Wetlands and Flood Mitigation in Ontario: Natural adaptation to extreme rainfall

Mason Marchildon P.Eng
Oak Ridges Moraine Groundwater Program
mmarchildon@owrc.ca

July, 2017

Prepared for:
Ducks Unlimited Canada

Wetlands and Flood Mitigation in Ontario: Natural adaptation to extreme rainfall

Mason Marchildon P.Eng
Oak Ridges Moraine Groundwater Program

July, 2017

Abstract

Wetlands and Flood Mitigation in Ontario: Natural adaptation to extreme rainfall

Wetlands are often recognized for their flood control value, but little research exists specific to Ontario, where extreme weather causing flooding poses ever-greater threats to urban areas. Ducks Unlimited Canada has undertaken new research to better understand the role of wetlands in storing and attenuating flood flows in an urban/rural watershed. The second phase of this research, reported here, employs advanced hydrologic modelling to address the questions of where and how wetlands are most effective at retaining water, what consequences further wetland loss may have on flooding, and what potential wetland restoration could have to improve flood storage within a watershed. The modelling was accomplished using fully-integrated, three-dimensional variably saturated hydrologic model built for the entire Credit River watershed at a high spatiotemporal resolution.

Disclaimer

The reader is reminded of the scope of this study, that is to determine capacity with which wetlands can mitigate flooding. Although the project is set within the Credit River watershed, information describing the complete hydrological process occurring with the Credit River watershed is incomplete, and thus the model and results obtained and described in this report represents a gross simplification of the real system. The findings of this report was solely prepared with the intention of fulfilling the scope of this study within the limits of a financial budget and a preset timeframe. The model should not be employed as a long-term water budget or as an operational/predictive model of the Credit River watershed without addressing certain information needs, some of which were addressed in this report. The author will remain available to those willing to improve the model should there be a need. This project in its detail was the first of its kind, and the procedures proposed were intentionally designed to be applicable to other watersheds in Ontario and abroad to investigate specific ecosystem services provided by wetlands.

Acknowledgements

This project could not have been completed without the financial support of Ducks Unlimited Canada. Special thanks goes out to Owen Steele for his unrelenting patience, support and inspiration: the passion you commit to the advocacy of wetland conservation I wish will one day become commonplace. I am indebted to Christie-Lee Hazzard for her unique insights into spatial information that were invaluable to the both the model design and scenario development: I cannot think of a time in my past modelling experience where your help wouldn't have been needed.

I am also grateful for having immediate access to the hard working conservation authority staff who are always open for discussion and to bounce ideas off of. Special thanks goes out the Dilnesaw Chekol, Michael Thorpe, Laura DelGiudice, Tim Mereu, and Scott Sampson: believe me that even our briefest of conversions had been of great help.

Much thanks goes out to Aquanty staff for their willingness to help me understand their fine model-code, and providing suggestions to my model design. Doctors Hyoun-Tae Hwang, Young-Jin Park, Ed Sudicky and Steve Berg: your open attitude and expedient support goes unparalleled—I wish you all great success and look forward to future endeavours. I also wish to thank Dr. Damian Merrick of HydroAlgorithmics, your support for and early release of AlgoMesh was much appreciated.

Additional thanks goes to the hard working staff at Environment Canada: Frank Seglenieks, Vincent Fortin and Sylvie Leroyer: I'm so glad to have been at the right place at the right time. I'm proud to be one of the first to break-out that amazing urban sub-kilometre atmospheric dataset: it sure took this project to the next level.

I must also make mention of the SciNet team: what a resource us modellers now have! SciNet was the backbone to this entire study; without it, the insight I gained would have been severely limited. Their openness, one-to-one consultation, free training and immediate support has been inspiring. I can't speak for all of the scientific disciplines that use you as a resource, but from now on, I will never cease to promote the utility of high-performance computing institutions such as yours. A special shout-out goes to Scott Northrup, your immediate assistance was invaluable.

I am only so lucky to have to opportunity to work for a group that has never resisted in my completing this work. To the thirteen partner agencies I help to support: thank you for giving me the time, the experience I gained here will no doubt be benefited by the services I will continue to provide for you. A special thank you goes out to Steve Holysh, you support never faltered and sincerely I admire that. So far, you and Rick Gerber have been exemplary workmates: thanks for your openness and willingness to discuss matter pertaining to this study at the drop of a hat.

And last but not least, I wish to send a special thanks to Alexandra Service. It would not do justice to say that your support and inspiration has been the foundation of this work, because as you are well aware, this project would have never got off the ground without you and I would have never gotten the chance to produce my best piece of work. For you to have the ability to get such important work off the ground, considering all of the modelling work completed in this province, just goes to show how well you are set on the correct path—kudos to you. I am encouraged that many others, society as a whole, and our natural environment will continue to gain from your presence. And to this, I dedicate this report to you.

Executive Summary

There exists a growing recognition that the services natural systems provide to society (i.e., ecosystem services) may be integral to our ability to adapt to a changing climate. The unsustainable costs associated with recent pluvial flooding that has been occurring with increased frequency in southern Ontario, Canada, has resulted in a renewed interest in valuating wetlands for their flood mitigation potential. When counted against the cost of recent flood events, the financial gains from the preservation of existing wetlands and the restoration of lost wetlands could be substantial. Wetlands could then be valued for the self-maintaining services they continue to provide free of charge. However, difficulties lie in understanding the role wetlands play in watershed hydrology.

A service often attributed to wetlands is their ability to mitigate flooding; however, this claim has often been made anecdotally, with little to no quantitative analysis to back it up, the kind of analysis that is ultimately required to assess the "natural capital" of wetlands. This is likely due to the inherent dangers associated with monitoring watershed hydrology during extreme high flow events, which presents a logistical difficulty in determining wetland function under high-flow conditions. Indirect means of quantifying wetland flood retention capacity are required.

This report employs the use of a numerical model of watershed hydrology to quantify wetland flood mitigation potential. The model was built to simulate the hydrology of the Credit River Watershed (CRW), a 950 km^2 basin located west of Toronto, Ontario, Canada. The CRW is a mixed land use watershed consisting of equal portions urban development, agriculture and natural cover, including some 4,000 wetlands and 1,400 km of mapped watercourses.

The investigation of wetland flood mitigation required a thorough model-code selection process to address the shortfalls of previously conducted wetland-flood modelling studies. The model ideally needs to be defensible, meaning that it should utilize state-of-the-art technology, current established and accepted theory, and the latest procedures of numerical modelling practice. The model design developed for this study and described herein ensured that a numerical model was built with the flexibility to:

i. simulate independent water balances for every CRW wetland, such that individual wetland function or the aggregated function of a group of wetlands could be assessed;

ii. ensure that any area within the CRW having a potential flood hazard/risk could be accounted for;

iii. accept additional modelling scenarios not investigated in the current study;

iv. provide discrete model states at virtually any location within the CRW at multiple points in time;

v. readily accept high-resolution spatiotemporal storm event information;

vi. adapt to alternate seasonal factors (i.e., snowmelt, frozen ground, varying antecedent moisture conditions, storm distribution/dynamics, etc.);

vii. simulate groundwater interactions that influence the function, storage and capacity of wetlands;

viii. simulate nutrient loading, fate and transport, and sediment loss and transport as needed; and,

ix. provide readily interpretable information necessary for flood impact assessment and wetland service valuation.

The modelling approach described in the report first set out to determine whether the flood mitigation capacity of wetlands is physically quantifiable through numerical simulation. Through a rigorous statistical framework it was determined that wetlands undoubtedly have the capacity to detain flood flows thereby mitigating flood hazards, at least within the CRW. This conclusion is realized beyond the uncertainty associated with model parameterization.

Next, a series of wetland loss and restoration scenarios were tested in an attempt to isolate the function of wetlands of various characteristics based, among other things, on wetland location within the watershed. In addition, these scenarios were modelled under the influence of a variety of extreme rainfall events, including the 2-, 5-, 10-, 25-, 50-, 100-year return period event plus an event representative of the highest short-term rainfall intensity recorded in Ontario.

Extreme rainfall events imposed onto the model were based on ultra-high resolution mapping of an actual 2015 southern Ontario convective storm event. The use of this advanced dataset ensured that the CRW was exposed to the appropriate storm dynamics that typify southern Ontario "extreme" events.

The first set of wetland loss scenarios attempted to isolate the function of wetlands in direct contact (i.e., connected) to mapped watercourses and drainage features. These scenarios were then compared with wetlands that were isolated (i.e., disconnected from drainage features). Although wetlands from both classes (connected vs. isolated) exhibited some influence on the CRW hydrology, connected wetlands proved to play the principle role in mitigating fluvial flooding. Removal of these connected wetlands would result in significant hazard to multiple reaches along the Credit River drainage network, including a number of mapped flood damage centres.

Other loss scenarios included the loss of all wetlands not deemed Provincially significant, and the removal of wetlands projected by Credit River Conservation (CVC) as potential near-term loss. Both of these scenarios closely resembled the function of isolated wetlands, as the majority of these wetlands were isolated themselves. Changes to isolated wetland distribution in the CRW tended to affect the hydrology of the landscape in close proximity to these wetlands, and thus areas that are converted from wetland may be inundated by waters normally detained by the lost wetlands.

Most notable in the model results is the potential flood reduction that can be gained by restoring the wetlands located at sites identified by CVC. Simulations show that restoring these wetlands can significantly reduce flood depths in Mississauga, and substantially reduce the number of locations along the Credit that pose risks to human health.

The report proposes a means of translating model results into an economic valuation of wetland function with respect to flood mitigation. The method's strength is that it allows for the translation of results from a complicated numerical procedure into a single figure that is easily communicable.

This report presents a novel attempt to quantifying wetland flood mitigation capacity. That said, great detail was added to ensure reproducibility of results. It is unclear whether the conclusions made here are specific to the CRW or can be translated elsewhere. Due to time and budget constraints, the study was restricted to a set of particular scenarios and was by no means established as the definitive set of model runs needed to quantify wetland-flood retention relationships; many other scenarios could possibly be investigated. The model was purpose built to ensure flexibility for future applications.

Contents

List of Figures

List of Tables

Section 1

Introduction

Since the turn of the century, Canadian cities have experienced a number of extreme precipitation and flooding events at high cost. According to the Insurance Board of Canada (IBC, 2016a,b), the total cost in terms of claimed damages from some eight major precipitation events occurring in Ontario over the past 12 years (Peterborough, July 2004; Eastern Ontario, September 2004; Toronto, August 2005; Hamilton, July 2009; Leamington & Windsor/Essex County, June 2010; Thunder Bay & Montreal, May 2012; Toronto, July 2013; Toronto, September 2014) approached $2.5 billion. Compounding this cost with the projection that extreme precipitation frequency and intensity are expected to increase in Ontario with a changing climate (Colombo et. al., 2007; Warren and Lemmen, 2014; Environmental Commissioner of Ontario, 2015), there is a growing need to develop and discover mechanisms for which society can adapt to this growing hazard.

Of the many potential adaptations society may turn to mitigate flood risk, ecosystem services are increasingly being recognized in Ontario especially since much of our natural capital (Maltby, 2009) that currently exists throughout many southern Ontario watersheds offer their services at no cost. Often referred to collectively as "green infrastructure," a diversity of stakeholders including conservation organizations (Hotte et. al., 2009; Conservation Ontario, 2013; Anielski et. al., 2014), municipalities (Ministry of Municipal Affairs and Housing, 2014; Environmental Commissioner of Ontario, 2014), businesses (Nature.org, 2013), state and national governments (USEPA, 2014), and international organizations (Millennium Ecosystem Assessment, 2005; European Environment Agency, 2015) are arguing for the preservation and enhancement of existing natural capital (such as wetlands) on the basis of its benefits to society and the valuation of its services.

Wetlands are defined areas on the landscape that are permanently or periodically inundated or saturated by surface and groundwater (Black, 1996), and offer a wide variety of ecosystem services including flood detention (Mitsch and Gosselink, 2015). Being generally characterized as independent landscape features regularly influenced by the presence of water, wetlands tend to be composed of hydric soils[1] that support a diverse range of hydrophytic vegetation[2] and aquatic fauna (Maltby and Acreman, 2011; Mitsch et. al., 2015) and provide conditions needed for anoxic biochemical processes that improve water quality (Mitsch and Gosselink, 2015). Considering their hydrological function and diversity of biological activity, in addition to flood mitigation, wetlands serve to (Wetzel, 2001; Mitsch and Gosselink, 2000, 2015; Maltby and Acreman, 2011; McLaughlin

[1]Hydric soils: soils that are formed under saturated conditions.
[2]Hydrophytic vegetation: plants that are adapted to grow in water.

and Cohen, 2013; Mitsch et. al., 2015):

- provide essential habitat and refuge;
- improve water quality—e.g., wetlands host a variety of biota that specialize in nitrogen fixation;
- sequester carbon/act as a carbon sink;
- retain sediment loadings—such as large organic carbon loadings that are derived from allochthonous sources;
- regulate/stabilize local and regional climate;
- regulate local temperatures through latent heat exchange;
- control erosion;
- reduce drought severity;
- regulate aquifers through surface water/groundwater exchange;
- offer food and fibre;
- offer timber, peat and other vegetation harvest; and
- offer cultural value and recreation areas.

From a hydrological perspective, wetlands are typically characterized as being regions where the runoff originating from rainfall or snowmelt collects. By collecting runoff, wetlands serve to attenuate the energy inherent in rainfall-runoff events (Black, 1996), thus offering potential flood mitigation services. Relatively little quantitative research has been performed to determine the exact role wetlands play in attenuating floods (Bullock and Acreman, 2003); and of that, research has predominantly focused on the role of riparian[3] (or floodplain) wetlands specifically, and not on wetlands in general at the watershed scale (Kadykalo and Findlay, 2016). Consequently, the generally accepted concept that wetlands mitigate flooding has tended to be somewhat anecdotal (Maltby and Acreman, 2011). The limited research conducted thus far has led to the general conclusion that riparian wetlands tend to be of higher value (see, for example, Mitsch and Gosselink, 2000).

Costanza et. al.(1997, 2014) long established that, with the exception of coastal estuaries, wetlands are significantly more valuable than lakes, rivers, grasslands, etc., in terms of the services they provide; however, assessing the value of ecosystem services specific to wetlands is not straight forward, but rather context-specific dependent on their location on the landscape (McLaughlin and Cohen, 2013). When considering flood mitigation, Ogawa and Male (1986) indicated that the location of wetlands must be taken into account when considering their influence on potential flood damage areas; however, the authors only considered the role of riparian wetlands. In contrast, Loucks (1989) concluded that for restoration considerations, smaller wetlands distributed throughout the headwater regions should provide better flood "buffering," thus reducing extreme flood pulses that could otherwise not be handled alone by fewer/larger downstream wetlands.

[3]Riparian wetlands being defined as wetlands that exist in close proximity/adjacent to a body of flowing water and is periodically influenced by flooding (after Mitsch and Gosselink, 2015).

What is apparent is that the flood-mitigation capacity of wetlands is not fully understood, especially the role of isolated wetlands,[4] which are thought to play a more-significant role in services other than flood mitigation such as aquifer regulation by attenuating groundwater response to rainfall variation (Mitsch and Gosselink, 2000; McLaughlin and Cohen, 2013). This highlights the attempt to acknowledge wetlands as "multiple-value systems," meaning different wetland types can provide different services (Mitsch and Gosselink, 2000) all while admitting that "it may become apparent that all wetlands are uniformly valuable" (McLaughlin and Cohen, 2013). What remains unclear is the cumulative role of smaller, isolated, headwater wetlands since there is limited knowledge on how the location, distribution and number of wetlands fulfil a particular ecosystem service such as flood mitigation (Erwin, 2009; Maltby and Acreman, 2011; Bradford, 2016).

Determining the role wetlands have to play in mitigating floods would require data collection that would be difficult and hazardous (McLaughlin and Cohen, 2013). Alternatives to empirical research include the application of numerical modelling; however, the many attempts at modelling the function of wetlands, in terms of water quantity, rarely consider wetland-flood relationships; rather they:

- are site-specific—concentrating on the impacts to individual wetlands from watershed development, rather than the role wetlands play on watershed hydrology (Gilvear et. al., 1993; McKillop et. al., 1999; Dietrich et. al., 2007; Gasca and Ross, 2009; Chen and Zhao, 2011; Trigg et. al., 2014);
- are focused on long-term wetland water balances and hydroperiod (Gilvear et. al., 1993; Krasnostein and Oldham, 2004; Krause and Bronstert, 2005; Dietrich et. al., 2007; Gasca and Ross, 2009; Rayburg and Thoms, 2009; Chen and Zhao, 2011); to investigate the impacts of land use change (Batelaan et. al., 2003) and groundwater extraction (Johansen et. al., 2014) on wetland function;
- attempt to identify wetland contribution to stream flow generation as regions of groundwater discharge (Partington et. al., 2013);
- investigate the dependence of groundwater flux on wetland bathymetry (Trigg et. al., 2014); or,
- identify recharge areas upon which groundwater-fed wetlands are dependent (Marchildon et. al., 2016).

As such, many wetland modelling studies reviewed focused on the relationships between groundwater and wetlands (Gilvear et. al., 1993; McKillop et. al., 1999; Batelaan et. al., 2003; Thompson et. al., 2004, 2009; Krause and Bronstert, 2005; Dietrich et. al., 2007; Gasca and Ross, 2009; Johansen et. al., 2014; Trigg et. al., 2014; Marchildon et. al., 2016), which is helpful in emphasizing their interdependence and relationship to local aquifer systems, however, do not investigate how wetlands could function under short-term extreme precipitation events that will likely be most detrimental to watershed vitality (Erwin, 2009).

Of the few studies that did investigate short-term (sub-daily) hydrology (McKillop et. al., 1999; Thompson et. al., 2004), they tended to be site-specific only focusing on a single wetland/complex. While others that did consider larger scales continued to focus on riparian wetlands only (Ogawa

[4] Isolated wetlands being defined as wetlands that are hydrologically isolated from any observable surface water connection (McLaughlin and Cohen, 2013; Bradford, 2016).

and Male, 1986; Krause and Bronstert, 2005; Rayburg and Thoms, 2009) disregarding the function of a number of isolated wetlands (see also Kadykalo and Findlay, 2016). Most importantly, these wetland-modelling efforts tended to be centred on wetlands and their sensitivity to watershed processes; whereas for a wetland flood mitigation study, efforts need to investigate the exact opposite, that is, how the *watershed* is sensitive to wetland flood mitigation capacity.

Ogawa and Male (1986) represents an early attempt to model wetland performance during flood events. Although restricted to riparian wetlands, this study did emphasize the importance of wetland distribution and of treating them independently. Wetland distribution was accomplished by applying a subwatershed-based modelling scheme, and the modelled watershed was exposed to a 10-, 100-, and 500-year, 24 hour duration storm event. Hydraulic flood routing was then required to route flood flows down the drainage network where it was concluded that downstream (riparian) wetlands were more valuable in their flood detention services; although one wonders what would have been concluded if the headwater/isolated wetlands had not been neglected. In all, the Ogawa and Male (1986) modelling effort was an excellent attempt at addressing wetland flood mitigation capacity at the watershed scale, and much of their model implementation and design was used to structure this study, including, but not limited to:

- the need to incorporate wetland size;
- the need to address wetland location and proximity to drainage features;
- the need to address wetland location in proximity to flood damage centres;
- the importance of capturing rainfall rate;
- the importance of antecedent moisture conditions; and,
- the importance of hydraulic routing.

With the abundance of literature documenting wetlands' ability to protect, improve, and enhance water quality (Maltby, 2009), and studies investigating impacts to wetlands from urbanization and climate change (Batelaan et. al., 2003; Erwin, 2009; Marchildon et. al., 2016), there is a critical need for a wetland modelling methodology to adequately valuate wetland services in flood mitigation. This report, which serves as the second of three phases of a comprehensive study, is such an attempt and will provide for a scientific methodology urgently needed to support wetland restoration (Erwin, 2009).

The following sections document the construction of a numerical model of the Credit River Watershed (CRW) situated west of Toronto, Ontario, Canada. The model was purpose-built to quantify wetlands' flood mitigation capacity at the watershed-scale—meaning that the capacity of the CRW wetland ensemble has been quantified, rather than the contribution of any particular wetland or wetland complex. That is not to say that the wetland function as a whole was lumped into a single numerical process, rather every mapped wetland was modelled independently, meaning the model has computed an independent water balance for each and every wetland.

1.1 A phased study

The assessment of the flood mitigation capacity of wetlands and the economic service they provide is being undertaken in three phases:

- Phase I: Literature review
- Phase II: Hydrologic modelling of the CRW
- Phase III: Economic valuation of the hydrologic modelling results

Phase I was a comprehensive literature review on academic research that focused on the role wetlands play in flood mitigation and the economic value of this service. The Phase I report has been appended to this report as Appendix A. As a brief summary of the Phase I report, broad evidence has been found linking wetlands to flood mitigation:

- Wetland drainage in the Canadian Prairies has led to an increase of up to 350% in flood peak flow (Pomeroy et. al., 2014).
- An acre wetland that is 1 foot deep can hold 330,000 US gallons of water (Hallock et. al., 2015).
- A 5.7-acre wetland can retain the natural runoff from a 410 acre watershed (Godschalk et. al., 1999).

In Ontario, a number of natural capital assessments have been completed that examine a range of ecosystem service benefits, including flood control from wetlands (Wilson, 2008a,b; Kennedy and Wilson, 2009; Troy and Bagstad, 2009). Reported estimates of flood protection in these studies are based on the application of primary research from other jurisdictions, then transferred to Ontario (i.e., benefit transfer); there is very little ecosystem valuation work based on research conducted in Ontario which highlights the need for this research project. Estimations of the economic value of flood mitigation provided by southern Ontario wetlands from these existing studies include:

- $380 million per year in the Greenbelt (Wilson, 2008a).
- $157 million per year in the Lake Simcoe Watershed (Wilson, 2008b).
- $16 million per year in the Credit River Watershed (Kennedy and Wilson, 2009).

Phase II of the study (this document) involves the development of a numerical hydrological model of the CRW that is used to quantify the flood attenuation capacity the watershed's many wetlands. As identified above, there is a lack of quantitative analyses of wetland flood attenuation capacity at the watershed scale (Kadykalo and Findlay, 2016). Since southern Ontario has experienced a number of costly extreme rainfall events over the past decade (IBC, 2016a,b), such an analysis is expected to provide a significant contribution. The quantitative modelling approach taken in this study has been coupled with a series of wetland loss and recovery scenarios that are tested against a range of extreme precipitation events varied by rainfall intensity. The Phase II results will inform Phase III, which will introduce an economic analysis to explore the cost associated with wetland loss and the potential financial gains that may be realized from wetland restoration. To ensure success of the economic analysis and the development of a business case for the conservation and restoration of wetlands, it is essential for the hydrological model outputs to serve as key inputs into such an economic analysis (Figure 1.1).

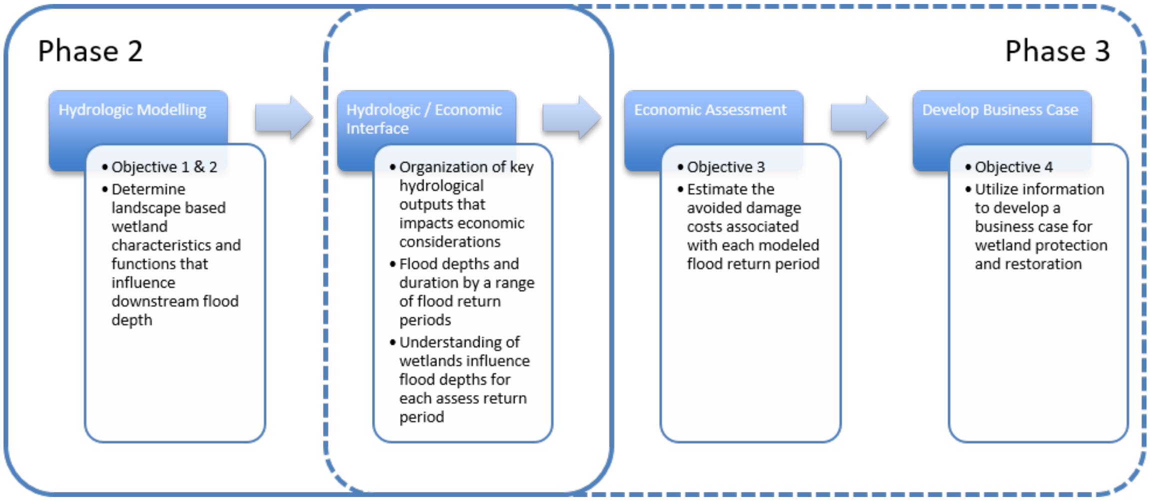

Figure 1.1: Interface between the hydrological (Phase II) and economic (Phase III) phases of this study.

1.2 Study scope

The purpose of this study is to determine the role, if any, wetlands play in attenuating flooding from high-intensity storm events occurring in the CRW, and to provide metrics to assist the economic valuation of this service. Prior to proceeding with this report, it is important for the reader to appreciate that the relationship between extreme rainfall and flooding is complicated, depending on a number of climatic and environmental factors which would be next-to-impossible to fully incorporate within a single modelling approach. Therefore, a clear Phase II project scope has been carefully defined as to:

> *Quantify the capacity for wetlands to detain flooding from an extreme late-summer rainfall event.*

The above scope is intentionally succinct, to ensure that the objectives of the study remain narrow in focus. The scope implicitly tests the hypothesis that a wetland service in the CRW includes flood retention during late-summer precipitation events, such as those costly events identified by the Insurance Board of Canada (IBC, 2016a,b). As will be discussed later in this report, this scope recognizes that extreme rainfall events experienced in southern Ontario are of the convective-type that typically occur during late summers when the land surface is super-heated and the near-surface (boundary-layer) atmosphere is humid. This mixture of super-heated humid air masses can induce atmospheric instability resulting in cumulus convection that can yield intense thunderstorms. The scope then dictates how the model is to be constructed and the assumptions underlying the model's initial state and boundary conditions; these include:

1. dry antecedent conditions;
2. seasonally low (deep) regional water table;

3. convective-type storm event that is isolated, of short-duration and high-intensity;
4. an event-based/short-term analysis; and,
5. late-season, late-stage vegetation growth.

The implication of an event-based hydrological modelling study is that the model is run with time-scales of short-duration (i.e., 1 to 5 days). This is different from other more common long-term wetland water-balance modelling efforts used in quantifying wetland hydrologic regime[5] and hydroperiod.[6] These long-term models require model run-times at the seasonal, annual or decadal time scales.

The Phase II modelling study is not wetland-centric, in that the purpose is not to assess impacts to any one wetland or wetland complex resulting from land use or climate change. Rather the focus is to quantify the cumulative role of all wetlands in the CRW, no matter their size or location on the landscape. The proposed study will not make an attempt to simplify the model by lumping any number of wetlands into a singular effective wetland element. This is to preserve the model's ability to quantify independent water balances for each individual wetland as part of the scenario-based model analysis.

1.2.1 Numerical model requirements

Phase II involves the construction of a watershed-scale numerical model of hydrology to quantify wetland flood mitigation capacity. A numerical model is an assembly of computer code that represents an approximation of a real phenomenon. Physical phenomena are simulated indirectly by means of governing (i.e., mathematical) equations thought to represent the physical processes that occur in reality (Anderson et. al., 2015). Here, the physical phenomena that are being modelled are the components of the hydrologic cycle—that is, the pathways water takes after being precipitated onto a watershed: where it collects, is absorbed, and directed into flowing streams that eventually drain the watershed.

Specifically, the watershed process being investigated is runoff generation (i.e., how rainfall is translated into runoff causing flooding) and its relationship to wetland distribution. The quantification of wetland flood mitigation capacity will be determined through a series of scenarios, in which a variety of hypothetical wetland loss and restoration options are tested to discern the role of individual wetlands of different types, size and distribution on the landscape. In addition, a series of extreme rainfall intensities will be forced upon each scenario to identify the range of wetland flood mitigation capacity.

1.2.2 Expected model outcomes

Once the results from proposed modelling are fed into the Phase III economic analysis, the anticipated outcomes are to:

1. gain a clearer understanding of what role, if any, wetlands can play in helping to reduce the cost of flooding in a typical southern Ontario watershed;

[5] Hydrologic regime is the mean, variance and rates of change in wetland water level (McLaughlin and Cohen, 2013).

[6] Hydroperiod is the recurring seasonal pattern of wetland water level (Mitsch and Gosselink, 2015).

2. determine the relationship of wetland location, extent and scale to flood attenuation;
3. assess the economic benefits the ecosystem service of wetlands may provide, including the return on investment of restoration activities;
4. identify "best bet" areas for wetland restoration; and,
5. provide information to assist municipalities, conservation authorities, provincial government, and others in planning for extreme rainfall events and adapting to climate change.

1.2.3 Numerical model requirements

With over 4,000 wetlands being identified within 24 wetland complexes of the CRW, varying in size, extent and proximity to dominant flowpaths, assessing their flood attenuation capacity requires a modelling approach that can account for the spatial distribution of wetlands across the landscape, as advocated by Mitsch and Gosselink (2000). The results of the hydrologic modelling are ultimately intended to provide input to the Phase III analysis that is aimed at determining the economic value of wetlands. Given that the value of wetlands is dependent on their spatial distribution, it is critical that wetland distribution be incorporated into the modelling approach; therefore, the numerical model chosen for this study must represent hydrologic and hydraulic processes in a fully-distributed manner (Shook et. al., 2013), meaning that processes are independently being simulated at discrete points in space. Process distribution should also be imposed at fine resolution in order to resolve small isolated wetlands, low-order headwater drainage features, and micro-topographic depressions (Thompson et. al., 2004). In addition, due to the short-duration nature of the events being simulated, the model must also simulate hydraulic and hydrologic processes at adequately small (sub-hourly) time scales (Ogawa and Male, 1986; McKillop et. al., 1999).

The influence of groundwater is also a recurring theme in many wetland studies (Roulet, 1990; Brassard et. al., 2000; Thompson et. al., 2004; Maltby and Acreman, 2011; McLaughlin and Cohen, 2013). The position of the groundwater table relative to the base of a wetland will have significant impacts on wetland hydrology, especially with respect to rainfall retention. A model must be chosen that can represent sub-surface processes at enough detail to (McKillop et. al., 1999):

1. identify wetlands that are either groundwater sources or sinks;
2. determine antecedent conditions; and,
3. establish initial wetland capacity.

A challenge in establishing initial capacity is the acknowledgment that groundwater interaction with wetlands can seasonally change direction from a groundwater recharge to a groundwater discharge regime (McLaughlin and Cohen, 2013; Bradford, 2016), and thus the initial state for this study will have to reflect a likely state occurring in late summer. Selecting a model that neglects the influence of groundwater will necessarily require the modeller to determine wetland capacity prior to performing any model runs, such as assuming (incorrectly) that wetlands are all empty prior to a storm event (as pointed out by Shultz and Leitch, 2001), thereby undermining the very purpose of the study.

In summary, the model fit for this study must be capable of accounting for the factors that contribute to wetland flood attenuation, which include:

1. basin morphometry—describing the shape of the watershed (Mitsch and Gosselink, 2000);
2. topography/bathymetry—describing the volumetric capacity (size) of a wetland (Ogawa and Male, 1986; McKillop et. al., 1999; Trigg et. al., 2014);
3. location and proximity to drainage features—describing the distribution and connectivity of wetlands to drainage features (i.e., streams, adjacent lower-gradient wetlands) that affects flood wave timing; i.e., the hydrogeomorphic principle (Mitsch and Gosselink, 2000);
4. depth to water table—dictating the (volumetric) absorptive capacity of wetland sediments (Maltby and Acreman, 2011);
5. sediment absorption—describing the sediment characteristics that dictate the rate at which absorption can occur (McKillop et. al., 1999; Maltby and Acreman, 2011; Mitsch and Gosselink, 2015);
6. vegetation—which effectively represents the surface roughness that retards the lateral movement of a flood wave (Tsihrintzis and Madiedo, 2000; Kadlec and Wallace, 2009);
7. adequate timescale—convective storms are characterized as being short-duration and spatially isolated (Weisman and Klemp, 1982; McKillop et. al., 1999); and,
8. hydraulic routing—physical constraints (i.e., energy and momentum) must be conserved to preserve the defensibility of model results (Ogawa and Male, 1986).

Few modelling codes and model approaches have the capability of accounting for all of the above-listed factors. Many model solutions commonly applied to wetland processes are incapable of assessing wetland flood-mitigation capacity because they either neglect:

1. spatial distribution—thus neglecting the value associated with wetland distribution and basin morphometry (Mitsch and Gosselink, 2000; Shook et. al., 2013);
2. short-term simulation—needed to resolve the isolated nature of extreme convective storms (Weisman and Klemp, 1982); or
3. sub-surface processes—putting reliance on the modeller to assume wetland absorptive (i.e., infiltration) capacity.

1.2.4 Data requirements

Prior to any modelling exercise, specifically for the fulfillment of the study scope and the numerical model requirements, certain fundamental datasets must be made accessible. How the data are to be utilized is discussed in detail later in §3. In short, the key baseline data needs to fulfil such a study must include:

1. distributed storm patterns;
2. representative/local historical rainfall intensities;
3. high resolution digital elevation model; and,

4. land cover mapping, describing:
    - land use
    - wetlands
    - drainage features (i.e., ditches, streams, rivers, etc.)
    - hydrostratigraphy/geology
    - surficial geology/soils mapping

Section 2

Study area, hydrology and climatology

The Credit River drains a 950 km^2 watershed extending from Orangeville in the north-west to the Lake Ontario shores of Mississauga Ontario in the south-east. The Credit River watershed (CRW) contains portions of some densely-populated regions of Ontario including the cities of Mississauga, Brampton, Georgetown, Orangeville and Oakville. Existing watershed mapping shows that the CRW is drained by roughly 1,370 km of drainage features that includes roadside ditches, ephemeral headwater streams and the river's mainstem that collectively drain some 24 subwatersheds (Figure 2.1. Port Credit, Mississauga is the outlet for the Credit River that discharges an average of 265M m^3 per year of runoff into Lake Ontario.

The CRW exists within the Mixedwood Plains ecozone that extends along the Quebec City-Windsor corridor. The ecozone is characterized by cool winters and warm summers and is prone to weather variability; the ecozone is known to be one of the major storm tracks of North America (Canadian Biodiversity Website, 2016). Urbanization and agriculture have made significant impacts on land cover. Forests that continue to exist are composed of a wide variety of coniferous and deciduous trees. Wetland types within the CRW consist mainly (74%—by area) of swamps, and 13% marsh, the remainder largely being unclassified.

2.1 Topography

Physiographically, the CRW is characterized by the north-south trending Niagara Escarpment that divides the watershed into two, roughly equal, portions: namely, the upper and lower watersheds (Figure 2.2). The digital elevation model (DEM) used in this study is the 2002 Greater Toronto Area (GTA) DEM completed in 2012 by the Spatial Data Infrastructure Unit of the Ontario Ministry of Natural Resources and Forestry (OMNR, 2002). The DEM has a spatial resolution of 5 m and a horizontal and vertical accuracy of 0.5 m, suitable for 1 m contour generation.

The 2002 GTA DEM does not capture Lake Ontario bathymetry beyond the Mississauga coastline. For the sake of completion, areas on the 2002 GTA DEM having reported elevations less than 75.1 meters above sea level (masl) were set to the Lake Ontario bathymetry layer offered by the National Centers for Environmental Information (NCEI) of the National Oceanic and Atmospheric

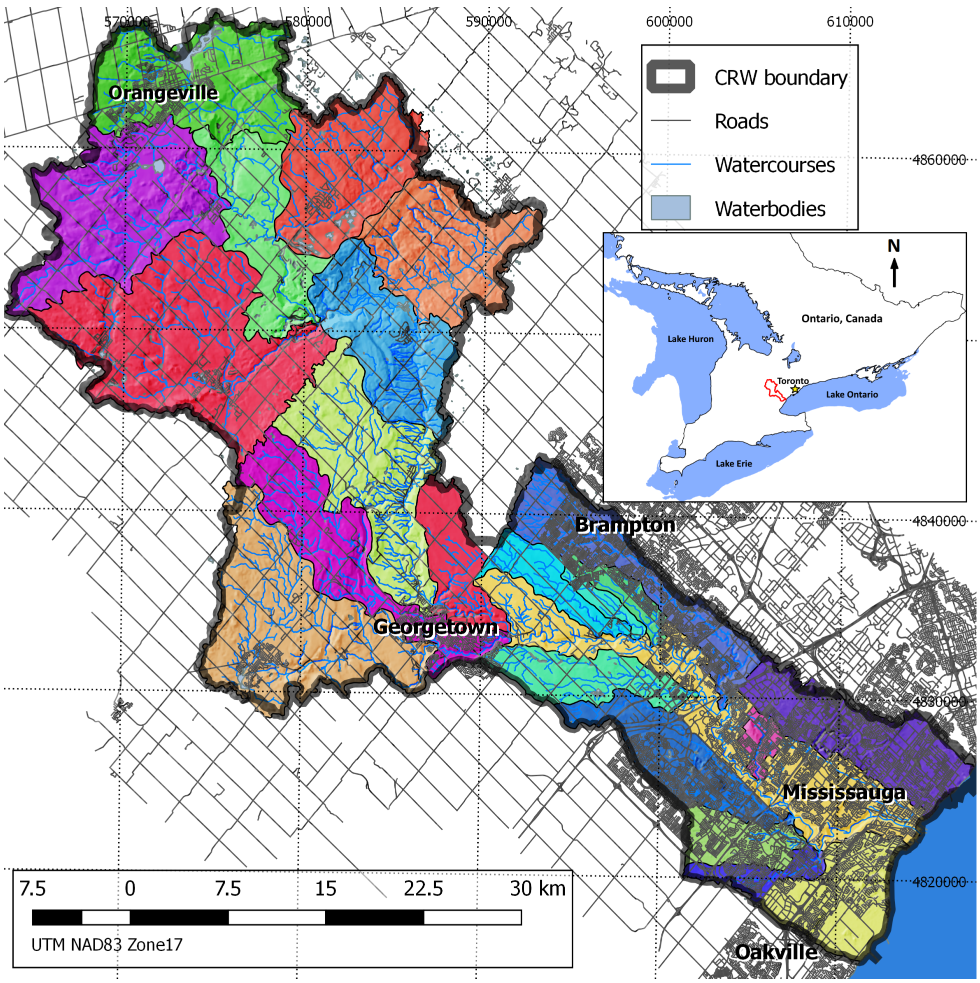

Figure 2.1: Credit River watershed including its 24 subwatersheds symbolized by the random colour scheme.

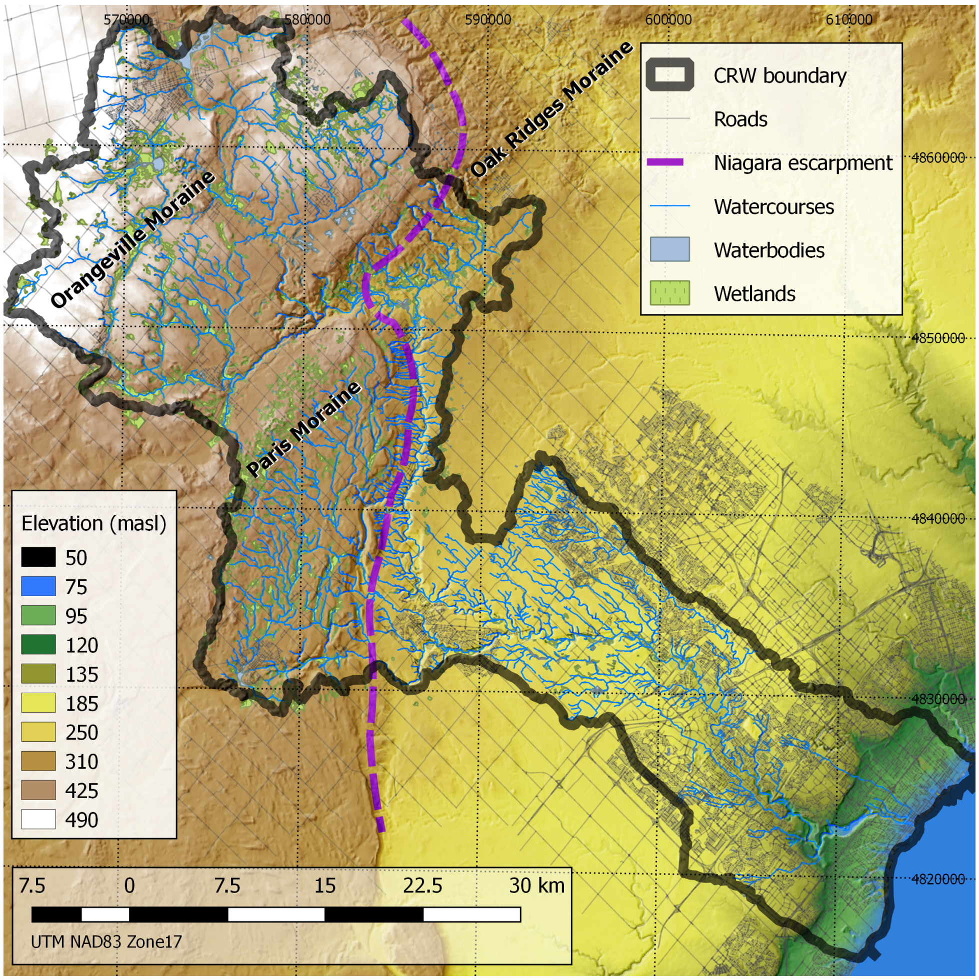

Figure 2.2: Credit River watershed topography.

Administration (NOAA), an agency of the U.S. Department of Commerce.[1]

CRW land surface elevation ranges from approximately 75 to 500 masl. Figure 2.3a presents the distribution of watershed elevation, which is quite smooth considering the presence of the escarpment. The reason for the apparent smoothness of the CRW hypsometric curve is: (i) the fact that the escarpment runs along the length of the CRW, covering significant portions of the watershed (Figure 2.2); and (ii) that the escarpment at many places exhibits gradual, but locally steep, talus slopes consisting of bedrock materials eroded from the escarpment face. According to the characterization of Strahler (1957), the downward-concaving nature of the hypsometric curve would indicate (correctly) that the CRW is in an early erosional stage of watershed geomorphology.

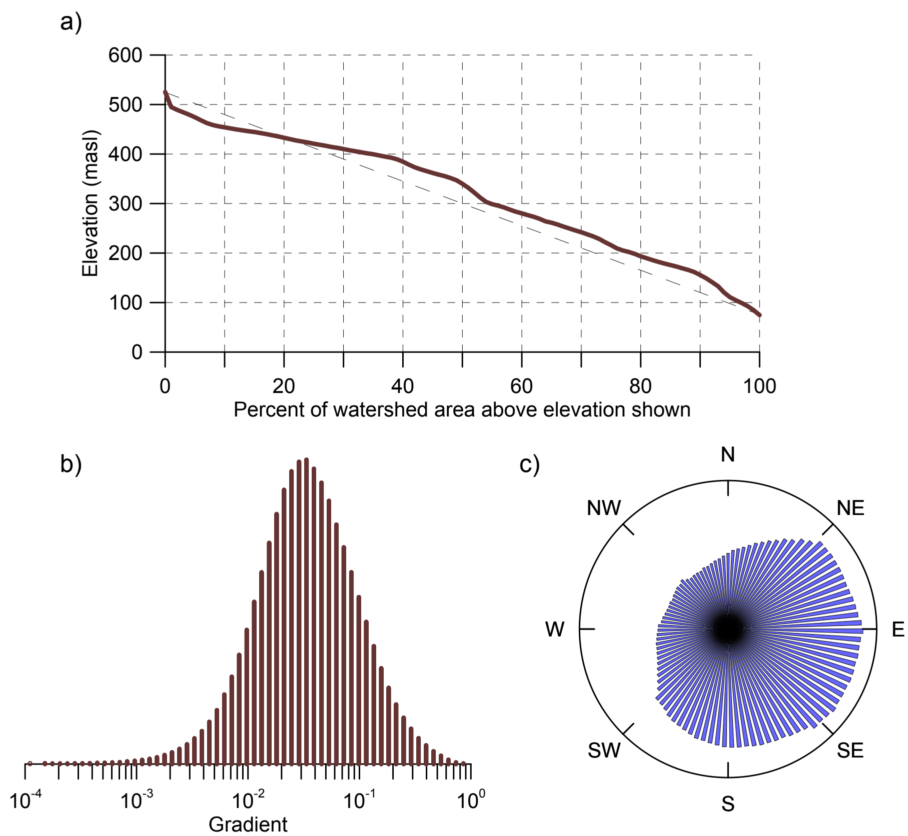

Figure 2.3: a) Hypsometric curve (Strahler, 1952) of the Credit River watershed; b) Histogram of bedslope distribution; c) Polar bar chart of aspect distribution.

Slope and aspect was computed using a nine-point planar regression performed at every cell and its surrounding eight cells of a 10 m-upscaled DEM. The majority of computed gradients span

[1]Data were accessed January, 2016 from http://www.ngdc.noaa.gov/mgg/greatlakes/ontario.html.

slightly over an order of magnitude, averaging at approximately 3% (Figure 2.3b). The slopes are predominantly facing east-south-east and span roughly 90° in either directions (Figure 2.3c). Hydrologically, this predominantly south-east facing watershed should, on average, receive a 3.6%[2] higher annual solar radiation flux relative to a horizontal surface, increasing the basin's drying potential.

2.2 Land cover

Land use and land cover information was provided by Credit Valley Conservation (CVC) in October, 2015 and is based on the southern Ontario Ecological Land Classification (ELC) system (Lee et al., 1998). The ELC mapping categorized the CRW's landscape into 72 distinct land cover types. For simplicity, the 72 types were grouped into 5 subclasses (see Figure 2.4), based on their hydrologic function, which include:

1. Agriculture—of all functions from growing of crops to the rearing of animals.
2. Anthropogenic—including all land coverage that has been altered by development or resources extraction. Generally, this subclass represents areas that are relatively impervious to rainfall infiltration.
3. Short vegetation—including all natural/pervious land areas whose land surface is partially to predominantly covered by vegetation (i.e., marshes, early succession growth, etc.).
4. Tall vegetation—similar to above, except the dominant vegetation types are deemed taller than anticipated flood depths (i.e., forests and swamps).
5. Waterbody.

Figure 2.5 presents the spatial distribution of the above-listed ELC subclasses. CRW land use cover is predominantly influenced by human activity, having most of the densely-populated areas residing in Brampton, Oakville and Mississauga to the southeast. In total, the anthropogenic subclass covers 29% of the CRW. Another 30% of the CRW is covered by agriculture, which can be found mostly to the north west in the upper watershed. Much of the natural landscapes (short vegetation–15%, tall vegetation–25%, and waterbodies–1%) is dispersed within the upper watershed and tends also to be found along the Niagara Escarpment.

2.2.1 Wetlands

Wetlands were identified using the wetland coverage provided by the Provincial Mapping Unit of the Ontario Ministry of Natural Resources and Forestry last updated on June 17, 2013. Through the Wetland Consolidation project of 2011, this wetland layer was built upon and improved from the Ontario Wetland Evaluation System (OWES) and includes the designated Provincially Significant Wetlands (PSW).

Within the CRW, roughly 4,000 wetlands and 610 waterbodies have been mapped, which suggests considerable groundwater interaction with the land surface. The CRW wetlands vary in size from 0.01 to 270 ha and exist mainly in the upper watershed. Figure 2.6 presents the distribution

[2] Calculated using potential solar irradiation theory (DeWalle and Rango, 2008).

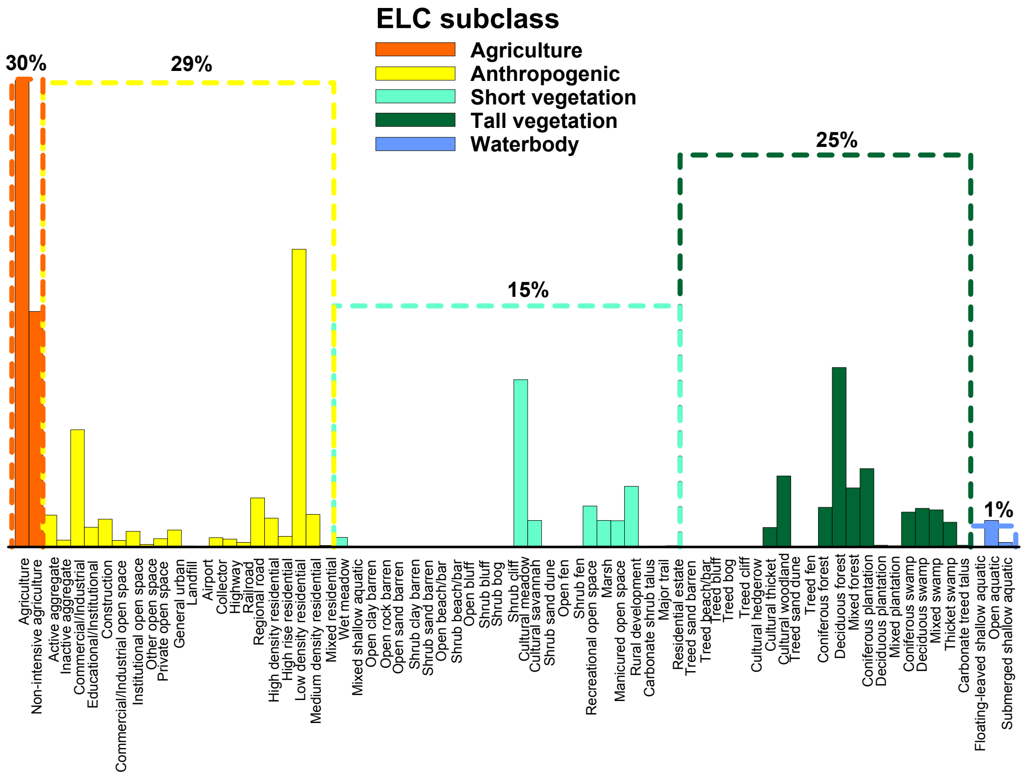

Figure 2.4: Distribution of ELC classifications and subclasses within the CRW.

of the mapped wetlands within the study area. On average, wetlands tend to be one hectare in areal extent, but vary by two orders of magnitude. It is important to note that the wetland area was measured directly from the provided geospatial data in which many wetland features could be found directly adjacent to one another, biasing the mode of the Figure 2.6 histogram to the left.

To explain the bias, individual spatial polygon features provided in the wetland mapping represent a discrete wetland type, either marsh, fen, swamp, bog, treed peatland, open water, etc., and not a contiguous wetland per se. Many individual wetlands were found to be comprised of multiple wetland "types," consequently conflating the wetland count. By applying a shapefile merge routine, thereby neglecting wetland type and joining all touching wetland polygon features, the total number of wetlands present in the CRW is reduced by 35% from 4,063 to 2,401. These merged wetland areas make up parts of the 23 larger wetland complexes found within the CRW. Table 2.1 lists the wetland complex with some additional attributes and Figure 2.7 shows their distribution within the CRW.

The wetland complexes tend to be rather dispersed and can extend across large swaths of the

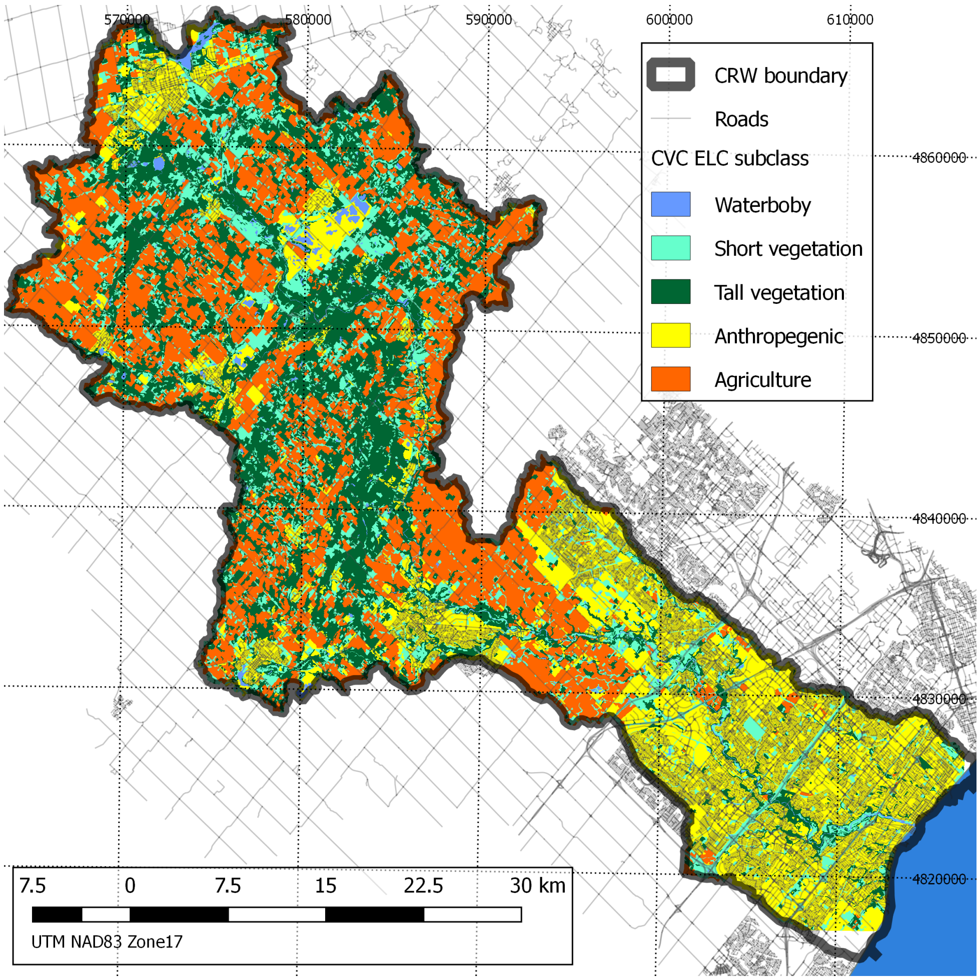

Figure 2.5: Spatial distribution of ELC subclasses within the CRW.

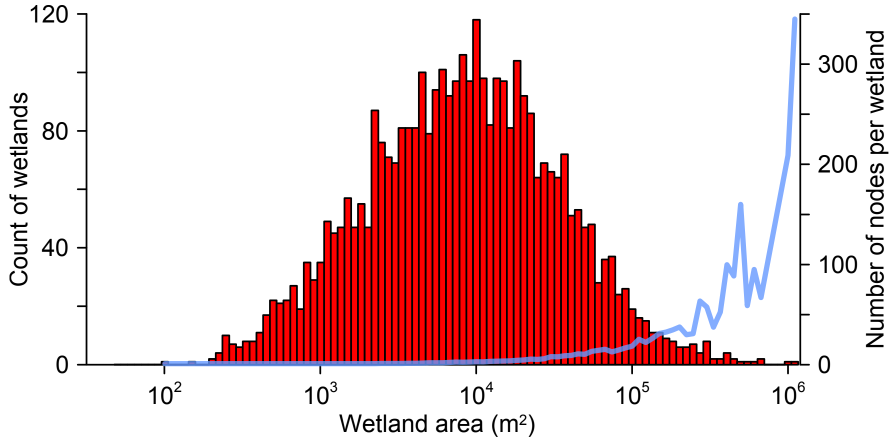

Figure 2.6: Distribution of wetland area within the CRW. Blue line represents the average number of model nodes used to represent wetlands of given size (see §3).

CRW. Most of the complexes exist in the upper watershed (83% by area) and will likely have the greatest influence on flood mitigation. In the lower watershed, it is likely that the dense urbanization has led to the removal of many pre-existing wetland complexes.

Wetlands that are hydrologically-isolated with no observable surface water connections (McLaughlin and Cohen, 2013) amount to 25% of all wetlands by area. Provincially-Significant Wetlands (PSWs) make-up 78% of all wetlands by area, but only 59% by number, suggesting a preference toward larger wetlands being established as significant. In Ontario, PSWs are identified through an evaluation process that assigns a score based on functions and values of wetlands from four perspectives: biological, social, hydrological and special features (Ontario Ministry of Natural Resources, 2014). It is apparent that within the CRW, the PSW evaluation system has assigned greater value to larger wetlands and wetland complexes. In addition, of the PSWs, only 19% by area make-up isolated wetlands, suggesting greater valuation given to connected wetlands.

Perhaps a better measure of wetland significance from a hydrological perspective, especially when considering their flood mitigation potential, is their contributing area (i.e., all up-slope areas draining toward the wetland). Applying terrain-analysis techniques to the 2002 GTA DEM, contributing areas to every wetland have been computed. As shown in Table 2.2, the relative contributing areas closely match relative wetland area suggesting that their value from a flood mitigation potential is equivalent. Notably, areas contributing to PSWs only make up twice the area contributing to non-PSWs, even though, by area of coverage, PSWs make up four times that of non-PSWs.

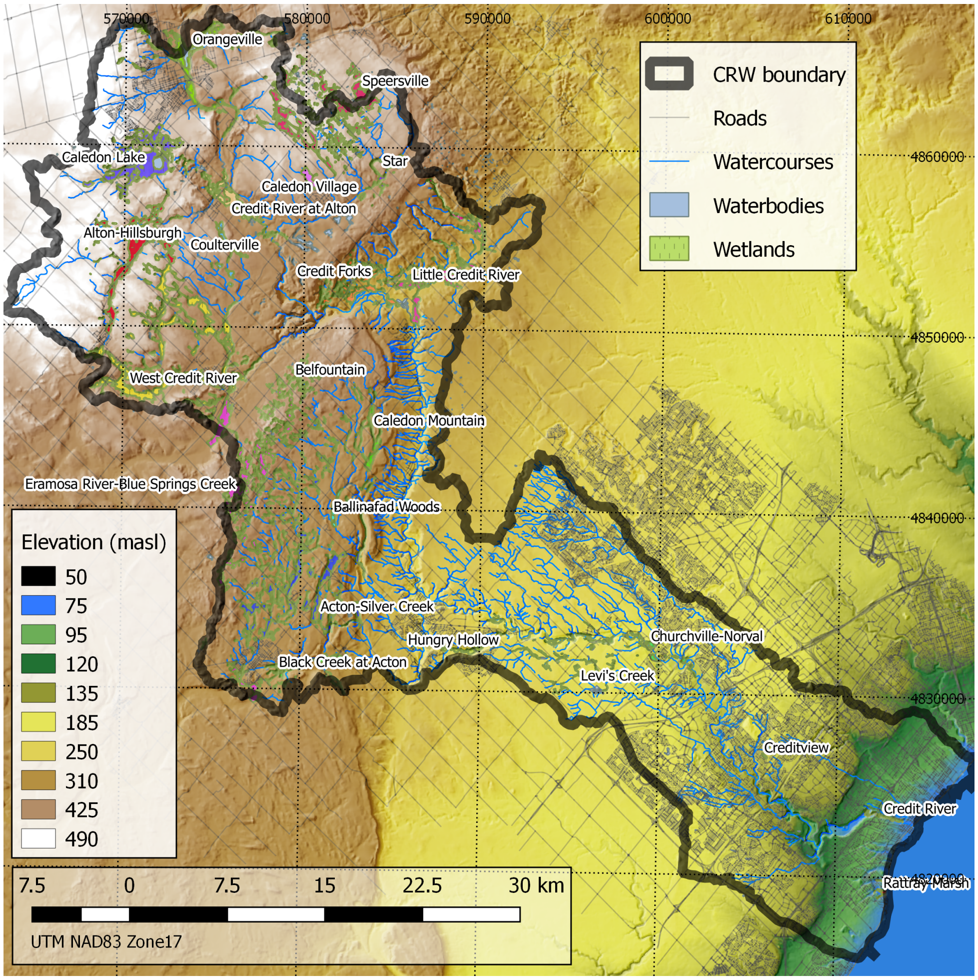

Figure 2.7: Distribution of wetland complexes within the CRW

Table 2.1: List of wetland complexes within the CRW (see also Figure 2.7).

Wetland Complex	General Watershed Location	Area (ha)
Acton-Silver Creek	Upper	823.1
Alton-Hillsburgh	Upper	436.6
Belfountain	Upper	70.2
Black Creek at Acton	Upper	113.0
Caledon Lake	Upper	533.3
Caledon Village	Upper	47.8
Coulterville	Upper	70.7
Credit River at Alton	Upper	194.8
Eramosa River-Blue Springs Creek	Upper	721.4
Orangeville	Upper	370.5
Speersville	Upper	634.3
Star	Upper	60.2
West Credit River	Upper	906.3
Ballinafad Woods	Escarpment	42.3
Caledon Mountain	Escarpment	154.1
Credit Forks	Escarpment	227.3
Little Credit River	Escarpment	353.5
Churchville-Norval	Lower	91.1
Credit River Marshes	Lower	22.0
Creditview	Lower	3.9
Hungry Hollow	Lower	62.2
Levi's Creek	Lower	50.7
Rattray Marsh	Lower	15.2

Table 2.2: Relative wetland coverage statistics from 4,063 CRW wetlands covering 78.6 km^2.

Wetland category/position	% (by count)	% (by area)	% (by contributing area)
PSW	59%	78%	65%
non-PSW	41%	22%	35%
All wetlands			
Connected	52%	75%	73%
Isolated	48%	25%	27%
PSW-only			
Connected	65%	81%	81%
Isolated	35%	19%	19%

2.2.2 Streams and waterbodies

Drainage features (i.e., streams, rivers, and some road side ditches, but not agricultural field tiles and municipal storm water management systems) and waterbodies (i.e., ponds, lakes, etc.) were extracted from the Ontario Hydro Network (OHN) watercourses and waterbodies GIS layers offered by the spatial data infrastructure unit of the Ontario Ministry of Natural Resources and Forestry and were accessed September, 2014.

All identified watercourses and waterbodies were retained for the purposes of this study, including all low-order headwater streams to the Credit River mainstem. Based on a Strahler (1952) stream-order analysis of the OHN watercourse layer, the Credit River mainstem is a 6^{th}-order watershed and has a maximum hydraulic length[3] of 110 km (Figure 2.8).

In total, there are 1,371 km of mapped drainage features used for this study. Table 2.3 breaks up the distance and number of reaches according to Strahler (1952) stream order. A reach is here defined as a continuous length of mapped channel without intersecting tributaries or divergences. Bedslope is computed on a reach basis but their average is weighted according to reach length.

Table 2.3: Statistics of drainage pathway geometry grouped by Strahler (1952) stream order.

Order	Number of reaches	Total length (km)	Weighted bedslope
1	1052	631.3	0.019
2	521	327.0	0.014
3	237	189.9	0.009
4	124	103.5	0.006
5	32	44.5	0.006
6	134	75.0	0.003
All	2100	1371.1	0.014

Through observation of the Credit River's longitudinal profile (Figure 2.9), tributaries can be differentiated by three characteristic bedslopes: The Credit's mainstem A has a low bedslope of approximately 0.3% and persists predominantly in the lowlands, B describes a set of tributaries with relatively high bedslopes of 3.6% that are mainly representative of those drainage pathways falling from the escarpment, and C the remaining mid-order tributaries have a low-moderate bedslope of 0.5%.

Of the CRW, only the upper reaches were included in Annable's (1996) morphologic database of rural streams: The CRW upland streams tend to be characteristically B- and C-type (Rosgen, 1994) channels that are low to moderately sloped, composed of sand to cobble beds with bankfull flow recurring roughly every 1.5 to 2.2 years.

[3] Hydraulic length is the longest path water could travel along the drainage network (Ponce, 1989).

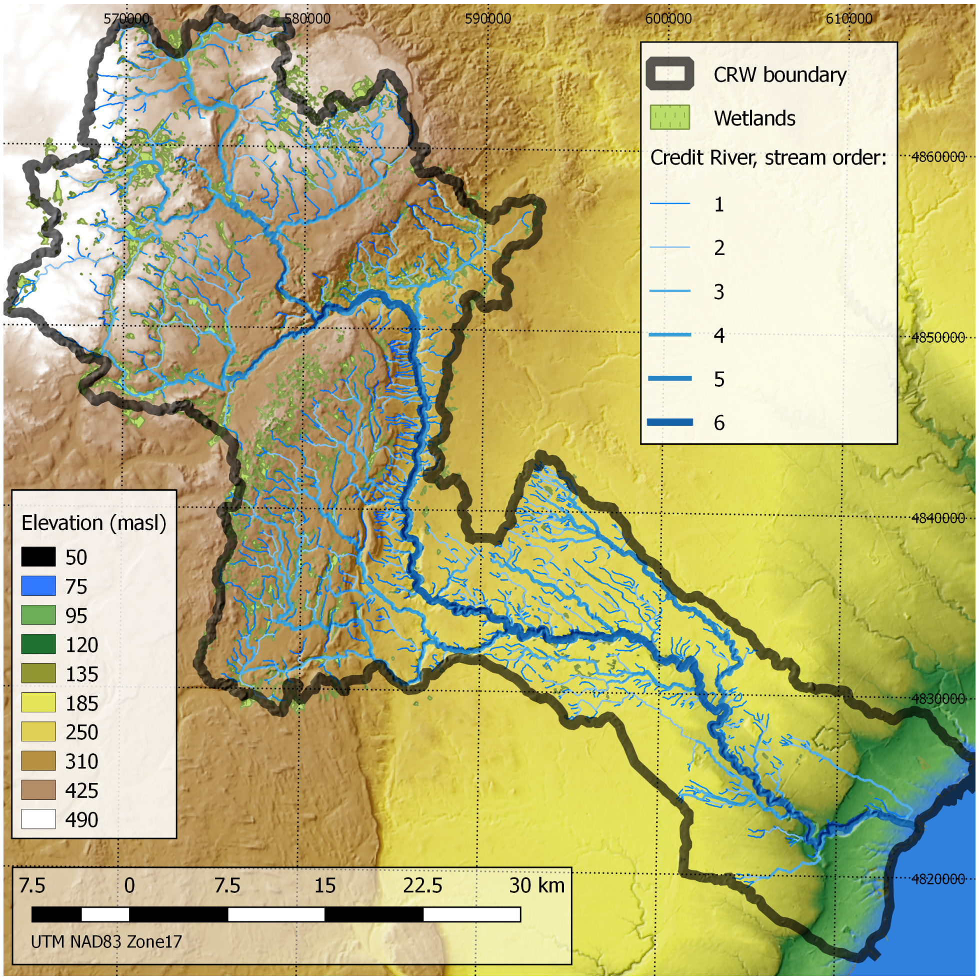

Figure 2.8: Credit River drainage network and wetland distribution.

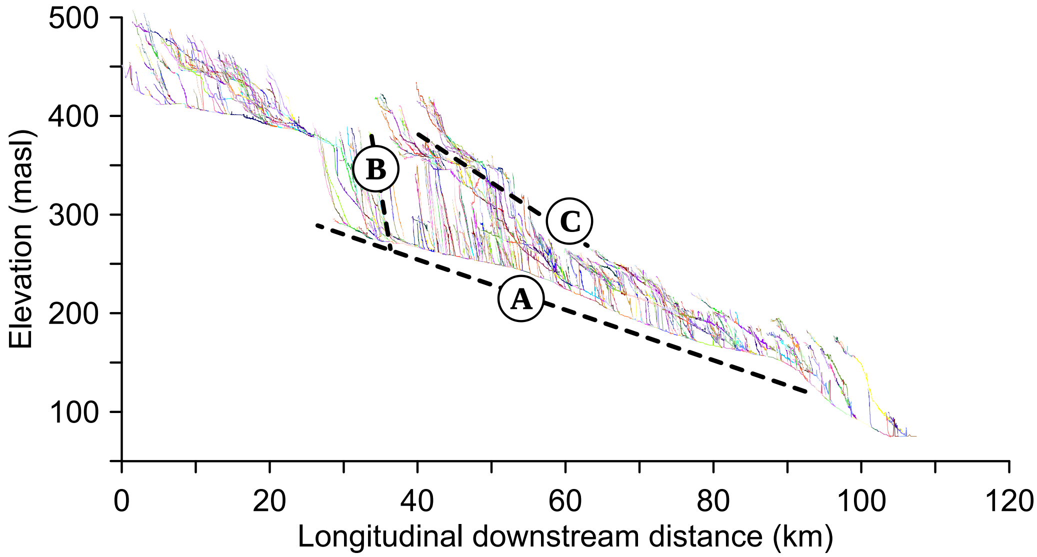

Figure 2.9: Longitudindinal profile of the Credit River hydrographic network. Dashed lines labelled A, B and C represent three characteristic bedslopes found along the Credit's flowpath. Colour scheme identifies individual reaches.

2.2.3 Flood damage centres

As a requirement to fulfilling the Phase III portion of this study, a list of 32 flood damage centres (FDC) and their locations have been provided by CVC (Figure 2.10). Within these FDC areas lie infrastructure and property of high value that has been or could be at risk from flood hazards. At these locations, determining flood risk will translate into a forecasted cost due to damage incurred from the flooding; and thus they will be used to valuate the ecosystem services of CRW wetlands and wetland complexes.

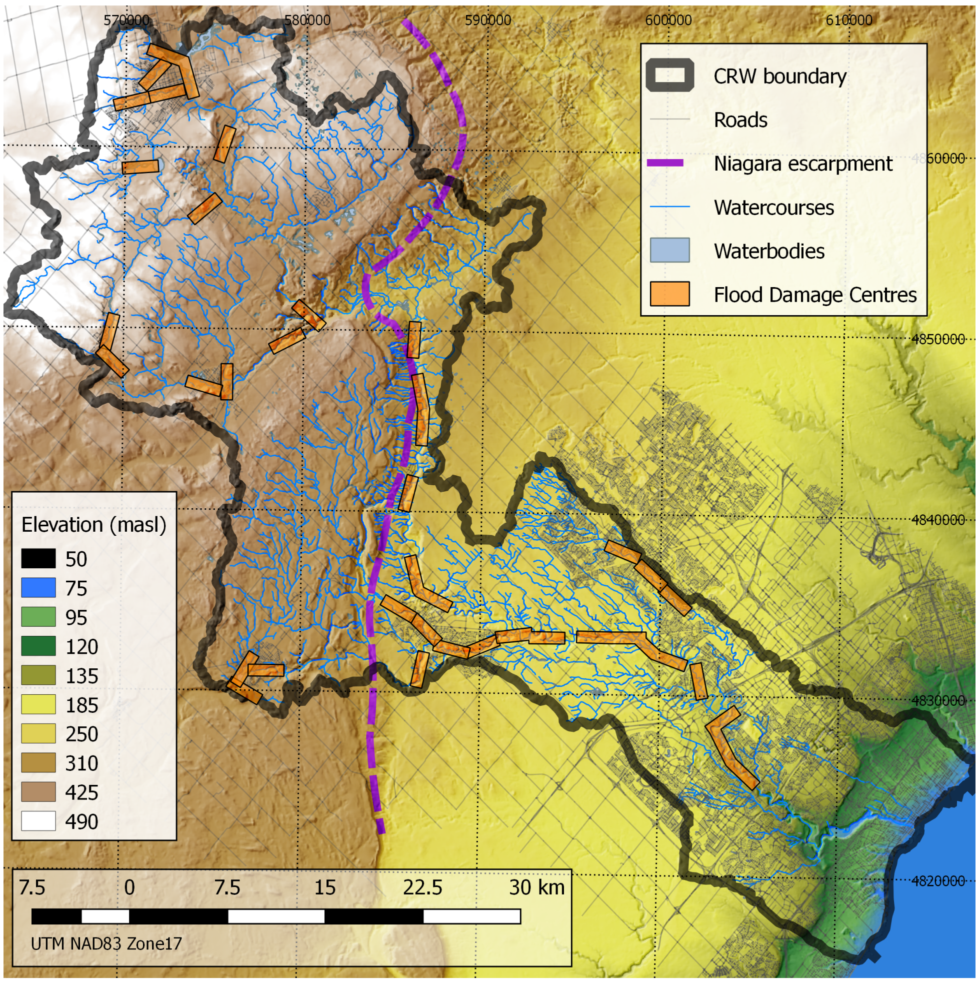

Figure 2.10: Location of flood damage centres within the CRW where focused hydrologic analysis will be conducted.

2.3 Hydrogeological conceptualization

The health and function of wetlands and cold-water streams within the CRW is dependent on a sustained water supply from the groundwater system (Richardson, 1956; CVC, 1994; CVC, 1998). In a subwatershed study conducted by the CVC (CVC et al., 1997), it was concluded that gaining a better understanding of groundwater-surface water interaction would be instrumental to managing the watershed's natural systems. However, understanding groundwater-surface water interactions requires an appreciation of the many physiographic and geologic features that characterize the CRW (CVC et al., 1997; AquaResource, 2009). Many residents within the CRW depend on groundwater for both private and municipal water supply and for the sustained baseflow needed for wastewater assimilation. In particular, the communities of Acton, Georgetown, Orangeville, Mono, Amaranth, Inglewood, Cheltenham, Alton, Erin, Hillsburgh and Caledon Village all rely on groundwater for their municipal water supplies (AquaResource, 2009).

Within southern Ontario, glacial activity has resulted in a complex arrangement of features including drumlinized till plains, moraines, glacial lakes and meltwater channels having been deposited over a network of bedrock valleys (CVC et al., 1997; Eyles, 2002; AquaResource, 2009). Combined with the Niagara Escarpment, the complex arrangement of glacial-derived sediment and bedrock valleys makes for a difficult characterization of the hydrogeological regime beneath the CRW. Fortunately, under the Source Water Protection program of the Clean Water Act (Ontario Ministry of the Environment, 2006) multiple groundwater models were built to assess groundwater flow and supplies in the CRW. One such model was a FEFLOW (Diersch, 2014) model covering the entire CRW that was constructed by AquaResource Inc. (2009) for Credit Valley Conservation. This model has served as the basis for understanding the subsurface flow regime of the CRW.[4]

Hydrogeology is the understanding of geology with an emphasis on how it affects the movement of groundwater. Within the CRW, from a water-movement perspective, glacial strata can broadly be classified into: aquifers—consisting of materials that tend to be highly permeable (e.g., sands and gravels) where water tends to move laterally; and aquitards—consisting of low-permeability materials (e.g., silts and clays) where water is typically restricted to vertical movement. Natural landscape features such as fens and headwater streams are typically located where aquifer materials daylight at surface and where there exists an upward hydraulic gradient. In such areas, groundwater is actively discharging to surface water features. When attempting to model such features, their interaction with the groundwater system must be realized, or else it would be left to the modeller to assume the features' function, biasing the very purpose of the modelling effort.

The following is an abridged description of the hydrogeological conceptualization as proposed by AquaResource (2009), relevant to the sustenance of CRW wetlands and cold-water streams. For a more-detailed review of the CRW geologic setting, the reader is referred to AquaResource (2009).

2.3.1 Physiography

The north-south trending Niagara Escarpment is characterized by steep slopes and significant rock outcrops with thin overburden. Prominent cliff faces are common along the escarpment edge. Groundwater discharge originating along the escarpment cliff face feeds numerous zero-order head water streams that, in areas north of Georgetown, flow directly into Credit River mainstem that flows parallel to the escarpment at its base.

[4] Details of the model to be discussed in §2.3.4.

The upper watershed lies west of the Niagara Escarpment. Found within this region are extensive till plains, moraines, and coarse-grained glacial spillways (AquaResource, 2009). Surficial geology in this area is characterized as having medium-high to high permeability materials (Chapman and Putnam, 1984). Portions of the CRW, especially in areas crossed by glacial moraines (i.e., the Horseshoe, Paris and Orangeville moraines) exhibit hummocky topography that limits overland flow from accessing drainage features (AquaResource, 2009) and provides potential locations for isolated wetlands. These moraine features have been recognized as being of hydrogeologic importance (AquaResource, 2009).

The lower watershed is a relatively flat landscape that slopes gently toward Lake Ontario. In this area below the escarpment, surficial soil permeability is typically low (Chapman and Putnam, 1984), however, localized pockets of sand and gravel exist in areas near the Credit River (AquaResource, 2009). The lower watershed is heavily urbanized and its drainage system is well engineered through a number of storm water management ponds and storm sewer networks. A small portion of the Oak Ridges Moraine covers the northern portions of the lower watershed and this area is also characterized as hummocky terrain composed of sand and gravels, thus supporting high localized groundwater recharge.

The physiographic regions found with the CRW identified by Chapman and Putnam (1984) and their formation are described in detail by AquaResource (2009). Of significant hydrological importance recognized by CVC et al. (1997) and AquaResource (2009), is the presence of various meltwater channels that formed as glacial ice lobes melted from the CRW area, depositing sorted mixtures of sand and gravel that can transmit large volumes of water below ground.

2.3.2 Bedrock geology

Bedrock geology beneath the CRW consists of a series of Paleozoic sedimentary rocks deposited some 400-500 million years before present. Some of the bedrock formations, particularly in the upper watershed and extending westwards into the Guelph area, have relatively high permeability making them highly productive groundwater sources. Like much of southern Ontario, paleo-fluvial erosion has left an array of bedrock valleys, some of which reflect the current-day Credit River drainage system. One bedrock valley essentially follows the mainstem of the Credit River. After the establishment of these valleys, glacial activity resulted in the deposition of materials into the bedrock valleys. Often the deposited materials were composed of coarser-grained sands and gravels, thus creating sub-surface regions of localized groundwater channelling.

2.3.3 Quaternary geology

Quaternary-aged sediments overlie the bedrock. These sediments were predominantly deposited during the most recent Wisconsinan glacial episode and comprise layers of varying composition (e.g., sands, silts, gravels, etc.). The thickness of the glacial sediment can exceed 75 m within the bedrock valleys and exceeds 100 m beneath the Oak Ridges Moraine. Many wetlands flank areas of thick overburden, especially around the Oak Ridges and Orangeville Moraines in the northern parts of the watershed. Given that these moraines are primarily composed of sands and gravels, a direct interaction between the moraines and adjacent groundwater-fed wetlands is expected.

Large parts of the upper watershed consist of the Orangeville and Paris Moraines composed of ice-contact stratified drift and/or glaciofluvial sands and gravels, all of which are relatively permeable. Topography on these moraines is rather hummocky, supporting many isolated wetlands and areas of concentrated recharge, which in turn support many headwater streams and riparian wetlands found along the flanks of the moraines (Figure 2.2).

The Halton Till overlies shale bedrock across the majority of the area in the lower watershed, east of the Escarpment. These low hydraulic conductivity materials provide a stark contrast to the high hydraulic conductivity overburden and bedrock units present west of the Escarpment in the upper watershed. The Chapman and Putnam (1984) mapping of surficial geology is presented in Figure 2.11.

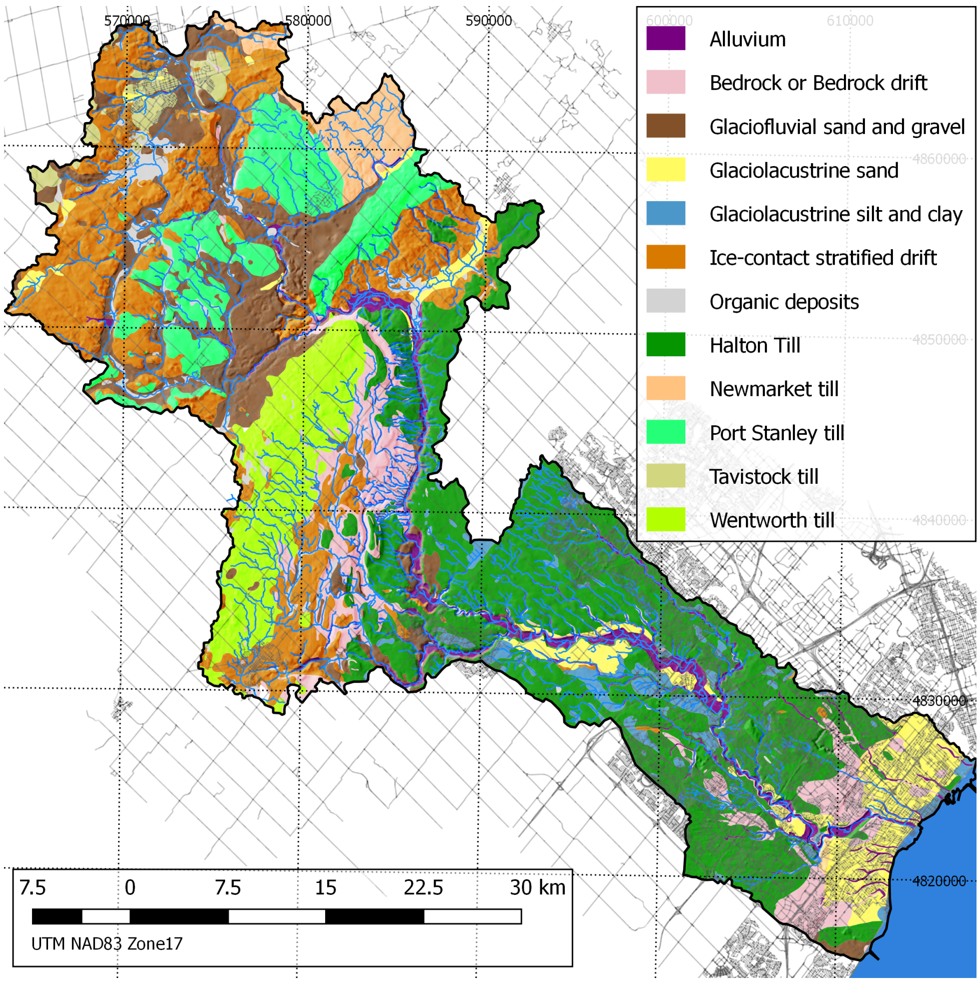

Figure 2.11: Quaternary geology of the CRW. (Modified from AquaResource, 2009.)

2.3.4 Hydrostratigraphy

It has long been recognized that the natural hydrologic systems (i.e., wetlands, headwater streams, etc.) within the CRW are inextricably linked with the groundwater system (Richardson, 1956; CVC, 1994; CVC et al., 1997; CVC, 1998; AquaResource, 2009). As discussed above, the scope of this project presumes dry antecedent conditions, which would imply that stream flow is entirely derived from groundwater sources. The project's focus is to investigate the flood mitigation capacity of thousands of wetlands that exist within the CRW. As recognized by Mitsch and Gosselink (2000), it is assumed that the proximity of these wetlands to nearby drainage features (i.e., streams) should play a role in flood mitigation. However, the ability of adjacent drainage features to route flood flows is also dependent on antecedent baseflow (Maltby and Acreman, 2011) and, in turn, on the locations along the channels where baseflow pick-up (i.e., groundwater discharge) is occurring. Identifying the occurrence of baseflow pick-up depends on an accurate conceptualization of the hydrostratigraphy, specifically the interaction between drainage features and shallow aquifers.

Based on the mapping of physiographic features, bedrock geology, glacial sediments, and high-order drainage features, AquaResource (2009) proposed an 11-layer conceptual hydrostratigraphic model that formed the basis for the model built for this study (Table 2.4). This conceptual model was incorporated into the 12-Layer Source Water protection Tier-2 FEFLOW model built by AquaResource (2009). The 10$^{\text{th}}$ layer representing the Queenston bedrock formation was split in two model layers due to its thickness below the upper watershed. A three-dimensional view of the Tier-2 FEFLOW model is given in Figure 2.12.

Table 2.4: Layering of the conceptual hydrostratigraphic model proposed by AquaResource (2009).

	Hydrostratigraphic unit	Zone	General lithology
1.	Surficial sediments	Overburden	as defined by Chapman and Putnam (1984), Figure 2.11
2.	Recent tills	Overburden	Halton, Wentworth, Newmarket till
3.	Upper aquifer	Overburden	Mackinaw Interstadial sediments
4.	Lower till aquitard	Overburden	Port Stanley, Tavistock, Northern till
5.	Intermediate aquifer	Overburden	Sand/gravel/Silt (Thorncliffe and Sunnybrook or Scarborough equivalent sediments)
6.	Weathered bedrock	Bedrock	Contact zone
7.	Guelph/Amabel aquifer	Bedrock	note: pinches out below escarpment
8.	Cabot Head aquitard	Bedrock	note: pinches out below escarpment
9.	Manitoulin/Whirlpool aquifer	Bedrock	note: pinches out below escarpment
10.	Queenston aquitard	Bedrock	Low conductance shale
11.	Georgian Bay aquitard	Bedrock	Low conductance shale an limestone

Capturing both the groundwater dependence of the wetland complexes and groundwater discharge to streams (and thus the flood mitigation capabilities of wetlands) requires the application of an integrated groundwater/surface water model (Thompson et. al., 2004; Erwin, 2009; Bradford, 2016). Such an integrated approach has been employed for this study. Details of the model development are discussed in §3.

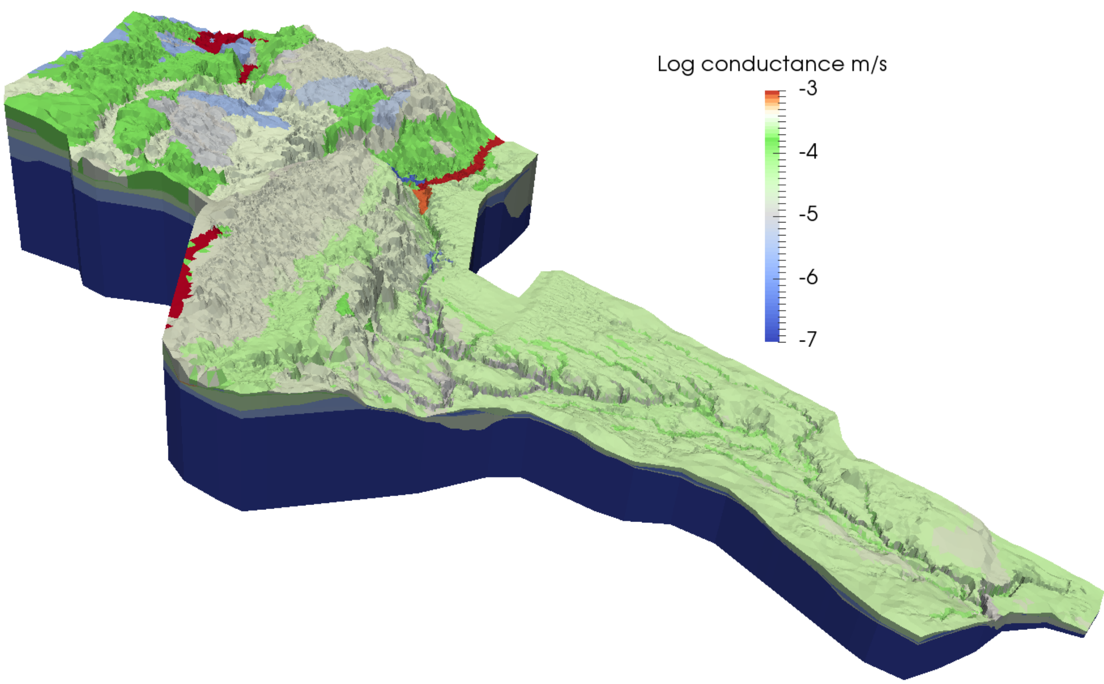

Figure 2.12: The three-dimensional hydrostratigraphic model proposed by AquaResource (2009). Model shown with a 10× vertical exaggeration.

2.4 Local hydrology and climatology

A total of 61 existing and historical Meteorological Service of Canada (MSC) climate stations (Figure 2.13) proximal to the study area were identified. Of the 61 stations, 54 reported daily rainfall amounts extending back to the year 1840, varying in terms of period of record and data quality. The number of reporting stations within the period of record is shown in Figure 2.14. This figure, shown in the form of a Gantt chart, illustrates how a number of stations were installed during the 1950s and 1960s culminating in almost 20 active stations reporting climate data during the 1970s. Since then, the number of active stations has been in steady decline.

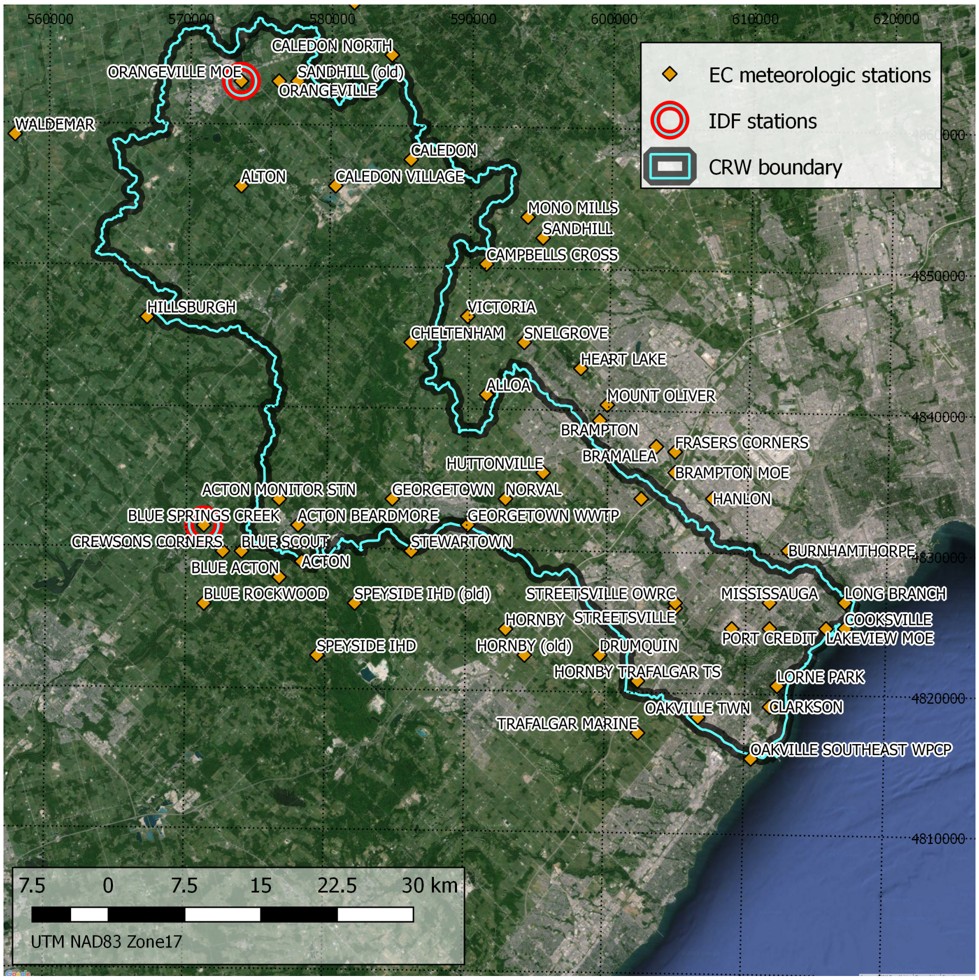

Figure 2.13: Location of climate stations in and around the CRW.

Two Environment Canada Intensity-Duration-Frequency (IDF) stations were identified next to the study area, namely, Orangeville MOE (6155790) and Blue Springs Creek (6140818) (circled red in Figure 2.13). Table 2.5 lists the 15 minute and 24 hour accumulations for a given return period.

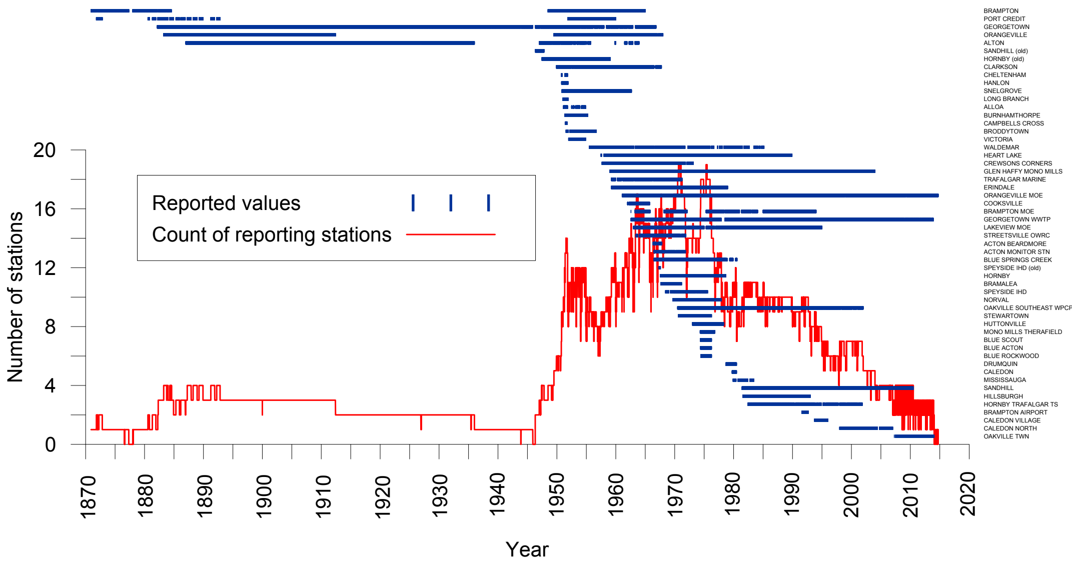

Figure 2.14: Period of record of rainfall at select Meteorological Service of Canada climate stations in and around the Credit River watershed. (Station names written on the right.)

There is a notable difference among these two proximal stations: the 2-yr return daily rainfall is reported to be either 40 mm and 55 mm per day, roughly a 30% deviation, albeit the IDF statistics built for these stations were derived from different time periods.

The requirement for high quality climate data is a necessity for numerical model development, as they drive the model to produce simulated floods. During model construction, the data are used to "calibrate" the model, generally by adjusting model parameters to adequately replicate measured stream flow discharge. However, a complication arises when attempting to calibrate to rare (i.e., extreme) events, in that, due to its rarity, data are hard to come by. Specifically, not only is high quality *rainfall* data required to model extreme events, but stream flow data measured during the same events (i.e., the *runoff response*) are also needed. When a numerical model is proposed to simulate this *rainfall-runoff response* phenomenon, as would be required to determine how wetlands function hydrologically, then all of the dependent data must be made available.

The rainfall-runoff response is dependent on a number of factors, primarily (i) the volume of rainfall, (ii) intensity of rainfall, (iii) location and extent of rainfall, and (iv) antecedent moisture conditions. Unfortunately, data commonly available in southern Ontario exclude information on the latter two (iii & iv), whereas (ii) is hard to come by—for example, of the many stations shown in Figure 2.13, most do not make available rainfall data measured at timescales less than a day. Consequently, should the model be calibrated, then only factor (i) must be relied upon.

Appendix B outlines the argument that rainfall volume alone is insufficient in describing the rainfall-runoff response within the CRW from a 2-year extreme precipitation event. Based on two rigorous statistical tests, it can only be concluded that the runoff-response to an extreme event

Table 2.5: Rainfall volumes (mm) of a given duration and return period observed in proximity to the CRW (ECCC, 2016).

Return Period (years)	Blue Springs Creek 15 min	24 hrs	Orangeville MOE 15 min	24 hrs
2	15.2	55.5	12.5	39.7
5	20.3	67.9	19.1	50.9
10	23.6	76.0	23.5	58.2
25	27.9	86.4	29.1	67.6
50	31.1	94.0	33.3	74.5
100	34.2	101.6	37.4	81.4

must be dependent on factors in addition to (i). Specifically, it cannot be demonstrated that peak flow response is correlated with rainfall amounts during a 2-year event. Consequently, this suggests that the data available do not contain the information required to calibrate a numerical model for the task at hand.

The same conclusion was demonstrated for 5-year return events; however, as longer return periods require longer datasets, it becomes impossible to assemble a sample size large enough to perform an informative statistical test.

To provide a more qualitative demonstration of this argument, consider the set of hydrographs observed at the 02HB008–Credit River West Branch at Norval gauge in response to the selection of 15 2-year return events occurring within a 30-year period (Figure 2.15). This figure overlays a set of stream flow hydrographs resulting from those events, colour-coded (cold to hot) according to the total daily volumes of precipitation that ranged from 35 to 54 mm. It is clear from these hydrographs that a 2-year precipitation event can manifest itself in a variety of stream flow hydrographs. Most notably is the occurrence of the most intense (by volume) rainfall events resulting in the lowest (peak) runoff response.

While this conclusion may appear counter-intuitive, the statistical testing suggests that the rainfall-runoff response to extreme rainfall events in the CRW has a greater dependence on antecedent moisture conditions (see Appendix B). Antecedent moisture conditions essentially describes the moisture state of the watershed prior to a precipitation event. Water can collect within surficial depressions and the pore spaces of the soil zone and can remain collected on vegetation from precipitation intercepted from past events. A high antecedent moisture state will equate to higher water levels in wetlands and relatively greater baseline stream flow (i.e., baseflow). With high antecedent moisture conditions, oncoming precipitation has fewer places to be retained and thus has no other option then to become runoff, resulting in increased peak flow volumes.

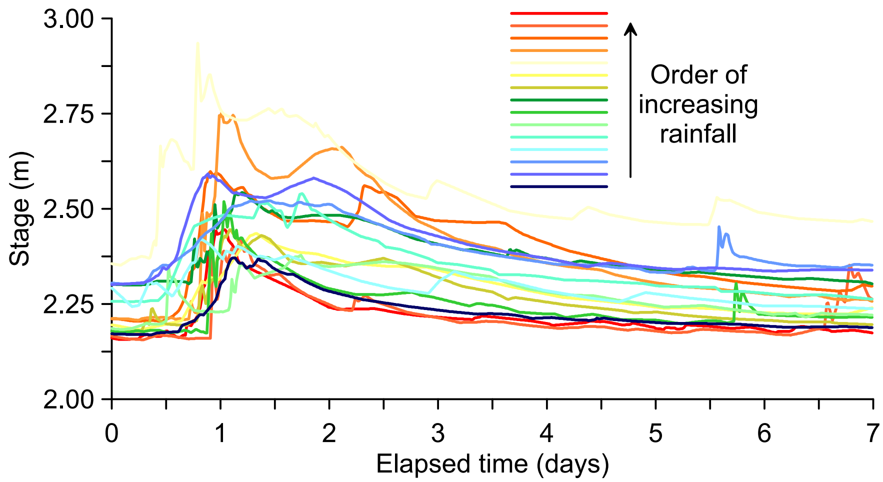

Figure 2.15: Set of 2-yr rainfall event response hydrographs illustrating the independence of rainfall volume to peak runoff.

2.5 Summary

On the basis of the discussion above, a number of model design constraints have been imposed. These constraints were incorporated into the model design plan for this study (§3), including:

Antecedent conditions. From the analysis of §2.4 and Appendix B, it was demonstrated that the antecedent moisture conditions of the watershed play a significant role in watershed rainfall-runoff response since correlation cannot be demonstrated between higher-magnitude rainfall events and peak stream flow. Consequently, as highlighted by Stephenson and Freeze (1974), determining initial watershed moisture states prior to simulating a rainfall event is not practically possible. In response, the model implementation plan will have to rely on a hypothetical initial state, a state kept consistent for all model runs. For a comparative study such as this, a consistent initial state eliminates structural bias associated with the high dependence between antecedent conditions and watershed response.

The influence of groundwater. Based on observations made from many watershed studies conducted in the CRW (Richardson, 1956; CVC, 1994; CVC et. al., 1997; AquaResource, 2009; CVC, 1998) and evidenced by the number of wetlands situated in close proximity to headwater streams and flanking the CRW's moraines (§2.3.3), there is little doubt that many of the wetlands being modelled are groundwater-connected. The depth of the groundwater table will play a factor in wetland capacity and initial moisture states and thus must be included in model-code selection and model design.

A high-resolution distributed modelling approach. The hydrological phase (II) of this study demands the incorporation of thousands of wetlands, thousands of kilometres of drainage features, a diverse and fragmented land use cover, a distinct physiography and 32 identified basin-wide flood damage centres. When coupled with the fact that extreme events observed in southern Ontario are of the convective type, defined as small-scale and isolated, the detailed spatial resolution required must also constrain the model-code selection and model design. Antecedent conditions within the CRW also appear to be location dependent, meaning that distinct locations within the CRW can be dry while other locations remain relatively wet (see Appendix B), and thus careful consideration must be taken when determining distributed initial conditions.

The simulated extreme event must also be distributed. According to the instantaneous hydrographs investigated, it is apparent that watershed response to extreme (>1.5-year return) events are characteristically non-similar and may depend, among other things, on rainfall distribution. Considering that the scope of the project is to compare watershed response to a variety of storm intensities, a set of climatic forcings having similar storm dynamics (i.e., scale, extent, orientation, location, velocity, and directionality) would need to be obtained. Given the rarity of the extreme events that are intended to be modelled (i.e., 2- through >100-year return events), acquiring a set of "similar" storm dynamics for each of these intensities is highly unlikely.

The modelling strategy cannot rely on traditional calibration schemes. As a follow-up to the previous points, the data that are available in the CRW are inadequate on their own to yield the information required for calibration. The rainfall-runoff response in the CRW is apparently dependent on certain information (e.g., storm distribution and antecedent conditions) that is simply unobtainable with the currently available data. A solution to this issue is presented in §3.3.

An alternate model evaluation approach is required. By establishing a scaled normalized climate forcing field and a constant initial state, an unbiased (with respect to boundary conditions) multi-model ensemble modelling approach (Matott et. al., 2009) must be pursued that will deliver a probabilistic means of quantifying wetland flood mitigation capacity to meet the requirements set in the project scope (§1.2). Such an approach may even prove to be more-amendable to a risk/actuarial analysis as planned in Phase III of this study (§1.1). More to be discussed below.

Section 3

Methodology

In §1.2, the scope of this modelling study was carefully defined such that the modelling approach remains constrained to within specific parameters. Firstly, implied in the scope is the requirement for the model to be event-based, meaning that the model needs to run at short temporal scales, neglecting the need for long-term hydrological simulation. The advantage of event-based modelling is that certain hydrologic processes (e.g., evapotranspiration) need not be modelled because their importance to the hydrologic cycle only emerges at larger (i.e., seasonal) time scales.

Secondly, as discussed below (§3.2.5), since the proposed study exists within southern Ontario, Canada, an "extreme" rainfall event implies a convective-type storm, which has a number of compounding implications on model design. One such implication is that southern Ontario convective-type storms typically occur in the late-summer (July–August–September), which coincides with a seasonally suppressed watertable and relatively dry conditions. The late summer condition also demands that terrestrial vegetation be at a late growth stage. This is important since vegetation itself can retard flood movement through its surface roughness (i.e., friction), which increases with vegetation density (Chow, 1959).

The study scope, coupled with previous research, and the CRW-specific modelling requirements, have also imposed a set of conditions for model selection (§3.1). These conditions include: process-based distributed modelling, adequate (sub-daily) time scales, and subsurface (i.e., groundwater, vadose zone) flow representation.

Process-based modelling approaches to simulate natural phenomena based on established physical theory. In the case of this hydrological study, the advantage is that as the proposed model simulates the movement of water over the landscape, physical principles such as the conservation of mass and momentum are not only obeyed, but form the basis of the mathematics used within the model. For example, when studying the dynamics of water movement along a stream network, hydraulic routing processes (i.e., depth and momentum) must be calculated using physical theory in order to obtain a realistic grasp of flood wave extent, magnitude, duration and timing (Ogawa and Male, 1986). This is critical where scientific defensibility is considered vital to the modelling process. Process-based modelling can also relieve the modeller from having to make too many assumptions about the processes themselves. The disadvantage to implementing processes at the physical level is that it tends to be rather expensive, in terms of computational time and resources.

Fully distributed modelling is the requirement to have physical processes simulated at multiple locations in space and time. This is critical for the proposed study as water moving downslope over the land surface must interact with any feature it may come in contact with, prior to entering, say, a stream channel. In many traditional models, for the sake of parsimony, overland flow is not explicitly represented. Rather, simplified mechanisms like transfer functions (Jakeman and Hornberger, 1993) are employed to delay runoff generated on the landscape from entering adjoining streams.

An objective of this study is to investigate the role of isolated wetlands and the cumulative role multiple isolated wetlands have on flood mitigation, which is not fully understood. With thousands of isolated wetlands distributed unevenly across the CRW, a distributed modelling approach is needed. Wetlands in their natural state come in many shapes and sizes. Distributed modelling is thus required to incorporate the impacts of wetland size, distribution and proximity to other features explicitly into the model design.

Sub-daily timescales are required simply because extreme rainfall events in southern Ontario tend to be isolated, of short-duration, fast-moving and locally intense (Weisman and Klemp, 1982). Not only does this further the need for a distributed approach, but it also requires a model that can simulate hydrologic processes at very fine (seconds to minutes) timescales. Rainfall rate, extent, distribution and velocity that define a southern Ontario extreme event can only be achieved by employing short timescales combined with a high spatial resolution.

Antecedent conditions appear to be the principal component to watershed rainfall-runoff response within the CRW. Given the connectedness of the wetlands in the study area to the groundwater system, the model must incorporate subsurface processes in order to quantify initial moisture conditions (Bradford, 2016). Water movement in the unsaturated zone and the depth to the watertable will dictate the CRW's overall flood retention capacity and thus it is essential that they be explicitly simulated. Without doing so, the initial capacity of the watershed has to be prespecified by the modeller, which undoubtedly adds bias to the model results.

In §1, it was identified that there is a need for the development of a practical approach to investigate wetland flood mitigation capacity. In pursuing this, a number of novel approaches were found necessary. In part this report, and specifically this section, will serve as the benchmark modelling approach to address wetland flood mitigation capacity at the watershed scale. The remainder of this section presents in detail the processes taken to achieve the results to ensure reproducibility. The details presented below are quite technical and can be safely skipped by the non-modeller.

3.1 Model selection

A total of eleven model codes were selected as potential solutions to address the model scope (§1.2). Many of the selected models are codes that are commonly used in watershed-scale hydrology in Ontario. Many were purpose-built for specific applications, and most have features that others do not. In no way is this an endorsement for any particular model, nor will the selection made here be universally applicable; rather, the model selected is best suited for the problem at hand in the CRW study area. The models considered include:

- **SWAT:** The Soil and Water Assessment Tool (`http://swat.tamu.edu/`) is a watershed-scale model built by the USDA. The model is free to use and was designed to use readily available data for application in ungauged basins. SWAT is a continuous long-term model, not intended to be used for single-event catchment routing. SWAT has the capability to model many water quality processes, such as nutrient loading, bacteria transport, sediment transport, etc.

- **HSP-F:** The Hydrological Simulation Program FORTRAN was developed under the USEPA to simulate hydrologic and water quality processes and was originally based on the Stanford Watershed Model (https://www.epa.gov/exposure-assessment-models/basins). Although freely available, the HSP-F code is proprietary and is managed by a third party. The model has the capability to run either continuous (i.e., long-term), event-based, or steady-state simulations. Water quality simulation includes point and non-point source pollution analyses; fate, transport, and exposure assessment; control of pesticides, nutrients, and toxic substances, etc. For more details, see Donigian et. al.(1995).

- **PRMS:** The Precipitation Runoff Modeling System is a hydrological model freely available from the USGS (http://wwwbrr.cr.usgs.gov/projects/SW_MoWS/PRMS.html). The original intent of PRMS was for application as a catchment-based semi-distributed model; however, PRMS can employ a cascading routing scheme that allows the user to pre-define flow pathways. While the cascade allows for processes to be spatially-dependent, the lateral translation of overland flow does not consider momentum nor compute back-water effects, it solely considers topological routing (Markstrom et. al., 2015).

- **HBV:** is a catchment-based model that has a long history of application all over the world. The model is highly simplified and thus optimized for quick computation at the expense of explicit process representation. The model is well described in Bergström (1995) and is freely available at http://www.geo.uzh.ch/en/units/h2k/services/hbv-model/.

- **HEC-HMS:** The Hydrologic Engineering Center Hydrologic Modeling System is a watershed-scale hydrologic modelling suite offered by the US Army Corps of Engineers (http://www.hec.usace.army.mil/software/hec-hms/). The model is better suited for event-based channel flow routing but can be used for continuous/long-term applications. The advantages of HEC-HMS is that it is packaged with an intuitive user interface, has some sediment and water quality simulations capabilities, and can be used as a real-time flood forecasting tool.

- **GAWSER:** The Guelph All-Weather Sequential Events Runoff model is a proprietary watershed based model purpose built for southern Ontario basins where snowmelt hydrology is of importance. Although the model has been employed in many southern Ontario watersheds (http://www.schroeter-associates.com/testweb2_002.htm), documentation and access to the model is limited. The model can be used for water quality purposes and flood forecasting.

- **GSFLOW:** The coupled Groundwater and Surface-water Flow model that is an integration of PRMS and MODFLOW: a modular groundwater flow model offered for by the USGS (http://water.usgs.gov/ogw/gsflow/). MODFLOW has a long history of application and is arguably the most-applied groundwater flow model. Combined with PRMS, GSFLOW provides excellent utility for long-term water balance analysis using this free, open-source and frequently updated tool. Complete description of the model can be found in Markstrom et. al.(2008).

- **SWAT-MODFLOW:** is an integrated hydrological model that couples SWAT land surface processes with MODFLOW. This version of SWAT has few documented applications (see http://swat.tamu.edu/software/swat-modflow/).
- **MIKE SHE:** is an integrated, process-based, fully distributed groundwater/surface water model offered by the DHI group (https://www.mikepoweredbydhi.com/products/mike-she). The model originates from the Système Hydrologique Européen (SHE) and has been vastly improved. The model comes coupled with MIKE 11, a fully-dynamic channel flow routing scheme. MIKE SHE is built using MIKE Zero, DHI's model construction suite. Further details can be found in Refsgaard and Storm (1995).
- **PARFLOW:** is an integrated, process-based, fully distributed groundwater/surface water model that is open-source and is optimized by use of parallel numerical solution schemes. PARFLOW is offered by the The Integrated GroundWater Modeling Center (IGWMC) at the Colorado School of Mines (Maxwell et. al., 2016). The model is rather simplified in that flow pathways are dictated solely by a digital elevation model; there is no way to add stream channels as linear features. As such, the model is best suited for very large-scale applications covering multiple watersheds at the continental scale.
- **HydroGeoSphere:** is a three-dimensional control-volume finite element integrated groundwater/surface water model distributed by Aquanty Inc. (https://www.aquanty.com/). The design of HydroGeoSphere incorporates physics-based formulations for many processes, including unsaturated flow processes in three dimensions, soil freeze and thaw, diffusive-wave overland flow, simulation of non-reactive and reactive chemical species transport, etc.

On the basis of the modelling criteria discussed above (fully distributed, process-based, groundwater integration, sub-daily timesteps), only three of the eleven models were deemed acceptable to address the flood mitigation potential of CRW wetlands, namely PARFLOW, MIKE SHE and HydroGeoSphere (see Table 3.1 for comparison).

Both a GAWSER (Schroeter and Associates, 2001) and an HSP-F (AquaResource, 2009) model have been built for the CRW. These models are semi-distributed, being subdivided into 186 and 216 sub-watersheds, respectively. These models were built for rainfall-runoff simulation and groundwater recharge estimation and thus do not take explicit account for wetland function and distribution. Given that a significant proportion of wetlands would have to be neglected (i.e., sub-watershed area averages 45 ha, compare that with Figure 2.6) and that groundwater interaction cannot be accounted for, these models are not suited to address the study scope (§1.2).

With respect to overland flow processes, the differences between the three potential model selections (e.g., PARFLOW, MIKE SHE and HydroGeoSphere) are subtle. The advantage of HydroGeoSphere is that a flexible mesh can be employed, whereas both PARFLOW and MIKE SHE use a grid-based (finite-difference) modelling scheme (Figure 3.1). The difference being that with a grid, cell sizes must remain constant in space, whereas the advantage of the flexible mesh is that the model design can be built such that the majority of its computation time is devoted to specific areas of concern; in this case, wetlands and drainage features. This leaves other areas of lesser concern from over-representation.

For example, using a grid-based approach, the modeller must decide on a representative resolution, which is a balance between model area (roughly 950 km^2 for the CRW) and the maximum number of computational elements (grids), say 100,000. This would restrict cell sizes to 100 m a side, meaning wetlands less than 1 ha in size could not be represented in the model. According to

Table 3.1: Model selection matrix (only the final three met all requirements).

Model	Process based[a]	Distributed[b]	TimeScale[c]	Groundwater integration
SWAT	✗	semi	sub-daily	✗
HSP-F	✗	semi	sub-daily	✗
PRMS	no momentum	semi/full	daily	✗
HBV	✗	✗	daily	✗
HEC-HMS	✗	semi	sub-daily	✗
GAWSER	✗	semi	sub-daily	✗
GSFLOW	no momentum	full	daily	✓
SWAT-MODFLOW	no momentum	semi	sub-daily	✓
PARFLOW	✓	full	variable	✓
MIKE SHE	✓	full	variable	✓
HydroGeoSphere	✓	full	variable	✓

[a] only considering overland processes here.
[b] *full*: forcings and processes are distributed; *semi*: only forcings are distributed, processes are left independent.
[c] *variable* indicates that there is no fixed time step, but it is implied that the timescale can be reduced to the seconds/minutes scale.

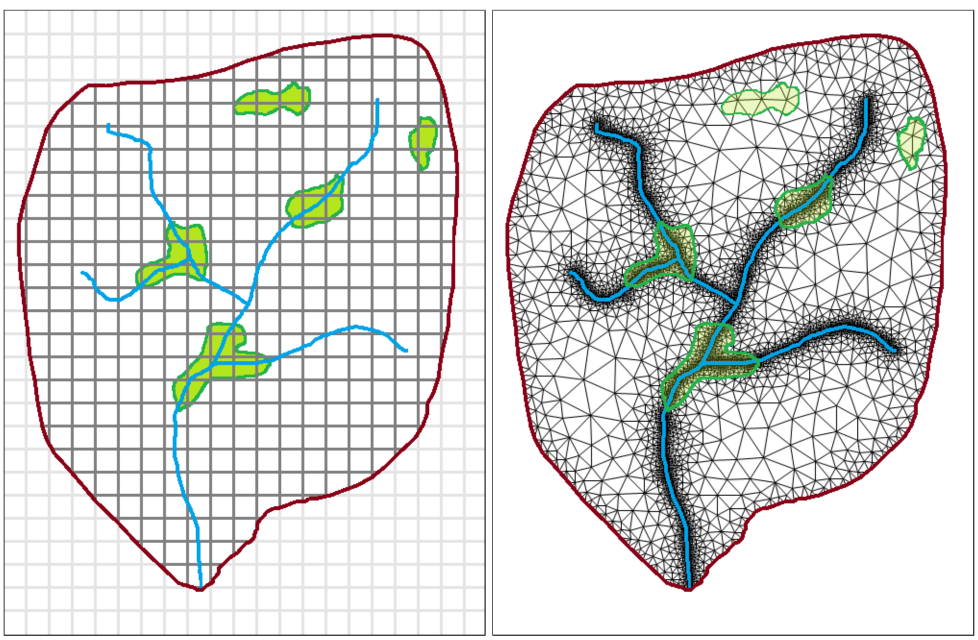

Figure 3.1: Illustrative samples of distributed modelling using grids (left) and flexible meshes (right).

Figure 2.6, this would prevent 46% of all CRW wetlands from being modelled. This restriction does not apply for a flexible mesh, where no size is, in a practical sense, too small and potentially all wetlands can be included.

As discussed in detail below, a flexible mesh was constructed with roughly 83,000 computational elements (i.e., finite-element nodes). This mesh design ensured that at least 1 computational element existed in every wetland, and 100s of nodes for wetlands exceeding 10 ha (Figure 2.6). Given its ability to gain a 27% improvement in model efficiency (in terms of the number of computational elements required—83,000 vs. 100,000) while ensuring all wetlands and drainage features remain represented in the model, the model selection ultimately went to the sole flexible mesh model: HydroGeoSphere by Aquanty Inc. A technical discussion of the mathematical theory of HydroGeoSphere and its outputs is given in Appendix C.

3.2 Model development

Two model builds were developed to accomplish this model study:

1. **Model A:** a quasi-steady state model to establish antecedent/initial and boundary conditions for

2. **Model B:** a shallow/reduced-layer transient model built for model parameter estimation and scenario analysis.

Model A incorporated the complete (12-layer) hydrostratigraphic interpretation (down to bedrock) of the CVC Tier-2 FEFLOW model (§2.3.4) re-sampled to the refined mesh (discussed below in §3.2.1) with the upper surface constrained by the digital elevation model discussed in §2.1. Based on its current and peer reviewed interpretation of regional geology, Model A's purpose was to define the shallow subsurface flow potentials, which established both the initial/antecedent conditions and the vertical flux boundary conditions for the bottom face of Model B.

Model B is a refinement of Model A where the deeper layers were removed to increase model efficiency (i.e., reduced run-times). Model B was used to determine model parameterization and was applied for all subsequent analysis reported in the results of this study. Model B utilized the same mesh and DEM constraints as Model A. The subsurface hydrostratigraphic representation was reduced to a 5-layer 3 m thick shallow soil-zone model. As the transient model runs were set to no longer than 5 days, it was assumed that changes to deep subsurface hydraulic potentials would be negligible. From this, the upper hydraulic potential of Model A served as the lower vertical flux boundary condition of Model B; thus providing the influence of the deeper groundwater system without explicitly modelling it.

In this section, the construction of the HydroGeoSphere models A and B is discussed. The following section (§3.3) discusses how the constructed model was prepared for scenario simulation to analyze wetland function (§3.4).

There are three main components that need consideration during model development: model structure, initial conditions, and boundary conditions. Model structure represents the physical dimensions and properties of the system being modelled and will generally remain constant throughout every model simulation. Initial conditions defines the antecedent state from which the simulation is to begin from and will differ here, for example, depending on the season from which the modeller wishes to assess wetland performance. (For the sake of this study, only late summer conditions are considered and thus only one initial condition was established.) Boundary conditions tend to change over the course of a model simulation (although they can remain constant) and are used to stress the model in order to observe its behaviour.

Below a brief description of the data requirements for the three components, and greater detail as to how the data were utilized is described in the subsections to follow. These subsections are intended for a technical audience and can be safely skipped by most readers to the following section (§3.3).

Model structure. Much of the datasets needed to define model structure has been discussed above: the digital elevation model and Lake Ontario bathymetry (§2.1); Land use (§2.2); wetlands, water courses and water body mapping (§2.2.1 and §2.2.2); and hydrostratigraphy (§2.3.4). What has yet to be discussed is how these data were employed to constrain the development of the flexible mesh (§3.2.1). To summarize, the developed mesh contained over 83,000 computational nodes that each, independently, calculate a hydrological water balance. Thousands of computations nodes have been preferentially placed within every CRW wetland and water body, along all mapped CRW drainage (i.e., stream) channels and within every flood damage centre (§2.2.3). A detailed image of the final mesh design can be found in Figure 3.2.

Initial conditions specify the antecedent moisture state of the model prior to applying storms. Model A's sole purpose was to determine the initial state for Model B. The initial state of Model A was full saturation, and was allowed to drain until the models baseflow discharge matched measured baseflow from eight stream gauge locations (see §3.2.4). Model A's results were then used to inform Model B—that is, to establish a late-summer antecedent moisture state driven by data and not prescribed by the modeller (for more discussion, see Appendix F).

Boundary conditions specify the flux of water entering or leaving the model domain throughout a model run. With the exception of the flux boundary conditions for the top of the model domains, the specified boundary conditions were kept constant for both model builds. Both Model A and B required the specification of five boundary conditions:

1. Constant head boundary at Lake Ontario—Model mesh perimeter nodes that lie within Lake Ontario were assigned a constant head of 74.8 masl, the long-term mean Lake Ontario water level.[1]

2. Flux/head boundary condition at the bottom of the model domain—For Model A, the bottom faces of the bottom layer were set to a zero-flux boundary. For Model B, the base of the model was set to the final potentials defined by the output of Model A, to be discussed further in §3.2.4.

3. Flux boundary condition at the top of the model domain—The top boundary condition of the model domain is essentially the precipitation the model is to receive. For Model A, this was set to a steady (i.e., constant) value of 134 mm/year, equivalent to the rate of late summer baseflow (see §3.2.4 for more details). For the Model B simulations that are ultimately used for the wetland flood mitigation analysis, a high-resolution distributed rainfall event was applied (§3.2.5).

[1] https://www.ec.gc.ca/eau-water/default.asp?lang=En&n=79962112-1

4. Flux boundary condition along the perimeter of the subsurface model domain—Vertical faces of subsurface model elements not lying within Lake Ontario were set to a zero-flux boundary condition.

5. Flux boundary condition along the perimeter of the overland flow model domain—the perimeter edges of the model's top surface was assigned a critical depth boundary condition for overland flow (see Aquanty, 2016).

3.2.1 Mesh generation

The model was built using a three-dimensional prismatic finite-element mesh constrained by the location of drainage features and wetlands, significant elevation changes such as the Niagara Escarpment and the Credit River valley, and the conceptual hydrostratigraphic model. The first three spatial constraints were used in the development of the finite-element mesh, while the hydrostratigraphic model was used to define the vertical stratification representing the interpolated geologic model described in §2.3.

Finite-element mesh

The lateral finite-element mesh (FEM) was constructed using AlgoMesh.[2] AlgoMesh is mesh building program that combines the common Delaunay refinement approach (Cheng et. al., 2012) with a comprehensive, multi-level optimization algorithm that incorporates Delaunay-based point insertion with a weighted Lloyd smoothing technique (Tournois et. al., 2008). The combination of these methods allows for the construction of a mesh of higher quality than what would be achieved by the Delaunay refinement approach alone (Merrick and Merrick, 2015). AlgoMesh creates a mesh that is robust and optimized resulting in an efficient model design having faster solver convergence and thus reduced simulation runtimes.

Processing of the mapped features used to constrain the FEM was required to prevent mesh over-refinement, while at the same time maintaining their influence on mesh design. Over-refinement occurs when points used in constraining the mesh are in unnecessarily close proximity or when two linear features intersect at sharp angles. The consequence of an over-refined mesh is that the model will be built with an excess of elements thus significantly increasing simulation runtimes. By simplifying the geometry of features used to constrain the mesh, a more efficient model was developed.

In the case of this study, "FEM constraining" refers specifically to the placement of FEM nodes. At the model's top surface, nodes are the locations where surface water depth is computed. Much of the purpose of this study is to account for water storage within wetlands and the routing of floods, therefore it is imperative that nodes be located within the wetland bounds and stream channels.

The procedures taken to ensure efficient model performance, while ensuring that every wetland, water body and low-order stream was represented in the model, are described below.

Drainage feature constraint

All 1,370 km of drainage features (i.e., streams, rivers, and some road side ditches) mapped within the CRW (§2.2.2) were used in constraining the FEM. In order to prevent over-constraining mesh

[2] version 1.0.6 developed by HydroAlgorithmics

geometry, simplification to the mapped stream geometry and drainage network had to be accomplished. In common practice, modellers traditionally reduce constraints imposed by the drainage network by simply neglecting low-order streams; for example, AquaResource (2009) constrained their CRW model to streams of Strahler order-2 and above, effectively eliminating the influence of 46% of the mapped drainage network (Table 2.3).

It must be acknowledged that the incorporation of a full drainage system is context-specific; in the case of this study, as discussed above, full drainage is necessary as many wetlands are connected to head water reaches and their hydrological influence would be altered if their connectivity to the drainage network were removed, effectively making them isolated wetlands.[3]

Simplification of the drainage network was accomplished by two means: (i) simplification of line geometry; and (ii) manual adjustment of channel confluence angles. For the entire length of every polyline used to represent a reach, the polylines were transformed into a continuous function using a standard cardinal spline interpolation technique with a tension[4] of 0.5. Points along the continuous spline spaced every 250 m were then selected as new vertices for the reach, significantly simplifying the channel geometry. In cases where the reach length was not divisible by 250 m, the vertex separation length was increased from 250 m until the simplified reach was divided into equal segment lengths.

Based on a trial mesh generation run using AlgoMesh, the generated FEM was inspected for areas where small confluence angles were over-constraining the mesh. These angles where adjusted manually to correct the over-constraint while maintaining the locality of the mapped drainage feature. In an iterative fashion, the mesh was re-generated and manual adjustment proceeded again until a satisfactory mesh was obtained based on the mesh quality reported below.

Wetland constraint

The challenge in accomplishing a mesh design for this study was the representation of wetland features. As shown in Figure 2.6, roughly half of the mapped CRW wetlands are less than 1 ha in size. Also, many of the wetlands form complicated shapes as many are physiographically constrained, and the mesh design must ensure that most (if not every) wetland be incorporated (i.e., represented by a mesh node).

Appendix D outlines a method devised by the author to overcome the complication of constraining the mesh design to include all CRW wetlands. The method adopts a topological shape recognition methodology that ensured at least one computational node existed within every mapped wetland. As wetland size increased, the number of nodes contained within the wetland perimeter increased (Figure 2.6). The methodology was also applied to every mapped water body, simply to ensure that any physiographic feature that resembles a depression on the landscape was accounted for in the model.

In total, the final model boundary included 3,679 of the 4,063 mapped CRW wetlands; many wetlands were remove either because they existed outside of, or intersected the model bound. It is important to note that the shape recognition methodology outlined in Appendix D is independent of whether the wetlands were merged according to the discussion of §2.2.1.

[3] An isolated wetland is defined as a wetland that is not connected to any observable drainage feature and thus has no outlet point (McLaughlin and Cohen, 2013; Bradford, 2015).

[4] Tension is a parameter to the cardinal spline technique.

Mesh quality

Once the constraints were set for wetlands, water bodies, drainage features and the model boundary, the AlgoMesh optimization routine was run to produce a high-quality finite element mesh. The final mesh (Figure 3.2) consisted of 164,781 finite elements consisting of 82,668 nodes. The longest elemental edge length was 946.0 m and the smallest element area was 19.2 m^2. Considering the number of constraints imposed on the model mesh design, AlgoMesh produced a mesh of exceptional quality. Appendix E details final mesh quality.

Achieving a high-quality mesh is paramount to reducing simulation runtimes. Considering the requirements for this modelling study, the approaches taken has assured that the model mesh has been optimized.

3.2.2 Nodal elevation mapping

With the generated mesh built, elevations occurring at each node had to be determined. For the first pass, nodal elevations were set to the digital elevation model discussed in §2.1. The majority of nodal elevations will remain equivalent to the DEM. However, to ensure channel-flow directionality, the stream vertices were re-assigned elevations based on the minimum elevation found within a 100 m radius from the stream vertices. The minimum radius procedure was employed for two reasons:

1. Mapped channel centrelines and the location of the channel as apparent on the DEM were not always coincident. In general, alluvial channels in equilibrium will naturally migrate within their meander belts (Julien, 2002). Significant migration can occur at and above bankfull flow, which is likely to recur every 1.5–2.2 years for CRW streams outside of urbanized areas (Annable, 1996). Therefore, it is reasonable to expect that the mapping of the channels and the measurement of the DEM occurred at different times, hence the discrepancy.

2. The DEM used is not hydrologically corrected, meaning that bridges and over-crossings will unrealistically become obstacles to flow if not accounted for. The selection of a 100 m radius was found to adequately remove any influence of these artifacts.

The last round of drainage feature pre-processing (designed by the author) involved the forcing of the channel's nodes[5] to become downward-sloping along the principle flow direction. This process began at the Credit River mainstem mouth and proceeded topologically upstream to every headwater reach, ensuring that each subsequent node is higher than the next.

For wetlands, nodes located within mapped wetland boundaries were assigned an elevation based on the lowest elevation found within a 50 m buffer of the node, to ensure that wetland bathymetry were kept true by avoiding potential DEM artifacts.

3.2.3 Hydrostratigraphic design

Hydrostratigraphic sub-layering for Model A was accomplished by intersecting the nodal locations of the generated FEM (§3.2.1) with the FEM of the AquaResource (2009) FEFLOW model (§2.3.4). With the exception of the model's top surface, layer elevations of the 12-layer AquaResource (2009) model were interpolated to the generated FEM node locations. Elemental properties from the

[5]Note that multiple channel nodes commonly exist between stream vertices originally spaced at 250 m (§3.2.1).

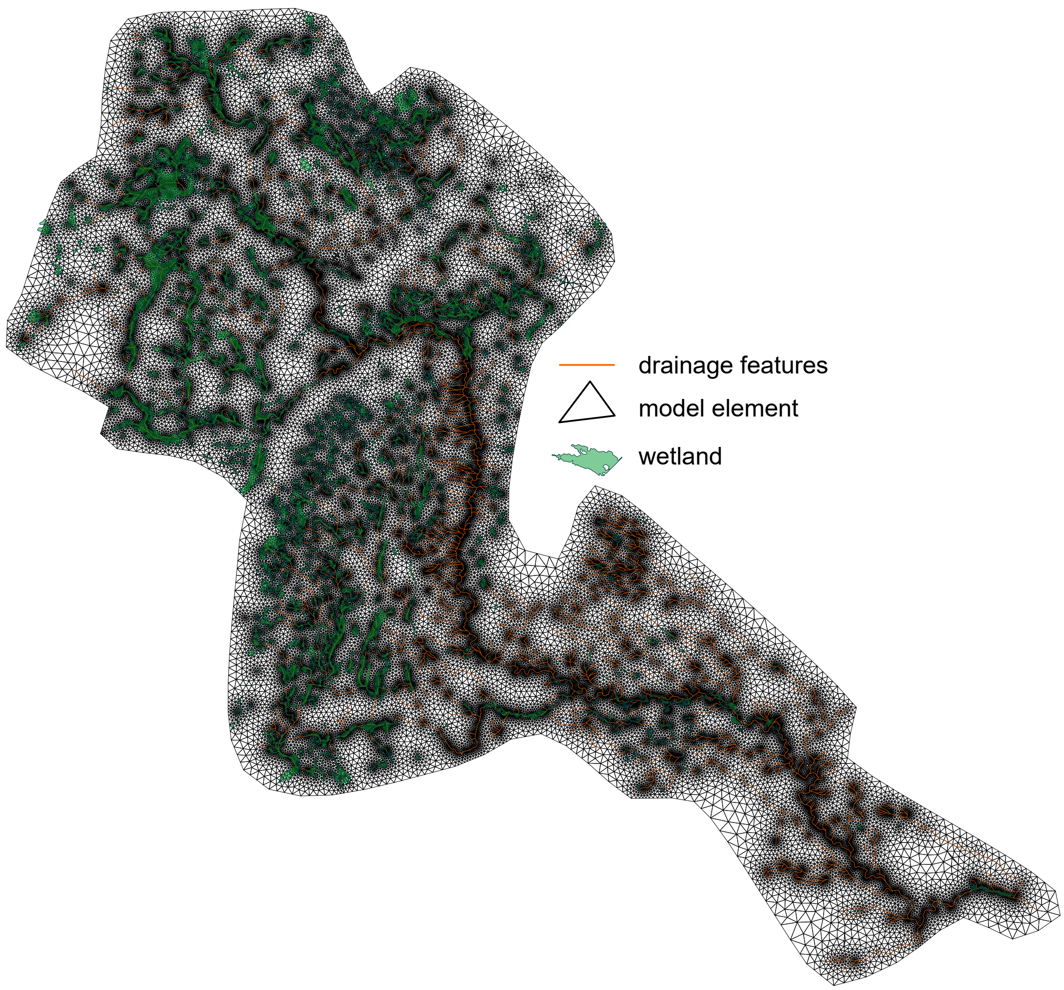

Figure 3.2: Final mesh design of the CRW. Note: if viewing from the original PDF, the figure is a vector image that will allow you to zoom in for greater detail.

AquaResource (2009) model were also interpolated to this model based on the location of where the generated elemental centroid intersected the AquaResource (2009) model mesh.

It is important to note that the AquaResource (2009) FEFLOW model was built with the intention of performing steady-state analysis of deep aquifer systems. For this reason, many characteristics of the CRW's hydrogeologic setting were simplified as they had little implication on the designed intent of that model. These simplifications include (AquaResource, 2009):

1. simplified representation of surficial materials;
2. bedrock fracture and regional faults have not been represented;
3. productive bedrock aquifer within the Amabel formation is not represented; and,
4. streams of Strahler (1952) order less than 2 were not represented.

Model B was built as a shallow soil zone model, and required a better representation of surficial materials. Layered at depths 0.25, 0.5, 1.0, 2.0, 3.0 meters below ground surface, material types were assigned according to Chapman and Putnam's (1984) surficial geology (Section 2.3.3) mapping. For consistency, mesh elements intersecting wetlands mapped from the Provincial wetland coverage (Section 2.2.1) had their top-most layer material properties converted to organics where not mapped from the surficial geology coverage.

Further sub-categorization of the Chapman and Putnam's (1984) surficial geology mapping type were required, specifically the "variable material" classification. Within the CRW, Chapman and Putnam (1984) used the variable material class to represent both the channel alluvium and the Niagara Escarpment's talus slopes, composed of erosional materials. While both these surficial deposits are variable in their composition, they have very different origins: one being alluvium while the other being mass wasting from the Niagara Escarpment. These two variable material types were defined as separate surficial material types into the model accordingly. Lastly, the Chapman and Putnam's (1984) surficial geology class "organics" was maintained because they coincided with CRW wetlands.

In the end, a total of six generalized surficial material types based on Chapman and Putnam (1984) were used to classify the CRW and set as distinct parameter zones within the model. The distribution of these material types are shown in Figure 3.3. The six generalized surficial material types include:

1. Low conductance materials (e.g., the Halton Till plain);
2. Low-medium conductance materials (e.g., Wentworth Till and Port Stanley Till);
3. High conductance materials (e.g., Orangeville, Oak Ridges and Paris Moraine sediments, glaciofluvial sand and gravels);
4. Variable materials (e.g., Niagara Escarpment's talus slopes);
5. Wetland sediments; and,
6. Fluvial materials (e.g., alluvium).

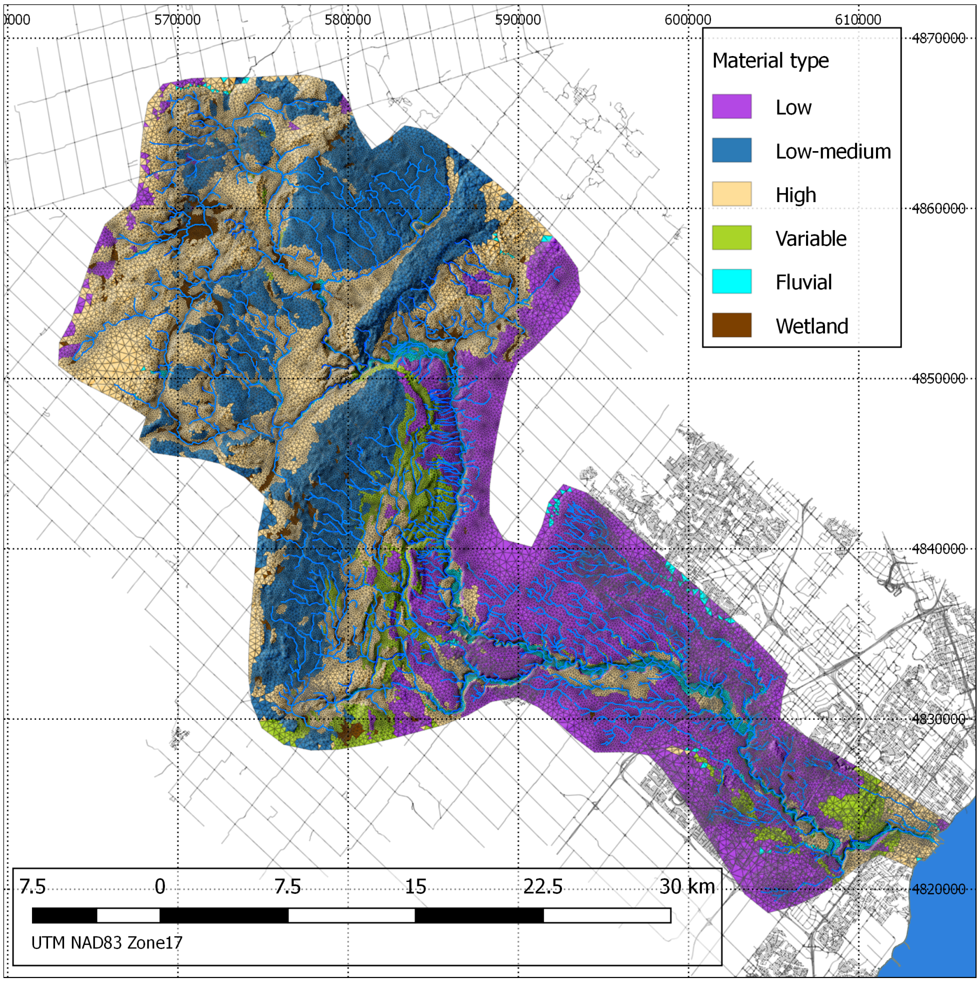

Figure 3.3: Distribution of material types across the CRW.

3.2.4 Initial conditions

Every model scenario is to be exposed to a set of late-summer convective storm events, and as discussed above, antecedent moisture conditions have implications for the watershed's response to these events. Therefore, crucial to the defensibility of results is the establishment of a likely moisture state prior to the onset of the imposed storm events. During the late summer, monthly stream flow in southern Ontario tends to be at its lowest; from this, two assumptions regarding the origin of late-summer baseflow are made: (i) groundwater discharge is the sole contributor to baseflow; and (ii) groundwater discharge is directly proportional to regional groundwater levels.

It is also assumed that the rainfall-runoff response is dependent on the antecedent moisture state by two primary means: (i) for much of the watershed, where the soil surface is dry, the antecedent moisture state will dictate the relative absorbability of the landscape; (ii) a number of CRW wetlands are expected to be perennially inundated dependent on their spatial location and their height above the watertable.

Determining these antecedent moisture dependencies required a modelling solution that explicitly incorporates land surface topography and the subsurface flow system. Model A (§3.2) was initially run in quasi-steady state to achieve a representative late-summer antecedent state. Model A was run having the entire subsurface domain initially set to fully-saturated and run with constant rainfall of 134 mm/year until a steady state was achieved. Based on this initial conditions model run, water table elevations that coincided with summer baseflow discharge within the CRW were determined and used as the initial conditions for the transient Model B runs. Summer baseflow discharge was determined from 13 Water Survey of Canada (WSC) stream gauges shown in Figure 3.4. For more discussion on this procedure, please refer to Appendix F. Stream flow and stage data were obtained from the following WSC stations:

02HB001: Credit River Near Cataract
02HB002: Credit River at Erindale
02HB008: Credit River West Branch at Norval
02HB013: Credit River Near Orangeville
02HB018: Credit River at Boston Mills
02HB019: Credit River Alton Branch above Alton
02HB020: Credit River Erin Branch above Erin
02HB024: Black Creek below Acton
02HB025: Credit River at Norval
02HB026: Credit River at Mississauga Golf Course
02HB029: Credit River at Streetsville
02HB030: Cooksville Creek near Cooksville
02HB031: Credit River Erin Branch at Hillsburgh

3.2.5 Extreme event selection

For this study a set of 7 rainfall events increasing in intensity was simulated to test wetland function under a variety of extreme conditions, and they included the 2-, 5-, 10-, 25-, 50-, and 100-year return period rainfall events plus the maximum obsevered rainfall intensity measure in southern Ontario.

A primary challenge with event-based hydrological modelling at the watershed scale is the difficulty in attaining an adequate spatial and temporal distribution of rainfall volumes. With respect

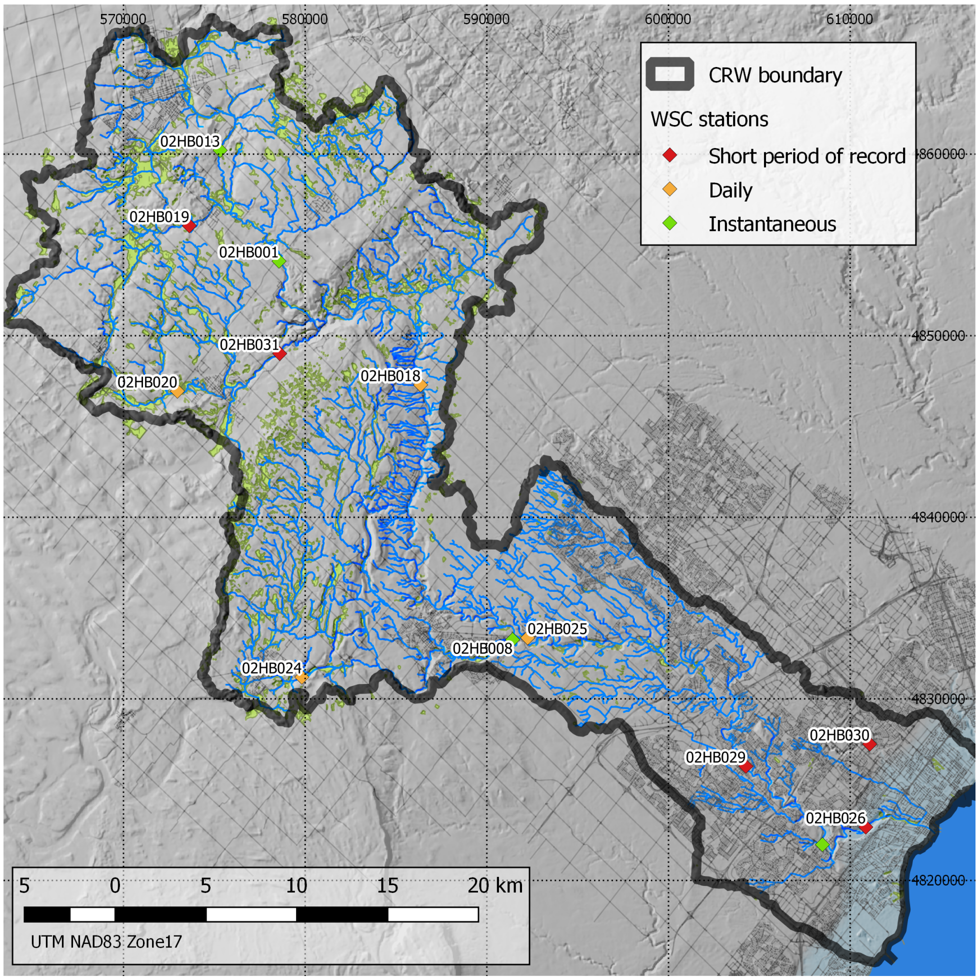

Figure 3.4: Location of WSC gauges within the CRW. Point symbology refers to: (i) Instantaneous—stream flow and stage reported every 15 min; (ii) Daily—average daily discharge and stage; (iii) Short POR—few data points exist at these locations and were thus not used for this study.

to rainfall, pluvial runoff generation is dependent on the amount of available surface retention and storm intensity and duration (Linsley et. al., 1975); and depending on the type of storm (convective, synoptic, orographic, etc.), attaining a proper representation of storm dynamics (i.e., distribution, extent, scale, and velocity) may be paramount to adequately representing the timing and intensity of rainfall on the watershed.

Appendix B demonstrated that there is a lack of correlation among rainfall event volume and stream peak stage and time to peak, which is an indication that the available observed data for the CRW does not have the "information content" (Beven, 2009) necessary for the event-based watershed-scale hydrological modelling needed to conduct this study. Based on the analysis, the rainfall-runoff response appeared more dependent on rainfall distribution rather than intensity and quantity.

Unfortunately, storm event information distributed in space and time at a fine resolution is extremely rare and poses a challenge to any watershed-scale modelling study. An event such as that required for this study should be reflective of the dynamics of a typical southern Ontario extreme storm event. Ontario rainfall climatology (Klaassen, 2014) is typified by mid-late summer convective storm events. As shown in Table 3.2, record storm events from the 5 minute to 24 hour duration observed in Ontario are all of the convective type; therefore, any study investigating the impacts of extreme (rainfall) events in southern Ontario must be able to incorporate the dynamics of these convective-type storms.

Table 3.2: Ontario record IDF station extreme rainfall amounts from Environment Canada's National Climate Data Archive for various durations.

Duration	Location	IDF station record amount (mm)	Average rate (mm/hr)	Date of occurrence	Dominant atmospheric process
5 min	St. Thomas	29.2	350.4	May 29, 1969	Convective
10 min	Toronto North York	44.7	268.2	Aug 19, 2005	Convective
15 min	Toronto North York	66.3	265.2	Aug 19, 2005	Convective
30 min	Toronto North York	90.2	180.4	Aug 19, 2005	Convective
60 min	Tobermory Cyprus Lake	112.0	112.0	Aug 21, 2003	Convective
2 hour	Toronto North York	131.7	65.9	Aug 19, 2005	Convective
6 hour	Kenora A	149.3	24.9	Jul 27, 1993	Convective
12 hour	Harrow CDA	187.7	15.6	Jul 19, 1989	Convective
24 hour	Harrow CDA	263.2	11.0	Jul 19, 1989	Convective
One-day[a]	Peterborough Trent U	239.8	10.0	Jul 14, 2004	Convective

[a] refers to the greatest measured total over one climate day (8am-8am) as opposed to a 24 hour continuous total. *Source:* Klaassen (2014)

Modelling the impacts of convective storms when assessing hydrological response at the watershed scale is difficult as convective storms are typically characterized as being relatively isolated and not strongly dependent on mesoscale or synoptic forcings (Weisman and Klemp, 1982). Capturing the dynamic processes of isolated events would necessarily require a dense observational network recording multiple measurements per day.

Just short of 400 Meteorological Service of Canada climate stations exist in Ontario reporting hourly rainfall amounts. A higher density of stations (282 of 398 total) are located in the southern portions of the province. Of these southern Ontario hourly stations, the average minimum spacing between adjacent station is roughly 10.8 km, which is far too sparse to capture convective storm patterns. In addition, it has long been recognized that many limitations exist with the various methods employed to interpolate point-scale rain station data into a distributed rainfall pattern (Coulibaly and Evora, 2007). Given the difficulties in obtaining good quality data at standard rain gauges (Sieck et. al., 2007), the accuracy of any interpolation method will ultimately depend on the accuracy of the gauges informing the method.

Another option would be to obtain RADAR-derived digital precipitation amounts. RADAR may collect data on roughly 10 minute intervals and are made available at finer resolutions compared with typical rain gauge networks (i.e., 4.3 km at NEXRAD in Buffalo, NY and 1 km at the Weather Radar King City, ON). The accuracy of RADAR data is dependent on a measurement's distance to the RADAR site and typically requires bias correction (Bedient and Huber, 2002). The quality of RADAR can be affected by beam interference and ground clutter, beam attenuation, beam overshooting, by capturing virga (precipitation that does not reach the ground), anomalous propagation and electromagnetic interference (Government of Canada, 2016), etc. While RADAR-derived data do provide a better distribution and the required temporal resolution, a >1 km spatial resolution may still fail to capture the spatial subtleties characteristic of localized convective storms.

This study was fortunate to receive an experimental very-high resolution urban-scale weather forecasting system dataset prepared for the 2015 Pan- and Parapan-American Games in Toronto by Environment Canada. The dataset came in a 1025×1025 250 m resolution, 15 minute snapshots of active weather distributions recorded in the southern Ontario region. The very-high resolution urban-scale weather forecasting system is a composite real-time dataset based on a double-moment microphysics planetary boundary-layer scheme (see Appendix G for details).

Four potential dates were selected in 2015 (May 30, June 27, Aug 2, and Aug 10) as they were dates where a number of stations in and around the CRW experienced significant (greater than 30.0 mm) daily rainfall accumulations. Of these dates, the August 2nd storm that swept through Toronto and much of the CRW, bringing heavy rains and hail was selected for the study (Figure 3.5).

The intended use of this dataset was not to replicate the August 2, 2015 storm, but rather to obtain a dynamic storm pattern to be used as a normalized rainfall-intensity distribution field for input into Model B. By increasing intensity factors applied to the normalized rainfall distribution field, a set of hypothetical rainfall patterns was derived. This avoided having to use a rainfall interpolation scheme from point measurements, or applying bias correction schemes to RADAR-derived rainfall data. (In addition, by employing identical rainfall distribution patterns scaled by varying intensities, watershed response can be compared without location bias that would be caused by a collection of storms from separate events.)

The preparation of the hypothetical set of distributed rainfall intensity fields based on the experimental very-high resolution urban-scale weather forecasting system that was read directly by Model B is discussed further in Appendix G.

3.3 Modelling strategy

Prior to the construction of any numerical model, an analysis of available data is required to help inform: (i) model conceptualization (Refsgaard and Henriksen, 2004); (ii) selection of the appropriate model structure (Butts et. al., 2004); and (iii) a model evaluation plan (Matott et. al., 2009—i.e., the

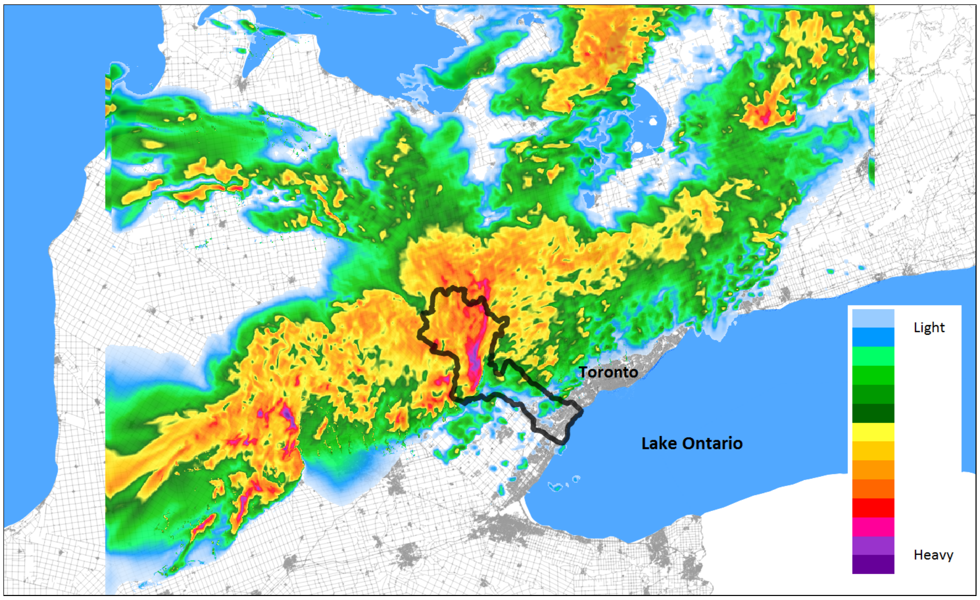

Figure 3.5: Snapshot of the very-high resolution urban-scale weather forecasting system showing the August 2, 2015 storm as it crossed the CRW (outline in thick grey)

means of model calibration and validation). Model conceptualization and model structure selection have been addressed above, and with that finalized, model calibration was needed.

Model calibration is the standard practice of adjusting model parameter values in order to obtain the best fit between observed and predicted variables, whereas validation is the process of evaluating the calibrated model to ensure that it reflects an acceptable representation of the system being modelled (Beven, 2009). Klemeš (1986) is often credited with establishing the approach to model calibration where a set of observations a model is intended to reproduce is split in two: the first set is used to calibrate the model; while the model is tested against the second set of observations. This split-sample calibration-validation approach is used to confirm the predictive capability of the model.

Ideally, when a modelling objective is to reproduce a particular phenomenon, then with perfect knowledge of boundary conditions (i.e., model boundary and initial conditions), the modeller should be able to replicate the observed phenomenon provided that all of the physical processes responsible for the observed phenomenon are fully represented in the model code; however, in practice, this is rarely, if ever, the case. For example, Stephenson and Freeze (1974) in their attempt to model snow melt runoff on a hillslope, realized the dependence of hillslope runoff parameters on the antecedent state and indicated that since initial states can never be fully known, then theoretically, a model can never be "calibrated."

The exercise conducted in §2.4 (and Appendix B) illustrated the issue raised by Stephenson and Freeze (1974) as it pertains to this study. From this exercise, it was possible to test the hypothesis of whether the observed stream flow response, defined by the metrics peak flow and time to peak were dependent on measured precipitation. If this hypothesis turned out to be true, then it could be said that the Credit River watershed's response to rare events is mostly dependent on rainfall quantity, and thus a calibration-validation procedure can be relied upon with the information available. However the hypothesis failed, meaning that climate data and stream gauging data alone cannot provide sufficient information to calibrate the model parameters. The tests did, however, reveal that the watershed's response is primarily dependent on antecedent conditions and rainfall distribution.

The lack of significant positive correlation between rainfall and time to peak, and between peak stage and time to peak further confirms that a *distributed* modelling approach, as the one proposed here, is necessary when assessing event-based hydrology of the CRW. Furthermore, the lack of correlation of initial stage among the set of high quality gauges prior to the onset of the same extreme rainfall event suggested a spatial dependence on antecedent state as well.

As a result, with the above hypothesis failing to be confirmed, the exact conundrum faced by Stephenson and Freeze (1974), which has also been raised by McKillop et. al.(1999), is reflected here—that is: there is insufficient data for model calibration. Therefore, on the basis of §2.4, a standard calibration-validation approach is not possible without access to additional data, such as high-resolution observed precipitation fields and a measured moisture profile at multiple locations distributed across the CRW; data that are simply unavailable.

3.3.1 Evaluation plan

With model conceptualization and model structure described in earlier sections, three issues related to data limitations remain: (i) establishing antecedent moisture conditions; (ii) determining distributed rainfall patterns; and, (iii) the model calibration/validation conundrum. The methods detailed above indirectly provided solutions to the first two issues provided that the modelling scenarios discussed below (§3.4) were performed as a comparative analysis, meaning wetland function was quantified by comparison to baseline conditions. In particular:

Antecedent moisture dependence was handled by establishing a initial state to be maintained constant for every model simulation. Although the established antecedent state was never directly measured, it was derived from measurement (§3.2.4). Most importantly, since the same antecedent state was applied for all model runs, the dependence/bias associated with initial conditions influencing the rainfall-runoff response was effectively circumvented. As shown by the lack of correlation of initial stage among a set of high quality gauges prior to the onset of extreme events, the spatial dependence on antecedent state was effectively considered.

Distributed rainfall intensity field described in §3.2.5 and Appendix B, is completely representative of the distributed nature of late-summer southern Ontario extreme rainfall events as the field itself was derived from an actual event that occurred in the region. Like antecedent moisture condition, the field was kept constant for all model runs, eliminating any bias associated with rainfall distribution and dynamics—only the magnitude of relative rainfall intensity was scaled according to the event that was being simulated.

Calibration/Validation. In the sections that follow, an alternative (to the calibration validation) modelling approach is described. The method employs a multi-model approach (Matott et. al., 2009) used more commonly for uncertainty assessment but can be thought to represent an aggregate treatment of error associated with parameter selection. The multi-model approach is an attempt to "generate ensemble predictions via consideration of multiple plausible models" (Matott et. al., 2009), which may "provide important benefits for hydrological simulation"

(Butts et. al., 2004). As will be discussed in the results section, one benefit the method offered was greater information as to the degree wetlands play in flood mitigation, which could not have been definitively provided through a typical calibrated-only model.

In the discussions that follow, all modelling was performed solely using Model B (§3.2). For the sake of simplicity and concision, the tools, processes and information employed in this study and discussed above (HydroGeoSphere, AlgoMesh, FEFLOW Tier-2, ELC, rainfall intensity field, Model A, Model B, etc.) will hereinafter be referred to in bulk as "The Model."

3.3.2 Multi-model analysis

The multi-model approach used for this study is a process where numerous model runs are performed while permuting a set of model parameters within a set "feasible range." Together, this number of model runs make up the model *ensemble*. A feasible range here is defined as the range of values a parameter is arguably going to take. For example, the height of ground-cover vegetation at late summer is likely going to range somewhere between 5 and 100 cm. The idea is that with the model ensemble, results would reflect a range of outcomes that would likely envelope the real behaviour of the CRW. In lay terms, this exercise would provide "ballpark" results, reflective of model uncertainty.

Clearly, the advantage here is that the modelling study proposed is conducted with an uncertainty analysis, which is lacking from many wetland modelling studies (see Kadykalo and Findlay, 2016). A detailed description of the Multi-model analysis procedure is provided in Appendix H.

Close to 10,000 model simulations[6] (i.e., realizations[7]) were run divided evenly among 6 (of 7) events, including the 2-, 5-, 10-, 25-, 50-, and 100-year return events (maximum observed rainfall intensity was excluded to the Monte Carlo analysis and the findings from the 100-year ensemble results were maintained for the maximum event). The multi-model simulations were performed at SciNet (`https://www.scinethpc.ca/`), Canada's largest supercomputer centre. SciNet's high-performance computing centre is hosted by the University of Toronto. SciNet's General Purpose Cluster (GPC) consists of 3,780 8-core nodes (IBM iDataPlex DX360M2), totalling 30,240 cores (Intel Xeon E5540) each at 2.53GHz, with 16GB RAM per node.

SciNet modelling for this project was, at times, able to run >100 simulations simultaneously which greatly expedited multi-model runtimes.

3.3.3 Esemble results

The multi-modelling analysis provided for an ensemble of model results as opposed to a single model realization; therefore, results are described on a statistical basis rather than a definitive result. Each model realizations, discussed in §3.3.2, was for a 2-day period and depth of overland flow was reported for every node at 15-minute increments. Therefore at every node (>82,000 in total), independent hydrographs were be produced providing for a ensemble/statistical distribution that was used for comparative analyses.

[6] This is an approximate number, as many trial/test runs (≈100–200) were accomplished and a few runs (<10) failed to complete in the allotted time.

[7] Realization refers to a separate model run based on a single permutation of model parameters; multiple realizations make up the ensemble.

At pre-defined points within the model domain, coincident with stream gauging stations, discharge passing that point was recorded. Hydrographs at these gauge location showing the distribution of discharge from the ensemble analysis were constructed, and is shown in Figure 3.6.

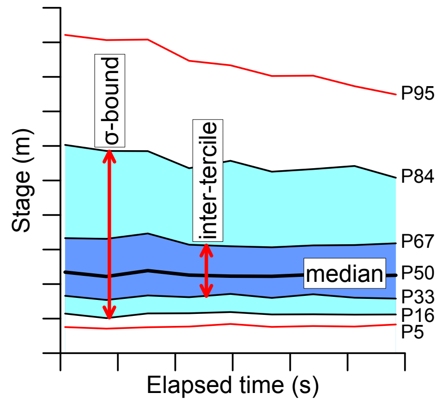

Figure 3.6: A sample multi-model simulation distribution hydrograph describing sample ranges.

Hydrograph distributions shown in Figure 3.6 were developed by evaluating the stage (i.e., flow depth[8]) distribution at every time increment. At every 15-minute time step, the simulated stages were sorted and a number of quantiles were computed to provide ranges against which individual model runs can be compared.

The median represents the stage that separates all simulated discharge into two equal parts, half lie above, the remaining below the median line. This "median hydrograph" does not represent a single realization, but the median stage of the ensemble at the given time step.

The tercile range divides the simulations in three equal parts, the bottom third (<p33) the middle third (p33–p67) and upper third (>p67). This helps qualify simulations as being relatively high or low, where pN represents the N^{th} percentile.

The sigma- (σ-)bound represents the middle range that is 2 standard deviations wide, and assuming a normal distribution, the mean simulation bisects the σ-bound. Statistically speaking, simulations that exist outside of these bounds can be said to be "significantly" high or low.

Lastly, the upper and lower 5^{th} percentile bounds 90% of all simulations and is useful in excluding potential outliers. These bounds are also very close to the 2σ-bound, a measure of "high-significance."

Validation with observation

The ensemble hydrographs from the 2 to 10-year return events were compared against the median storm hydrographs measured from the same 15 events discussed in §2.4 at four Water Survey of Canada (WSC) gauges: 02HB001—Credit River Near Cataract, 02HB002—Credit River at

[8]Flow depth is defined as the depth of flowing water moving at some flow velocity.

Erindale, 02HB008—Credit River West Branch at Norval, and 02HB013—Credit River Near Orangeville (refer to Figure 3.4). Figure 3.7 shows the hydrograph distributions superimposed by the observed median hydrographs.[9]

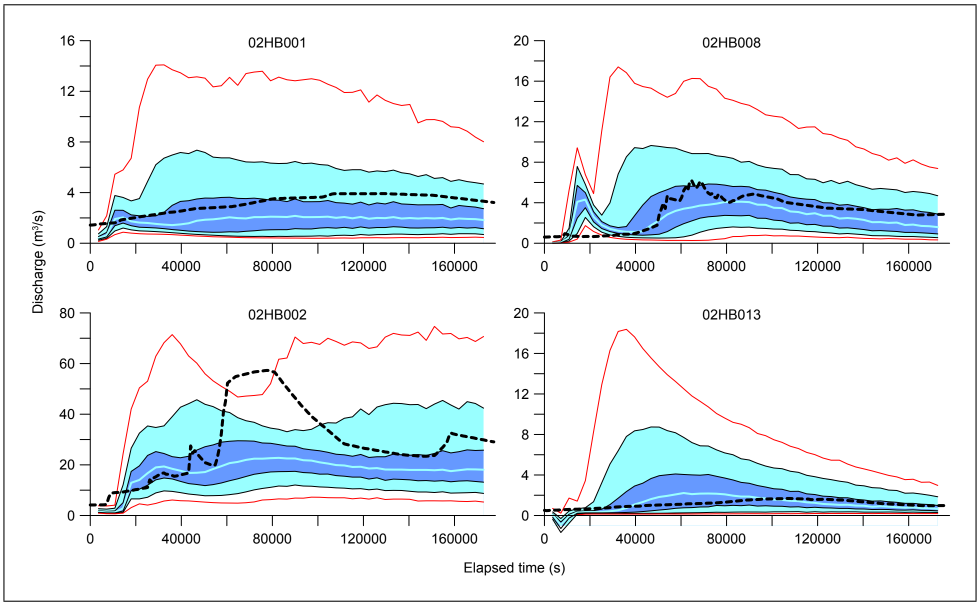

Figure 3.7: Validation of four WSC gauges to the multi-model simulation, showing overall significant agreement. Dashed line is the observed median hydrograph, the remaining colour scheme is illustrated in Figure 3.6.

Here it is evident that the ensemble simulation faired well in bounding the observed phenomena, thus validating the model design, approach and parameter range selection. For most of the time, the median observed hydrograph lies within the σ-bound and for roughly two thirds of the time, lies within the middle-tercile range.

Gauge 02HB002—Credit River at Erindale is a highly urbanized gauge and is the sole gauge that experiences significant deviation from the simulation distribution. It is likely that this deviation is reflective of the lack of urban storm infrastructure (i.e., storm sewers) implemented in the model. More on this is discussed in §6.

Nodal distribution

In a similar fashion to the hydrograph distributions, the maximum flow depths at every model node was also be built into a distribution function. Maximum flow depth, a measure of peak flow, is a primary metric that is used to analyze the degree of flooding. From the ensemble distributions, significant impacts can be discerned on a nodal basis, that is at 82,668 locations. For example, the distribution of maximum flow depth of a 2-year storm at node 48930 (chosen at random) is shown

[9]Please recall that the median hydrograph is not represented by an actual event, but reflects the median stage of all 15 events (§2.4) at each time increment.

in Figure 3.8. By fitting a normal distribution to the histogram of simulated heads, σ-bounds can be extracted for subsequent analysis.

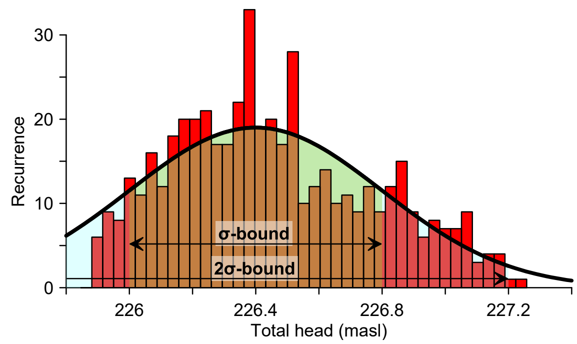

Figure 3.8: The 2-year return simulation histogram of maximum flow depth (represented as total head) occurring at node 48930 fitted with a normal distribution function.

The σ-bound is a direct indication of the degree to which model results are sensitive to the adjustment of free parameters within their feasible ranges. Any deviation beyond these bounds can be said to be beyond the parameter uncertainty of the model. This means of analysis will be utilized below to indicate significant impacts due to changes in wetland distribution.

Baseline parameter selection

From the ensemble, the parameter set that yielded the median response in terms of accumulated flow volume was selected as the baseline parameter set. The median response included all storm intensity scenarios, equally weighted. A baseline model parameter set was required for the subsequent wetland removal/restoration scenarios. By maintaining the baseline parameters, alternative wetland scenarios will be tested to quantify impact. In other words, while model parameterization remains constant, model structure will be changed.

Changes to the model results from a structural change will be deemed "significant" based on the difference in rainfall-runoff response among scenario results relative to the nodal σ-bound defined from the (baseline) ensemble. Should the difference exceed the σ-bound at a given location, then it can be said that the hydrological impact due to the change in model structure is beyond what can be attributed to model uncertainty.

The set baseline parameters are given in Table 3.3 for overland flow properties (§2.2) and Table 3.4 for surficial material properties (§3.2.3). The saturation–pressure–relative conductivity tables used in the model are plotted in Figure 3.9 and were based on standard van Genuchten (1980) parameters established by Schaap et. al.(2001). Please refer to Aquanty (2016) for more details on HydroGeoSphere parameterization.

It should be made aware that the chosen range for Manning's (1891) roughness is well below many published values measured in marsh wetlands (see, for example, Tsihrintzis and Madiedo, 2000) or used for the design of treatment wetlands (Kadlec and Wallace, 2009). In these publications, the roughness values provided represent bulk roughness, and not specifically surface roughness as interpreted in the model design. Bulk roughness includes the effects of tortuosity and extended flow pathways associated with treatment wetland design in addition to surface roughness, which is similar, in principle, to the Cowan (1956) method for estimating hydraulic roughness of natural channels.

The Manning's roughness coefficients applied to HydroGeoSphere represents the base/minimal roughness, as rill storage and obstruction height both serve to effectively increase roughness as overland flow decreases (Aquanty, 2016); therefore, direct application of these published bulk values would greatly overestimate uniform flow roughness. This method employed by HydroGeoSphere is actually most appropriate as the published Manning's roughness coefficients, which are typically back-calculated from free water surface wetlands, tend to show great depth-dependency (Kadlec and Wallace, 2009), a feature explicitly accounted for in the model code.

Table 3.3: List of baseline overland flow parameters set for subsequent analysis (see Aquanty, 2016 for more details).

Parameter	Type	Units	Value
Manning's roughness coefficient	Waterbody	$\frac{s}{m^{1/3}}$	0.06
	Short vegetation		0.18
	Tall vegetation		0.17
	Urban		0.01
	Agriculture		0.24
Rill storage height	All	m	0.0001
Height of ground vegetation	Waterbody	m	0.1
	Short vegetation		0.47
	Tall vegetation		0.48
	Urban		0.0
	Agriculture		0.3
Coupling length	All	m	0.001

Table 3.4: List of baseline surficial geology parameters set for subsequent analysis (see Aquanty, 2016 for more details).

Parameter	Type	Units	Value
Saturated hydraulic conductivity[a]	Low	m/s	10^{-8} (10^{-9})
	Low-medium		10^{-7} (10^{-8})
	High		10^{-4} (10^{-5})
	Variable Materials		10^{-6}
	Wetland Sediments		10^{-5}
	Alluvium		10^{-5} (10^{-6})
Porosity	Low	–	0.40
	Low-medium		0.37
	High		0.30
	Variable Materials		0.40
	Wetland Sediments		0.50
	Alluvium		0.35
Specific storage	Low	m^{-1}	1.27×10^{-7}
	Low-medium		1.27×10^{-7}
	High		1.27×10^{-7}
	Variable Materials		1.27×10^{-7}
	Wetland Sediments		10^{-6}
	Alluvium		1.27×10^{-7}

[a] Rounded to the nearest OM, vertical conductivity given in brackets

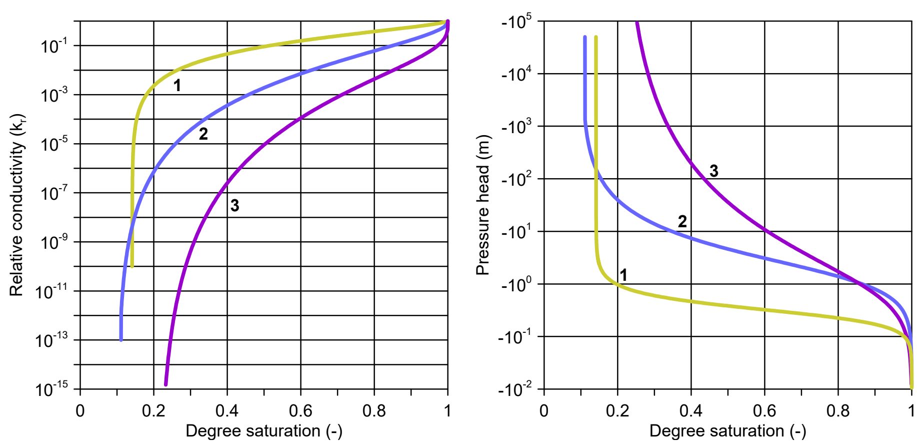

Figure 3.9: Saturation–relative conductivity (left) and pressure–saturation (right) curves used for the baseline model. Surficial geology types: 1—High, variable, and alluvium; 2—Low-medium and wetland sediments; and 3—Low conductivity materials.

3.4 Modelling scenarios

A total of 7 wetland distribution scenarios were run for each of the 7 event intensities, totalling 49 model runs for the subsequent analysis. Of the seven scenarios, one scenario reflects the existing condition run used for the basis of comparison. Five wetlands loss scenarios attempt to identify the flood-mitigation role of particular wetland types, and the seventh is a wetland restoration scenario. The wetland scenarios are as follows:

1. Baseline model, with existing wetland coverage;
2. Loss of all isolated wetland (i.e., wetlands disconnected from any observable drainage feature);
3. Loss of all connected (to observable drainage features) wetlands;
4. Loss of all non-Provincially significant wetlands (§2.2.1);
5. Projected near-term loss of wetlands according to Credit Valley Conservation (CVC);
6. Loss of all wetlands (i.e., worst case scenario); and,
7. Restored wetlands at all potential restoration sites as determined by CVC.

The implementation of model scenarios and model outputs collected are discussed below. Due to time and budget constraints, the study was restricted to these particular scenarios and was by no means established as the definitive set of model runs needed to quantify the wetland-flood retention relationship. Other scenarios could possibly be evaluated and the model was designed for future application. Model runtimes ranged from 4 to 12 hours.

Temporal scale

The model employs a variable time-stepping scheme to optimize the solving of model numerics. A maximum time step of 15 minutes was selected for all model runs to ensure a high temporal resolution of model result outputs. The models were run for a period of 2 days, in which there are 192 15-minute increments. With 192 time steps $\times$ 49 model runs $\times$ 82,668 model computational elements (i.e., nodes) yielding over 3GB of single-precision data per model output metric, timestep selection also has logistical limitations.

3.4.1 Modelling wetland removal

This modelling study investigated five scenarios that involved varying degrees of wetland loss. As each of the 3,679 wetlands existing within the model bounds were individually modelled, a systematic means of removing their hydrologic affect was implemented.

This study employed a "boundary condition link" (BCL) feature that has been newly implemented into HydroGeoSphere. The BCL establishes a direct link from any two points within the model domain. For wetlands that were set to be removed under a given scenario, a BCL was established that would drain any existing water that has ponded within a wetland and route the water to the nearest drainage feature. Essentially, wetland removal was accomplished by means of drainage, and the drainage system was assumed to be 100% efficient.

With the aid of Ducks Unlimited Canada (DUC) GIS staff, it was determined whether removed wetlands were to be reclassified as either agricultural or anthropogenic (see §2.2) depending on the location of the wetland being removed. Model parameters in these reclassified areas were re-parameterized accordingly.

3.4.2 Baseline scenario

Scenario 1: The baseline scenario represents existing wetland distribution and is used as a benchmark for comparison to the remaining scenarios. All mapped wetlands, drainage features, land use and surficial geology discussed in §2.2.1, §2.2.2, §2.2 and §3.2.3, respectively, have been preserved in their current state.

3.4.3 Wetland loss scenarios

To quantify the flood mitigation capacity of existing wetlands, five wetland-loss scenarios were devised to identify the role of specific subsets of characteristically-similar wetlands relative to the baseline scenario. The modelling of wetland loss was accomplished using the wetland drainage methodology discussed above. The selection of wetland subsets was accomplished by identifying wetlands that are deemed hydrologically connected/isolated, Provincially significant, or are currently situated in areas of potential development.

With the exception of Scenario 6: all wetland loss, a geospatial exercise was undertaken in preparation for the model runs.

Connected/isolated wetlands

For Scenario 2: wetlands that are not connected to any observable drainage feature (McLaughlin and Cohen, 2013) were removed from the system. This was to test whether the position of wetlands in the landscape has an impact on flood mitigation and to test the hypothesis that isolated wetlands play a negligible role in flood mitigation. Isolated wetlands tend to be small and are likely not evaluated under the Provincially Significant Wetlands (PSW) evaluation process, which may neglect their aggregate contribution to flood mitigation at the watershed scale even though they still may have an important role to play (Bradford, 2016).

Connected wetlands were identified by applying a proximity selection routine common to many commercial Geographic Information System (GIS) software packages. A search for any wetland within 10 m of a mapped drainage feature was deemed connected. A second sweep for wetlands within 10 m of connected wetlands was also deemed connected to ensure that wetland disconnection was not a result of mapping artifacts or due to the presence of right-of-ways cut into the wetland feature for other services such as roadways and hydro corridors.

Once the connected-wetland selection was complete, the remaining un-selected wetlands were deemed isolated, and the wetland mapping was established for Scenarios 2 and 3.

Provincially significant

Provincially Significant Wetlands are identified through a wetland evaluation system, which ranks the relative values of wetlands in Ontario following the guidelines of the Ontario Ministry of Natural Resources (2014). The wetland coverage used for this study was attributed with a field that indicated whether each wetland had a PSW designation. Any wetland that was not given PSW status was drained for Scenario 4.

It is the intent of this study to address whether, from a flood-retention perspective, non-PSWs are significant. As it is acknowledged that wetlands that are not PSWs may still play an important role (Bradford, 2016), Scenario 4 will reveal their importance with respect to flooding.

Projected near-term loss

Scenario 5: Projected near-term loss wetlands were those that existed outside of the CVC Natural Heritage System (NHS). CVC indicated that these wetlands would be most vulnerable in the near-term since they would not have the additional protection that their Natural Heritage System (NHS) provides within their watershed. All wetlands outside of the NHS boundary were selected regardless of whether or not the wetland was provincially significant. A quick manual screening was also undertaken to ensure that any projected wetland that had a low likelihood of actually being lost (i.e., existed within protected flood plains, deemed Provincially significant, etc.) were maintained in the model.

3.4.4 Restoration scenario

Scenario 7 reflected potential wetland restoration plans as informed by CVC. Similar to above, manual screening was also undertaken to ensure that potential restoration sites were reasonable (i.e., not in areas either developed or planned for development). In total, the potential restoration plan yielded and additional 2,085 wetlands, some being completely isolated, while others being extensions of existing wetland features (Figure 3.10).

Again with the aid of DUC, the potential restoration sites were attributed with the likely added storage depth (i.e., maximum ponding depth) the restored wetland should achieve. The restorable wetlands were given either a 40 or 65 cm impoundment depth for incorporation into the model. These depths were achieved by assigning them to the overland rill storage parameter (Aquanty, 2016) to all elements whose centroid existed within the potential restoration site bounds.

3.5 Model output metrics

Two forms of model outputs are produced: direct and derived. Strictly speaking, direct outputs are values that are outputted from every model run, and derived outputs are calculated based on the direct outputs. Table 3.5 list the outputs collected for the subsequent analysis.

Post-processing of model above-surface (i.e., overland flow) heads are required to produce a set of metrics used for the flood flow analysis. Based on resultant heads, flow depths, flow velocities, and additional derived flow metrics such as velocity-depth and depth-duration were determined. Heads were output from the model at every node in 900 second increments. With a two-day model run, this results in 192 timesteps totalling 15.8 M datapoints.

The method of derived output calculation was added to Appendix C.2.

Table 3.5: List overland flow model outputs used for the wetland-flood mitigation analysis.

Output[a]	Units	Description
Direct outputs		
Head	m	height of water surface relative to sea level
Flow velocity[b]	m/s	depth-averaged velocity of flowing water
Derived outputs		
Flow depth	m	depth of flowing water above surface
Depth-duration	ms	time-average depth at a point multiplied by duration offers a pseudo-measure of the total volume of water existing in any one location
Volumetric flux	m^3/s	total volume of water passing any given point over a period of time
Velocity-depth	m^2/s	velocity-depth is a common factor used in storm water hazard analysis. The metric relates the power of moving water against the buoyancy objects at risk (generally people)
Maximum depth	m	the maximum depth of flood at any given point
Maximum velocity	m/s	the maximum velocity of flood flow at any given point

[a] Only considering overland flow outputs
[b] Although velocity is a direct output, the values used for this study were calculated (see §C.2)

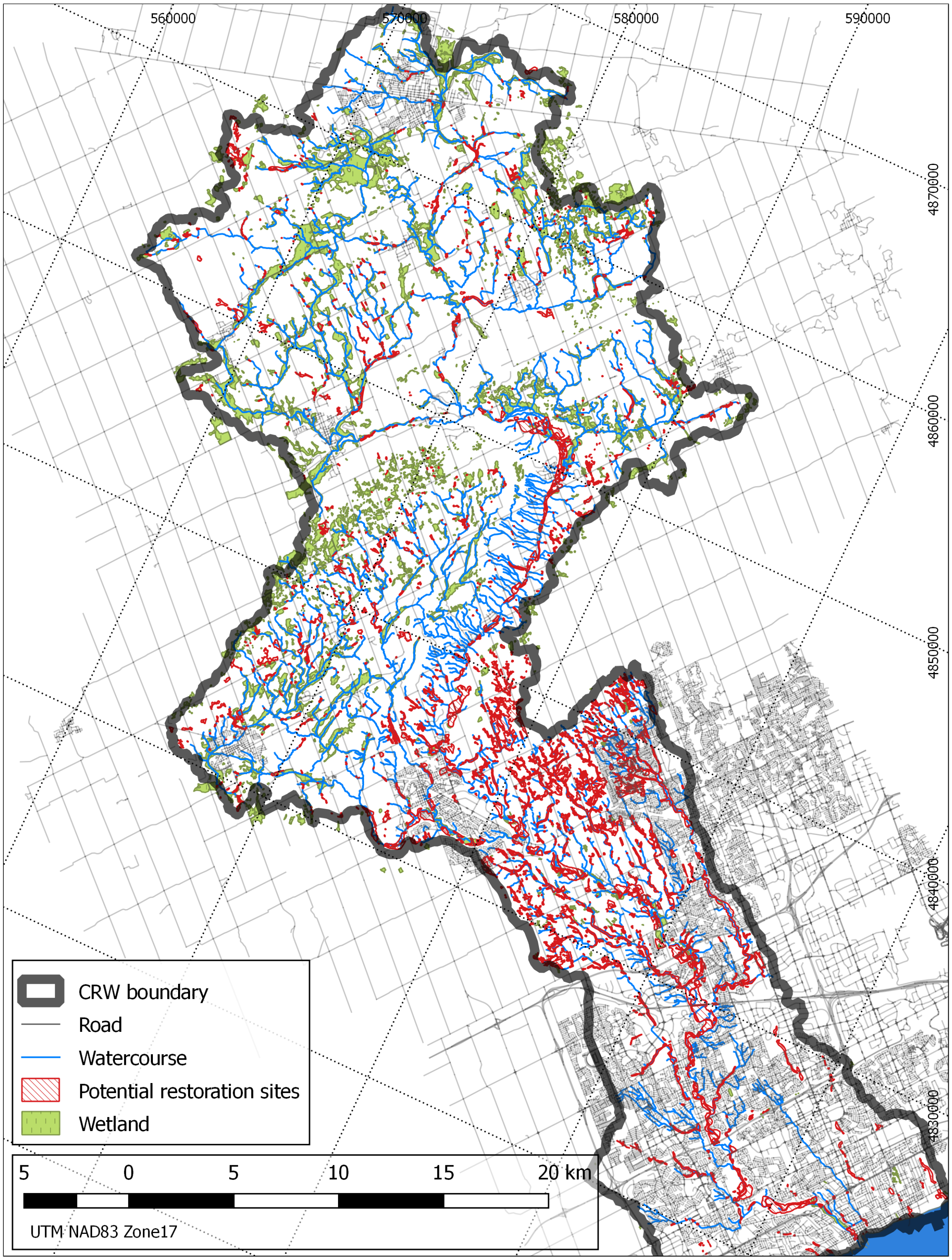

Figure 3.10: Wetland areas slated for potential restoration.

Section 4

Results

For much of the preceding sections of this report, many arguments were made for a process-based distributed modelling approach to address the scope of this study (§1.2). Besides the need to incorporate state-of-the-art rainfall event data (§3.2.5) and to establish a realistic basin-wide antecedent state (§3.2.4), advantages of distributed modelling continue to emerge once analyzing model results at the watershed scale.

Generated model results from past modelling efforts introduced in §1 were typically dependent on pre-defined calibration locations, or based on a sub-watershed/catchment area/drainage basin model structure. For example, the GAWSER (Schroeter and Associates, 2001) and HSP-F (AquaResource, 2009) models discussed in §3.1 had sub-divided the Credit River Watershed (CRW) into ~200 sub-watersheds. Given that this is a large number of sub-watersheds, the modeller would still have had to predetermine the location of the sub-watershed outlets according to where results would need to be recorded. Compare that to the tens of thousands of locations (i.e., model nodes) recording results with the current model, more-or-less distributed evenly across the CRW (see §3.2).

Although it would be onerous to report model results at every node, the high resolution gained from the modelling strategy has enabled this analysis to identify regions within the CRW that are apparently impacted from wetland alteration. These impacts may not have coincided with the predetermined locations (i.e., sub-watersheds) needed for a semi-distributed model such as the GAWSER and HSP-F models, and thus would have been overlooked.

A total of seven wetland distribution scenarios (§3.4) have each been exposed to seven extreme rainfall events (§3.2.5), totalling 49 independent model simulations. With 82,668 nodes reporting flow depths and 164,781 finite elements reporting 3D flow velocities at every 15-minute interval for two days (192 timesteps in total), over 5.4 billion readings were recorded, amounting to ~21 GB of single-precision data. Lots of insight can be gained from these data, but it would not be prudent to describe them in full under one cover.

In this section, model results are selected, first and foremost, to highlight the role of wetlands in terms of answering the study scope (§1.2), followed by a set of potential interpretations one can make using the model output. Complete model output data will be made available upon request.

The results presented below have been organized according to the degree with which insights are uncovered from a less-detailed lumped/sub-catchment approach to the distributed modelling approach taken here. The idea is to convince the reader of the limitation of *not* taking a distributed approach through the understanding that the subsequent results from later sections would not be possible. The results of the numerical analysis are presented as follows:

§4.1: **At-a-station results**

These results reveal the least amount of information from the modelling exercise. However, discussion is included here because it reflects the limitations of model results from a model that is not fully-distributed. All of the previous attempts at wetland modelling, discussed in §1 and §3.1, did not utilize a fully-distributed model, and would themselves be restricted to presenting results in this manner.

§4.2: **A test for significance: do wetlands contribute to flood reduction? (Basin-scale results)**

The use of a process-based fully-distributed modelling solution provides greater flexibility in revealing the hydrologic role of wetlands (for details on model selection, see Section 3.1). Most telling is how significant impact to CRW hydrology due to wetland alteration is identified at a number of locations. "Significance" here is statistically robust, beyond what can be attributed to model uncertainty, and is founded on the multi-model ensemble results generated (see §3.3.3).

Here, the argument is given that alteration to wetland distribution within the CRW will have a measurable impact to watershed hydrology; however the impacts are found to be quite localized and context specific.

§4.3: **Evaluation of hydrological change—suggestions for model evaluation**

After demonstrating that wetlands influence CRW hydrology during extreme rainfall events (§4.2), a sample set of model results and interpretations are illustrated. Here, the true power of the distributed model comes to light, as one is able to zoom into any particular portion of the model domain (i.e., a wetland, FDC, etc.) and investigate local hydrology.

What is quite revealing is the potential gain in watershed safety from the incorporation of potential wetland restoration sites (§4.3). In areas such as in the heart of Mississauga, significant reduction to flow depths and thus hazard to human health is apparent.

§4.4: **Suggested economic analysis**

Lastly, a brief demonstration is made to illustrate how the immense collection of model results can be aggregated into an easily-interpretable chart detailing the economic benefit to wetland preservation and restoration (§4.4). This proposed chart is a suggested path for the economic analysis (Phase III) to follow this report (see §1.1).

4.1 At-a-station results

Prior to the design of any lumped-parameter or semi-distributed model is a requirement for the modeller to decide on locations within the watershed where model outputs are to be computed. The choice of output location is not an arbitrary one, but is dependent on the model design itself.

Typically, the watershed location where outputs are computed coincides with locations where calibration data are available, i.e., at stream gauging stations. Within the CRW, 8 of 13 Water Survey of Canada (WSC) gauges have good quality daily records over long periods of record (≥10 years). These gauges are listed in Table 4.1 and shown in Figure 3.4.

Table 4.1: List of long-record WSC stream gauges available for at-a-station model analysis.

Gauge Name	Contributing Area (km^2)	Number of reported values	Record begin	Record end
02HB001: Credit River near Cataract	199.4	36,399	1915-05-07	2014-12-31
02HB002: Credit River at Erindale	769.6	16,547	1945-10-01	1993-09-15
02HB008: Credit River West Branch at Norval	136.5	19,741	1960-10-01	2014-12-31
02HB013: Credit River near Orangeville	76.0	17,259	1967-10-01	2014-12-31
02HB018: Credit River at Boston Mills	389.8	11,815	1982-08-27	2014-12-31
02HB020: Credit River Erin Branch above Erin	58.3	11,598	1983-04-01	2014-12-31
02HB024: Black Creek below Acton	28.2	9,909	1987-03-16	2014-06-29
02HB025: Credit River at Norval	666.9	9,563	1988-10-26	2014-12-31

At-a-station results are presented in Figures 4.2 through 4.7. In general, all the hydrograph patterns are the same among events, only their relative magnitude increases with event rainfall intensity. Based on this pattern similarity, it is clear that the dependence of hydrograph form on storm dynamics has been eliminated by selecting a single storm pattern scaled to the various event intensities (§3.2.5); only the time to peak flow appears to decrease slightly as event intensity increases.

Recall from §3.3.3 the definition of the hydrograph distribution, which is a representation of ensemble results from the multi-model analysis (see also, Figure 3.6). The Figure 4.2–4.7 hydrograph distributions mainly reveal the degree with which wetland alteration has impacted the stream flow regime at the given location. Points where the scenario hydrographs (dashed lines in Figures 4.2–4.7) lie outside of the σ-bound is indicative of a "statistically significant" impact, outside of what can be attributed to model uncertainty. In general, peak flows tend to lie outside the σ-bound; however, in some cases, a sustained hydrograph recession after peak flow can lie outside the σ-bound, reflecting an overall significant change in streamflow volume.

Based on the selected at-a-station locations, only 5 of the 8 locations appear to show results of any significance with respect to the ensemble results (§3.3). This could be misleading, because as will be discussed below, the relationship between wetlands and their watershed is location-specific, and these 3 "insignificant" locations simply exist in "uninteresting" locations with respect to the CRW's wetlands. Without a fully-distributed modelling effort, as performed here, many location-specific affects due to wetland loss would remain undetected.

It is also interesting to note how inconsistent the at-a-station results can be; for instance, the gauges with the smallest catchment areas (02HB008, 02HB013, 02HB020, and 02HB024) appear to be most affected by changes to wetland distribution, while gauge locations immediately downstream of these (02HB001 and 02HB018) show little impact, especially 02HB002 which lies near the mouth of the CRW. On the other hand, stream discharge at 02HB025, the location having the second-largest catchment area, does experience significant change. From this, it cannot be concluded that wetland loss impacts are reduced with increasing catchment area; however, this conclusion may have been erroneously made if location 02HB025 was not included in a non-distributed model design.

An interesting phenomenon associated with hydrographs located immediately below the escarpment (02HB018 and 02HB025 included), is the presence of a delayed (by often a day) secondary peak event. This bimodal hydrograph was indeed present in the 02HB008 instantaneous (observed) hydrograph on occasions where only typical unimodal hydrographs were occurring elsewhere within the CRW.

Each location experiencing the bimodal hydrograph coincides with a buried bedrock valley coming off the escarpment (AquaResource, 2009). The second flood pulse is indicative of groundwater entering headwater streams along the escarpment, fed by discharge originating from the Paris Moraine, lagged by the relative speeds of shallow groundwater flow. This unique phenomenon only emphasizes the need to include groundwater/sub-surface flow processes when constructing basin-wide hydrological models within the CRW, even at small temporal scales.

Gauge 02HB008—Credit River west branch at Norval—is situated in the lower catchment, just upstream of where Silver Creek connects with the mainstem Credit. This station tends to exhibit high sensitivity to wetland alteration, especially with the loss of connected wetlands. With the loss in connected wetlands, the initial peak increases significantly, causing the west branch to become more flashy, which may pose hazards to the communities of Acton and Georgetown.

Unique to gauge 02HB008 is the appearance of an intermediate third peak that occurs almost immediately after the onset of the first peak (Figure 4.2), but becomes consumed by the main (initial) flood peak as the event forcing increases in intensity (i.e., compare with Figure 4.7).

The location at gauge 02HB013 lies immediately downstream of the community of Orangeville, and like the Georgetown and Acton gauges (02HB008 and 02HB024), experiences significant increases in peak flow with the loss of connected wetlands.

Location 02HB020, above Erin, is a small catchment that shows minor sensitivity to very extreme ($\geq$50-year return) events, but otherwise shows no real impact from wetland alteration. An interesting result at 02HB020 is that although the all-loss scenario continues to mimic the isolated-only scenario, neither of these scenarios appear to have any significant impact on hydrology, based on them persisting within the σ-bound. It is the remaining scenarios, including the restoration scenarios, that appear to show significant increases to peak flow. One possible explanation is that at two locations, there are two large (connected-type) wetlands (part of the Alton-Hillsburgh wetland complex and the West Credit River wetland complex) that extend beyond 02HB020's immediate catchment area (Figure 4.1). This connection is possibly providing additional pathways for water to enter 02HB020's catchment. By removing the connected wetlands, these pathways are cut-off, effectively reducing 02HB020's catchment area.

Location 02HB024—Black Creek near Acton—has the smallest catchment area and is significantly affected by the absence of connected wetlands. Considering that the catchment lies entirely in the upper CRW upstream of 02HB008, notice the lack of the delayed secondary peak experienced by 02HB008. Only, the third (intermediate) peak experienced by 02HB008 can definitely be found to originate above the 02HB024 location, and like 02HB008, is consumed as event intensity increases.

Downstream of 02HB008, on the Credit River mainstem, location 02HB025 appears also to be sensitive to connected wetland removal with a significant increase in the hydrograph's initial peak during all events. However, hazards associated with this peak may be inconsequential, as the secondary delayed peak exceeds the primary peak in magnitude in all cases and does not differ much from the baseline peak.

As a general observation from the at-a-station hydrographs, Scenario 3: loss of connected wetlands and Scenario 6: loss of all wetlands exhibit nearly identical results. These results would appear to justify the assumption made by many (§1) that connected wetlands play a bigger role in flood mitigation. From these at-a-station results, connected wetlands are entirely responsible for in channel (fluvial) flood mitigation.

Scenario 7, being the sole restoration scenario, seems to demonstrate significant gains achievable at locations 02HB002, 02HB008, 02HB024 and 02HB025 as shown by the green dashed hydrograph dropping below the σ-bound. With the exception of 02HB024, all of these locations represent relatively large catchments that are situated in the lower CRW. Potential restoration plans would gain a 20–50% decrease in peak flow, which would be of significant benefit to the communities of Acton, Georgetown, and the City of Mississauga.

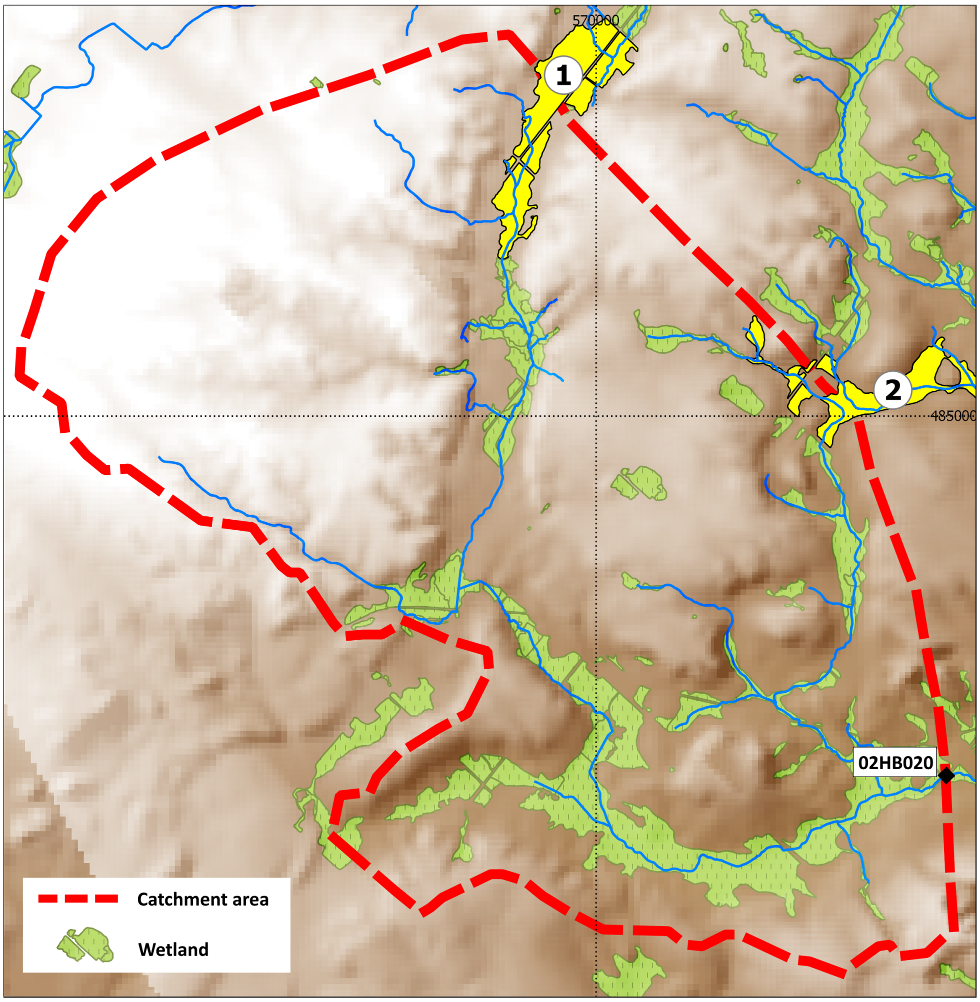

Figure 4.1: The Alton-Hillsburgh wetland (1) and the West Credit River wetland (2) that extend the effective catchment area contributing to gauge 02HB020.

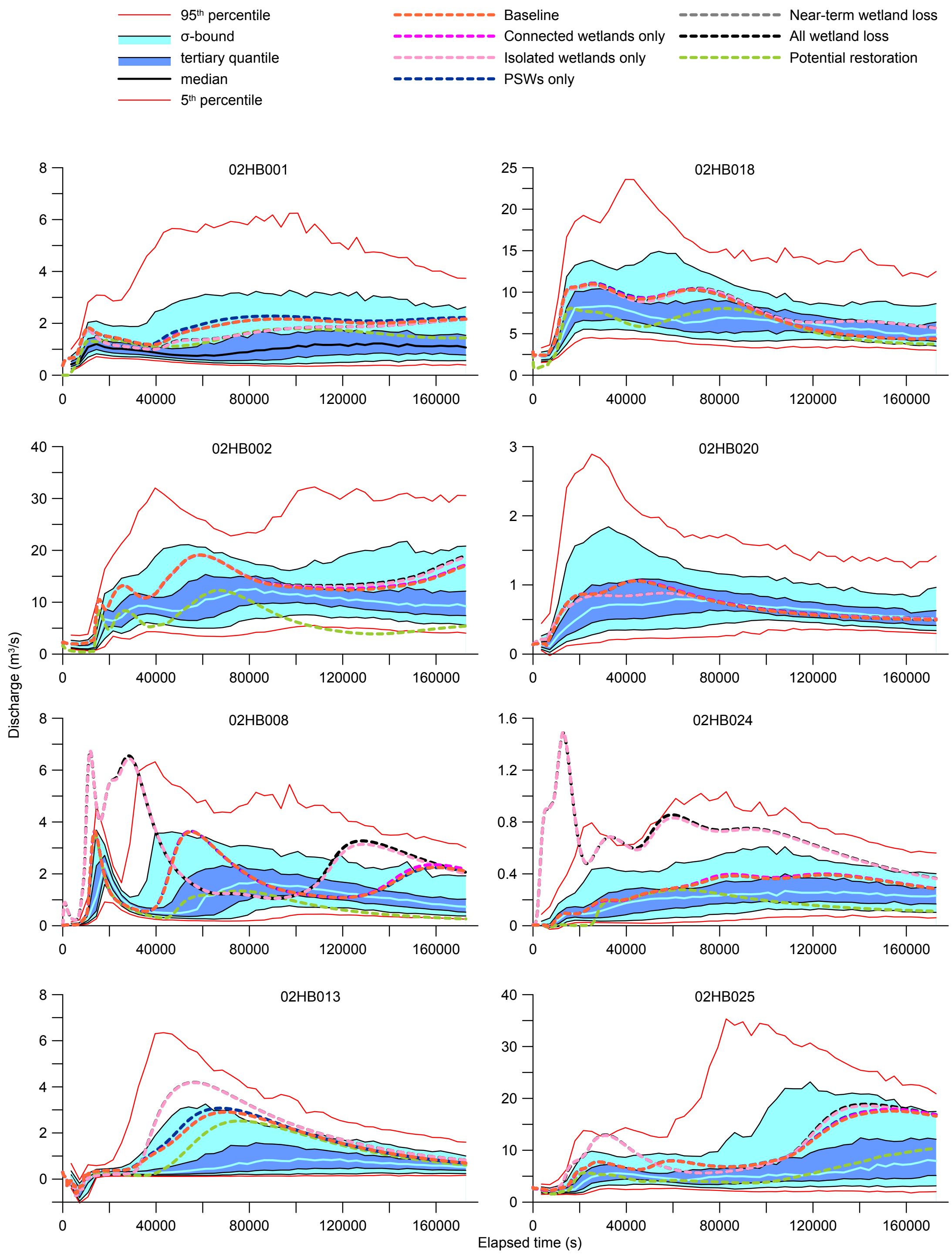

Figure 4.2: At-a-station results for the 2-year return event.

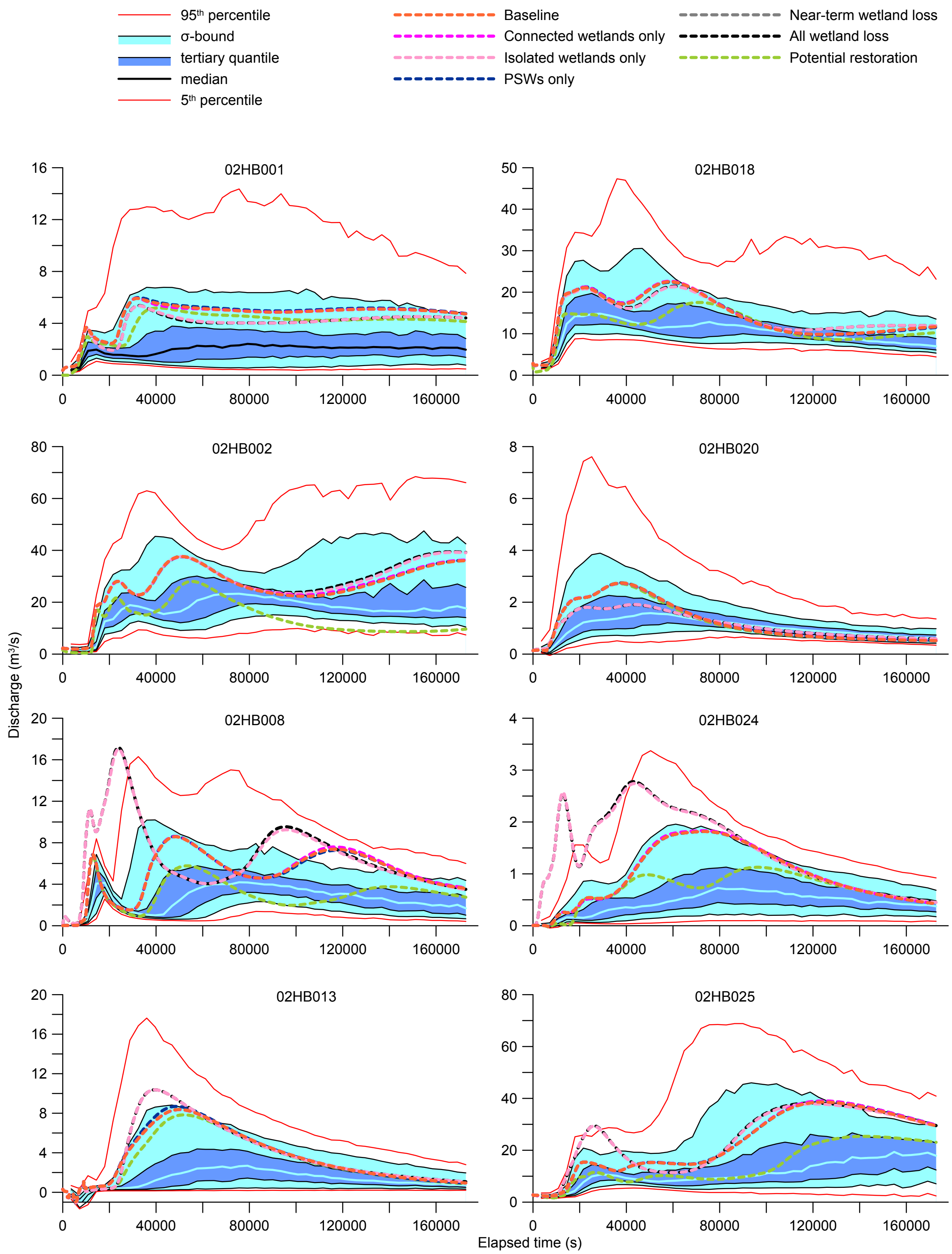

Figure 4.3: At-a-station results for the 5-year return event.

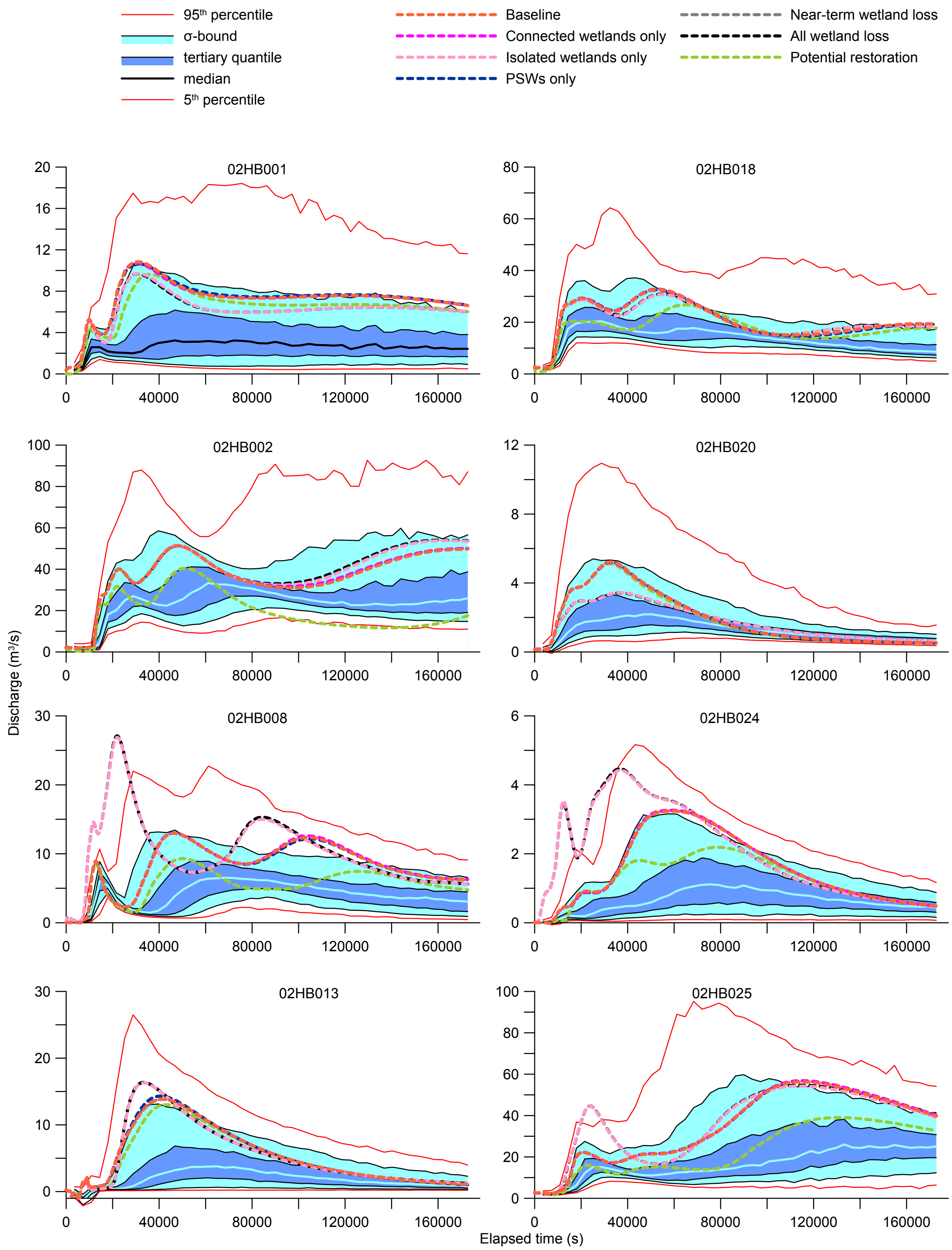

Figure 4.4: At-a-station results for the 10-year return event.

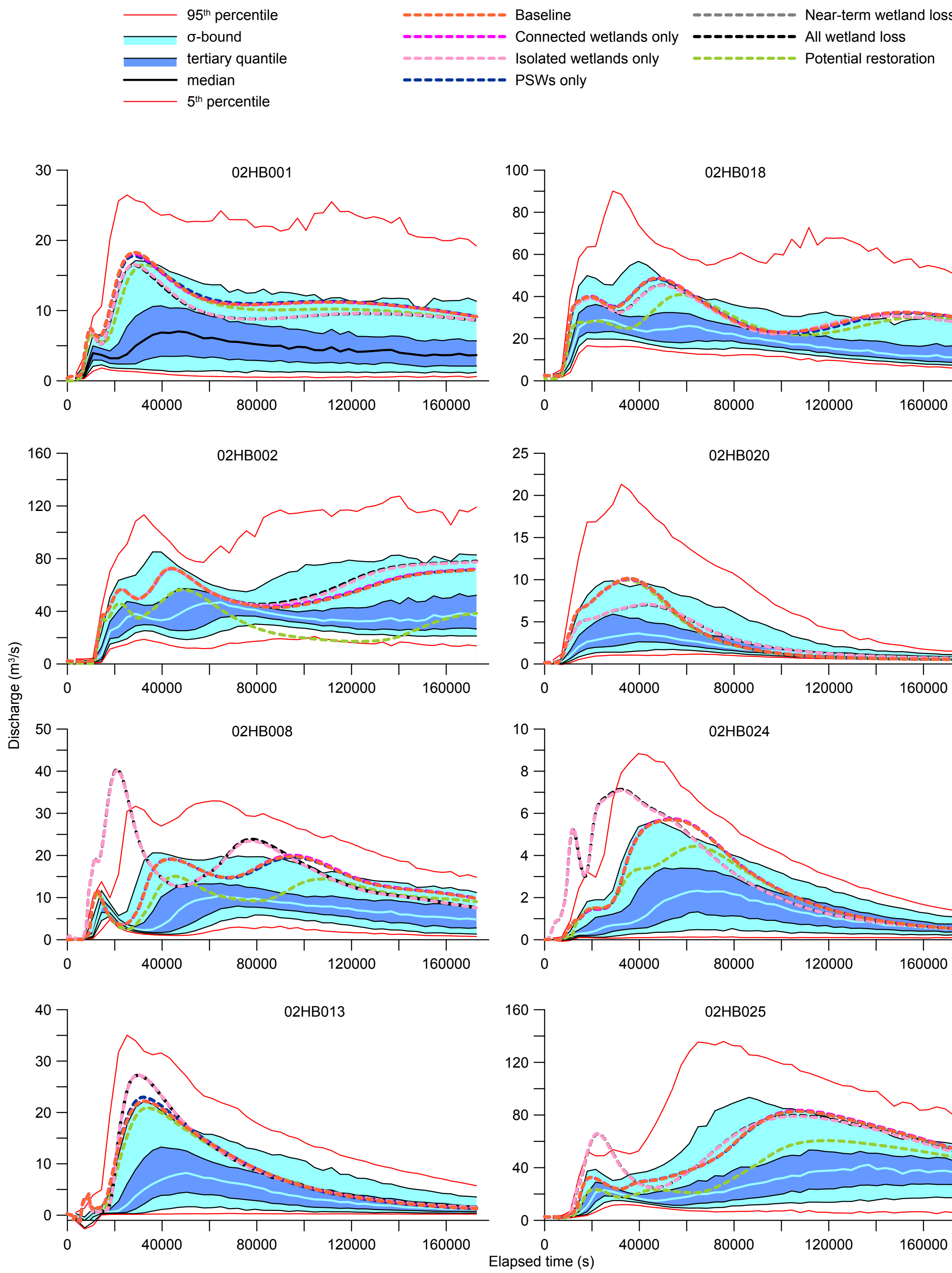

Figure 4.5: At-a-station results for the 25-year return event.

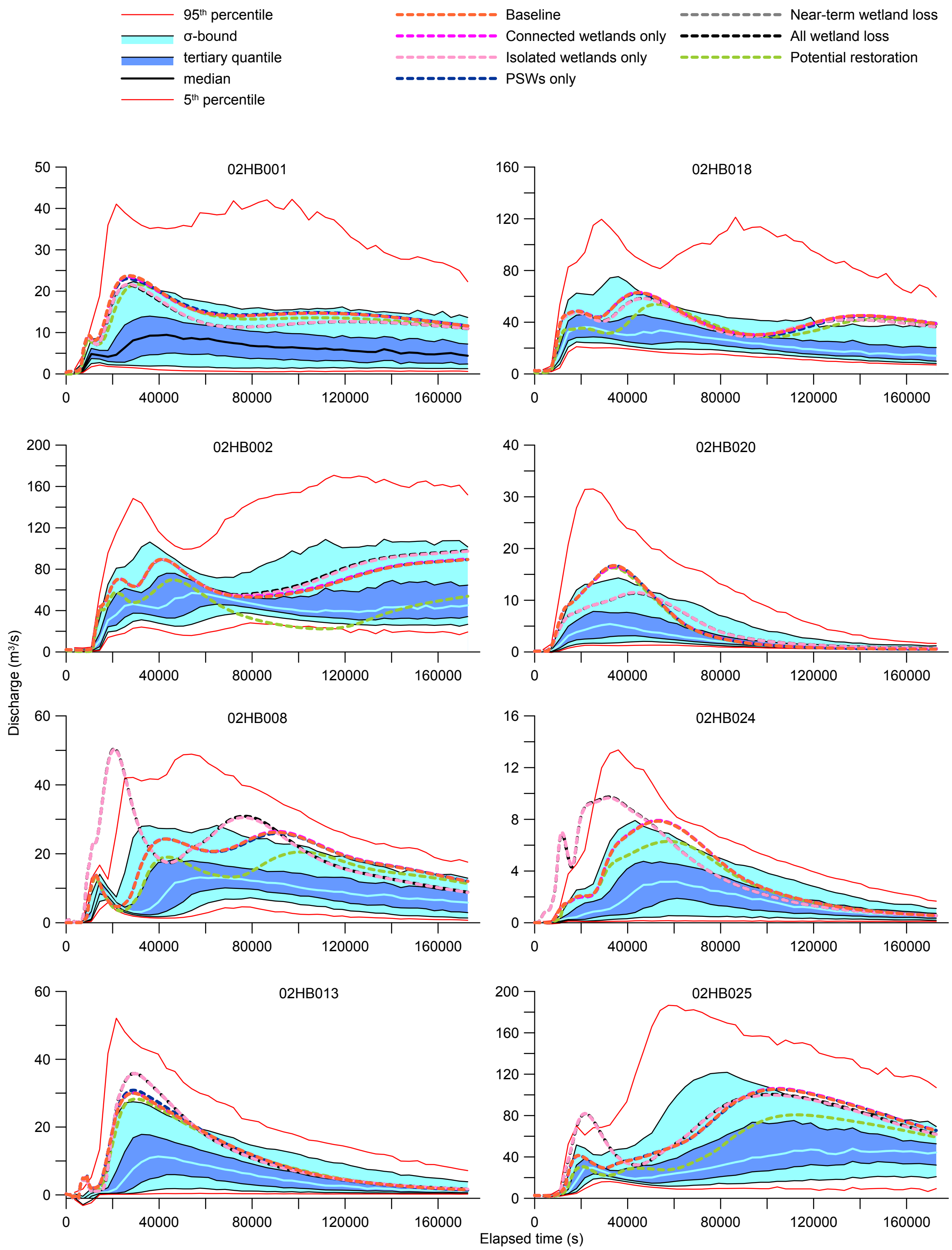

Figure 4.6: At-a-station results for the 50-year return event.

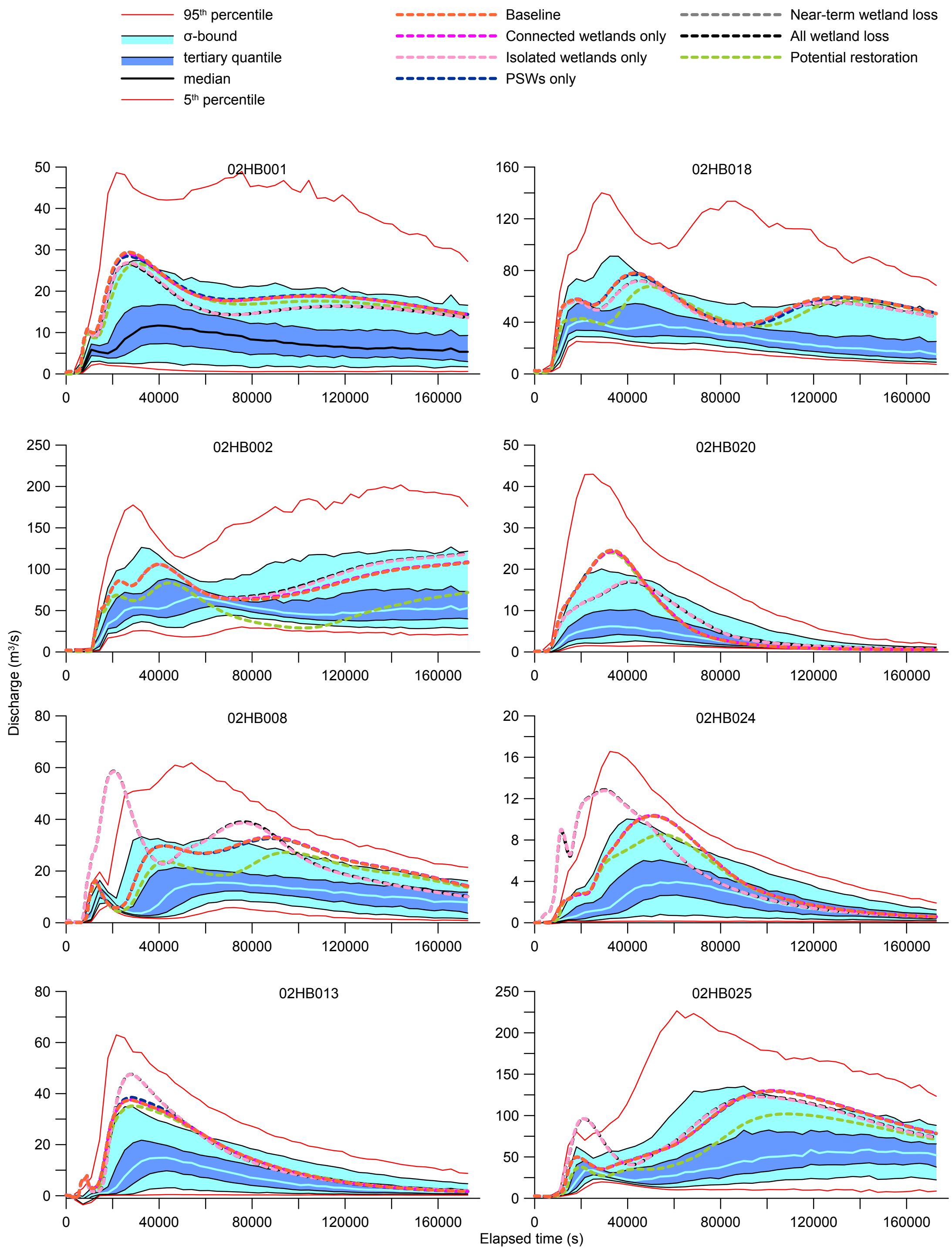

Figure 4.7: At-a-station results for the 100-year return event.

4.2 Basin-scale results

The model employed for this study was a fully-distributed model such that the results are not restricted to any pre-defined location. As shown below, this methodology has the advantage of providing results everywhere within the CRW compared to the at-a-station results presented above. The results presented thus far would have been the limit of results produced from the majority of the model codes listed in §3.1.

A motivator for the distributed modelling approach was the need for a flexible modelling solution that could be applied for future use. The model proved to elucidate CRW hydrology and its interplay with wetlands in areas that would have been hard to identify with another modelling strategy. For example, many of the areas most significantly affected by changes in wetland distribution could not have been determined prior to model design, as they are indicative of the complex interplay among topography, land use, geology and position within the watershed. For the remainder of this section, the results from the distributed model are discussed.

4.2.1 Test for hydrological significance

Model uncertainty

In §1.2, the scope of the study was identified as to determine the capacity of CRW wetlands in retaining flood flows from a set of extreme rainfall events. The model presented here was designed with the capability to satisfy this scope and more results are presented below. Prior to discussing the distributed results, the validity of the model and its ability to discern the hydrological affects of wetlands must first be established.

As with any modelling exercise, the ideal objective of creating an exact replication of real-world processes cannot be achieved due, in part, to epistemic uncertainty. This uncertainty will always prevent the model from providing definitive answers typically demanded from such a modelling exercise, unavoidably resulting in model uncertainty.

Epistemic uncertainty is closely tied with parameter uncertainty—the limit a parameter value can practically be "known," which can, in reality, only be reduced to a range of possible values.[1] Parameter uncertainty, combined with other sources of uncertainty, will emerge in aggregate as model uncertainty; that is, the limit model results will reflect real observation. Other sources of model uncertainty include (Beven, 2009):

1. Model structural error—associated with errors in model formulation, assumptions used in the model code, and the boundary conditions that define the model domain. For the most part, it is conjectured that the magnitude of structural error associated with the current modelling approach can be deemed negligible relative to parameter uncertainty, because:

    a. The selected model code is well tested and is the most comprehensive model code in terms of the physical processes incorporated, which reflect current and established physical theory; and,

    b. The initial and boundary conditions are hypothetical (yet realistic) by design (§**??**); therefore, the dependence of boundary conditions on model results is circumvented. Otherwise, this dependence would have implications on the results if the established calibration-validation approach was taken (see Stephenson and Freeze, 1974).

[1] Similar to the idea of a feasible range discussed in §3.3.2.

2. Modeller uncertainty—associated with the interpretations and assumptions made by the modeller during the conceptualization phase. (This report serves to document the procedures taken by the author to as much detail as possible. It is encouraged that the methods described herein be challenged for the sake of addressing potential biases that may result in differing conclusions.)

3. Aleatoric uncertainty—associated with the randomness inherent with all information. Such random errors tend to become negligible when interpreted (or averaged) over the long term or addressed through ensemble modelling (e.g., a multi-model approach as applied here—Matott et. al., 2009).

Parameter uncertainty

The multi-model approach (§3.3.2) employed for this study allowed for a direct quantification of parameter uncertainty. Section 3.3.3 described how the ensemble simulation was translated into a distribution of maximum flow depth[2] at every node within the model domain (82,668 nodes in total). The envelope bounding the uncertainty in simulated flow depth was quantified at every node on the basis of the distribution σ-bound, which is a measure of the degree to which parameter uncertainty translated into model uncertainty. This is similar to the at-a-station results (§4.1); except here, σ-bounds reflect the uncertainty in maximum simulated flow depth (Figure 3.8), rather than the σ-bound of the hydrograph distribution (Figure 3.6) which represents stream discharge.

It is important to note that stream discharge alone is not necessarily indicative of flood potential, and thus the results demonstrated thus far (§4.1) would not be fully capable of answering the study scope, not without additional modelling tools.[3] Only with the distributed model built here can the physics of water be properly accounted for, allowing streams to overbank and wetlands to drain, inundating (flooding) the CRW landscape as quantified from simulated flow depth.

For every wetland removal and restoration scenario (§3.4), changes in maximum flow depth (Δd) observed at any given node with respect to the baseline scenario can be compared against the nodal σ-bound (Figure 3.8). When maximum flow depth differences lie outside of the σ-bound from either an increase or decrease in depth relative to the baseline, hydrological change resulting from a change in wetland distribution is said to be statistically "significant." In other words:

> *Change to local (i.e., nodal) hydrology due to the loss (or restoration) of wetlands is beyond what can be attributed to the uncertainty associated with the model parameters.*

Furthermore, a secondary "very-significant" qualifier can be assigned to those maximum flow depth differences lying outside of the 2σ-bound, representing an assurance that wetlands have an influence on flood mitigation with 95% confidence.

Figure 4.8 illustrates a few samples of the significance testing. "Significance" is symbolized as a set of red and blue points, located at every model node. Two sizes of points are used to represent the degree of significance: largest for 2σ, and smallest for 1σ; the remaining (insignificant) nodes are left invisible. The colour red indicates a significant decrease in maximum flow depth, while blue represents an increase.

[2] Flow depth is defined as the depth of flowing water moving at some flow velocity.

[3] Additional 1D hydraulic modelling would be required, but would still be restricted to the Credit River floodplains and would remain incapable of addressing isolated wetlands.

The first sample (Figure 4.8b) shows the effect of the removal of a rather large connected wetland at Dragonfly Park, south of Orangeville under Scenario 3 and experiencing a 100-year event. The red coloured points around Dragonfly Park verify the effect of draining the wetland, since the depths within the wetland have decreased significantly. The effect of the Dragonfly Park wetland drainage caused a significant increase in maximum flow depth (blue points) within the floodplain immediately downstream, approaching Melville.

In this example, the flooding (blue coloured points) near Melville is occurring within a connected wetland, which under scenario 3 has been removed and is being drained. This suggests that the increase in depth associated with upstream wetland loss would have been unmanageable by the Melville wetland, should it have been preserved.

Not only does the Figure 4.8b example provide quantitative evidence of the role of wetlands under flood conditions, but it also serves to verify the methodology used (i.e., red points in drained wetlands).

Figure 4.8c illustrates the effect of removing non-PSW wetlands (Scenario 4) also under a 100-year event. The set of wetlands shown in Figure 4.8c were formed by a multitude of small depressions characteristic of the hummocky terrain on top of the Paris Moraine. In this particular case, the wetlands have been converted to agricultural land as part of the scenario (§3.4.3). As water is drained from these small isolated wetlands, the runoff that would have normally been retained and retarded is redistributed and quickly collects in low-land depressions, essentially pooling the drained water into nearby areas (outlined in red). The modelling suggests that the removal of these isolated non-PSW wetlands would result in a redistribution of water, placing it in areas that may have already been developed.

The redistribution effect illustrated in Figure 4.8c suggests a likely impact of draining many small-scale isolated CRW wetlands. The retention of rain water at these many wetland locations is spread over the landscape resulting in a greater groundwater recharge potential. Since these wetlands exist on top of the Paris Moraine, maintaining their groundwater recharge function will also maintain the ecological function of headwater streams flanking the moraine (Marchildon et. al., 2016); therefore, removing isolated wetlands may put these groundwater dependent ecosystems at risk.

Due to their isolated nature, decreased flood retention from the loss of isolated wetlands do not appear to affect flooding within the floodplains of the Credit River drainage network. Consequently, very few reaches identified as flood damage centres (FDC—§2.2.3), which are predominantly located along stream channels (see Figure 4.10 below), are significantly affected by the loss of isolated wetlands.

Some exceptions do occur in cases where isolated wetlands are in close proximity to an FDC; most notably, Norval just north of Guelph St. at Adamson St. (Figure 4.9). This highlights the nature of flood mitigation services of isolate wetlands: although their impact may not be as ubiquitous as connected wetlands, they continue to provide a service, generally for lands in close proximity. This then would counter the assumption made by many authors that isolated wetlands do not provide flood protection services at all (§1), it just happens that their impact cannot be measured from a streamflow hydrograph.

Figure 4.8d illustrates the gains associated with the restoration of wetlands after a 2-year event. Here, the blue points continue to indicate a significant increase in maximum depth, but in this case, that is by design. Introducing wetland restoration by means of an impoundment (§3.4.4) has increased the retention capacity of the wetlands providing for significant reductions (red points) in flow depths downstream, as the Credit courses through downtown Mississauga. Note the presence of blue points located within the boundaries of the restored wetlands, confirming the method used to impound water within these sites (see §3.4.4).

As this example reflects a relatively frequent (i.e., once every other year) extreme event, the benefit associated with the increase in water retention would be accrued just as frequently. It is evident that the value of wetland restoration has the potential to save the City of Mississauga from considerable costs associated with damaged infrastructure and property, and could even have the potential to save lives (see §4.3 below).

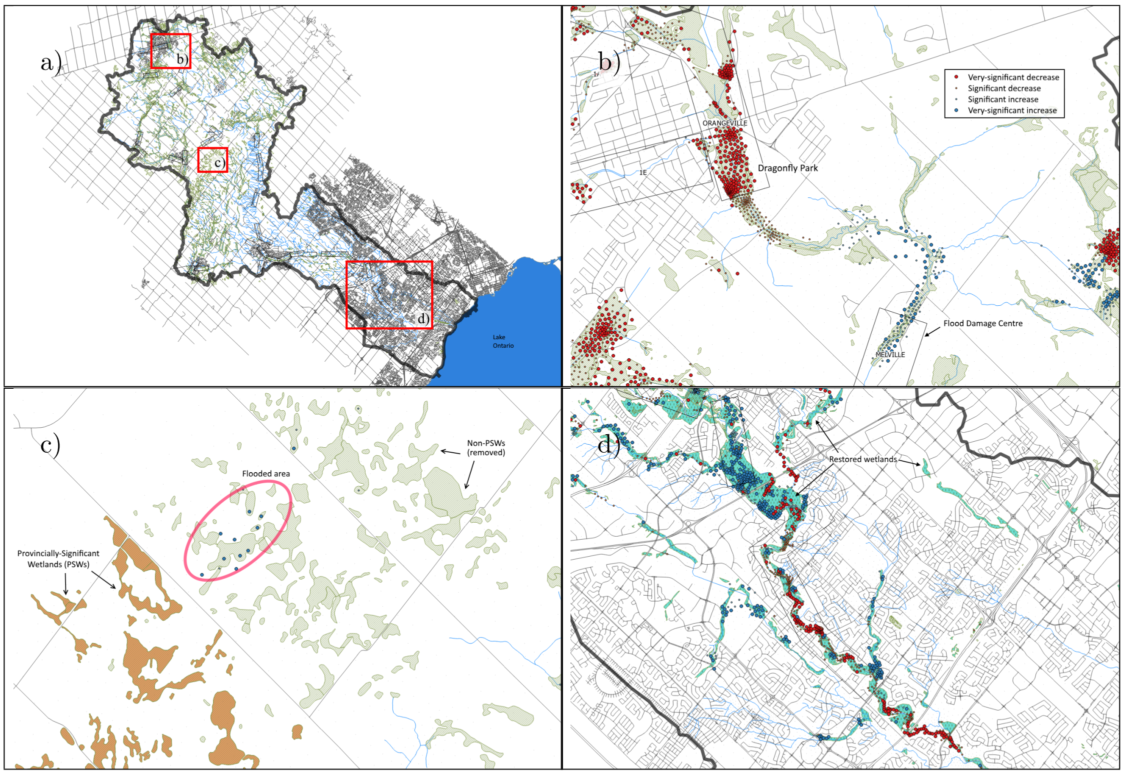

Figure 4.8: Close-ups of the significant flooding test results. Figure a) shows the location of b), c), and d). (Note: density of points relate only to mesh design (§3.2.1), and is not indicative of flow depth significance.)

4.2.2 Hydrological significance, basin-scale

Figures 4.11 through 4.16 present the significance mapping at the basin-scale with respect to the CRW FDCs (Figure 4.10). These maps were prepared by aggregating model significance testing from all event scenarios. First, every element was screened and was deemed significant if any of its adjoining nodes were themselves deemed significant. If significant, the element was then given a score equivalent to the probability of event occurrence (i.e., the reciprocal of the event return period). Scores were then accumulated for all 7 events (2-, 5-, 10-, 25-, 50-, 100-, and 500-year return storm), for a maximum possible score of 0.872. (Note: elements that not coloured demonstrate insignificant changes to flow depth.)

The scores mapped in Figures 4.11 through 4.15 provided for a relative scale flood vulnerability (in terms of potential significance) associated with the loss of wetlands. Figure 4.16, on the other hand, uses the same relative scale to rate the potential gains associated with wetland restoration.

Like the at-a-station results, the total wetland loss (Scenario 6, Figure 4.15) closely resembles the results from the loss of connected wetlands only (Scenario 3, Figure 4.12). It is apparent from this resemblance that the function of connected wetlands outweigh that of isolated wetlands in terms of flood flow reduction in the Credit River, particularly within the flood prone widths of the Credit River network in the upper watershed.

To begin, Scenario 6 represents the worst-case scenario in which all wetlands within the model were drained (Figure 4.15). The all-wetland loss scenario appears to be an aggregation of the previous loss scenarios and the same flood hazard conclusions discussed above apply here. This finding suggests that future modelling effort may be able to avoid this worst case scenario, and the results from all other scenarios can be accumulated in its place.

In all, 72% (23 of 32 FDCs) were affected by the loss of some wetland in terms of increased flood potential. Four FDC regions (Figure 4.10) that did not appear to be affected from wetland loss included:

1. West Credit River upstream of Hillsburgh (FDC 6A);
2. Ferndale Park and Terra Cotta—the reach from Inglewood to Glen Williams is a 15-20 km stretch of the Credit River with little added contributing area;
3. Silver Creek in Georgetown (FDC 16A, B, C, D); and,
4. Fletchers Creek, west Brampton (FDC 19B and C).

Scenario 2—Loss of isolated wetlands: Although not too extensive, the flood mitigation function of isolated wetlands is present (Figure 4.11). Their hydrological effects appear to be isolated themselves, generally localized in close proximity to the wetlands that have been removed, such as in Norval (Figure 4.9). Another implication, reduction in flow retention caused by the loss of isolated wetlands on top the Paris Moraine (Figure 2.2) tended to be immediately collected by the hummocks in the surrounding terrain. In this way, much of the flood increase caused by the removal of isolated wetlands never reached the Credit's drainage network.

Scenario 3—Loss of connected wetlands: Modelling indicates that the removal of connected wetlands results in a significant increase in flooding at many locations along the Credit River, including a number of upper CRW flood damage centres (Figure 4.12). In particular:

1. the Melville flood damage centre just downstream of Orangeville and the Black Creek reach between Acton and Georgetown appear to be quite affected by the loss of connected wetlands;
2. the Erin (west) branch of the Credit River from Hillsburgh through Belfountain also appears to lose flood protection from the loss of connected wetlands (FDCs 6B, 7A, 7B and 8A);
3. Caledon Creek upstream of Caledon village (E:580,000; N:4,860,000);

4. the Ken Whillans Resource Management Area at the north end of the Inglewood FDC; and,

5. Caledon Lake south of Orangeville (near FDC 3A).

The modelling results of Scenario 3 closely resemble that of Scenario 6, and justify the assumptions made by earlier modelling studies that only riparian wetlands have a role in flood control (§1). However, this justification does not, in turn, justify the used on a lumped parameter or semi-distributed model (see §3.1); rather, as illustrated (again) by the Scenario 2 results, wetland flood retention of isolated wetlands is location dependent, and likely have some flood control, just not with respect to fluvial flooding in particular.

Scenario 4—The loss of non-PSWs—demonstrated, like Scenario 2, that the flood retention offered by non-PSW wetlands is located in areas proximal to the wetlands themselves (Figure 4.13) and thus not necessarily offering fluvial flood protection. (Recall, from §2.2.1, that many non-PSWs are isolated themselves.) That said, there are exceptions, such as significant flood potential observed in the Orangeville and Brimstone FDC's for events exceeding the 2-year return.

Scenario 5—near-term potential loss—consisted of a set of wetlands that are typically isolated and exist along the CRW watershed divide. Like Scenarios 2 and 4, the hydrological affect of losing the wetlands subject to potential near-term loss tend to be isolated to areas surrounding the wetlands themselves (Figure 4.14). Although no FDCs appear to be directly affected, one particular area of west Brampton near Creditview Rd. and Bovaird Dr. W. (E:595,400; N:4,836,000) is experiencing additional flooding due to the loss of a wetland currently being developed as a residential area.

Scenario 7—wetland restoration: Prior to discussing the results, it is important to recall that the majority of the CRW wetlands exist within the upper watershed, above the Niagara Escarpment. The lower CRW has experienced extensive development in the past which has led to the removal of numerous wetlands (DUC, 2010). Not surprisingly, most of the potential restoration sites lie in the lower CRW (Figure 3.10).

Consequently, most of the gains (i.e., reduced flood potential from the restoration of wetlands) occurs in the lower CRW (Figure 4.16). The communities of Orangeville, Georgetown, Brampton and Mississauga all appear to benefit from significant flood reduction. All but 12 FDCs, all of which exist in the upper watershed, experienced a reduction in maximum flow depth as a result of the restoration scenario.

As was clear from the resemblance of the Scenario 2 and 6 results, the effect of wetland flood retention appears to be additive. From this, Scenario 7 results could represent the increased flood potential caused by historical development, which neglected the preservation of the existing wetlands. Fortunately, much of what has been lost in terms of flood mitigation potential can be regained, and future costs associated with poor development planning can potentially be mitigated.

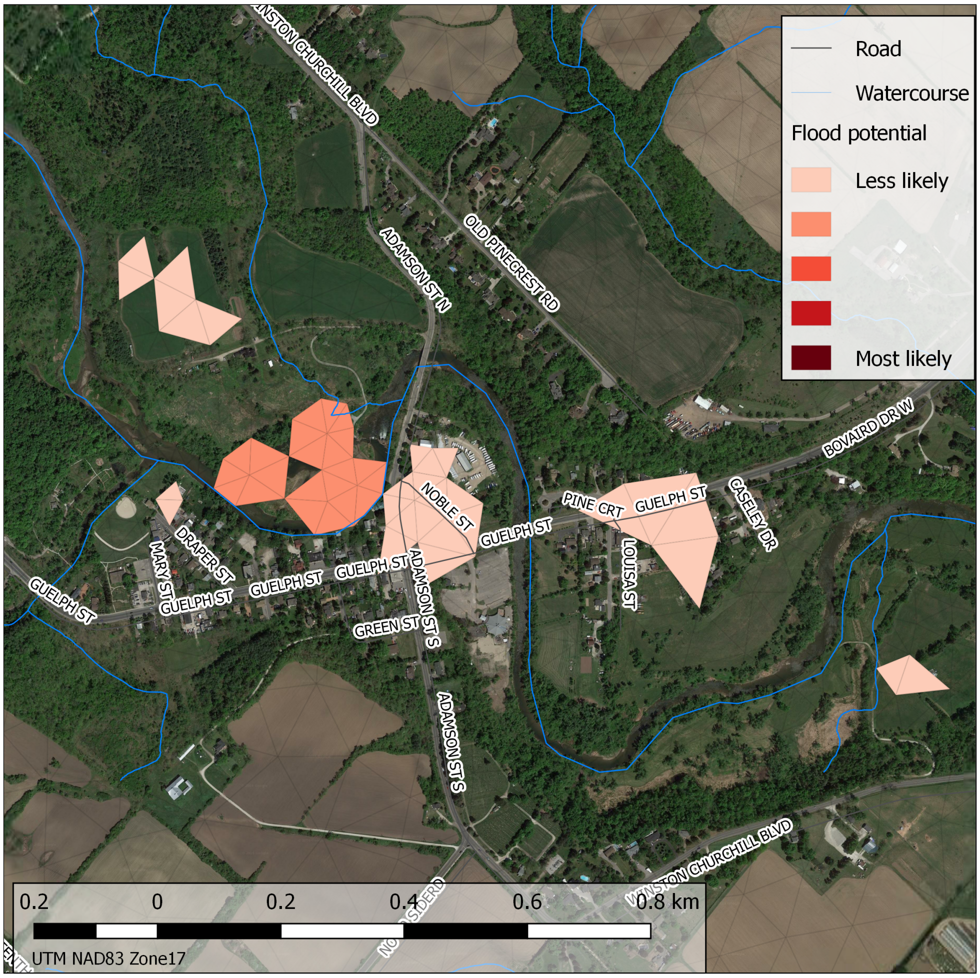

Figure 4.9: View of flooding potential within Norval due to the loss of isolated wetlands.

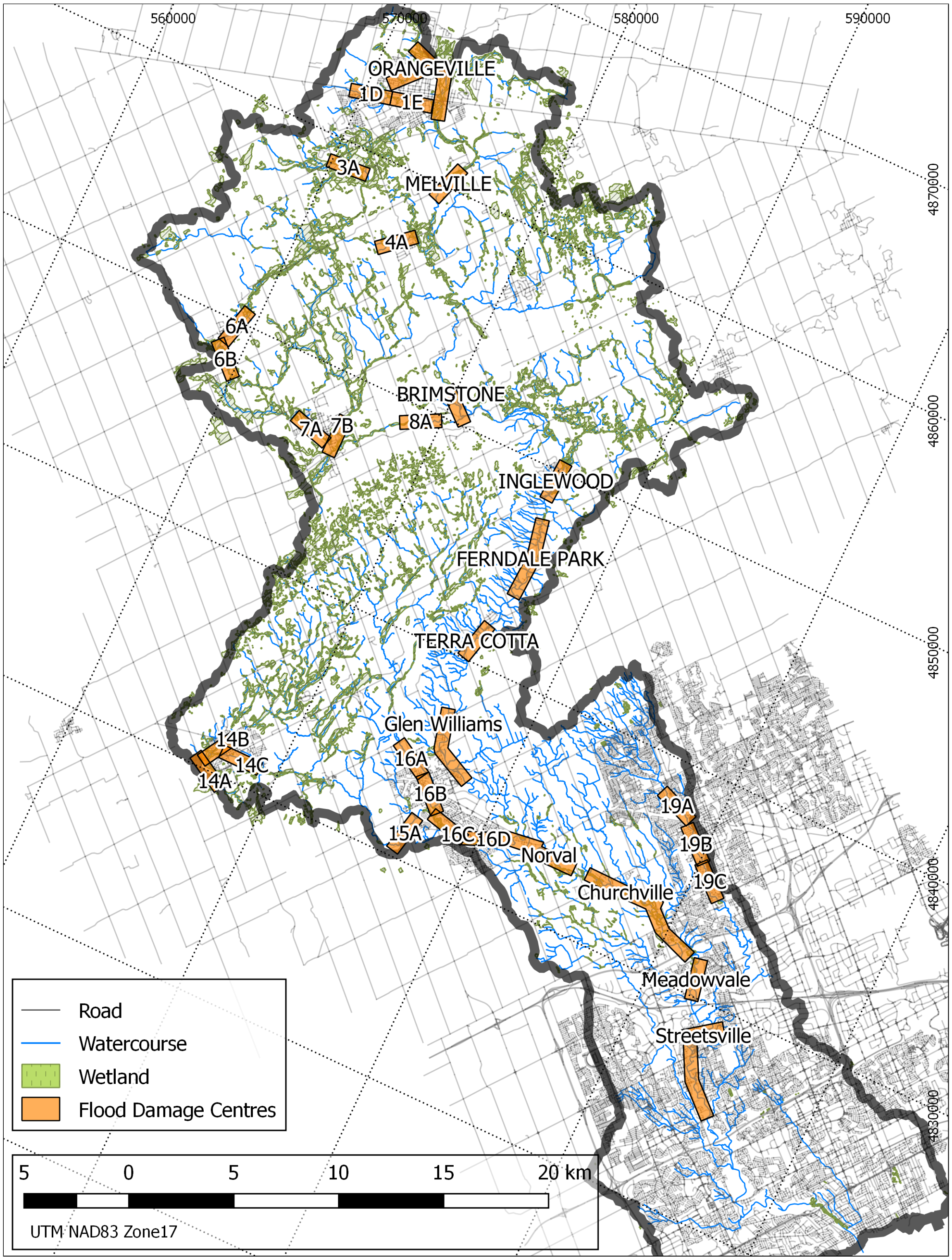

Figure 4.10: Flood damage centres within the CRW.

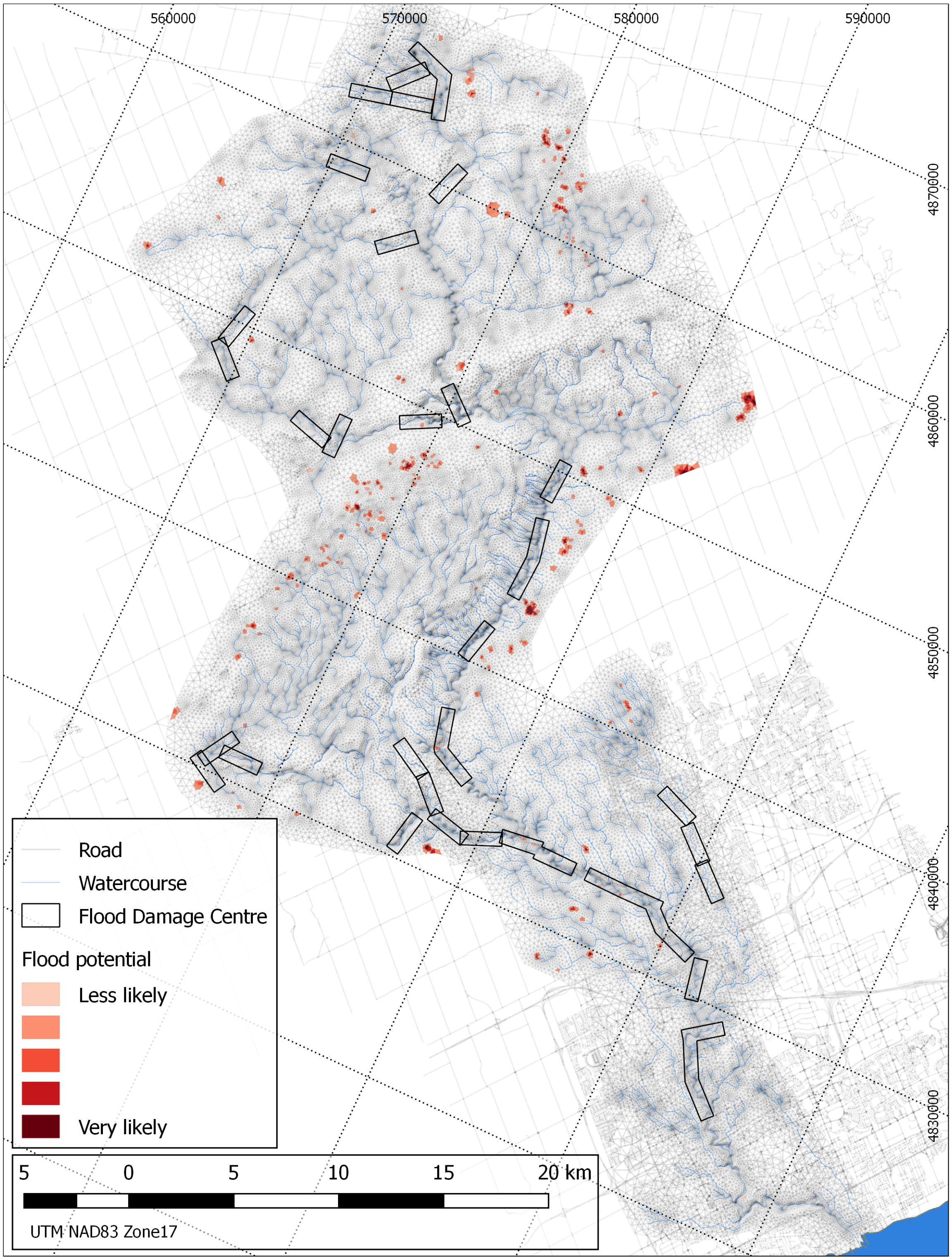

Figure 4.11: Basin wide significant flood potential mapping, Scenario 2: Loss of isolated wetlands.

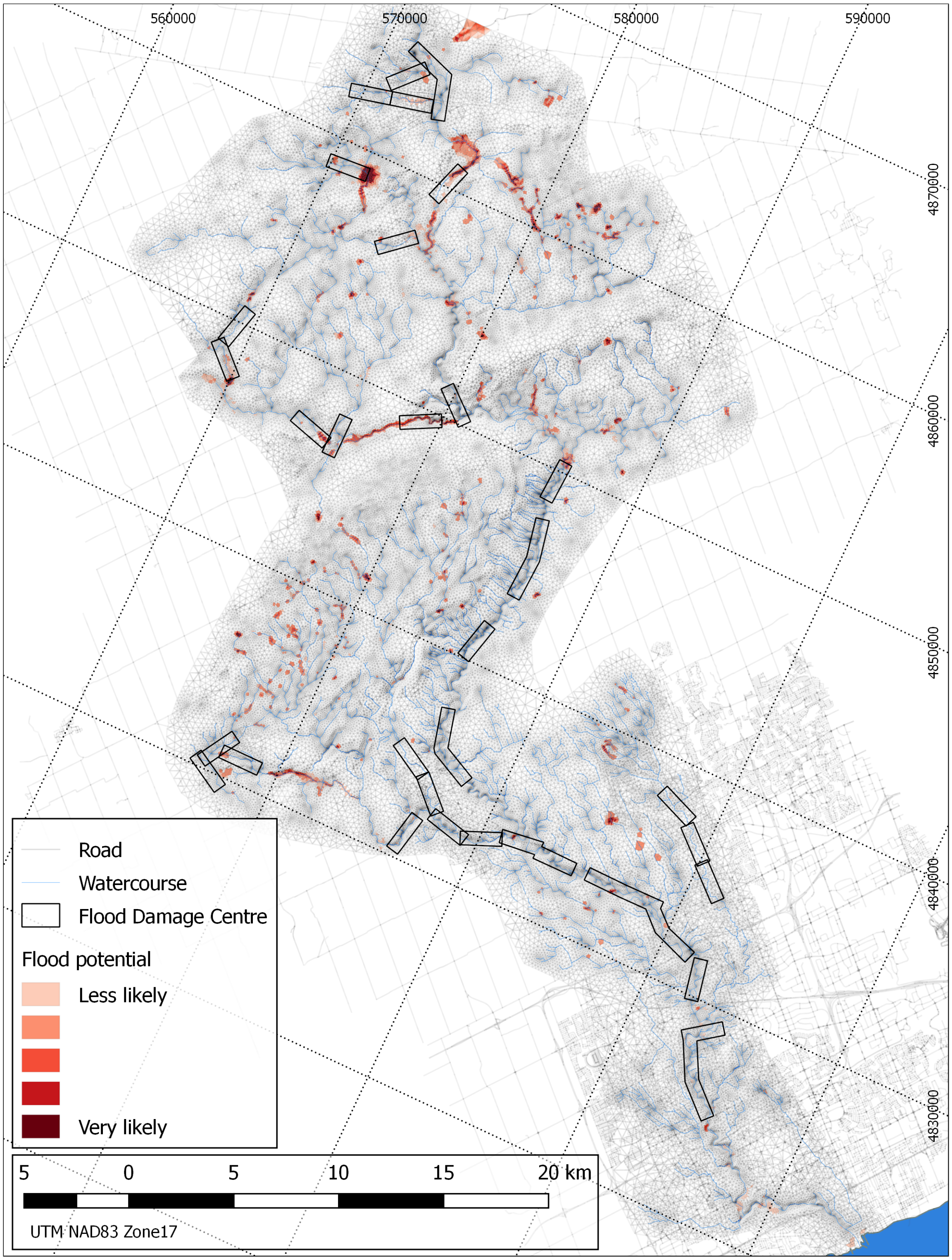

Figure 4.12: Basin wide significant flood potential mapping, Scenario 3: Loss of connected wetlands.

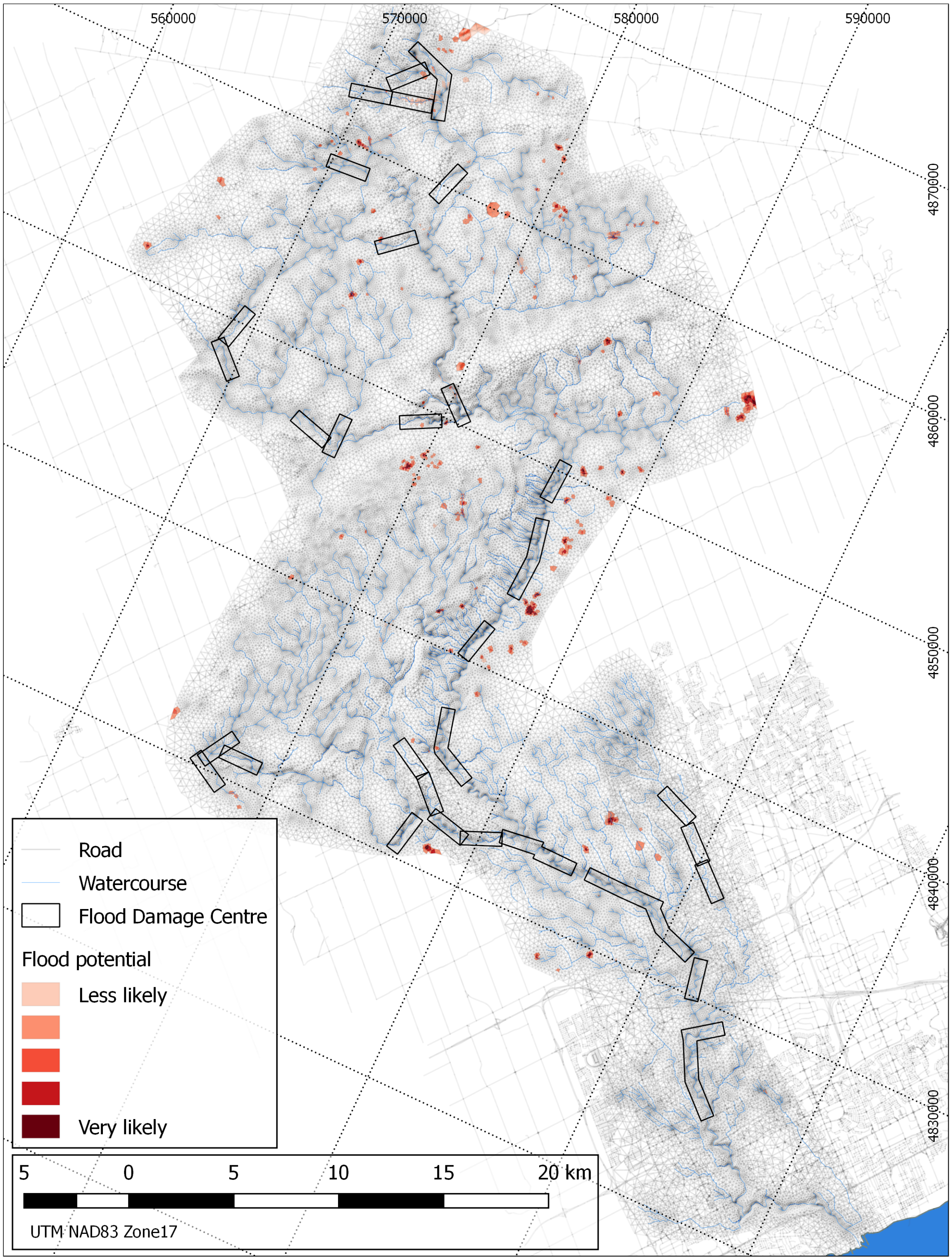

Figure 4.13: Basin wide significant flood potential mapping, Scenario 4: loss of non-Provincially significant wetlands.

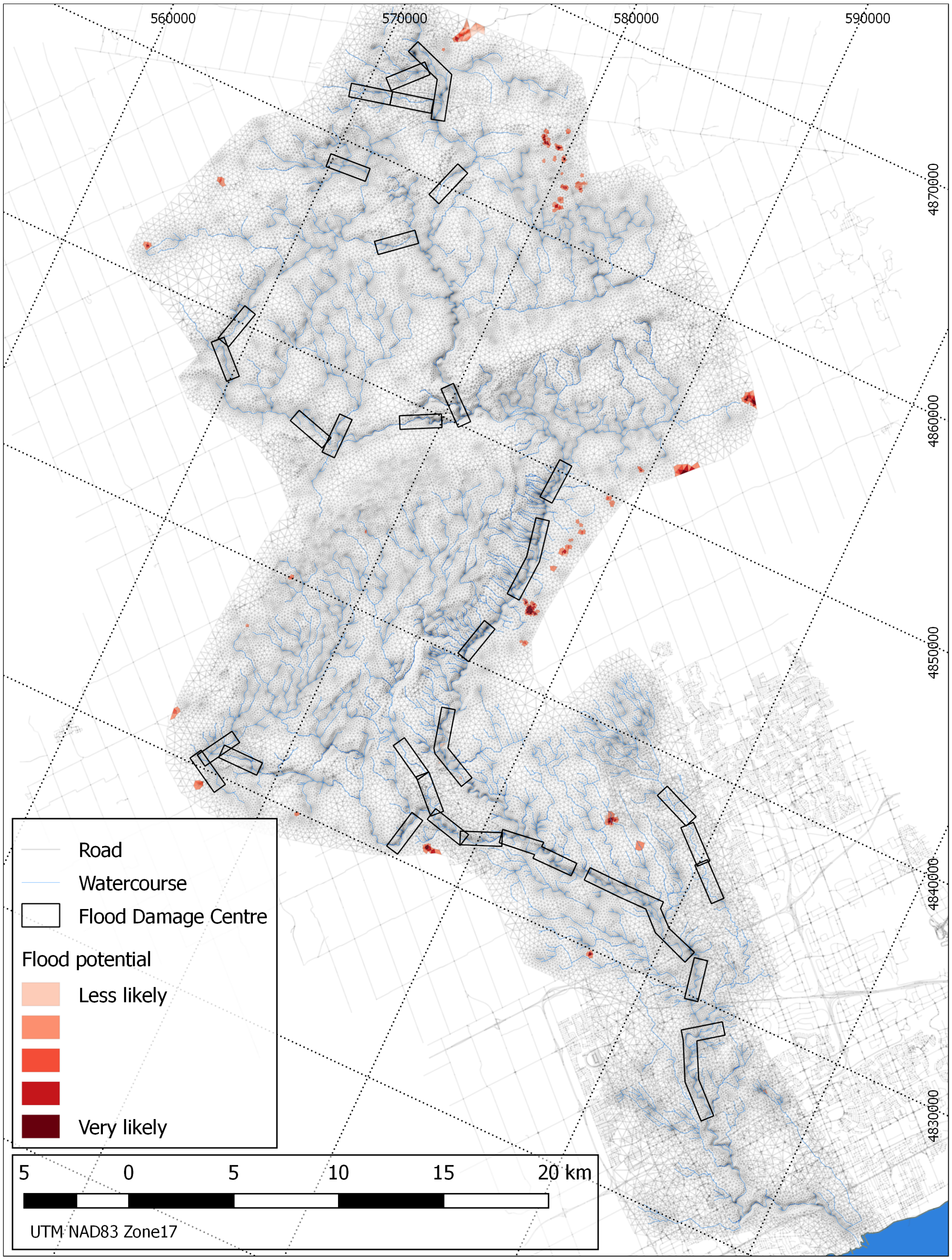

Figure 4.14: Basin wide significant flood potential mapping, Scenario 5: Near-term wetland loss.

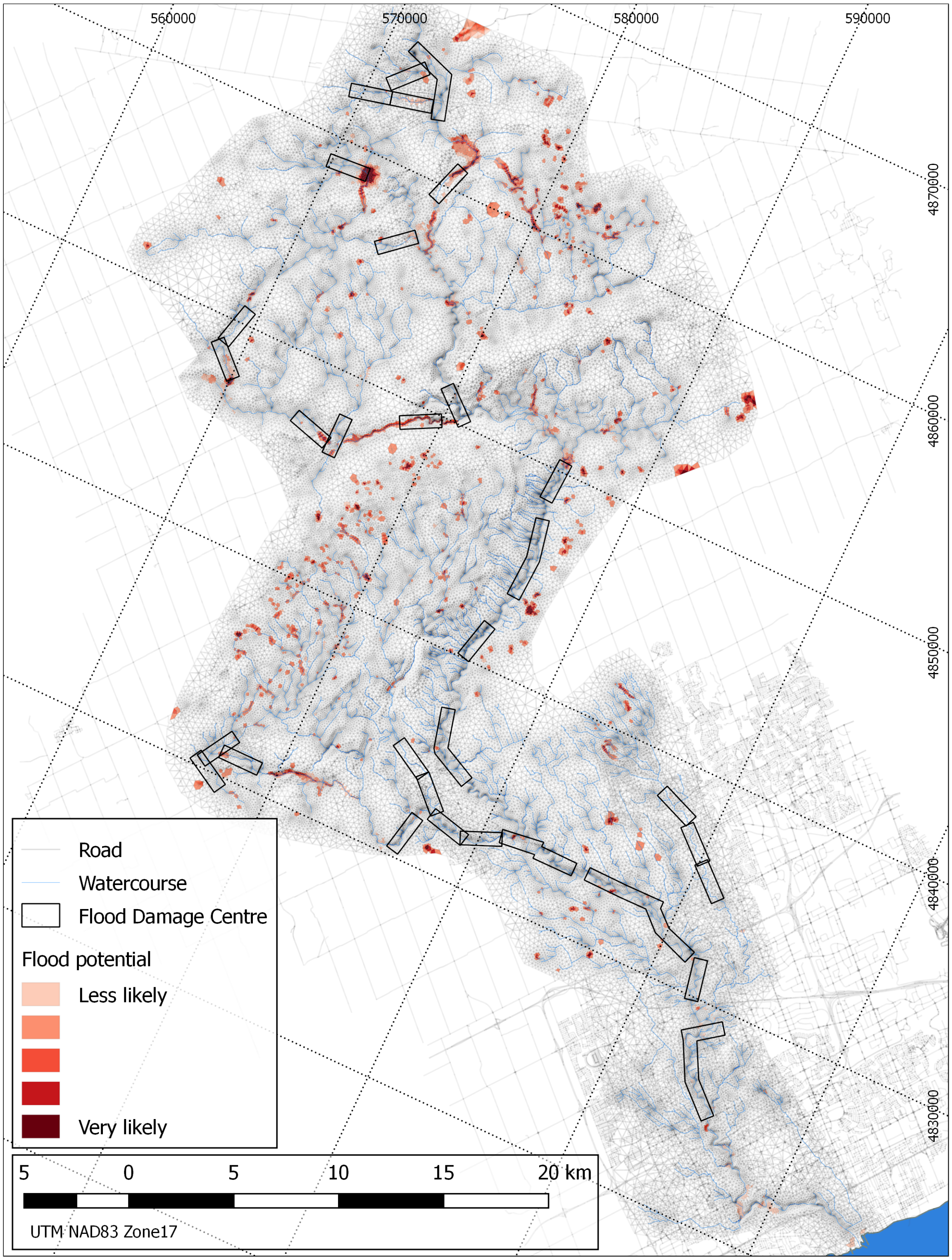

Figure 4.15: Basin wide significant flood potential mapping, Scenario 6: Loss of all mapped wetlands.

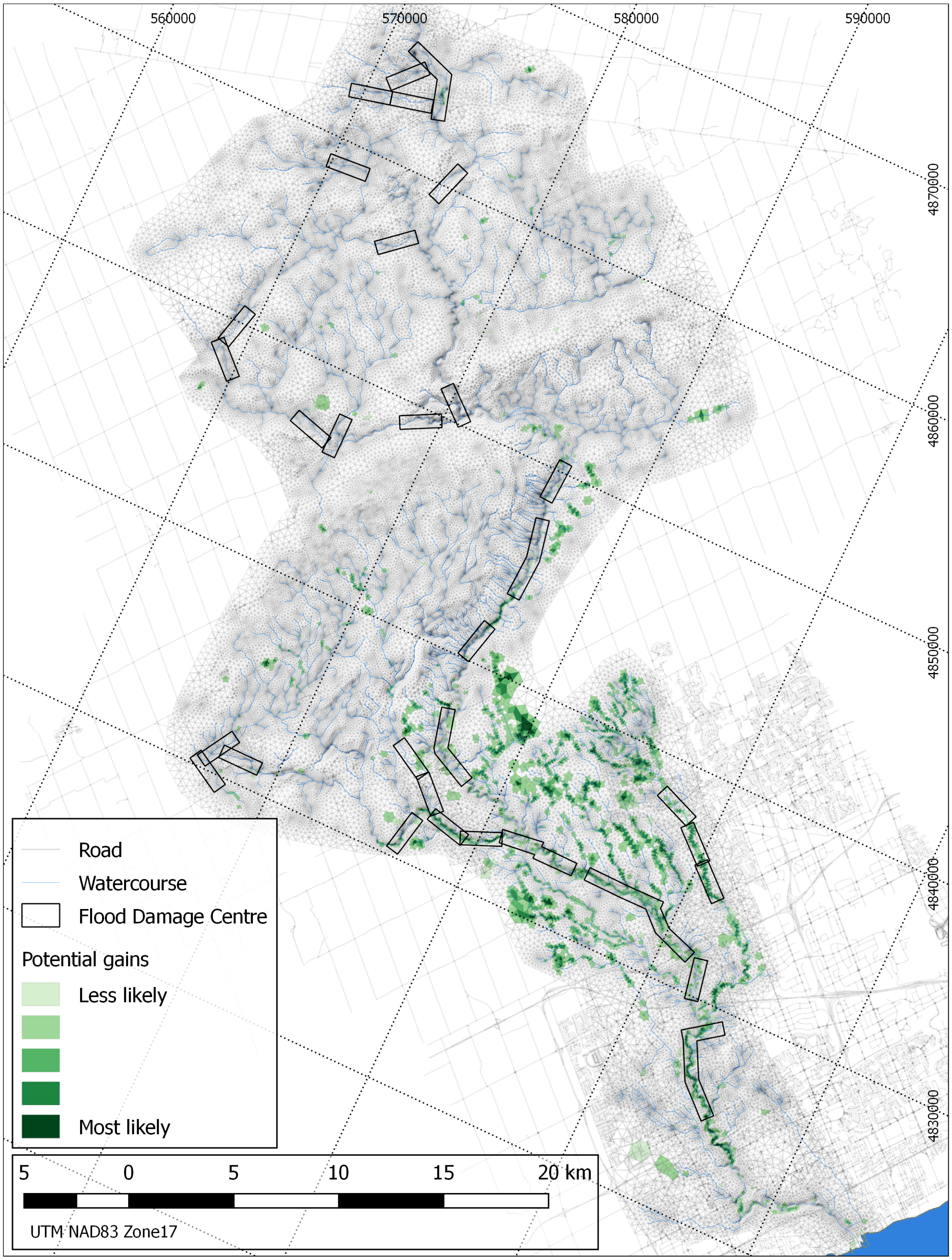

Figure 4.16: Basin wide significant flood reduction based on Scenario 7: Potential restoration.

4.3 Evaluation of hydrological change

With 7 scenarios, 7 extreme events, and 4 overland flow metrics (§3.5) reported for each of the 192 timesteps over the model domain consisting of over 160,000 elements, it would be quite onerous to report all of the model findings here. To save from including hundreds of figures within this report, the following section provides an overview of the how the output data can be used and interpreted.

As part of the deliverable of the model, all of the model output data that could potentially be reported here will be available for future analysis. The intention of the model design, in addition to meeting the model scope (§1.2), was to provide for a variety of simulation results covering many water quantity metrics that would be useful for future analysis, including the Phase III portion of this study that will conduct an economic valuation of the ecosystem services of wetlands within the CRW (1.1). The suite of model output metrics that are available include (§3.5):

1. Flow depth
2. Flow velocity
3. Velocity-depth
4. Depth-duration
5. Groundwater exchange (i.e., infiltration and seepage)
6. Sub-surface saturation
7. Sub-surface total head (including pressure)
8. Shallow sub-surface groundwater flux

With every parameter having outputs for 49 separate scenario model runs, a dataset in excess of 6–7 GB of single-precision data was produced per parameter. As the scope of the current study is limited to flood (i.e., overland) flow processes, only the first four of the above output metrics are discussed below. Furthermore, since these parameters are output as a time series of 192 15-minute time steps, the 192 outputs are reduced into a single result so they can be discussed in an aggregate form. Flow depths, flow velocities and velocity-depths are aggregated by reporting the maximum recorded value at each node/element; while depth-duration in itself is an aggregate result (Equation C.10).

Below presents a sample discussion of changes to flow metrics at specific/focused locations within the CRW. Both flow depth and flow velocity are discussed in the Dragonfly Park region immediately downstream of Orangeville, velocity-depth is discussed for Mississauga where it has greater implications to human safety, and depth-duration is discussed for the Credit River west branch in the Georgetown-Action area and above the Paris Moraine. See Figure 4.8a for reference.

Changes to maximum flow depth

Flow depth is an obvious metric to quantify flood extents. For example, depth-damage curves, a function that relates flow depth to potential property damage, is a common tool used by storm water engineers when assessing flood vulnerability and risk. Figure 4.17 illustrates the extent of increased/decreased flooding south of Orangeville (i.e., the upper CRW) under a 100-year event simulated by the model. The results illustrate how the various wetland scenarios affect the CRW hydrology relative to current (baseline conditions)—determined by subtracting baseline (Scenario 1) flow depths from the remaining scenarios. For reference, OMNR (2002) states that flow depths greater than 1.4 m would put the average person at risk. Recall the scenarios sequence as follows (§3.4):

Scenario 1: Baseline (existing) conditions
Scenario 2: Isolated wetland loss
Scenario 3: Connected wetland loss
Scenario 4: non-PSW loss
Scenario 5: Near-term potential loss
Scenario 6: All wetland loss
Scenario 7: Potential wetland restoration

Scenarios 2 and 5 continue to reveal similar consequences as many of the near-term loss wetlands tend also to be isolated and exist along the CRW perimeter (thick shaded line in at the top of the 4.17 Figures). Note, however, that from these Figures, it is evident where the wetland draining occurred by the brown colour-coded elements.

Scenario 3—loss of connected wetlands—continues to show the greatest impact in terms of maximum flow depth augmentation. Wetlands lost in Orangeville have an immediate effect to wetlands upstream of the Melville FDC. Wetlands draining in and around Caledon Lake next to FDC 3A appear to augment the Lake's levels, and increases flood depths downstream of the Lake's outlet into the west Credit.

Scenario 4—loss of non-PSWs—has an immediate impact to the Dragonfly Park wetland next to Orangeville's waste water treatment plant (note that this change in depth was not found to be significant relative to model uncertainty). Nonetheless, there is a marked change to wetland flooding at Dragonfly Park and may warrant further investigation.

Again, Scenario 6—all wetland loss—is an aggregate of the remaining four wetland-loss scenarios. Interestingly, due to the additional water added to the Dragonfly Park wetland from the loss of non-PSWs (Scenario 4), a greater reduction in Dragonfly Park wetland flow depth has occurred compared with Scenario 2. This can be attributed to the support the Dragonfly Park wetland has from local (non-PSW) wetlands, where water drained from the Dragonfly Park wetland is replenished through groundwater seepage originating from recharge at surrounding wetlands. By draining the local (non-PSW) wetlands, the supporting seepage rates are suppressed, further lowering flow depths in the Dragonfly Park wetland. This also warrants further investigation.

Since much of the potential wetland restoration exists in the lower watershed, gains from flood reduction in the upper watershed is limited to: i) the Orangeville FDC; and, ii) within the Credit River immediately downstream of the west Credit confluence in the south-west corner of Figure 4.17.

Changes to maximum flow velocity

Like flow depth, flow velocity is also a natural metric for quantifying potential flood-incurred damage. While depth alone can only indicate areas on the landscape that are inundated, velocities have the effect of transporting material from sediment, to people, to trees that can result in further damage. Velocities are also indicative of erosion and scour potential which could have direct consequences to buried infrastructure. Figure 4.18 illustrates the distribution of flow velocity changes under the various wetland scenarios exposed to a 100-year rainfall event.

To reiterate, the model was designed with future utility in mind. The flow velocity maps are quite amendable to sediment transport analysis through the use of many soil loss formulations, such as the Modified Universal Soil Loss Equation (MUSLE), the Watershed Erosion Prediction Project (WEPP), the Agricultural Non-Point Source model (AGNPS), the Areal Non-point Source Watershed Environment Response Simulation (ANSWERS) model, or the Chemical Runoff and Erosion from Agricultural Management System (CREAMS) model (Singh, 1995; Merritt et. al., 2003). This flexibility was obtained by ensuring for a process-based, fully-distributed model design that allows for the highly discretized flow field needed for sediment transport analysis and yield quantification.

As a reference, flow velocities ranging from 0.8 to 1.5 m/s can, in general, cause unwanted erosion around building foundations, depending on other factors (e.g., vegetative, slope, etc.—OMNR, 2002).

Overland flow velocity is quite sensitive to wetland distribution. For all scenarios, there is clear impact to many model elements within the model domain. All but Scenario 5—near-term potential loss—look to have much of the upper CRW under the influence of wetlands in terms of overland flow velocity. Changes to the velocity are quite variable, with the general trend of flow velocities decreasing within drained wetlands and increasing around drainage features.

Although velocity may be indicative of potential sediment erosion/deposition, the metric on its own is quite deceiving without the context of depth. The model will continue to transport water over the land surface at inconceivable flow depths (i.e., $<$1 mm), which is unrealistic from a practical standpoint. Combining the metrics of velocity and depth is therefore more informative.

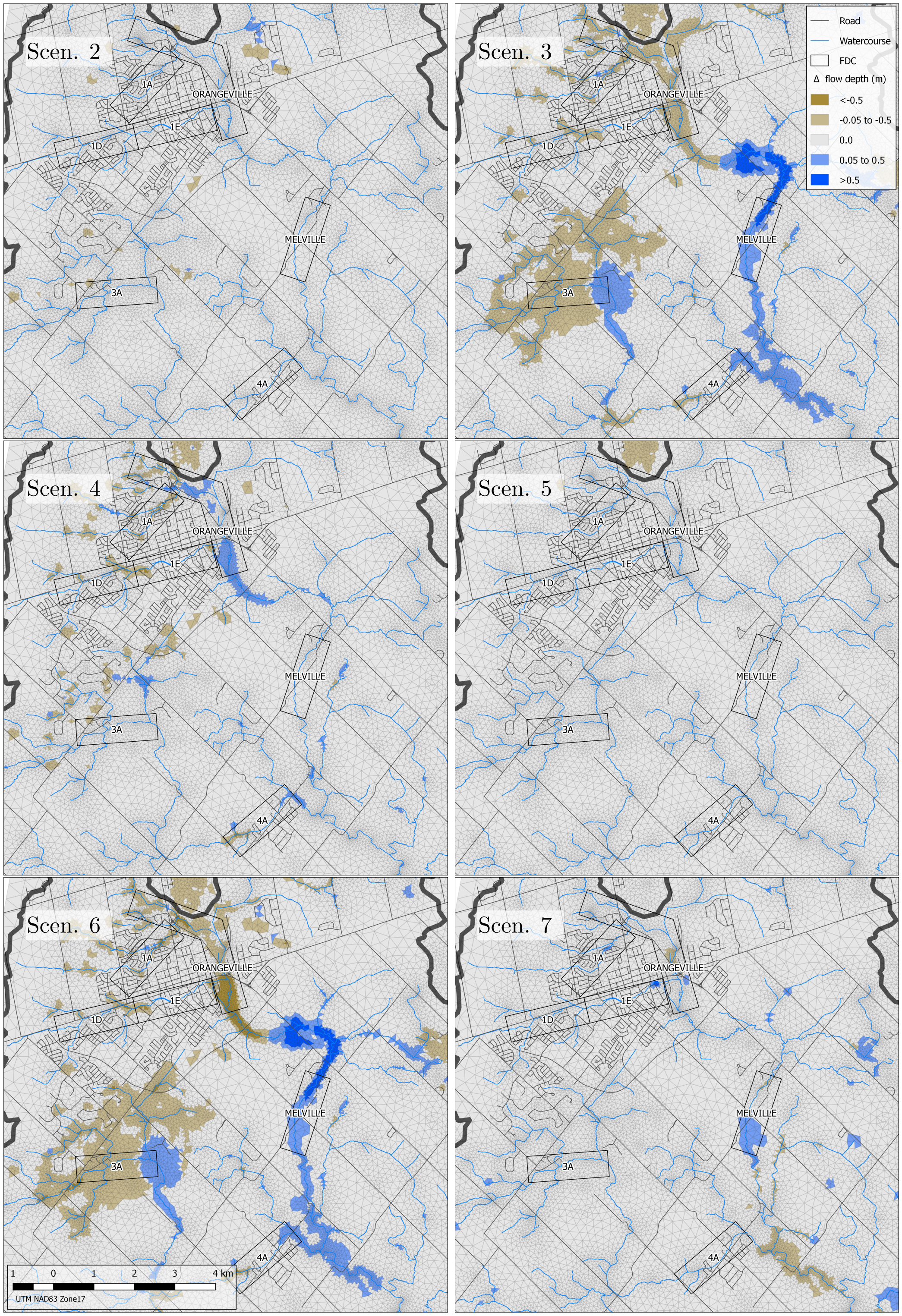

Figure 4.17: A comparison of changes (Δ) in maximum flow depth after a 100-year event between the 7 scenarios and the baseline.

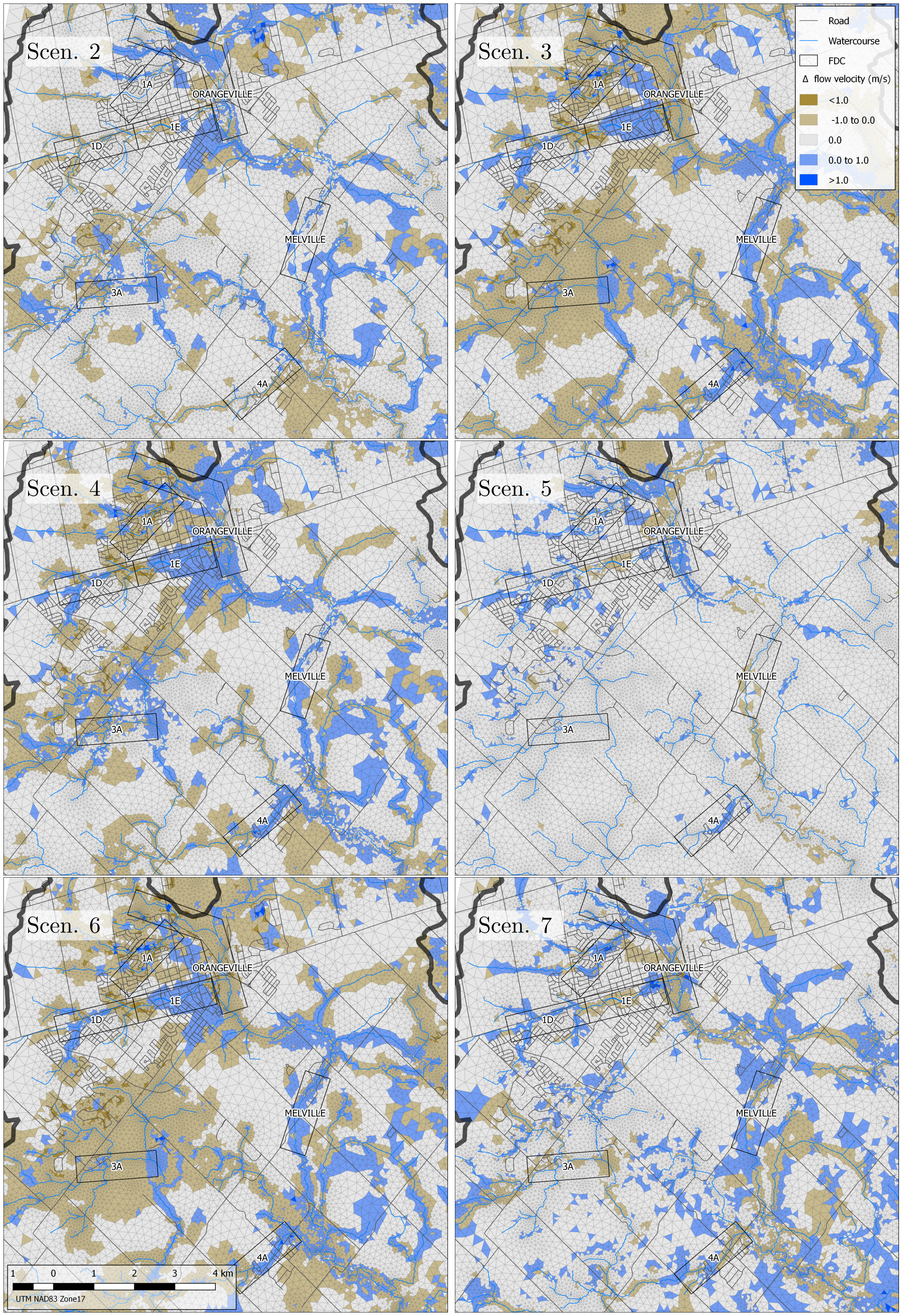

Figure 4.18: A comparison of changes (Δ) in maximum flow velocity after a 100-year event between the 7 scenarios and the baseline.

Peak velocity-depth

Velocity-depth is a combination of both flow velocity and depth (Equation C.9) commonly used as a criteria for safe access/egress for people. Mapping using this metric can help evaluate the dangers imposed on citizens from the various scenarios. The risks to a person being swept away by a flood is dependent on the buoyant force equal to the weight of water displaced by that person (a function of flow depth), and the moment and friction instability of a person standing in flowing water (a function of flow velocity—OMNR, 2002; Jonkman and Penning-Rowsell, 2008).

The OMNR (2002) technical guidance states that an average adult can remain stable standing in 1.4 m of water. For children aged 6–10 years old the stable depth reduces to 1.1 m, and <1 m for younger children. With the added momentum thrust of flowing water, a general rule-of-thumb for adult stability can be gauged by the 3×3 rule developed in the United States, relating to a 3 ft depth of water flowing at 3 ft/s ($\approx$0.8 m^2/s).

Results are available for the entire CRW, but discussion is reduced to one example showing how the results can be used. Figure 4.19 illustrates the velocity-depth distribution in Mississauga (location ⓓ in Figure 4.8a) for the baseline scenario experiencing 2- to 100-year events.

Within Mississauga, the Credit River valley is fairly incised and it is thus apparent that most of the human flood risk is situated within the floodplain regions. Other areas outside of floodplain region experiencing high risk include areas with local surface depressions, such as at the intersection of Erin Mills Pkwy. and Britannia Rd., near the centre-left of Figure 4.19, and the Hurontario and Queensway area, a known flooding "hotspot."[4] As expected, the severity of risk increases with increasing storm intensity, however, the extent of the high risk areas is roughly the same. Risk levels illustrated in Figures 4.19 and 4.20 are described in Table 4.2.

Table 4.2: Description of human-flood risk levels used in Figures 4.19 and 4.20.

Velocity-depth range (m^2/s)	Rule	Description
<0.09	—	No risk
0.09–0.37	$> 1 \times 1$	Low risk
0.37–0.84	$> 2 \times 2$	Low risk to adults, high risk to children
0.84–1.50	$> 3 \times 3$	High risk to adults
≥1.50	—	Extreme risk

Figure 4.20 contrasts human risk levels between the baseline and the potential restoration scenarios exposed to a 2-year rainfall event. Reduction in risk to human lives according to this velocity-depth rule-of-thumb is apparent, especially within Mississauga. Although the restoration scenario does not eliminate all high risk zones, it does reduce the risk at multiple locations. Any gains from reduced risk to human life results in the greater protection of Mississauga residents.

[4] http://www.t4tdrestoration.ca/flooding-restoration/flooding-hotspots-mississauga/

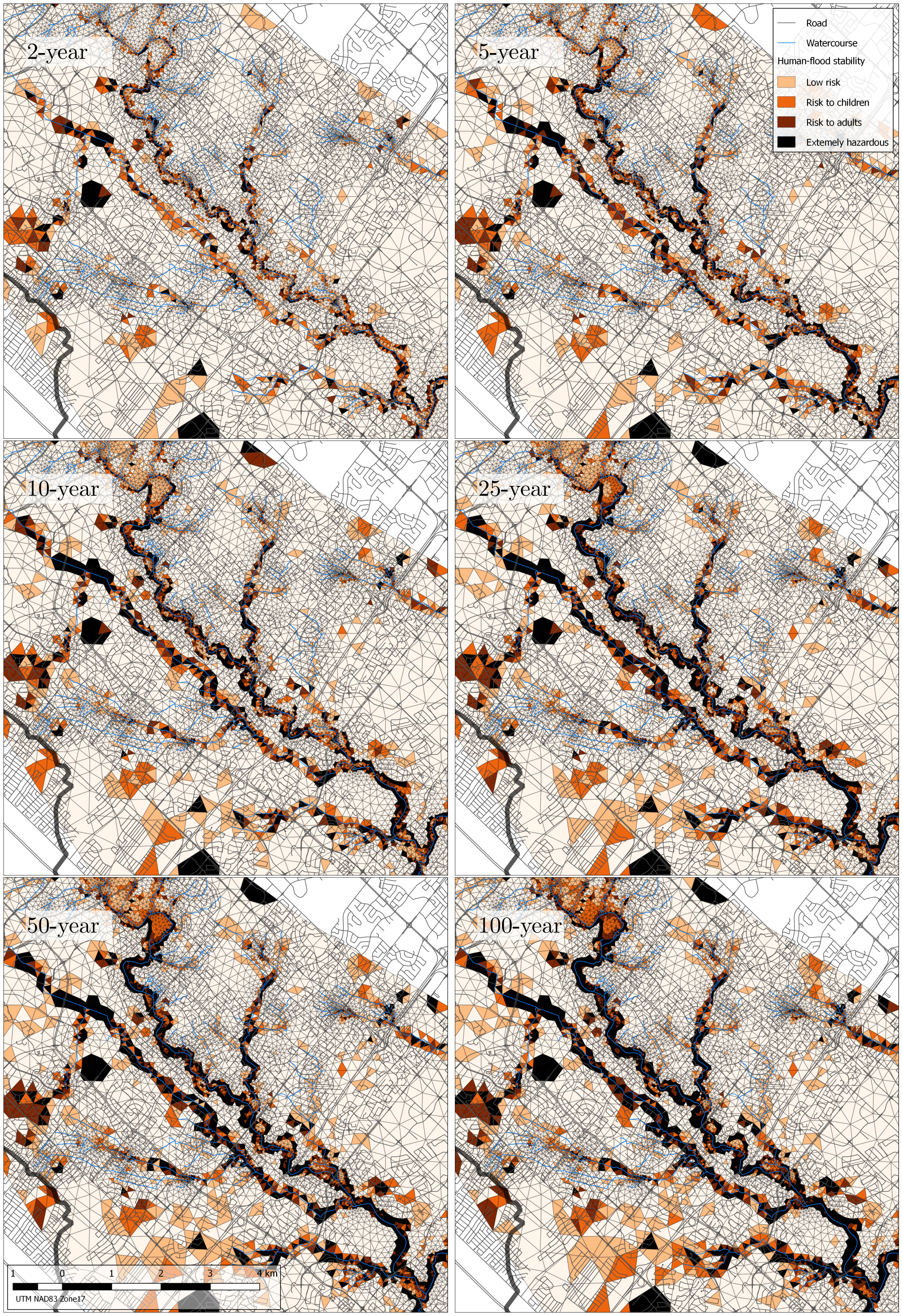

Figure 4.19: A series a results illustrating the degree of human risk associated with increasing storm intensity.

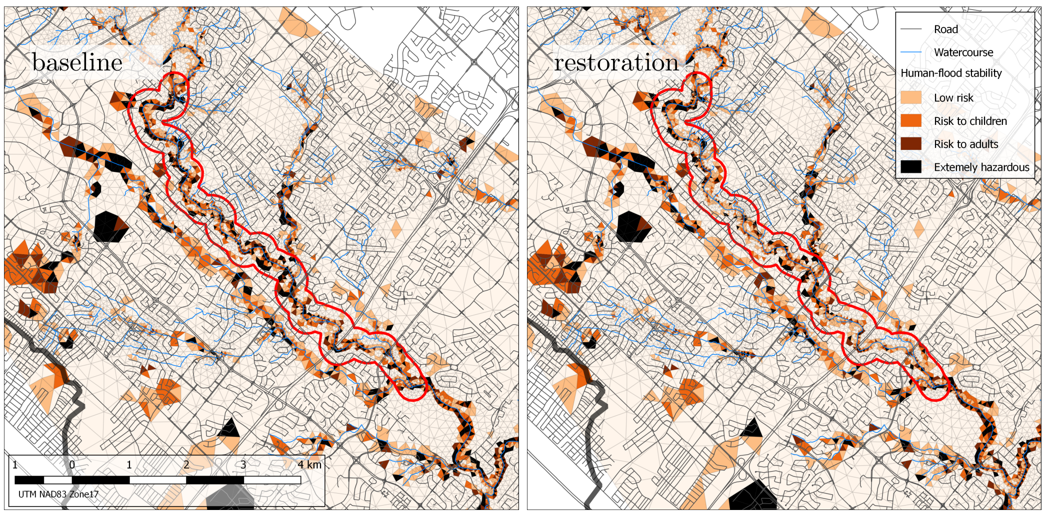

Figure 4.20: Evident reduction to the degree of human risk from a 2-year return event after wetland restoration efforts, especially within the Credit River mainstem between HWY 401 and Burnhamthorpe Rd. (outlined in red). (Note: size of elements relate only to mesh design (§3.2.1), and is not indicative of risk.)

Depth-duration

Depth-duration is an aggregate function that is essentially the average depth over the 2-day modelling period. Within the river valley, depth-duration relates to the efficiency of the channel to convey flowing water. The duration of inundation will also dictate the level of impact the flood may have on property and infrastructure as well as the degree of channel erosion.

Depth-duration can also be thought of as the total volume of water a landscape area is being exposed to, during an event, for any given model element. The greater the depth-duration, the more severe is the impact from flooding is likely to be. Figure 4.21 compares the baseline depth-duration for the 2- and 100-year event, in the Acton-Georgetown and Paris Moraine area. Comparisons among scenarios shows little discernable difference, especially at the watershed scale.

The depth-duration figures give a good interpretation of where water collects. Most notably, hummocky depressions on top of the Paris Moraine emerge, which stretches from north to south along the west edge of Figure 4.21. Contrast that with the high-permeability areas downslope of the Moraine that appear to remain dry, independent of storm intensity, based on the lighter shades of blue in Figure 4.21. Other than the mainstem Credit, which is expected to see an increase in depths from upstream sources, the rest of the depth-duration distribution remains more or less constant.

An exception would be the headwater streams coming off the Paris Moraine. These streams appear to swell with the 100-year storm. Interestingly, the added headwater flow depths occur without any apparent increase in depth-duration on top of the moraine. This area appears to remain below 1 cm on average. This is a sign of groundwater discharge being the primary source of the headwater stream flow, originating from the Paris Moraine and travelling through the shallow subsurface. The role of the moraine in supporting low-order streamflow illustrates a hydrological function of the CRW that could not have been correctly simulated without the use of an integrated groundwater/surface water flow model.

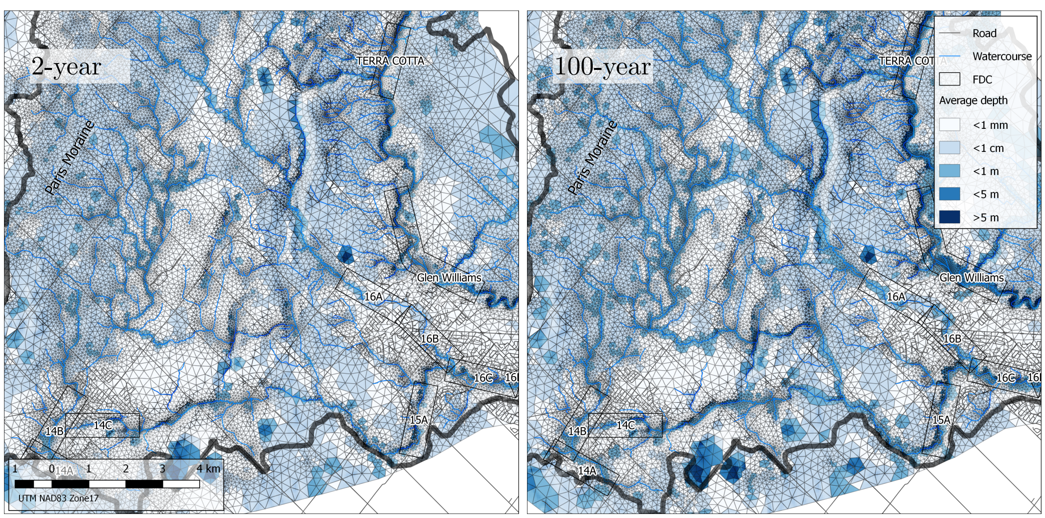

Figure 4.21: Comparison between the 2- and 100-year baseline event in terms of depth-duration (expressed as average depth of flow during the 2-day simulation).

4.4 Recommendation for economic analysis

This brief section discusses a potential avenue for how the results of this modelling effort can be easily translated into a basic economic valuation tool of wetland conservation and restoration. The method was inspired through discussions with Mr. J. Wilson of Green Analytics in 2015 prior to the design of the modelling strategy.

The economic analysis assumes a viable relationship between a model output (§3.5) and the cost of damage to infrastructure, property or perhaps the loss of life. Because of the flexibility in the modelling strategy, the economic analysis can be applied either:

- over the entire model domain;
- to sub-sections (e.g., individual communities) of the CRW; or
- to an accumulation of independent areas of interest (e.g., Flood Damage Centres—FDCs).

As an example, this section will utilize the velocity-depth metric, as it is a standard metric used by storm water engineers to assess risk due to flooding (OMNR, 2002). The assessment will also focus on the FDCs as they are representative of areas within the CRW that have immediate flood risk to property and infrastructure (§2.2.3). The economic analysis will also focus solely on three of the seven scenarios: Scenario 1: baseline; Scenario 3: loss of connected wetlands; and, Scenario 7: potential wetland restoration.

The economic valuation tool is presented in Figure 4.22. For the y-axis, the model metric of choice (in this case velocity-depth) is used to represent the relative severity of the extreme rainfall event. Ideally, the metric would be translated into a direct cost. This would first require a flood damage function to relate model outputs to a monetary value. On the x-axis, the return period of the extreme events allows for costs to be estimated for a given return period rainfall event.

Provided that the y-axis is translated into units of cost per annual maximum event rainfall ($/yr) and time (years) remains on the x-axis, then the area under a line in Figure 4.22 would equate to the value of flood retention service forecasted over an arbitrary period of time.[5] For example, the forecasted cost associated with the loss of connected wetlands over the next 25 years would simply amount to the difference between the loss scenario line and the baseline (red region), integrated from 0 to 25 years, which equals the area of the yellow-highlighted region in Figure 4.22.

Likewise, the time required to recover the cost of a wetland restoration plan can be determined by integrating the green region up to the expected final cost. The point where the integrated region extends in time (along the x-axis) will identify the required design lifetime where equivalent gains accrued through damage reduction outweigh the design costs (i.e., a simplified cost-benefit analysis tool).

The plot was created by averaging the elemental values within the area of interest, weighted by the elemental area. For this particular plot, velocity-depths less than $0.01\,\mathrm{m^2/s}$ were omitted.[6] The metric averages are then plotted against the return period relating to the extreme event from which the scenario was run.

[5]Assuming that the recurrence of a given return event can be predicted by a maximum order statistic (i.e., Gumbel distribution) for the arbitrary time period.

[6]Omitting these lower values eliminates bias caused by areas where flooding does not occur, and focuses primarily on flood-prone areas.

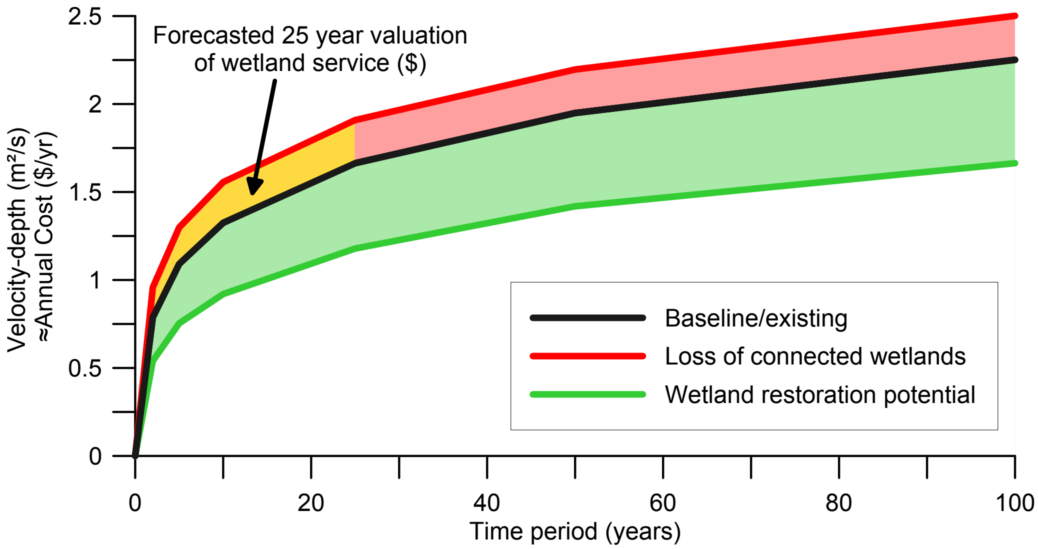

Figure 4.22: A sample of a potential means of performing an economic analysis from the model outputs.

Section 5

Conclusions

A numerical modelling study was conducted to resolve an outstanding question of watershed hydrology, namely: do wetlands have the ability to reduce flooding? Little quantitative analysis has been performed to date likely due to the danger inherent in measuring watershed response during high-flow (i.e., extreme) events. Consequently, wetlands have been said to have flood mitigation potential based on little more than anecdotes and intuition (see Maltby and Acreman, 2011). However, while hydrology has the knack of being counter-intuitive, an attempt had to be made to provide some form of quantitative support for this claim. If true, wetland preservation and restoration could be of high value to society, but in order to valuate the natural capital of southern Ontario wetlands, such quantitative support is required.

Section 1.2 provided the study scope for the investigation that followed. In short, the purpose was to determine whether wetlands have the physical capacity to reduce the impact of flooding from extreme rainfall events. Once the scope was confirmed, the study then proceeded to:

1. quantify the cumulative capacity of existing individual wetlands of any size, type, and proximity, to detain water from a set of high intensity storm events;
2. determine the relative effectiveness of wetlands of various size, type, and proximity to mitigate extreme pluvial events through the design of scenarios representing potential future wetland distribution; and
3. obtain a detailed set of hydrological response metrics for the purpose of informing an economic analysis to assist in assessing the natural capital of wetlands with respect to flood mitigation services.

Model selection and design

Quantifying the flood mitigation service provided by wetlands was accomplished using a numerical model. A rigorous process of model selection was performed as part of the model design. Ultimately, the model needed to be defensible and flexible to allow for future applications. A review of the Credit River Watershed (CRW) and the function of its wetlands, along with a review of previous wetland ecosystem service research, concluded that the model had to simulate:

1. distributed hydraulic processes in space and time;

2. hydraulic processes using established theory;
3. overland flow interactions with the shallow groundwater system; and,
4. all of these processes at sub-hourly time steps.

Using these criteria, it was found that many of the model-codes commonly applied to modelling wetland function were not applicable. The model code that was selected was HydroGeoSphere, a process-based, fully-distributed model that simulates groundwater/surface water interactions. The numerical model design ensured that the model remained purpose built for expandability, having the ability to model other factors affecting wetland function (e.g., frozen ground and nutrient loading, etc.).

The model was built for the entire CRW, a 950 km^2 mixed land use basin consisting of some 4,000 wetlands and 1,400 km of mapped drainage features. By developing novel methodologies to constrain the model domain, the resulting model was able to independently account for each wetland, ranging in size from 19 m^2 to over 100 ha. HydroGeoSphere permits the implementation of a flexible model mesh, which has allowed for the inclusion of every mapped drainage feature. This detail was deemed necessary as the model results were dependent on the multiple wetlands in contact with low-order streams.

Multi-model strategy

After a review of the information available for the CRW, it was revealed that no correlation existed between rainfall volumes and the resulting peak streamflow. Consequently, the available CRW data had insufficient information content required to perform model calibration and validation. Relative to rainfall volumes, the CRW storm response has a greater dependency on antecedent moisture conditions (with an added spatial dependency) and, to a lesser extent, rainfall distribution. Unfortunately, both antecedent moisture and storm distribution information are difficult to come by, especially when considering that extreme events are rare by definition. As an alternative to the standard calibration-validation approach, a multi-model ensemble approach, resembling an uncertainty analysis, was undertaken.

Antecedent moisture conditions was prescribed by adjusting groundwater potentials until mid-late summer observed median baseflows were obtained. This procedure, bounded by CRW topography and hydrogeology, helped distinguish those wetlands that are permanently inundated from those that are ephemeral.

Storm distribution was prescribed from an ultra-high resolution reconstruction of a 2015 southern Ontario storm event. Rainfall intensity was distributed using this normalized storm distribution field, keeping storm dynamics constant and thus eliminating any bias associated with storm distribution influences on runoff response. By scaling of the normalized field according the to 2-, 5-, 10-, 25-, 50-, 100-year return 15 minute intensities (as monitored by nearby IDF stations), plus the Ontario record 15 minute intensity to represent an absolute extreme, the rainfall distribution field satisfied the need to model a variety of event intensities.

Thousands of 2-day model runs were conducted while permuting a total of 17 model parameters. The parameters, all being physically interpretable (a criterion of the model selection process), were allowed vary within a predefined feasible range. This resulted in a set of model realizations that are assumed to bound the CRW's actual hydrological response. Sets of model realizations applied over the existing CRW were collected for each storm intensity.

The ensemble of model realizations were used to quantify how the uncertainty in parameter selection affects model results. Independent parameter uncertainty bounds were computed at over 82,000 discrete locations within the model domain and were used to test the hydrological impact of wetland loss and restoration. At multiple locations in the CRW, no matter the scenario applied, changes to wetland distribution affected the hydrological response beyond the range attributed to parameter uncertainty. From this, wetlands demonstrated a quantifiable capacity to control flood flows within the CRW, meeting the study scope objective.

The wetland-loss scenarios provided an opportunity to compare isolated versus connected wetlands. The literature reviewed tended to assume that riparian (i.e., connected) wetlands play a greater role in flood mitigation than isolated wetlands. From the at-a-station results, this did appear to be the case; however, when observed at the watershed-scale it is evident that all wetlands affect watershed hydrology. The hydrologic affect of isolated wetlands remained in close proximity to the location of the altered isolated wetlands, and did not appear to affect fluvial flooding. With respect to fluvial flood mitigation, the functional difference between connected and isolated wetlands is that the former provides two flood prevention functions: detention storage and surface roughness (i.e., friction), while the latter only contributes to storage.

Isolated wetlands within the CRW generally exist in hummocky terrain. Rainfall that is not detained within these wetlands, after being removed, tends to collect in adjacent hummocks and does not reach the drainage network. From an in-stream perspective, this local redistribution mutes the effect of isolated wetland loss to (fluvial) flood prone areas. Isolated wetland loss appeared to only contribute to the creation of additional nearby wetlands (i.e., inundated areas). Similar to the findings of previous wetlands studies, the hydrological function of isolated wetlands in the CRW is to retain water evenly spread over the landscape, providing for increased recharge potential. Removing these wetlands would not guarantee the removal of hummocks, and the water that would have been retained by the isolated wetlands can only migrate to nearby depressions. While this may not affect in-stream flood conditions, it nonetheless can create excess water levels in unwanted areas.

The broad perception that isolated wetlands are not relevant to flood mitigation may not be justified. For this CRW study, the isolated wetlands were formed on top of moraines characterized by hummocky topography. This may be unique to recently glaciated landscapes typical of southern Ontario watersheds. Thus identifying the role of isolated wetlands in general, remains unresolved.

Other investigated loss scenarios (e.g., loss of non-PSWs, near-term potential loss, etc.) appeared to select wetlands that were primarily isolated; therefore, these scenarios exhibited similar results to the isolated wetland loss scenario. The lesson learned here is that more effort should have been made to ensure that the scenarios chosen had distinct wetland selections, in order to avoid repetition of results. Of note, however, was the apparent additive quality exhibited by the various wetland loss scenarios. The worst-case/all wetland loss scenario was indistinguishable from the collection of results of the remaining loss scenarios. This would imply that the affect of sequential wetland losses does not compound and that wetland impacts are independent. Further work on this matter should be accomplished.

The restoration scenario showed a significant reduction in flood potential, especially along the Credit mainstem through Mississauga. Most of the potential restoration sites were connected-type wetlands that existed in the lower CRW below the Niagara Escarpment. Within the lower watershed, many of the original wetlands have been lost to development. Combined with the relatively impervious surficial geology underlying this area, it is apparent from the results of the wetland restoration scenario that neglecting the flood-mitigation service of wetlands during past development has increased Credit River flood hazards. For example, restoration of wetlands showed marked reductions in the extent of velocity-depths exceeding $1\,\mathrm{m}^2/\mathrm{s}$, the upper threshold for which an adult can stand in flowing water without being swept away.

Although a pre-development scenario was not performed to demonstrate wetland function prior to urbanization, the restoration scenario can serve as a surrogate. By taking the restoration scenario results in reverse, the gains achieved could be estimated as being roughly equivalent with the hazards associated with wetland loss. Pending successful translation into the cost of wetland services (phase III to follow), it may prove that the restoration of wetlands in the Mississauga area will come with a high return. It can at least be said that restoration will provide a reduction in risk to human health and safety.

Reflecting on the model approach

In general, the communities of Acton, Georgetown, Erin, Norval and Orangeville would experience increases in flood risk due to the further loss of wetlands, while Mississauga would achieve significant flood hazard reduction through a wetland restoration plan. The lack of available CRW monitoring data would normally be a limitation for typical modelling studies that apply a calibration-validation approach. The multi-model ensemble approach taken in place of a calibration-validation approach provided for the framework to leverage model uncertainty as a means of determining, with statistical significance, that wetlands do have the physical capacity to mitigate flood hazards. In retrospect, should there have been available adequate data to perform a typical calibration-validation modelling approach, it may have not been possible to identify the hydrologic function of wetlands during extreme rainfall events with such certainty.

One of the model selection criteria during the model design phase was to ensure a fully-distributed modelling approach. It is clear that without this approach, the model results would have been hampered, if not misleading. For example, the at-a-station results confirmed the assumption that connected/riparian wetlands offer flood protection. However, the at-a-station results could not detect any reduction in flood potential associated with isolated wetlands. The at-a-station results reflect the limit of semi-distributed and lumped-parameter models common to hydrology. In contrast, the distributed approach confirmed that isolated wetlands do offer flood mitigation services, albeit in close proximity to the wetlands.

In hindsight, with an at-a-station/lumped approach, many of the areas that were found to be affected by changes in wetland distribution could not have been determined prior to model design, and thus would have avoided detection. This emphasizes that in hydrology, there exists a complex interplay amongst topography, land use, and geology at any particular location within the watershed, and thus the need for distributed modelling. Replicating the results presented here to other watersheds would necessarily require the re-application of the modelling methodology described.

Another modelling criteria that proved essential was the inclusion of the groundwater system. Since the CRW storm response is highly dependent on antecedent moisture conditions, the groundwater conceptualization provides the only data-driven means of predetermining moisture states, which assisted in establishing the initial water levels at certain low-land wetlands. Without incorporation of the groundwater system, the initial conditions for the model, including the initial storage capacity of all wetlands, would have been predefined by the modeller. Given the purpose of the modelling study was to quantify wetland capacity, this arbitrary predefining of initial wetland capacity would pose an obvious bias in model conclusions, thus questioning the defensibility of the study.

The groundwater integration also revealed interesting phenomena within the CRW that merits further investigation: Hydrographs immediately below escarpment showed secondary peaks, delayed by a day, likely contributed from delayed shallow water discharge into the headwater and talus slope streams originating on the Paris Moraine and routed through meltwater channels. Upon inspection, this dual peak phenomenon can be observed from instantaneous stream flow records, adding a qualitative validation of the approach taken and justifying the need to include groundwater processes.

The economic analysis described offers a quick and easily accessible means of determining the cost of wetland loss and restoration. The economic valuation plot described has the added ability of translating a rather complicated modelling procedure into readily available economic terms that can quickly set a monetary value to wetland flood mitigation services.

In closing, it's clear that wetlands affect watershed hydrology, no matter the scale of rainfall event. It is unclear, however, whether these conclusions are specific to the CRW or can be translated elsewhere. A suggested plan for a future application of this methodology would be to test the hypothesis that wetland function in a watershed is strictly additive, as it appears to be here. One way to test this would be to simulate impacts from the incremental loss of random wetlands. Should the impact be truly additive, then the changes resulting from this random wetland loss should converge to the modelled results of the complete wetland loss scenario. Otherwise, a set of random wetland loss realizations may reveal a threshold level of loss, beyond which, substantial and unmanageable impacts would result (e.g., the "marginal value paradox" of Mitch and Gosselink, 2000).

The design of this model not only ensured flexibility for application within the CRW, but the methodology ensures expandability to watersheds elsewhere.

Section 6

Model limitations

The hydrological model used was built at the watershed-scale with the intention of producing a watershed analysis. Variability and uncertainty of model results will increase when looking at the results at finer spatial scales. It is suggested that for a proper/rigorous interpretation of the model results, more attention should be paid to comparing changes of scenario results relative to the baseline.

The model was constructed with a variety of simplifying assumptions that are listed below. Assumptions made in the development of the physical theories applied in the model-code are not discussed here, as there are many other resources available. Also, assumptions and simplifications made in the conceptualization of hydrostratigraphy have been documented in AquaResource (2009).

Due to time and budget constraints, the study was restricted to a particular set scenarios and was by no means established as the definitive set of model runs needed to quantify the wetland-flood retention relationship. Since the model was designed for future application, other scenarios can be readily simulated.

Increased monitoring will prove invaluable to evaluating flood control capabilities of wetlands (Erwin, 2009), and would undoubtedly help in refining these model results.

Little research has been undertaken to determine the sensitivity of groundwater systems to changes in climate as it relates to wetland function (e.g., shifts in the depth to the water table). Reduced groundwater recharge can have severe long-term impacts on large head water systems like the CRW, and thus influence the results presented here. In addition, models that directly simulate the impact to wetlands from the alteration of the watershed hydrology are rare (Poff et. al., 2010), and was not the focus of the study's scope. In its current state, the model built here cannot address these issues; however, with minor alteration, the model can be made amenable to address such concerns.

Simplifications and assumptions

No water takings considered. Communities within the CRW rely on both groundwater and surface water for their drinking water supply and waste assimilation. Because the model's purpose was to simulate short-term events, it was assumed that these takings and any changes in takings or wastewater discharges over a two day period can be deemed negligible.

No urban infrastructure built into the model. Within the CRW, there are many storm water control/management facilities and other hydraulic structures (e.g., weirs, culverts, bridge piers, etc.); these were not included, and can all impact CRW hydrology and flow patterns (e.g., back-water effects). The addition of such detailed infrastructure was deemed infeasible when modelling at the watershed-scale. This would have had significant implications on model run times, potentially prohibiting the model from converging. Rather, the prime importance of the modelling was to ensure that the function of wetlands and streams was fully represented. In the future, should there be a need for detailed urban-scale modelling, this model can easily serve to provide hydrological input to such detailed modelling efforts.

Spatial scale. To reiterate, the model was built to analyze watershed-scale hydrology. Capturing watershed function as a whole comes at a cost of sacrificing small-scale phenomena.

Temporal scale. The model was intended to analyze the impact of short-term events and hydraulics at the sub-hourly scale. As the model stands, it is not immediately suitable for long-term seasonal analysis of watershed hydrology. That said, the model can be readily reformulated, which would allow the model to be used for water balance computations, climate change analysis, nutrient loading assessments, etc.

Results are seasonal. Many wetlands have hydroperiods that include wetter and dryer phases (Maltby and Acreman, 2011) and thus the results may differ depending on the initial model states that are dependent on the time of year.

References

Anderson, M.P., W.W. Woessner, R.J. Hunt, 2015. Applied Groundwater Modeling, 2nd edition, Academic Press, London, UK.

Anielski, M., J. Thompson, S.J. Wilson, 2014. A genuine return on investment: The economic and social well-being value of land conservation in Canada. Ducks Unlimited Canada, Stonewall, Manitoba, Canada.

Annable, W.K., 1996. Database of morphologic characteristics of watercourses in southern Ontario in: Adaptive management of stream corridors in Ontario, Section G.3. 237pp.

Aquanty Inc., 2016. HydrpGeoSphere reference and user manual, Release 1.0. 241pp.

AquaResource Inc., 2009. Integrated Water Budget Report–Tier 2 (SPC Accepted Draft) Credit Valley Source Protection Area. Report prepared for Credit Valley Conservation. April, 2009. 169pp.

Batelaan, O., F. De Smedt, L. Triest, 2003. Regional groundwater discharge: Phreatophyte mapping, groundwater modelling and impact analysis of land-use change. Journal of Hydrology 275(1): 86-108.

Bedient, P.B., W.C. Huber, 2002. Hydrology and Floodplain Analysis, 3rd ed. Prentice Hall. NJ. 763pp.

Bélair, S., L.P. Crevier, J. Mailhot, B. Bilodeau, Y. Delage, 2003a. Operational implementation of the ISBA land surface scheme in the Canadian Regional Weather Forecast Model Part I: Warm season results. Journal of Hydrometeorology 4: 352-370.

Bélair, S., R. Brown, J. Mailhot, B. Bilodeau, L.P. Crevier, 2003b. Operational implementation of the ISBA land surface scheme in the Canadian Regional Weather Forecast Model. Part II: Cold season results. Journal of Hydrometeorology 4: 371-386.

Bergström, S., 1995. The HBV model, in: Computer Models of Watershed Hydrology (Chapter 13), ed. Singh, V.P.. Water Resources Publications, Highlands Ranch, Colorado, USA: 443-476.

Beven, K., 2009. Environmental Modelling: An Uncertain Future? Routledge. 310pp.

Black, P.E., 1996. Watershed Hydrology, 2nd ed. Ann Arbor Press, Inc. 449pp.

Bradford, A., 2015. Averting degradation of southern Ontario wetlands due to hydrologic alterations associated with development. Canadian Water Resources Journal.

Brassard, P., J.M. Waddington, A.R. Hill, N.T. Roulet, 2000. Modelling groundwater-surface water mixing in a headwater wetland: implications for hydrograph separation. Hydrological Processes 14: 2697-2710.

Brunner, P., C.T. Simmons, 2012. HydroGeoSphere: A fully integrated, physically based hydrological model. Groundwater 50(2): 170-176.

Bullock, A., M.C. Acreman, 2003. The role of wetlands in the hydrological cycle. Hydrology and Earth System Sciences. 7(3): 358-389.

Butts, M.B., J.T. Payne, M. Kristensen and H. Madsen, 2004. An evaluation of the impact of model structure on hydrological modelling uncertainty for streamflow simulation. Journal of Hydrology 298: 242-266

Canadian Biodiversity Website, 2016. Mixedwood Plaines ecozone. [ONLINE] Available at: http://canadianbiodiversity.mcgill.ca/english/ecozones/mixedwoodplains/mixedwoodplains.htm. [Accessed 6 July, 2016]

Chapman, L.J., D.F. Putnam, 1984. The Physiography of Southern Ontario 3rd ed. Ontario Geological Survey. Special Volume 2. 270pp.

Chapman, T.G., A.I. Maxwell, 1996. Baseflow separation—comparison of numerical methods with tracer experiments. Institute Engineers Australia National Conference. Publ. 96/05, 539-545.

Chen, H., Y.W. Zhao, 2011. Evaluating the environmental flows of China's Wolonghu wetland and land use changes using a hydrological model, a water balance model and remote sensing. Ecological Modelling 222: 253-260.

Cheng, S-W., T.K. Dey, J.R. Shewchuk, 2012. Delaunay mesh generation. CRC Press. 410pp.

Chow, V.T., 1959. Open Channel Hydraulics. McGraw-Hill. New York. 680pp.

Clarifica Inc., 2002. Water Budget in Urbanizing Watersheds—Duffins Creek Watershed. Report prepared for the Toronto and Region Conservation Authority.

Colombo, S.J., D.W. McKenney, K.M. Lawrence, P.A. Gray, 2007. Climate change projection for Ontario: Practical information for policymakers and planners. Ontario Ministry of Natural Resources, Ontario Forest Research Institute, Applied Research and Development Branch, Sault Ste. Marie, Ontario, Canada.

Conservation Ontario, 2013. Dodging the "Perfect Storm:" Conservation Ontario's business case for strategic reinvestment in Ontario's flood management programs, services, and structures. Conservation Ontario, New Market Ontario, Canada.

Costanza, R., R. d'Arge, R. De Groot, S. Farber, M. Grasso, B. Hannon, B, K. Limburg, S. Naeem, R.V. O'Neill, J. Paruelo, et. al., 1997. The value of the world's ecosystem services and natural capital. Nature 387: 253-260.

Costanza, R., R. De Groot, P. Sutton, S. Van Der Ploeg, S.J. Anderson, I. Kubiszewski, S. Farber, R.K. Turner. 2014. Changes in the global value of ecosystem services. Global Environmental Change 26: 152-158.

Coulibaly, P., N.D. Evora, 2007. Comparison of neural network methods for infilling missing daily weather records. Journal of Hydrology, 341(1): 27-41.

Cowan, W.L., 1956. Estimating Hydraulic Roughness Coefficients. Agricultural Engineering 37: 473-475.

Credit Valley Conservation, 1994. A Conservation Areas Strategy for the Credit River Watershed, November, 1994. 56pp.

Credit Valley Conservation, 1998. Credit Watershed Natural Heritage Project Detailed Methodology: Identifying, Mapping and Collecting Field Data at Watershed and Subwatershed Scales, April, 1998. 139pp.

Credit Valley Conservation, Environmental Water Resources Group, Ortech Corporation, Terraqua Investigations Ltd. and B. Kilgour, 1997. Caledon Creek and Credit River Subwatershed Study (Subwatersheds 16 and 18), prepared for the Region of Peel, July 1997. 76pp.

DeWalle, D.R., A. Rango, 2008. Principles of Snow Hydrology. Cambridge University Press. 410pp.

Diersch, H-J.G., 2014. FEFLOW–Finite element modeling of flow, mass and heat transport in porous and fractured media. Springer. Berlin Heidelberg, XXXV, 996pp.

Dietrich, O., M. Redetzky, K. Schwärzel, 2007. Wetlands with controlled drainage and sub-irrigation systems—modelling of the water balance. Hydrological Processes 21: 1814-1828.

Donigian, A.S., B.R., Bicknell, J.C. Imhoff, 1995. Hydrological simulation program–FORTRAN (HSP–F), in: Computer Models of Watershed Hydrology (Chapter 12), ed. Singh, V.P.. Water Resources Publications, Highlands Ranch, Colorado, USA: 395-442.

van Dorp, J.R., S. Kotz, 2003. Generalized Trapezoidal Distributions. Metrika, 58(1): 85-97.

van Dorp, J.R., S.C. Rambaud, J.G. Perez, R.H. Pleguezuelo, 2007. An Elicitation Procedure for the Generalized Trapezoidal Distribution with a Uniform Central Stage. Decision Analysis, 4(3): 156-166.

Ducks Unlimited Canada, 2010. Southern Ontario wetland conservation analysis. Ducks Unlimited Canada, Barrie, Ontario, Canada. 51pp.

Dupont, F., P. Chittibabu, V. Fortin, Y.R. Rao, Y. Lu, 2012. Assessment of NEMO-based hydrodynamic modeling system for the Great Lakes. Water Quality Research Journal of Canada 47(3-4): 198-214.

Eckhardt, K., 2005. How to construct recursive digital filters for baseflow separation. Hydrological Processes 19: 507-515.

Environment and Climate Change Canada, 2016. Engineering Climate Datasets. [ONLINE] Available at: http://climate.weather.gc.ca/prods_servs/engineering_e.html [Accessed 30 May 2016].

Environmental Commissioner of Ontario, 2014. Sink, Swim or Tread Water? Adapting infrastructure to extreme weather events. Toronto. [ONLINE] Available at: http://docs.assets.eco.on.ca/reports/climate-change/2014/2014-GHG-Sink-Swim.pdf. [Accessed 6 July, 2016]

Environmental Commissioner of Ontario, 2015. Feeling the Heat: Greenhouse gas progress report. Toronto [ONLINE] Available at: http://docs.assets.eco.on.ca/reports/climate-change/2015/2015-GHG.pdf. [Accessed 6 July, 2016]

Erwin, K.L., 2009. Wetlands and global climate change: the role of wetland restoration in a changing world. Wetlands Ecology and Management 17: 71-84.

European Environment Agency, 2015. Exploring Nature Based Solutions: The role of green infrastructure in mitigating the impacts of weather- and climate-related natural hazards. Luxembourg.

Eyles, N. 2002. Ontario Rocks: Three Billion Years of Environmental Change. University of Toronto Press. Fitzhenry and Whiteside.

Fillion, L., and Coauthors, 2010. The Canadian Regional Data Assimilation and Forecasting System. Weather Forecasting 25: 1645-1669.

Gabriel, K.R., 1971. The biplot graphic display of matrices with application to principal component analysis. Biometrika 58(3): 453-467.

Gasca, D., D. Ross, 2009. The use of wetland water balances to link hydrogeological processes to ecological effects. Hydrogeology Journal 17: 115-133.

van Genuchten, M.Th., 1980. A closed-form equation for predicting the hydraulic conductivity of unsaturated soils. Soil Science Society of America Journal 44: 892-898.

Gilvear, D.J., R. Andrews, J.H. Tellam, J.W. Lloyd, D.N. Lerner, 1993. Quantification of the water balance and hydrogeological processes in the vicinity of a small groundwater-fed wetland, East Anglia, UK. Journal of Hydrology 144: 311-334.

Godschalk, D.R., T. Beatley, P. Berke, D.J. Brower, E.J. Kaiser, 1999. Natural hazard mitigation: Recasting disaster policy and planning. Island Press, Washington, DC, USA.

Government of Canada, 2016. About Radar. [ONLINE] Available at: http://www.ec.gc.ca/meteo-weather/default.asp?lang=En&n=2B931828-1. [Accessed 2 May, 2016]

Hallock, L., T. van Heeke, J. Burr, J. Rumpler, 2015. Shelter from the storm: How wetlands protect our communities from flooding. Environment Virginia Research & Policy Center, Richmond Virginia, USA.

Hotte, N., M. Kennedy, V. Lantz, 2009. Valuing wetlands in southern Ontario's Credit River watershed: Wetland ecosystem services characterization and literature review. Credit Valley Conservation, Mississauga, Ontario, Canada.

Institute of Hydrology, 1980. Low Flow Studies report. Wallingford, UK.

Insurance Bureau of Canada, 2016a. Facts of the Property and Casualty Insurance Industry in Canada, 38th edition. 66pp.

Insurance Bureau of Canada, 2016b. Media Release: Burlington flooding insured damages estimated at $90 million. [ONLINE] Available at: http://www.ibc.ca/qc/resources/media-centre/media-releases/burlington-flooding-insured-damages-estimated-at-$90-million. [Accessed 5 July, 2016]

Jakeman, A.J., G.M. Hornberger, 1993. How much complexity is warranted in a rainfall-runoff model? Water Resources Research 29(8): 2637-2649.

Johansen, O.M., J.B. Jensen, M.L. Pedersen. 2014. From groundwater abstraction to vegetative response in fen ecosystems. Hydrological Processes 28(4): 2396-2410.

Jonkman, S.N., E. Penning-Rowsell, 2008. Human Instability in Flood Flows. Journal of the American Water Resources Association 44(4): 1-11.

Julien, P.Y., 2002. River mechanics. Cambridge University Press. 434pp.

Kadlec, R.H., S.D. Wallace, 2009. Treatment Wetlands 2nd ed. CRC Press, New York. 928pp.

Kadykalo, A.N., C.S. Findlay, 2016. The flow regulation of wetlands. Ecosystem Services 20: 91-103.

Kennedy, M., J. Wilson, 2009. Natural credit: Estimating the value of natural capital in the Credit River watershed. The Pembina Institute, Drayton Valley, Alberta, Canada.

Klaassen, J., 2014. Ontario Rainfall Climatology. Internal Environment Canada (Meteorological Service of Canada) publication. Prepared in support of the Toronto 2015 Pan Am and Parapan Am Games. Toronto, Ontario.

Klemeš, V., 1986. Operational testing of hydrological simulation models. Hydrological Sciences Journal, 31(1): 13-24.

Krasnostein, A.L., C.E. Oldham, 2004. Predicting wetland water storage. Water Resources Research 40(W10203). 12pp.

Krause, S., A. Bronstert, 2005. An advanced approach for catchment delineation and water balance modelling within wetlands and floodplains. Advances in Geosciences 5: 1-5.

Kurowicka, D., R. Cooke, 2006. Uncertainty Analysis with High Dimensional Dependence Modelling. John Wiley & Sons, Ltd. 284pp.

Lee, H., W. Bakowsky, J.L. Riley, J. Bowles, M. Puddister, P. Uhlig, S. McMurray, 1998. Ecological Land Classification for Southern Ontario: First Approximation and Its Applications. Report prepared for the Ontario Ministry of Natural Resources: SCSS Field Guide FG-02, September 1998.

Lemieux, C., 2009. Monte Carlo and Quasi-Monte Carlo Sampling. Springer Science. 373pp.

Leroyer, S., S. Bélair, S.Z. Husain, J. Mailhot, 2014. Sub-Kilometer Numerical Weather Prediction in an Urban Coastal Area: A Case Study over the Vancouver Metropolitan Area. Journal of Applied Meteorology and Climatology 53: 1433-1453.

Linsley, R.K., M.A. Kohler, J.L.H. Paulhus, 1975. Hydrology for Engineers 2nd ed. McGraw-Hill, Inc. 482pp.

Loucks, O.L., 1989. Restoration of the pulse control function of wetlands and its relationship to water quality objectives in: Kusler, J.A., M.E. Kentula (eds.), Wetland creation and restoration: the status of the science Vol. II. USEPA Environmental Research Laboratory, Corvallis, OR. 170pp.

Maltby, E., M.C. Acreman, 2011. Ecosystem services of wetlands: Pathfinder for a new paradigm. Hydrological Sciences Journal 56(8): 1341-1359.

Maltby, E., (ed.), 2009. Functional assessment of wetlands: Towards evaluation of ecosystem services. Cambridge: Woodhead Publishing. 672pp.

Manning, R., 1891. On the flow of water in open channels and pipes. Transactions of the Institution of Civil Engineers of Ireland. 20: 161-207.

Marchildon, M., P.J. Thompson, S. Cuddy , E.J. Wexler, K. Howson, J.D.C. Kassenaar, 2016. A methodology for identifying ecologically significant groundwater recharge areas. Canadian Water Resources Journal (4): 515-527.

Markstrom, S.L., R.G. Niswonger, R.S. Regan, D.E. Prudic, P.M. Barlow, 2008. GSFLOW–Coupled groundwater and surface-water flow model based on the integration of the Precipitation-Runoff Modeling System (PRMS) and the Modular Ground-Water Flow Model (MODFLOW-2005): U.S. Geological Survey Techniques and Methods 6-D1: 240pp.

Markstrom, S.L., R.S. Regan, L.E. Hay, R.J. Viger, R.M.T. Webb, R.A. Payn, J.H. LaFontaine, 2015. PRMS-IV, the precipitation-runoff modeling system, version 4: U.S. Geological Survey Techniques and Methods, book 6, chap. B7. 158pp.

Masson, V., 2000. A physically based scheme for the urban energy budget in atmospheric models. Boundary-Layer Meteorology 94: 357-397.

Matott, L.S., J.E. Babendreier, S.T. Purucker, 2009. Evaluating uncertainty in integrated environmental models: a review of concepts and tools. Water Resources Research 45(6).

Maxwell, R.M., and Coauthors, 2016. ParFlow User's Manual. Integrated GroundWater Modeling Center Report GWMI 2016-01. 167pp.

Merrick, D.P., N.P. Merrick, 2015. AlgoMesh: A new software tool for building unstructured grid models. Proceedings of MODFLOW and More, Colorado.

McKillop, R., N. Kouwen, E.D. Soulis, 1999. Modeling the rainfall-runoff response of a headwater wetland. Water Resources Research 35(4): 1165-1177.

McLaughlin, D.L., M.J. Cohen, 2013. Realizing ecosystem services: wetland hydrologic function along a gradient of ecosystem condition. Ecological Applications 23(7): 1619-1631.

Merritt, W.S., R.A. Letcher, A.J. Jakeman, 2003. A review of erosion and sediment transport models. Environmental Modeling and Software 18: 761-799.

Milbrandt, J.A., M.K. Yau, 2005. A multimoment bulk microphysics parameterization. Part I: Analysis of the role of the spectral shape parameter. Journal of Atmospheric Science 62: 3051-3064.

Milbrandt, J.A., S. Bélair, M. Faucher, M. Vallee, M. Carrera, A. Glazer, 2016. The Pan-Canadian High Resolution (2.5 km) Deterministic Prediction System. Weather Forecasting 31: 1791-181.

Millennium Ecosystem Assessment, 2005. Ecosystems and human well-being: Synthesis. Island Press, Washington, DC, USA.

Ministry of Municipal Affairs and Housing, 2014. Provincial Policy Statement. Toronto.

Mitsch, W.J., J.G. Gosselink, 2000. The value of wetlands: Importance of scale and landscape setting. Ecological Economics 35: 25-33.

Mitsch, W.J., J.G. Gosselink, 2015. Wetlands 5th ed. John Weily and Sons, Inc. New Jersey. 736pp.

Mitsch, W.J., B. Bernal, M.E. Hernandez, 2015. Editorial: Ecosystem services of wetlands. International Journal of Biodiversity Science, Ecosystem Services & Management 11(1): 1-4.

Nathan, R.J., T.A. McMahon, 1990. Evaluation of Automated Techniques for Baseflow and Recession Analyses. Water Resource Research 26(7): 1456-1473.

Nathan, R.J., T.A. McMahon, 1991. Comment on the evaluation of automated techniques for base flow and recession analyses. Water Resource Research, 27(7): 1783-1784.

Nature.org, 2013. The case for green infrastructure, a joint-industry white paper, June 2013. [ONLINE] Available at: http://www.nature.org/about-us/the-case-for-green-infrastructure.pdf. [Accessed 6 July, 2016]

Ogawa, H., J.W. Male, 1986. Simulating the flood mitigation role of wetlands. ASCE Journal of Water Resourses and Planning Management 112: 114-127.

Ontario Ministry of the Environment. 2006. Clean Water Act. Queen's Printer for Ontario.

Ontario Ministry of Natural Resources, 2002. Greater Toronto Area Digital Elevation Model 2002, Metadata record, Geographic Information Branch, Science and Information Resources Division.

Ontario Ministry of Natural Resources, Water Resources Section, 2002. River & Stream Systems: Flooding Hazard Limit, a Technical Guide. 118pp.

Ontario Ministry of Natural Resources, 2014. Ontario wetland evaluation system: southern manual. 3rd ed., Version 3.3. Toronto, ON: Queen's Printer for Ontario. 296pp.

Partington, D., P. Brunner, S. Frei, C.T. Simmons, A.D. Werner, R. Therrien, H.R. Maier, G.C. Dandy, J.H. Fleckenstein. 2013. Interpreting streamflow generation mechanisms from integrated surface-subsurface flow models of a riparian wetland and catchment. Water Resources Research 49: 5501-5519.

Piggott, A.R., S. Moin, C. Southam, 2005. A revised approach to the UKIH method for the calculation of baseflow. Hydrological Sciences Journal 50(5): 911-920.

Poff, N.L., B.D. Richter, A.H. Arthington, S.E. Bunn, R.J. Naimann, E. Kendy, M. Acreman, et. al., 2010. The ecological limits of hydrological alteration (ELOHA): A new framework for developing regional environmental flow standards. Freshwater Biology 55: 147-170.

Pomeroy, J.W., K. Shook, X. Fang, S. Dumanski, C. Westbrook, T. Brown, 2014. Improving and testing the prairie hydrological model at Smith Creek research basin. University of Saskatchewan, Canada.

Ponce, V.M., 1989. Engineering Hydrology: Principles and Practices. Prentice Hall, N.J. 640pp.

R Core Team, 2013. R: A language and environment for statistical computing. R Foundation for Statistical Computing, Vienna, Austria. ISBN 3-900051-07-0, URL: http://www.R-project.org/.

Rayburg, S., M.C. Thoms, 2009. A coupled hydraulic-hydrologic modelling approach to deriving a water balance model for a complex floodplain wetland system. Hydrology Research 40(4): 364-379.

Refsgaard, J.C., H.J. Henriksen, 2004. Modelling guidelines–terminology and guiding principles. Advances in Water Resources 27(1):71-82.

Refsgarrd, J.C., B. Storm, 1995. MIKE SHE, in: Computer Models of Watershed Hydrology (Chapter 23), ed. Singh, V.P.. Water Resources Publications, Highlands Ranch, Colorado, USA: 809-846.

Richards, L.A., 1931. Capillary conduction of liquids through porous media. Physics 1, 318-333.

Richardson, A.H., 1956. Credit Valley Conservation Report prepared for the Department of Planning and Development. Toronto. 709pp.

Rosgen, D.L., 1994. A classification of natural rivers. Catena 22: 169-199.

Roulet, N.T., 1990. Hydrology of a headwater basin wetland: groundwater discharge and wetland maintenance. Hydrological Processes 4: 387-400.

Rutledge, A.T., 1998. Computer Programs for Describing the Recession of Ground-Water Discharge and for Estimating Mean Ground-Water Recharge and Discharge from Streamflow Records-Update, Water-Resources Investigation Report 98-4148.

Schaap M.G., F.J. Leij, M.Th. van Genuchten, 2001. ROSETTA: a computer program for estimating soil hydraulicparameters with hierarchical pedotransfer functions. Journal of Hydrology 251: 163-176.

Shook, K., J.W. Pomeroy, C. Spence, L. Boychuk, 2013. Storage dynamics in prairie wetland hydrology models: evaluation and parameterization. Hydrological Processes 27(13): 1875-1889.

Schroeter and Associates, 2001. Credit River Watershed Hydrology Model Summary Report. Prepared for Credit Valley Conservation.

Shultz S.D., J.A. Leitch, 2001 The feasibility of wetland restoration to reduce flooding in the Red River valley: A case study of the Maple River watershed, North Dakota. Agribusines and Applied Economics, report No. 432a. 22pp.

Sieck, L.C., S.J. Burges, M. Steiner, 2007. Challenges in obtaining reliable measurements of point rainfall. Water Resources Research 43(W01420)

Singh, V.P., (ed.), 1995. Computer Models of Watershed Hydrology. Water Resources Publications, Highlands Ranch, Colorado, USA. 1144pp.

Sloto, R.A., M.Y. Crouse, 1996. HYSEP: A Computer Program For Streamflow Hydrograph Separation And Analysis U.S.Geological Survey Water-Resources Investigations Report 96-4040.

Stedinger, J.R., V.W. Griffs, 2011. Getting from here to where? Flood frequency analysis and climate. Journal of the American Water Resources Association 47(3): 506-513.

Stephenson, G.R., R.A. Freeze, 1974. Mathematical simulation of subsurface flow contributions to snowmelt runoff, Reynolds Creek watershed, Water Resources Research 10: 284-294.

Strahler, A.N., 1952. Hypsometric (area-altitude) analysis of erosional topography. Geological Survey of America. Bulletin 63: 1117-1142.

Strahler, A.N., 1957. Quantitative analysis of watershed geomorphology. Transactions of the American Geophysical Union 38(6): 913-920.

Thompson, J.R., H. Refstrup Sørenson, H. Gavin, A. Refsgaard, 2004. Application of the coupled MIKE SHE/MIKE 11 modelling system to a lowland wet grassland in southeast England. Journal of Hydrology 293: 151-179.

Thompson, J.R., H. Gavin, A. Refsgaard, H. Refstrup Sørenson, D.J. Gowing, 2009. Modelling the hydrological impacts of climate change on UK lowland wet grassland. Wetlands Ecology and Management 17(5): 503-523.

Tournois, J., P. Alliez, O. Devillers, 2008. Interleaving Delaunay refinement and optimization for 2D triangle mesh generation, in proccedings of the 16th international meshing roundtable. Springer Berlin Heidelberg.

Trigg, M.A., P.G. Cook, P. Brunner, 2014. Groundwater fluxes in a shallow seasonal wetland pond: The effect of bathymetric uncertainty on predicted water and solute balances. Journal of Hydrology 517: 901-912.

Troy, A., K. Bagstad, 2009. Estimating Ecosystem Services in Southern Ontario. Spatial Informatics Group, LLC. Pleasanton, California. 73pp.

Tsihrintzis, V.A., E.E. Madiedo, 2000. Hydraulic resistance determination in marsh wetlands. Water Resources Management 14: 285-309.

U.S. Environmental Protection Agency, 2014. Green Infrastructure for Climate Resiliency. EPA Publication #832F14007.

Warren, F.J., D.S. Lemmen (eds.), 2014. Canada in a changing climate: Sector perspectives on impacts and adaptation. Natural Resources Canada, Ottawa, Ontario, Canada.

Weisman, M.L., J.B. Klemp, 1982. The dependence of numerically simulated convective storms on vertical wind shear and buoyancy. Americal Meteorological Society Monthly Waterher Review 110: 504-520.

Wetzel, R.G., 2001. Limnology: Lake and River Ecosystems 3rd ed. Academic Press, New York, NY. 1006pp.

Wilson, S.J., 2008a. Ontario's wealth, Canada's future: Appreciating the value of the Greenbelt's eco-services. David Suzuki Foundation, Vancouver, British Columbia, Canada.

Wilson, S.J., 2008b. Lake Simcoe basin's natural capital: The value of the watershed's ecosystem services. Friends of the Greenbelt Foundation Occasional Paper Series 6. David Suzuki Foundation, Vancouver, British Columbia, Canada.

Zadra, A., D. Caya, J. Côte, B. Dugas, C. Jones, R. Laprise, K. Winger, and L-P. Caron, 2008. The next Canadian regional climate model. Physics in Canada 64: 75-83.

Appendix A

Phase I Literature Review: Natural Solutions for a Changing Climate

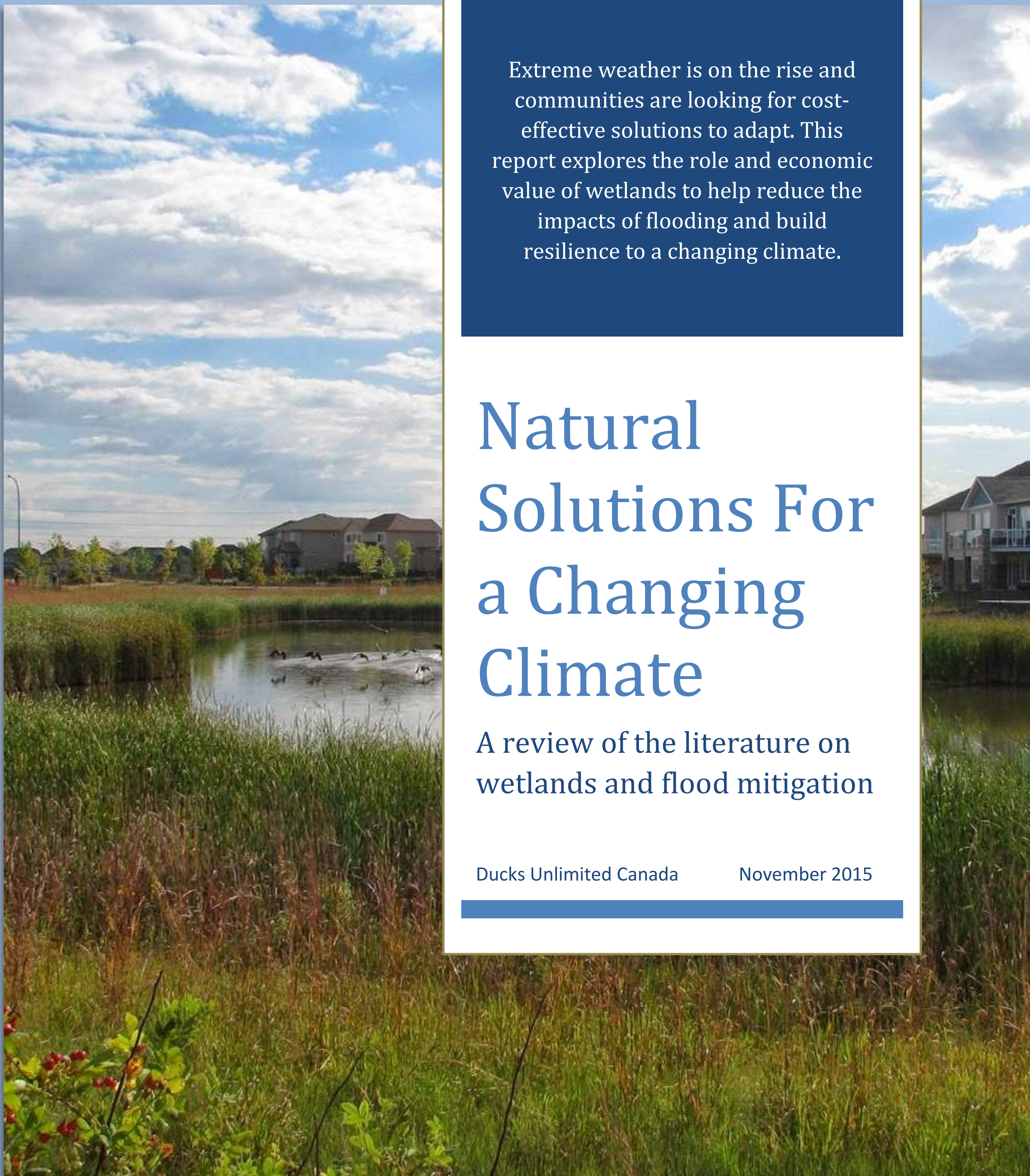

Extreme weather is on the rise and communities are looking for cost-effective solutions to adapt. This report explores the role and economic value of wetlands to help reduce the impacts of flooding and build resilience to a changing climate.

Natural Solutions For a Changing Climate

A review of the literature on wetlands and flood mitigation

Ducks Unlimited Canada

November 2015

Natural Solutions for a Changing Climate: A review of the literature on wetlands and flood mitigation. Ducks Unlimited Canada. November 2, 2015.

Report prepared by:

Ian Glass, Institute for Wetlands and Waterfowl Research, Ducks Unlimited Canada
Alexandra Service, Ducks Unlimited Canada

With special acknowledgement to:

Owen Steele, Ducks Unlimited Canada
Jeff Wilson, Green Analytics

With generous funding from:

RBC Blue Water Project
Ontario Ministry of Natural Resources and Forestry

Introduction

Extreme weather events related to climate change are on the rise in Ontario, largely manifested in the form of flooding. Major flood events have occurred with increasing frequency (Environmental Commissioner of Ontario (ECO) 2014) over the past 20 years in places like Peterborough, London, Thunder Bay, Mississauga and Burlington. The July 8, 2013 storm that hit the Toronto area was the most expensive natural disaster in Ontario's history, costing almost $1 billion in flood-related damages. It's clear that infrastructure in many Ontario cities is struggling under the weight of these major storm events.

While investments in stormwater, sewer and other infrastructure are clearly needed, many practitioners are increasingly turning to green infrastructure as a complementary and often more cost-effective solution to managing flooding. Wetlands are recognized as having significant flood control benefits, and are often considered a form of 'natural' green infrastructure. Although there is considerable evidence globally for this wetland benefit, there are still gaps in research, particularly specific to Ontario. Some studies have looked at Ontario wetlands (Ahmed et al 2009, Bertulli 1981, Taylor 1982, Whitely and Irwin 1986), largely confirming their significant capacity for flood control, however they do have limitations in terms of methodology, scope, and economic considerations. Ducks Unlimited Canada (DUC) is undertaking new research in the Credit River watershed (CRW) in southern Ontario to help fill some of these research gaps, and provide a better understanding of the role and economic value of wetlands to manage flooding in a typical southern Ontario watershed. The purpose of this literature review is to compile and summarize existing research into the role of wetlands for flood mitigation, including the economic value of this service to society, identify gaps in our current understanding, and demonstrate why new research is urgently needed.

Ontario in a Changing Climate

Canada is expected to see an increase in temperature of 1.3°C between 1948 and 2007 due to climate change – this represents twice the global average, and temperatures are expected to increase by another 1.5°C by 2050 (Roy et al. 2001, Insurance Bureau of Canada (IBC) 2012, Warren et al. 2014, Rasmussen 2015). Climate change modelling for southern Ontario indicates even more significant temperature increases of 5°C during the summer and 6°C during the winter by 2100 when compared to 1971-2000 average temperatures (Colombo et al. 2007). Because warmer air can hold more moisture, rising temperatures mean precipitation rates throughout Canada have increased by an average of 12%, or 20 more days of rain per year since 1950. However, precipitation levels can be highly variable depending on region – southern Ontario could actually experience an average10-20% reduction in rain during the summer and winter months (Colombo et al. 2007, IBC 2012, Warren et al. 2014), but this precipitation is also expected to be more volatile, with frequent intense storms potentially interspersed with periods of drought (ECO 2015).

Increasing average temperatures and precipitation, combined with greater areas of impervious surfaces related to population shifts and growth in urban areas, are contributing to increasingly costly flood events. Research by Brody et al. (2007a) found that flood peak discharges increased 80% in urban catchments with greater than 50% impervious surface (e.g., concrete, asphalt). Modelling predicts that 1:25 and 1:50 year flood events in the Credit River watershed in southern Ontario will cause damages estimated at \$6.5 million and \$7.7 million per event (Kennedy and Wilson 2009). Twenty-first century flood events in Canada have caused significant damage including the 2005, \$7 million flood in Fredericton, the \$90 million spring 2011 flood along the Richelieu River, the Assiniboine River floods of 2011 that caused \$1.2 billion in damages, and the 2013 floods in Toronto and Calgary that caused \$850 million and \$6 billion in damages, respectively (Lantz et al. 2012, Conservation Ontario 2013, Burn et al. 2015, Saad et al. 2015). Floods also cause significant issues in the United States each year, averaging between \$2.9 and \$5.2 billion per year and killing 140 people – it is estimated that flood damages could increase to \$1 trillion per year by 2050 (Brody et al. 2007b, 2011, Kaiser et al. 2012, Ziemba et al. 2014, Hallock et al. 2015).

It is clear that future land use, infrastructure, and urban development decisions can no longer be planned based on historic weather patterns (ECO 2014). Climate change is already causing significant challenges for Ontario, especially due to flooding, and this will only increase over time. We need new solutions for a new climate and that includes rethinking infrastructure to incorporate natural features like wetlands.

The Value of Green Infrastructure

"In conjunction with gray infrastructure, interconnected networks of green infrastructure can enhance community resiliency by increasing water supplies, reducing flooding…and improving water quality" (US EPA 2014). Many US cities are starting to adopt green infrastructure techniques to help deal with the increased burden of extreme weather brought on by climate change. For example the U.S. Army Corps of Engineers recognized that the loss of coastal wetlands around New Orleans significantly worsened the impacts of Hurricane Katrina, and is now actively working to restore wetlands in partnership with several different organizations (ECO Annual Report 2010/11). Cities like Philadelphia and Portland are increasingly investing in green infrastructure and maintaining natural ecosystems to avoid the skyrocketing costs of traditional pipes and concrete (ECO Annual Report 2010/11).

Ontario cities have been somewhat slower to adopt green infrastructure on a large scale, but there is increasing recognition that new solutions are needed to deal with the impacts of extreme weather. For the first time the most recent 2014 Provincial Policy Statement (PPS), which guides municipal land use planning in Ontario, includes a provision that planning authorities should promote green infrastructure to complement traditional forms of infrastructure (MMAH 2014). The PPS defines green infrastructure as, "natural and human-made elements that provide ecological and hydrological functions and processes. Green infrastructure can include components such as natural heritage features and systems, parklands, stormwater management systems, street trees, urban forests, natural channels, permeable surfaces, and green roofs" (MMAH 2014). Notably, this definition not only includes man-made structures that are meant to mimic natural processes, but also natural features and systems in and of themselves.

A recent report released by the European Environment Agency concludes unequivocally that green infrastructure approaches are not only effective in dealing with climate change impacts, they are also on balance cheaper than using traditional grey infrastructure alone. According to the report this is largely due to the 'multifunctionality' of green infrastructure, which means that it can provide a number of functions and benefits within the same spatial area (EEA 2015). "It is the multifunctionality of [green infrastructure] that sets it apart from the majority of its grey counterparts, which tend to be designed to perform one function alone…without contributing to the broader environmental, social and economic context" (Naumann et al, 2011). In this way, green infrastructure tends to be able to produce greater benefits within a given cost framework, and generally require lower costs over the long term.

Wetlands are slowly starting to be recognized as a form of natural green infrastructure for the many different benefits they provide to society. As the climate continues to change, natural features like wetlands will become increasingly important to help communities adapt to these changes in a sustainable and cost-effective manner.

What is a wetland?

Wetlands are dynamic ecosystems that are continuously receiving and losing water from evapotranspiration, precipitation, groundwater and surface flow (Winter and Woo 1990). The Canadian National Wetland Working Group (NWWG 1997) defines a wetland as "land that is saturated with water long enough to promote wetland or aquatic processes as indicated by poorly drained soils, hydrophytic vegetation, and various kinds of biological activity which are adapted to a wet environment." There are five classes of wetlands in Canada: bogs (mossy peat), fens (sedges), marshes (emergent, floating and submergent plants), shallow water, and swamps (wooded wetlands) (Whiteley and Irwin 1986, NWWG 1997). The Ontario Ministry of Natural Resources and Forestry (MNRF) also recognizes four types of wetlands based on their position in the landscape: isolated, lacustrine (lakeside), palustrine (upland with an outlet watercourse), and riverine (river or streamside) (MNRF, 1993, Whiteley and Irwin 1986).

Wetlands cover 1.5% of the Earth's surface and are among the most threatened ecosystems in the world (Cox 1993). In Canada, 1.27 million square kilometers of wetlands cover 14% of our total land area, which equals approximately 25% of the world's wetlands (Natural Resources Canada 2009). Like the rest of world, Canada's wetlands are highly vulnerable, with an estimated 70% of original wetlands lost to drainage for agricultural, commercial and residential development projects since European settlement (Natural Resources Canada 2009). Cox (1993) estimated that 20 million hectares (ha) of Canada's wetlands have been drained since 1800.

Wetland loss is an ongoing issue in Canada. Ducks Unlimited Canada (DUC, unpublished data) estimates that on average 32 ha of wetlands per day or 11,817 ha of wetlands per year are lost in Canada. One dramatic example is southern Ontario, which has sustained some of Canada's most significant wetland losses with 1.4 million ha (72%) drained since 1800 (DUC 2010, Lantz et al. 2013). Loss occurs for a number of different reasons, but in southern Ontario, the primary causes of wetland loss are urban development, agriculture, infrastructure, and resource extraction. Population growth in and around the Greater Toronto Area (GTA), and in other areas of the province, continues to put pressure on the existing land base often leading to impairment of wetland function, if not outright loss. According to the Ontario Biodiversity Council's latest State of Ontario Biodiversity Report, while the rate of wetland loss has slowed in recent years, it has continued with an average loss of 0.6% over the period of 2000-2011 with loss as high as 1.8% in some areas (SOBR 2015).

The loss of wetlands is highly problematic – wetlands are recognized among the most productive ecosystems on earth, and contain some of the highest biodiversity levels in Canada (Environment Canada 2013). However, they are also incredibly valuable resources from a human standpoint, providing numerous social, economic, and environmental services, all of which are lost when wetlands are damaged or drained.

Flood Attenuation Benefits

A key service that wetlands provide is their ability to reduce the potential damage of flood events. Wetlands have the ability to "act like a sponge" and detain water, which helps reduce and attenuate floodwater peak flows and timing to downstream portions of the watershed (Turner 1757, Winter and Woo 1990, De Laney 1995, Gabor et al. 2001, Mitch and Gosselink 2007, Southern Tier Central Regional Planning and Development Board 2012, Acreman and Holden 2013, McLaughlin and Cohen 2013). Wetlands are capable of storing significant amounts of water. For instance, a one acre wetland that is 1 foot deep can hold 330,000 US gallons of water (Hallock et al. 2015). This storage capacity allows wetlands to temporarily store floodwaters before overflowing and releasing some of the water downstream. This process is also commonly referred to as "fill and spill" and is common in geographically isolated wetlands such as those found in the Prairie Pothole Region (Winter and Woo 1990, Brody et al. 2007, Mitch and Gosselink 2007, Acreman and McCartney 2009, Kusler 2009, Acreman and Holden 2013). Wetland soils also reduce floodwater peak flows and timing by absorbing some of the excess floodwaters (Baker et al. 2009, Ziemba et al. 2014). Finally, friction created by flood waters flowing over and through wetland vegetation reduces the velocity of floodwaters and has the ability to desynchronize flood waters across the landscape (Wamsley et al. 2010, Gedan et al. 2011, Shepard et al. 2011, Gittman et al. 2014, Garssen et al. 2015).

Numerous studies (see Table 2) have shown the flood attenuation benefits of wetlands, however, the ability of wetlands to reduce peak flows and timing can be variable depending on wetland type and location in the watershed, and the wetland's antecedent condition (e.g., already full) prior to the flood event (Juliano and Simonovic 1999, Schultz and Leitch 2001, Simonovic and Juliano 2001, Kirby et al 2002, Schultz and Leitch 2003). The balance of academic literature from around the world clearly demonstrates that wetlands can in fact help moderate the impacts of flooding. Clearly, given the high costs of flooding in Ontario communities, this service must also provide some economic value to society. The study of ecosystem goods and services (EGS) can help give us an indication of the value of these 'non-market' services that communities benefit from on a daily basis.

Table 2: Flood attenuation benefits provided by wetlands

Benefit	Region	Researchers
Maintaining 3,800 ha of floodplain wetlands would save $17 million in downstream flood damage	Charles River, MA	U.S. Army Corps of Engineers 1972
Reduction of flood peak flow discharge from 150 cubic meters per second (m^3/s) to 80 m^3/s.	Napanee River, ON	Bertulli 1981
Increased stormwater detention times	Chandler Slough Marsh, FL,	Ammon et al. 1981
Play a key role in controlling summer storm runoff	Peterborough, ON, Canada	Taylor 1982
Watersheds that are comprised of 4 to 5% wetlands have a 50% peak	Northeastern U.S. States	Novitzki 1985

flow period compared to watersheds lacking wetlands		
Reduction in the number of wetlands lead to significant increases in flood peak flow	Charles, Neponset, and Ten Mile Rivers, MA	Ogawa and Male 1986
Downstream peak flows slowed by 24 to 48 hours	Southern Ontario	Whiteley and Irwin 1986
Peak flood flow 50% less during 50 year flood event along rivers with intact wetlands	Kankakee River, IL and Iroquois River, IN	Demissie and Kahn 1993
Restoration of upland wetlands reduced flood peak flows by 10 to 23%	Mississippi River basin	U.S. Army Corps of Engineers 1994
Watersheds comprised of 5 to 10% wetlands are capable of reducing flood peak flows by 50%	-	De Laney 1995
A 5.7 acre wetland can retain the natural runoff from a 410 acre watershed	Des Plaines River, IL	Godschalk et al. 1999
13 million acres of wetlands could retain all the flood water of the 1993 Mississippi River flood	Upper Mississippi River Basin	Godschalk et al. 1999
1:100 year flood peak flows would increase 4% if all non-provincially significant wetlands (PSW) are removed	Rideau River Valley watershed, ON	Ahmed et al. 2009
1:100 year flood peak flows would increase 2.4% if all non-PSW are removed	Ottawa, ON	Ahmed et al. 2009
870 dry prairie pothole basins are capable of holding 19.79 million m³ of flood water	Stutsman County, ND	Huang et al. 2011

Wetlands reduce flood peak flows by 10%	Rideau Valley watershed, ON	Ahmed 2014
Peak flow reductions of 20-41% depending of flood type	Eagle Creek watershed, IN	Javaheri and Babbar-Sebens 2014
Flood velocity reduced by up to 13%	Eagle Creek watershed, IN	Javaheri and Babbar-Sebens 2014
Flood peak flow discharges during moderate to low flow years increased 150 to 350% if all wetlands are drained	Smith Creek basin, SK	Pomeroy et al. 2014
Flood peak flows decrease 35 to 70% if wetlands were restored to 1958 levels	Smith Creek basin, SK	Pomeroy et al. 2014
Small wetlands provide $6.11 of flood protection services to road infrastructure.	Prairie Pothole Region, USA	U.S Fish and Wildlife Service 2014
Each acre of wetlands on agricultural landscapes provides $29.23 in flood protection services to agricultural landscapes	Prairie Pothole Region, USA	U.S. Fish and Wildlife Service 2014

Ecological Goods and Services and Economic Value

Ecological goods and services (EGS) play a key role in supporting human life (Millennium Ecosystem Assessment 2005). EGS can be defined as ecosystem functions that are of benefit to humans and generally do not have a market value (Barbier 2011). Zedler (2003) estimates that wetlands provide 40% of all the world's EGS. The EGS provided by wetlands include carbon sequestration, water quality improvement, nutrient retention, flood and erosion control, groundwater recharge, maintenance of biodiversity, wildlife habitat, recreational opportunities and aesthetic benefits (Brander et al. 2006, Hotte et al. 2009, Barbier 2011).

Research conducted by Costanza et al. (1997) estimates the world's biomes provide EGS worth $16-$54 trillion per year with an average annual value of $33 trillion. Anielski et al. (2014) estimated the EGS benefits provided by the 2.54 million ha of wetlands and associated habitats maintained by Ducks Unlimited Canada (DUC) to be approximately

$4.27 billion per year. Of this, the wetland habitat maintained by DUC provided the greatest estimated annual EGS benefits at $3.1 billion, followed by forests at $808.8 million; grasslands provided $369.9 million and croplands provided $456,355 (Anielski et al. 2014). The estimated EGS services provided by DUC conservation projects could be divided as follows: 31% of the benefits were attributed to carbon sequestration, 28% to groundwater recharge and water storage, 19% to wastewater treatment and water purification, 9% to pollination services, 6% to hydrological benefits such as flood control, 2% for genetic diversity maintenance, 2% for food provisioning, 1% for biological control benefits and 1% to erosion prevention (Anielski et al. 2014). However, the reported flood control benefits are likely an underestimate as the author points to a lack of available data on the economic value of this wetland service.

In Ontario a number of natural capital assessments have been completed that examine a range of ecosystem service benefits, including flood control from wetlands (Wilson 2008; Kennedy and Wilson 2009; Troy and Bagstad 2009). As shown in Table 1, wetlands provide significant economic value to the residents in these study areas. However, estimates of wetland value do vary considerably from a reported average annual flood value of $2,711 per ha in the Credit River Watershed (Kennedy and Wilson 2009) to $99,318 per ha for southern Ontario wetlands within a suburban or urban context (Troy and Bagstad 2009). Reported estimates of wetland EGS values in these studies tend to be based on the application of primary research from other jurisdictions, that is then transferred to Ontario (through a benefit transfer methodology); there is very little ecosystem valuation work based on primary research conducted in Ontario. While these estimates are useful for drawing attention to the importance of ecosystem services, they do not always accurately reflect the spatial realities that ultimately lead to economic benefits.

Table 1: Estimates of Wetland Economic Value in Ontario from 4 Studies

	Southern Ontario* (Troy and Bagstad 2009)	**Greenbelt** (Wilson 2008)	**Lake Simcoe Watershed** (Wilson 2008)	**Credit River Watershed** (Kennedy and Wilson 2009)
Annual wetland EGS value/hectare	$161,420	$14,153	$11,172	-
Total annual wetland EGS value	$39.5 billion	$1.3 billion	$435 million	$187 million
Annual wetland flood value/ hectare	$99,318	$4,039	$4,039	$2,711
Total annual wetland flood value	-	$380 million	$157 million	$16 million

**Urban/suburban wetlands only*

It is likely that increasingly costly flood events will continue as a result of climate change. As a result, the benefits that wetlands provide regarding flood attenuation and other EGS will become more valuable, making wetland protection and restoration critical. A fulsome understanding of these benefits requires an assessment that considers wetland location within a hydrologic system relative to built infrastructure (roads, bridges, homes, etc.). DUC's research will seek to fill a gap in the current literature by conducting primary research in an Ontario watershed, then using the findings to conduct an economic analysis of the flood damage mitigated by the presence of wetlands. This research is critical because, without a clear understanding of the economic value that wetlands provide, land use decisions may determine the fate of wetlands based on the value of alternatives that generate tax revenue (e.g. commercial or residential buildings), rather than on a complete evaluation that includes the value of natural green infrastructure assets, and the potential costs of losing them.

Conclusion

As this literature review shows, wetlands can play an important role in mitigating the impacts of flooding, and the economic value of this service is in fact substantial. The flood protection benefits provided by wetlands will only continue to grow due to the impacts of climate change and the resulting weather extremes it produces (Burn and Whitfield 2015). Ongoing research is critical to creating a better understand this wetland service, its economic value, and the contribution that wetlands can provide to society through sustainable development. This is why Ducks Unlimited Canada is piloting new research in the Credit River watershed of southern Ontario. This research will quantify the capacity of wetlands to slow and store flood water during a major storm event, assess the impacts of further wetland loss and potential restoration on flooding, and determine the economic value of wetlands for flood mitigation. Ultimately, this information may provide opportunities for more informed land use decisions that can help mitigate the impacts of flooding and enhance resilience to climate change in Ontario.

Climate change will require a shift in how communities manage water, and increasingly this means turning to more natural solutions. 'Hard' or 'grey' infrastructure can be costly, time consuming to construct, and on its own has not proven able to handle the kinds of storm events that are expected in future. More and more research is showing that investments made in green or natural infrastructure provide significant returns in avoided costs down the road. It's time for governments, businesses, and citizens to recognize these natural values, and invest in maintaining them.

References

Acreman, M.C. and M.P. McCartney. 2009. Hydrological impacts in and around wetlands. Pages 643-666 *in* E. Maltby and T. Barker, editors. The wetlands handbook. Wiley-Blackwell, Hoboken, New Jersey, USA.

Acreman, M. and J. Holden. 2013. How wetlands affect floods. Wetlands 33: 773-786.

Ahmed, F. 2014. Cumulative hydrologic impact of wetland loss: Numerical modeling study of the Rideau River watershed, Canada. Journal of Hydrologic Engineering 19: 593-606.

Ahmed, F., N. Howlander, C. Enguelz, and A. Soutar. 2009. Quantifying the importance of wetlands in the management of floods and droughts in the Rideau Valley watershed Rideau Valley Conservation Authority, Monotick, Ontario, Canada.

Ammon, D.C, H.C. Wayne, and J.P. Hearney. 1981. Wetlands use for water management in Florida. Journal of Water Resources Planning and Management 107: 315-327.

Anielski, M., J. Thompson, and S. Wilson. 2014. A genuine return on investment: The economic and social well-being value of land conservation in Canada. Ducks Unlimited Canada, Stonewall, Manitoba, Canada.

Babbar-Sebens, M., R.C. Barr, L.P. Tedesco, and M. Anderson. 2013. Spatial identification and optimization of upland wetlands in agricultural landscapes. Ecological Engineering 52: 130-142.

Baker, C., J.R. Thompson, and M. Simpson. Hydrological dynamics I: Surface waters, flood and sediment dynamics. Pages 120-168 *in* E. Maltby and T. Barker, editors. The wetlands handbook. Wiley-Blackwell, Hoboken, New Jersey, USA.

Barbier, E.B. 2011. Wetlands as natural assets. Hydrological Science Journal 56: 1360-1373.

Barbier, E.B. and B.S. Enchelmeyer. 2014. Valuing the storm surge protection service of US Gulf Coast wetlands. Journal of Environmental Economics and Policy 3: 167-185.

Bertulli, J.A. 1981. Influence of a forested wetland on a southern Ontario watershed. Pages 33-48 *in* A. Champagne, editor. Proceedings of the Ontario wetland conference. Federation of Ontario Naturalist, Don Mills, Ontario, Canada.

Brander, L.M., R.J.G.M. Florax, and J.E. Vermaat. 2006. The empirics of wetland valuation: A comprehensive summary and a meta-analysis of the literature. Environmental & Resource Economics 33: 223-250.

Brody, S.D., W.E. Highfield, H.-C. Ryu, and L. Spanel-Weber. 2007a. Examining the relationship between wetland alteration and watershed flooding in Texas and Florida. Natural Hazards 40: 413-428.

Brody, S.D., S. Zahran, P. Maghelal, H. Grover, and W.E. Highfield. 2007b. The rising costs of floods: Examining the impact of planning and development decisions on property damage in Florida. Journal of the American Planning Association 73: 330-345.

Brody, S.D., S. Zahran, W.E. Highfield, H. Grover, and A. Vedlitz. 2008. Identifying the impact of built environment on flood damage in Texas. Disasters 32: 1-18.

Brody, S.D., J. Gunn, W. Peacock, and W.E. Highfield. 2011. Examining the influence of development patterns on flood damages along the Gulf of Mexico. Journal of Planning Education and Research 31: 438-448.

Brody, S.D., W.G. Peacock, and J. Gunn. 2012. Ecological indicators of flood risk along the Gulf of Mexico. Ecological Indicators 18: 493-500.

Brody, S.D., R. Blessing, A. Sebastian, and P. Bedient. 2014. Examining the impact of land use/land cover characteristics on flood losses. Journal of Environmental Planning and Management 57: 1252-1265.

Bullock, A. and M. Acreman. 2003. The role of wetlands in the hydrological cycle. Hydrology and Earth Systems Sciences 7: 358-389.

Burn, D.H. and P.H. Whitfield. 2015. Changes in floods and flood regimes in Canada. Canadian Water Resources Journal: in press.

Cai, Y.P., G.H. Huang, Q. Tan, and B. Chen. 2011. Identification of optimal strategies for improving eco-resilience to floods ecologically vulnerable regions of a wetland. Ecological Modelling 222: 360-369.

Chu, C. 2014. Climate change vulnerability assessment for aquatic ecosystems in the Great Lakes basin, Ontario. Ontario Ministry of Natural Resources, Peterborough, Ontario, Canada.

Colombo, S.J., D.W. McKenney, K.M. Lawrence, and P.A. Gray. 2007. Climate change projection for Ontario: Practical information for policymakers and planners. Ontario Ministry of Natural Resources, Ontario Forest Research Institute, Applied Research and Development Branch, Sault Ste. Marie, Ontario, Canada.

Conservation Ontario. 2013. Dodging the 'Perfect Storm': Conservation Ontario's business case for strategic reinvestment in Ontario's flood management programs, services, and structures. Conservation Ontario, New Market Ontario, Canada.

Costanza, R., R. D'Arge, R. de Groot, S. Farber, M. Grasso, B. Hannon, K. Limburg, S. Naeem, R.V. O'Neill, J. Paruelo, R.G. Raskin, P. Sutton, and M. van den Belt. 1997. The value of the world's ecosystem services and natural capital. Nature 387: 253-260.

Costanza, R., O. Pérez-Maqueo, M.L. Martinez, P. Sutton, S.J. Anderson, and K. Mulder. 2008. The value of coastal wetland for hurricane protection. Ambio 37: 241-248.

Cox, K. 1993. Wetlands: A celebration of life. North American Wetlands Conservation Council (Canada) Sustaining wetland issues paper no. 1993-1, Ottawa, Ontario, Canada.

Cunderlik, J.M. and T.B.M.J. Ouarda. 2009. Trends in the timing and magnitude of flood in Canada. Journal of Hydrology 375: 471-480.

De Laney, T.A. 1995. Benefits to downstream flood attenuation and water quality as a result of constructed wetlands in agricultural landscapes. Journal of Soil and Water Conservation 50: 620-626.

Demissie, M. and A. Kahn. 1993. Influence of wetlands on streamflow in Illinois. Illinois State Water Survey report 561, Champaign, Illinois, USA.

Ducks Unlimited Canada. 2010. Southern Ontario wetland conservation analysis. Ducks Unlimited Canada, Barrie, Ontario, Canada.

Environmental Commissioner of Ontario. 2011. Engaging Solutions: 2010/11 Annual Report. Toronto.

Environmental Commissioner of Ontario. 2015. Feeling the Heat: Greenhouse gas progress report. Toronto

Environmental Commissioner of Ontario. 2014. Sink, Swim or Tread Water? Adapting infrastructure to extreme weather events. Toronto.

European Environment Agency. 2015. Exploring Nature Based Solutions: The role of green infrastructure in mitigating the impacts of weather- and climate-related natural hazards. Luxembourg.

Ferreira, C. 2011. Sensitivity of hurricane storm surge numerical simulations to wetland parameters in Corpus Christi, TX. World Environmental and Water Resources Congress 2011: Bearing knowledge for sustainability: 3149-3157.

Gabor, T.S., A.K. North, L.C.M. Ross, H.R. Murkin, J.S. Anderson, and M.A. Turner. 2001. "Beyond the Pipe". The importance of wetlands and upland conservation practices in watershed management: Functions and values for water quality and quantity. Ducks Unlimited Canada, Stonewall, Manitoba, Canada.

Garssen, A.G., A. Baattrup-Pedersen, L.A.C.J. Voesenek, J.T.A. Verhoeven, and M.B. Soons. 2015. Riparian plant community response to increased flooding: A meta-analysis. Global Change Biology 21: 2881-2890.

Gedan, K.B., M.L. Kirwan, E. Wolanski, E.B. Barbier, and B.R. Silliman. 2011. The present and future role of coastal vegetation in protecting shorelines: Answering recent challenges to the paradigm. Climatic Change 106: 7-29.

Gittman, R.K., A.M. Popowich, J.F. Bruno, and C.H. Peterson. 2014. Marshes with and without sills protect estuarine shorelines from erosion better than bulkheads during a Category 1 hurricane. Ocean & Coastal Management 94-102.

Godschalk, D.R., T. Beatley, P. Berke, D.J. Brower, and E.J. Kaiser. 1999. Natural hazard mitigation: Recasting disaster policy and planning. Island Press, Washington, DC, USA.

Gombault, C., M.-F. Sottile, F.F. Ngwa, C.A. Madramootoo, A.R. Michaud, I. Beaudin, and M. Chikhaoui. 2015. Modelling climate change impacts on the hydrology of an agricultural watershed in southern Québec. Canadian Water Resources Journal 40: 71-86.

Hallock, L., T. van Heeke, J. Burr, and J. Rumpler. 2015. Shelter from the storm: How wetlands protect our communities from flooding. Environment Virginia Research & Policy Center, Richmond, Virginia, USA.

Hey, D.L. and N.S. Philippi. 1995. Flood reduction through wetland restoration: The upper Mississippi River basin a case history. Restoration Ecology 3:4-17.

Higfield, W.E. and S.D. Brody. 2006. Price of permits: Measuring the economic impacts of wetland development on flood damages in Florida. Natural Hazards Review 7: 123-130.

Hillman, G.R. 1998. Flood wave attenuation by a wetland following a beaver dam failure on a second order boreal stream. Wetlands 18: 21-34.

Hotte, N., M. Kennedy, and V. Lantz. 2009. Valuing wetlands in southern Ontario's Credit River watershed: Wetland ecosystem services characterization and literature review. Credit Valley Conservation, Mississauga, Ontario, Canada.

Hubbard, D.E. and R.L. Linder. 1986. Spring runoff retention in prairie pothole wetlands. Journal of Soil and Water Conservation 41: 122-125.

Huang, S., C. Young, M. Feng, K. Heidemann, M. Cushing, D.M. Mushet, and S. Liu. 2011. Demonstration of a conceptual model for using LiDAR to improve the estimation of floodwater mitigation potential of Prairie Pothole Region wetlands. Journal of Hydrology 405: 417-426.

Institute for Catastrophic Loss Reduction. 2012. Telling the weather story. Insurance Bureau of Canada, Toronto, Ontario, Canada.

Javaheri, A. and M. Babbar-Sebens. 2014. On comparison of peak flow reductions, flood inundation maps, and velocity maps in evaluating effects of restored wetlands on channel flooding. Ecological Engineering 73: 132-145.

Johnston, C.A, N.E. Detenbeck, and G.J. Niemi. 1990. The cumulative effect of wetlands on stream water quality and quantity: A landscape approach. Biogeochemistry 10: 105-141.

Johnston, D.M., J.B. Braden, and T.H. Price. 2006. Downstream economic benefits of conservation development. Journal of Water Resources Planning and Management 132:35-43.

Juliano, K. and S.P. Simonovic. 1999. The impact of wetlands on flood control in the Red River Valley of Manitoba. University of Manitoba, Natural Resources Institute, Winnipeg, Manitoba, Canada.

Kennedy, M. and J. Wilson. 2009. Natural credit: Estimating the value of natural capital in the Credit River watershed. The Pembina Institute, Drayton Valley, Alberta, Canada.

Kirby, D.R., K.D. Krabbenhoft, K.K. Sedivec, and E.S. DeKeyser. 2002. Wetlands in the northern plains prairies: Offer societal values too. Rangelands 24: 26-29.

Kusler, J. 2009. Wetlands and natural hazards. Association of State Wetland Managers, Berne, New York, USA.

Langridge, S.M., E.H. Hartge, R. Clark, K. Arkema, G.M. Verutes, E.E. Prahler, S. Stoner-Duncan, D.L. Revell, M.R. Caldwell, A.D. Guerry, M. Ruckelshaus, A. Abeles, C. Coburn, and K. O'Connor. 2014. Key lessons for incorporating natural infrastructure into regional climate adaptation planning. Ocean & Coastal Management 95: 189-197.

Lantz, V., P. Boxall, M. Kennedy, and J. Wilson. 2010. Valuing wetlands in southern Ontario's Credit River watershed: A contingent valuation analysis. Credit Valley Conservation, Mississauga, Ontario, Canada.

Lantz, V., P.C. Boxall, M. Kennedy, and J. Wilson. 2013. The valuation of wetland conservation in an urban/peri urban watershed. Regional Environmental Change 13: 939-953.

Lantz, V., R. Trenholm, J. Wilson, and W. Richards. 2012. Assessing market and non-market costs of freshwater flooding due to climate change in the community of Fredericton, eastern Canada. Climatic Change 110: 347-372.

Leschine, T.M., K.F. Wellman, and T.H. Green. 1997. The economic value of wetlands: Wetlands' role in flood protection in western Washington. Washington State Department of Ecology, Bellevue, Washington, USA.

Martinez-Martinez, E., A.P. Nejadhashemi, S.A. Woznicki, and B.J. Love. 2014. Modeling the hydrological significance of wetland restoration scenarios. Journal of Environmental Management 133: 121-134.

McCauley, L.A., M.J. Anteau, M. Post van der Burg, and M.T. Wiltermuth. 2015. Land use and wetland drainage affect water levels and dynamics of remaining wetlands. Ecosphere 6: art. 92.

McLaughlin, D.L., and M.J. Cohen. 2013. Realizing ecosystem services: Wetland hydrologic function along a gradient of ecosystem condition. Ecological Applications 23: 1619-1631.

Millennium Ecosystem Assessment. 2005. Ecosystems and human well-being: Synthesis. Island Press, Washington, DC, USA.

Miller, M.W. and T.D. Nudds. 1996. Prairie landscape change and flooding in the Mississippi River valley. Conservation Biology 10: 847-853.

Mitsch, W.J. and J.G. Gosselink, editors. 2007. Wetlands. Fourth edition. John Wiley & Sons, Hoboken, New Jersey, USA.

Mitsch, W.J. and M.E. Hernandez. 2013. Landscape and climate change threats to wetlands of North and Central America. Aquatic Sciences 75: 133-149.

Ministry of Municipal Affairs and Housing. 2014. Provincial Policy Statement. Toronto.

National Wetlands Working Group. The Canadian wetland classification system. Second edition. B.G. Warner and C.D.A. Rubec, editors. Wetlands Research Centre, University of Waterloo, Waterloo, Ontario, Canada.

Natural Resources Canada. 2009. Distribution of freshwater wetlands. Natural Resources Canada, Ottawa, Ontario, Canada.

Naumann, S., D. McKenna, T. Kaphengst, M. Pieterse, and M. Rayment. 2011. Design, implementation and cost elements of green infrastructure projects. Final report to the European Commission, DG Environment.

Novitzki, R.P. 1985. The effects of lakes and wetlands on flood flows and base flows in selected northern and eastern states. H.A. Gromman, editor. Proceedings of the wetlands conference of the Cheasapeake. Environmental Law Institute, Washington, DC, USA.

Ogawa, H. and J.W. Male. 1986. Simulating the flood mitigation role of wetlands. Journal of Water Resources Planning and Management 112: 114-128.

Ontario Biodiversity Council. 2015. State of Ontario's Biodiversity.

Ontario Ministry of Natural Resources. 1993. Ontario wetland evaluation system: Southern manual. Third edition. Ontario Ministry of Natural Resources, Toronto, Ontario, Canada.

Pattison, J.K., W. Yang, Y. Liu, and S. Gabor. 2011. A business case for wetland conservation: The Black River subwatershed. Ducks Unlimited Canada, Barrie, Ontario, Canada.

Pomeroy, J.W., K. Shook, X. Fang, S. Dumanski, C. Westbrook, and T. Brown. 2014. Improving and testing the prairie hydrological model at Smith Creek research basin. University of Saskatchewan Centre for Hydrology Report no. 14, Saskatoon, Saskatchewan, Canada.

Qaiser, K., Y. Yuan, and R.D. Lopez. 2012. Urbanization impacts on flooding in the Kansas River basin and evaluation of wetlands as a mitigation measure. Transactions of the ASABE 55: 849-859.

Rasmussen, P.F. 2015. Assessing the impact of climate change on the frequency of floods in the Red River basin. Canadian Water Resources Journal: in press.

Rémillard, L., J. Rousselle, F. Ashkar, and D. Sparks. 2004. Analysis of the seasonal nature of extreme floods across Canada. Journal of Hydrologic Engineering 9: 392-401.

Riboust, P. and F. Brissette. 2015. Analysis of Lake Champlain/Richelieu River's historical 2011 flood. Canadian Water Resources Journal: in press.

Roy, L., R. Leconte, F.P. Brissette, and C. Marche. 2001. The impact of climate change on seasonal floods of a southern Quebec River basin. Hydrological Processes 15: 3167-3179.

Saad, C., A. St-Hilarie, P. Gachon, and S. El Adlouni. 2015. The 2011 flood event in the Richelieu River basin: Causes, assessment and damages. Canadian Water Resources Journal: in press.

Schottler, S.P., J. Ulrich, P. Belmont, R. Moore, J.W. Lauer, D.R. Engstrom, and J.E. Almendinger. 2014. Twentieth century agricultural drainage creates more erosive rivers. Hydrological Processes 28: 1951-1961.

Schultz, S.D. and J.A. Leitch. 2001. The feasibility of wetland restoration to reduce flooding in the Red River Valley: A case study of the Maple River watershed, North Dakota. North Dakota State University, Agricultural Experiment Sate Agribusiness & Applied Economic Report no. 432a, Fargo, North Dakota, USA.

Schultz, S.D. and J.A. Leitch. 2003. The feasibility of restoring previously drained wetlands to reduce flood damage. Journal of Soil and Water Conservation 58: 21-29.

Shepard, C.C., C.M. Crain, and M.W. Beck. 2011. The protective role of coastal marshes: A systematic review and meta-analysis. PLoS ONE 6: e27374.

Sierszen, M.E., J.A. Morrice, A.S. Trebitz, and J.C. Hoffman. 2012. A review of selected ecosystem services provided by coastal wetlands of the Laurentian Great Lakes. Aquatic Ecosystem Health & Management 15: 92-106.

Simonovic, S.P. and K.M. Juliano. 2001. The role of wetlands during low frequency flooding events in the Red River basin. Canadian Water Resources Journal 26: 377-397.

Southern Tier Central Regional Planning and Development Board. 2012. Flood attenuation opportunities in the Binghamton area (Broome County, NY): Guidance for identifying potential projects that enhance the ability of the watershed to absorb and store water. Southern Tier Central Regional Planning and Development Board, Binghamton, New York, USA.

Spatial Informatics Group, A. Troy, and K. Bagstad. 2009. Estimating ecosystem services in southern Ontario. Ontario Ministry of Natural Resources, Peterborough, Ontario, Canada.

Taylor, C.H. 1982. The hydrology of a small wetland catchment near Peterborough, Ontario. Pages 105-129 *in* M.J. Bardecki, editor. Proceedings of the Ontario Wetland Conference. Ryerson Polytechnical Institute, Toronto, Ontario, Canada.

Turner, N. 1757. An essay on draining and improving peat bogs: In which their nature and properties are fully considered. Baldwin and Pew, London, United Kingdom.

Turner, R.K., J.C.J.M. van den Bergh, T. Söderqvist, A. Barendregt, J. van der Straaten, E. Maltby, and E.C. van Ierland. 2000. Ecological-economic analysis of wetlands: Scientific integration for management and policy. Ecological Economics 35: 7-23.

U.S. Army Corps of Engineers. 1972. Charles River, Massachusetts: Main Report and Attachments. U.S. Army Corps of Engineers, Waltham, Massachusetts, USA.

U.S. Army Corps of Engineers. 1994. Sharing the challenge: Floodplain management into the 21st century. Interagency Floodplain Management Review Commission, Washington, DC. USA.

U.S. Environmental Protection Agency. 2014. Green Infrastructure for Climate Resiliency. EPA Publication #832F14007.

U.S. Fish and Wildlife Service. 2014. Small wetlands in the U.S. Prairie Pothole Region: Values worth conserving! U.S. Fish and Wildlife Service, Lakewood, Colorado, USA.

Wamsley, T.V., M.A. Cialone, J.M. Smith, J.H. Atkinson, and J.D. Rosati. 2010. The potential of wetlands in reducing storm surge. Ocean Engineering 37: 59-68.

Warren, F.J. and D.S. Lemmen, editors. 2014. Canada in a changing climate: Sector perspectives on impacts and adaptation. Natural Resources Canada, Ottawa, Ontario, Canada.

Whiteley, H.R. and R.W. Irwin. 1986. The hydrological response of wetlands in southern Ontario. Canadian Water Resources Journal 11: 100-110.

Wilson, S.J. 2008. Lake Simcoe basin's natural capital: The value of the watershed's ecosystem services (Friends of the Greenbelt Foundation Occasional Paper Series 6). David Suzuki Foundation, Vancouver, British Columbia, Canada.

Wilson, S.J. 2008. Ontario's wealth, Canada's future: Appreciating the value of the Greenbelt's eco-services. David Suzuki Foundation, Vancouver, British Columbia, Canada.

Winter, T.C. and M.K. Woo. 1990. Hydrology of lakes and wetlands. Pages 159-187 *in* M.G. Wolman and H.C. Riggs, editors. Surface water hydrology. Geological Society of America, Boulder, Colorado, USA.

Woodward, R.T. and Y.-S. Wui. 2001. The economic value of wetland services: A meta-analysis. Ecological Economics 37: 257-270.

Yang, W., X. Wang, Y. Liu, S. Gabor, L. Boychuk, and P. Badiou. 2010. Simulated environmental effects of wetland restoration in a typical Canadian prairie watershed. Wetlands Ecology and Management 18: 269-279.

Zedler, J. 2003. Wetlands at your service: Reducing the impacts of agriculture at the watershed scale. Frontiers of Ecology and Environment 1: 65-72.

Ziemba, E.J., A.M. Borchers, and M.D. Heintzelman. 2014. The value of wetlands for flood mitigation.

Appendix B

Analysis of local climatology and watershed response

An analysis of 61 existing and historical Meteorological Service of Canada climate stations (Figure 2.13) proximal to the study area was conducted to obtain records of extreme rainfall events. Of the 61 stations, 54 reported daily rainfall amounts extending back to the year 1840, varying in terms of period of record and data quality. The number of reporting stations within the period of record is shown in Figure 2.14.

A search for days where median daily rainfall totals ranged from 40 mm to 55 mm was conducted. This chosen range reflects the 2-year return, 24 hour totals of 39.7 mm and 55.5 mm reported at the Environment Canada Intensity-Duration-Frequency (IDF—ECCC, 2016) stations Orangeville MOE (6155790) and Blue Springs Creek (6140818), respectively; these stations were selected based on their proximity to the study area (see Figure 2.13 and Table 2.5). The 2-year return event was selected here for the simple fact that it is anticipated that a larger sample of events of this magnitude would be obtained; longer return periods = increased rarity.

In total 17 dates within the period of 1969 to 1996, inclusive (a period with the greatest number of stations reporting and to coincide with the available stream discharge data, see below), were detected to fall within this 40 mm to 55 mm range, two of which were rejected as they occurred within the months of December through April. These months were excluded in order to avoid potential rain-on-snow or rain on frozen soil events and ensure that the events collected are most-likely of the late-summer convective type. Fifteen events over a 28-year period equates to an event of this particular magnitude occurring once every 1.9 years, confirming the 2-year return selection objective. The dates when these selected events occurred are listed in Table B.1.

Instantaneous stage and discharge data was obtained from the Water Survey of Canada for a number of Credit River watershed gauges during the period of 1969 through 1996. Only four of eight gauges contained near-complete records of 15-minute instantaneous data, and they include: 02HB001—Credit River Near Cataract, 02HB002—Credit River at Erindale, 02HB008—Credit River West Branch at Norval, and 02HB013—Credit River Near Orangeville (see Figure 3.4). Fifteen hydrographs were then extracted from each of the four gauge records according to the dates given in Table B.1. Initial stage (d_0), peak stage (d_{max}) and time to peak (t_p) were determined from an automated time series analysis script written by the author. Time to peak is defined as time elapsed from the initiation of the rising limb to the maximum stage observed (Figure B.1).

Table B.1: List of fifteen 2-year-return 24 hr events occurring in the Credit River watershed area between 1969-1996.

Median 24 hr rainfall volume	Date	Number of stations reporting
35.3	1969-11-01	17
36.6	1992-11-12	9
37.6	1976-05-06	14
37.9	1973-10-29	14
38.2	1969-05-18	14
38.8	1992-08-27	10
39.9	1987-07-19	10
40.1	1996-05-20	6
41.4	1971-07-05	17
41.6	1972-10-22	14
42.9	1986-09-29	10
48.4	1986-08-26	10
51.0	1977-09-24	12
51.8	1975-08-23	18
54.2	1995-10-05	7

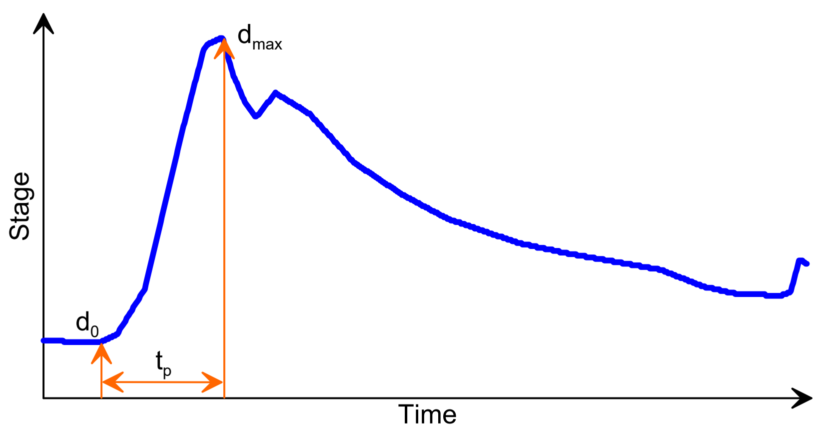

Figure B.1: Sample hydrograph illustrating metrics used in characterizing stream flow response.

B.1 Test for correlation

The range of the selected 2-year events in Table B.1 is roughly ±20% of the 42.3 mm overall mean, thus providing an adequate range of rainfall amounts that can be tested for correlation between rainfall event volume and stream stage. A Spearman's rank-order correlation test was used to determine the relationship between rainfall event volume (P) and stream peak stage (d_{max}). The results of the Spearman's test presented in Table B.2 indicates that there does not exist any correlation between 2-year return 24 hr rainfall accumulation and peak stream flow stage at any of the four gauges ($p > 0.05$).

Table B.2: A Spearman's rank-order correlation (ρ_s) testing of the Credit River watershed response to 2-yr rainfall events from 1969 to 1996.

Gauge	n pairs	Spearman's ρ_s [a]			
		P vs. d_{max}	P vs. t_p	d_{max} vs. t_p	d_{max} vs. d_0
02HB001	13	-0.40	0.04	0.22	0.77[b]
02HB002	13	0.13	-0.26	-0.75	0.92[b]
02HB008	15	0.26	-0.38	-0.24	0.61[b]
02HB013	15	-0.13	-0.48	-0.21	0.75[b]

[a] P = precipitation; d_0 = initial stage; d_{max} = peak stage; t_p = time to peak.

[b] Significant correlation ($p < 0.01$)

A Spearman's rank-order correlation test was also used to determine correlation between rainfall amount (P) and time to peak (t_p), and between peak stage (d_{max}) and time to peak (t_p). Neither of these were significantly correlated ($p > 0.05$), perhaps suggesting that the Credit River watershed's response to 2-year events is dependent on the spatial distribution of precipitation, thus affecting the time of concentration.

As a qualitative demonstration of the lack of event volume-to-peak flow correlation, a set of hydrographs observed at the 02HB008–Credit River West Branch at Norval gauge in response to the selection of 2-year events were considered (Figure 2.15). It is clear from this gauge (and the other Credit River gauges—not included here) that a 2-year storm event can manifest itself into a variety of stream flow hydrographs. Interestingly, some of the most intense rainfall events experienced the lowest flows in this 1969-1996 time period, as shown be the deeper-red hydrograph lines.

Amongst the four gauges tested, a comparison between initial stage (d_0) and peak stage (d_{max}) did demonstrate significant correlation ($p < 0.01$—Table B.2). Assuming that the initial stage prior to the onset of a rainfall event is entirely representative of baseflow discharge, this would indicate that antecedent conditions is likely the principle component of rainfall response in the Credit River watershed. However, a further complication is revealed when attempting to correlate initial stage ranking amongst the four gauges (Table B.3). Only three of the possible six pairings among the four gauges showed correlation, indicating that antecedent conditions are also dependent on watershed location; meaning two separate locations within the CRW can be, at the same time, relatively moist and dry and thus cannot be said that antecedent moisture condition is a ubiquitous basin-wide characteristic.

Table B.3: Spearman's rank-order test correlation matrix of antecedent (baseflow) stage among four Credit River watershed gauges prior to 2-yr rainfall events from 1969 to 1996.

Gauge	Spearman's ρ_s		
	02HB001	02HB002	02HB008
02HB002	0.13		
02HB008	0.38	0.59[b]	
02HB013	0.88[a]	0.47	0.66[a]

[a] Significant correlation ($p < 0.01$)
[b] Significant correlation ($p < 0.05$)

B.2 Analysis of principle components to runoff generation

To test the dependency peak flow has on any of the remaining hydrograph characteristics, a Principal Components Analysis (PCA) was performed. The advantage of PCA is that it can used to identify the relative independencies among a set of observed and calculated phenomena. In contrast with Spearman's rank correlation coefficient which only considers the relationships among two variables, PCA will reveal the multicollinearity among all variables, thus alleviating the analysis from the assumption of variable independence. The analysis was performed using the `prcomp` R-package (R core team, 2013).

Five variables were complied for the PCA analysis including the four addressed with the Spearman rank correlation analysis plus peak duration, defined as the time the hydrograph stage exceeded its median level. All of the data were standardized prior to performing the analysis in order to prevent scaling issues, as per standard procedure. Flow-based metrics (i.e., peak and initial flow) where also normalized according to their gauge's catchment areas in order to transform their discharge from m^3/s to an equivalent mm/d.

Analysis of variable interdependence was accomplished qualitatively using a set of three PCA biplots (Gabriel, 1971) representing the first three principal components (PCs). These three PCs explain 77.4% of the variance found in the data. The biplots shown in Figure B.2 show observation scores (points that are colour-coded according to the gauge the data were reported from), superimposed with the variable loadings (brown arrows). Simply by inspection, the biplots will reveal correlation among a set of variables based on the equivalence between a pair of loading vectors.

For example, biplot B.2b, which explains 51.9% of the variance among the data, illustrates that event volume and peak duration show some potential correlation; however, both loadings project only 60–70% onto the PC1–PC3 plane. However, by inspection of the other two planes (B.2a and c), it's apparent that the two loading are in fact orthogonal, meaning that they are not truly correlated. Any evidence from these three plans that show orthogonality between a pair of loading vectors, which are representative of the flow variables, is evidence against their correlation, provided that a significant proportion of the vectors' magnitudes project onto the Principal Component (PC) plane. The closer a loading vector reaches the unit circle shown in black on Figures B.2a–c, the greater influence that vector has in explaining the variance of that PC plane.

For the purpose of this study, in support the conclusions drawn from the Spearman rank correlation analysis, the main interest from these biplots is to identify any relationship between peak flow and event volume, as they represent the two datasets that are available for calibration. With a)

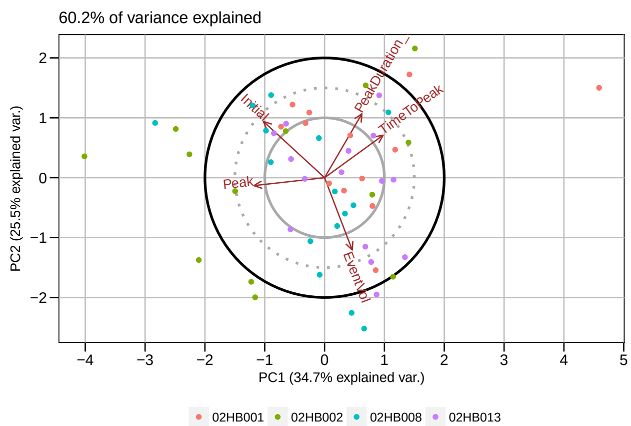

b)

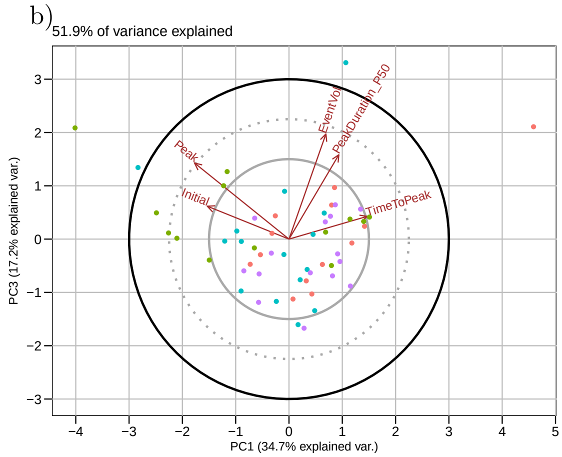

c)

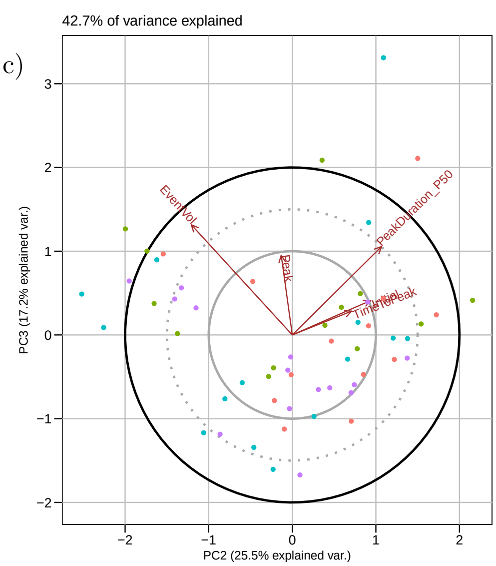

Figure B.2: PCA biplots that explain 77.4% of the variance among rainfall event volume (i.e., precipitation accumulation), initial discharge, peak discharge, time to peak, and peak duration. Brown arrows indication PCA loadings projected onto the Principal Component (PC) planes: a) PC1 vs. PC2; b) PC1 vs. PC3; and c) PC2 vs. PC3. Solid-grey, dotted-grey, and solid black circles represent the 50%, 75%, and 100% degree of loading projection onto the PC plane, respectively.

the exception of biplot B.2c, no correlation between peak flow and event volume can be determined due to their orthogonality. While the loadings are not orthogonal from the PC2–PC3 plane (biplot B.2c), peak flow explains less the half of the plane's variance, which in itself only explains 42.7% of total variance, and thus should not considered.

Peak duration and time to peak tended to project equally on all plains suggesting their correlation. These two parameters can be assumed to be reflective of storm location, distribution and dynamics (i.e., time of concentration), and thus it is understandable that these variables show correlation. While peak flow and peak duration tend not to exhibit much correlation, the first two PC planes (B.2a and b) tend to reveal that peak flow and time to peak are negatively correlated, judging by their tendency to point in opposite directions. If time to peak is assumed to be reflective of time of concentration, then the same can be said for peak flow.

The greatest correlation appears to be between initial flow and peak flow, as they tend toward the same direction on the first two PC planes. Only the third PC plane does the orthogonality between the two loading begin to emerge; however, both loadings explain roughly half of the third PC plane's variability. Their explanatory power to the PC2–PC3 plane (B.2c) is less than the remaining planes and thus can be a safely neglected. This provides confirmation the above Spearman rank correlation analysis in which antecedent conditions tend to be the dominant factor in the rainfall-runoff response of the CRW, followed by storm location/time of concentration and not event volume.

Appendix C

HydroGeoSphere: mathematical theory

C.1 Model description

HydroGeoSphere (Aquanty, 2016) is a three-dimensional fully-distributed, physics-based integrated groundwater/overland flow numerical model. Its capabilities as an integrated model are wide ranging, and includes dynamic overland and stream channel flow routing, sub-surface unsaturated flow simulation with dual media, fracture flow and frozen soil capabilities, contaminant and thermal transport, and hydrological processes including interception and evapotranspiration.[1] For the purposes of this study, only the mechanisms relevant to wetland function, with respect to their handling of water quantity, are described below.

HydroGeoSphere simulates the movement of water through the subsurface using the variably-saturated three-dimensional groundwater equation, commonly referred to as the Richards (1931) equation (modified from Aquanty, 2016):

$$-\nabla \mathbf{q} - \Gamma_0 + Q = \frac{\partial \theta}{\partial t}, \tag{C.1}$$

where Q is the volumetric fluid flux in or out of the domain, θ is the water content within the void spaces of the sub-surface medium, t is time, Γ_0 is the fluid exchange between the surface and sub-surface domains, and $\mathbf{q}$ is the fluid flux vector given by:

$$\mathbf{q} = -\mathbf{K} \cdot k_r \nabla h, \tag{C.2}$$

where $\mathbf{K}$ is the hydraulic conductivity tensor, k_r is the relative permeability of the medium that is dependent on the degree of saturation $S_w = \frac{\theta}{\phi}$ and varies between zero and unity, ϕ is porosity, and $h = \Psi + z$ is total hydraulic head where Ψ is the pressure head and z is elevation.

[1] The reader is referred to Brunner and Simmons (2012) for a more-complete description of the capabilities and applications of HydroGeoSphere.

Overland flow is simulated using the diffusive wave approximation of the shallow water equations (modified from Aquanty, 2016):

$$-\nabla(d_0\mathbf{q_0}) + d_0\Gamma_0 + Q_0 = \frac{\partial \phi_0 h_0}{\partial t}, \tag{C.3}$$

where d_0 is overland flow depth, $h_0 = d_0 + z_0$ is the water surface elevation, z_0 is land surface elevation, ϕ_0 is a surficial porosity representing volume exclusion caused by the presence of physical obstructions such as vegetation and varies from zero at the land surface to unity at depths above obstruction heights, Q_0 is the volumetric flow rate per unit area representing external sources and sinks, and surficial fluid flux $\mathbf{q_0}$ is given by:

$$\mathbf{q_0} = -\mathbf{C_0} \cdot c_r \nabla h_0, \tag{C.4}$$

where c_r is a hyperbolic conductance reduction factor that varies from zero at the land surface to unity at depths above heights of obstructions such as vegetation, and $\mathbf{C_0}$ is the overland flow conductance derived from Manning's (1891) uniform flow equation (modified from Aquanty, 2016):

$$\mathbf{C_0} = \frac{d_0^{2/3}}{\mathbf{n}} \left(\frac{\partial h_0}{\partial s}\right)^{-1/2}, \tag{C.5}$$

where $\mathbf{n}$ is Manning's resistance factor, given in two dimensions and s is a length taken in the direction of maximum slope.

Both the subsurface equations and shallow water equations are solved simultaneously with the fluid exchange term (Γ_0) providing the flow coupling between the groundwater and surface water domains. The fluid exchange term is given by (modified from Aquanty, 2016):

$$\Gamma_0 = \begin{cases} \dfrac{k_r K_{zz}}{d_0 l_c}(h - h_0) & \text{when } h \geq h_0 \\ \dfrac{c_r K_{zz}}{d_0 l_c}(h - h_0) & \text{otherwise} \end{cases} \tag{C.6}$$

where l_c is the coupling length separating the subsurface and overland flow domains and K_{zz} is the vertical conductance through this coupling length described by the vertical conductance of the underlying sub-surface material.

C.2 Calculation of model outputs

Following the procedure outlined in Panday and Huyakorn (2004), flow depth (m) at each node i (and for every timestep) is calculated from:

$$d_i = h_i - (z + h_{ds})_i\,, \tag{C.7}$$

where d_i is the depth at node i, h_i is total head (metres above sea-level—$masl$), z is land surface elevation ($masl$), and h_{ds} is the height of depression storage (m—refer to Aquanty, 2016). Water pooling above surface can only move laterally if its depth exceeds depression storage height. Depth computed at every element is simply the average of depth from the three nodes that make-up the element.

Velocity is also calculated following Panday and Huyakorn (2004), using nodal heads to determine the gradient in the direction of maximum slope ($S = \partial h/\partial s$). Elemental velocity is then calculated based on Manning's equation for uniform flow assuming a shallow flow surface (i.e., sheet-flow):

$$v_i = \frac{1}{n_i} d_i^{2/3} S^{1/2}, \tag{C.8}$$

where v is the computed flow velocity (m/s) at element i, n is the Manning coefficient ($s/m^{1/3}$) set for element i, and d is elemental flow depth (m) computed as discussed above. Velocity-depth (vd—m^2/s), a standard engineering metric used to assess flood risk is computed by:

$$vd_i = \frac{1}{n_i} d_i^{5/3} S^{1/2}, \tag{C.9}$$

and depth-duration (dd—ms) is calculated from:

$$dd_i = \Delta t \sum_{ts=1}^{192} d_{i,ts}, \tag{C.10}$$

where ts is the timestep index and Δt is the model output constant timestep of 900 s.

Appendix D

Medial axis finite element mesh constraint

Within the final model boundary, 3,679 wetland features and 610 water bodies of varying shapes and sized were identified. As the purpose of this study was to quantify the function of these features and how their aggregated function affects the hydrology of the CRW, ideally all of them had to be explicitly accounted for. This requirement posed logistical problems as flexible mesh building routines have limited means of ensuring their inclusion. Of the mesh building routines that could be applied, they would consequently result in the addition of too many elements that would significantly hinder model run times. There are four approaches one could use to constrain the finite element mesh (FEM) to these features:

1. Apply no constraint—this option avoids the spatial location of the wetland features altogether, but would ensure an efficient FEM design. As the purpose of this study is to quantify the hydrological role of wetlands, this was not an option.

2. Constrain mesh to wetland boundary—As many of these mapped features are small ($< 1\,\text{ha}$), they are bounded by a number of vertices that are in very close proximity to one another ($< 1\,\text{m}$) and thus would greatly over-constrain the mesh—this would not be a feasible option.

3. Constrain mesh to feature centroids—This is a viable option in that the mesh would be constrained to *some* wetlands of circular shape. Issues arise when a wetland takes on a concave or irregular shape, and the wetland centroid lands in areas outside of the wetland bounds. This provides little improvement from option 1 (see Figure D.1)—an alternative method would be preferable.

4. Employ a mesh-refinement procedure—Mesh-generating software (including AlgoMesh used for this study) offers a feature where elemental edge lengths can be constrained to a minimum length within selected features, such as wetlands—This may appear to be a viable option; however there are two consequences to this approach:

    (a) this method restricts edge lengths only and not nodal placement, thus it tends to avoid nodes being placed in thinner elongated wetland features, precisely where they're needed (see Figure D.1); and,

(b) although not nearly to the extent of option 2., this procedure does come at a cost to model efficiency, as a significant increase of finite-elements need to be included.

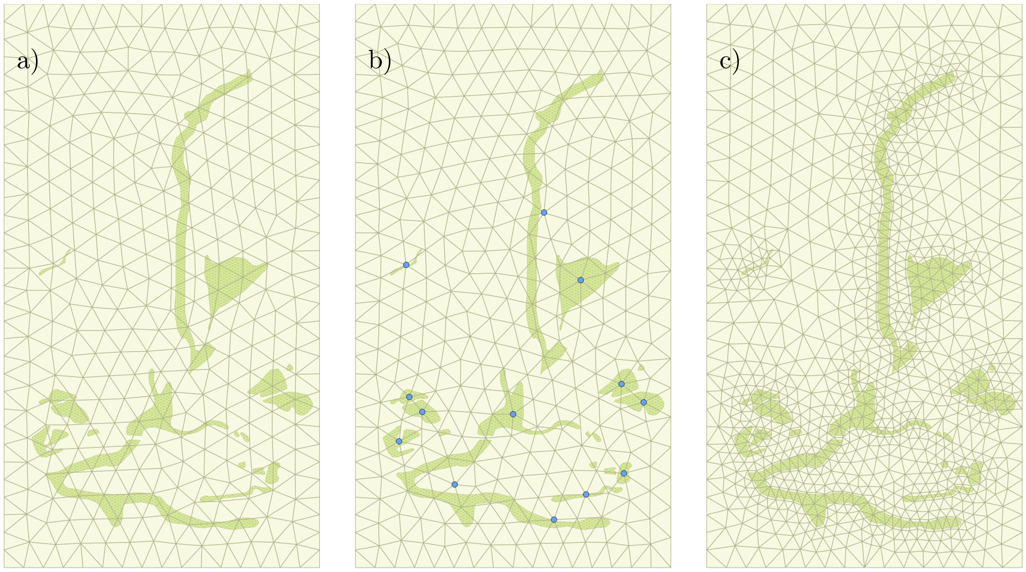

Figure D.1: Alternative methods to constraining an FEM around wetlands: a) no constraint; b) centroidal constraint; and c) edge length refinement within wetlands.

An alternative means to wetland-mesh constraint involved systematically identifying ideal node locations within the bounds of every wetland feature, and is based on a topological shape recognition methodology used to define a shape's "medial axis." The medial axis procedure is an automated procedure used to determine the "centreline" of a polygon, which is defined as a line whose perpendicular distance to a polygon bound is at its maximum without crossing other polygon boundaries. The technique was originally developed for "skeleton detection" as a means of creating an approximate skeleton of a two-dimensional figure (see, for example, the skeleton detection of a horse silhouette[1] in Figure D.2).

The automated medial axis technique designed for this study proceeded by determining all possible circles that touch at least two points of the wetland boundary while remaining completely contained within the wetland bound. Let the outline of the wetland be defined by curve γ. A circle of centre c is bitangent to γ at points s and t if:

$$(c - \gamma(s)) \cdot \mathbf{T}(s) = (c - \gamma(t)) \cdot \mathbf{T}(t) = 0, \tag{D.1}$$

where

$$\mathbf{T}(t) = \frac{d\gamma}{dt}, \tag{D.2}$$

[1] http://pages.cs.wisc.edu/~csverma/CS558_11/MedialAxis.html

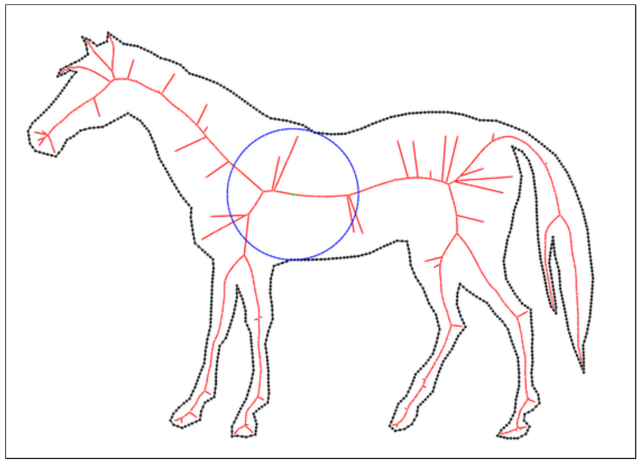

Figure D.2: An example of medial axis applied to skeleton detection of a horse's silhouette.

and $\mathbf{T}(t)$ is the unit tangent vector of curve γ at point t. The radius (r) of the interior circle can be computed as:

$$|c - \gamma(s)| = |c - \gamma(t)| = r. \tag{D.3}$$

A collection of interior bitangent circle centroids were collected as potential nodal FEM constraints. A final screening of these points was accomplished to ensure that no two points were within 25 m of each other. The final product of the medial axis technique is illustrated in Figure D.3a and yielded some impressive results. In the example used to illustrate the procedure, the mesh node locations were successfully constrained to within the wetland bounds at very little cost (Figure D.3b). When compared with the no constraint option, the medial axis only yielded a 15% increase in the number of elements, as opposed to a three-fold increase after using the common mesh-refinement procedure.

In total, 3,679 wetlands were located with the model boundary and were each independently represented in the model by allocating at least one computational node with the spatial domain of every wetland feature. Wetland-node representation varied widely. Figure 2.6 presents a histogram of wetland area and the average number of nodes used to compute a water balance within a wetland of a given size. As shown in Figure 2.6, as the area of wetland increases, so does the number of computational nodes used in representing the wetlands increase.

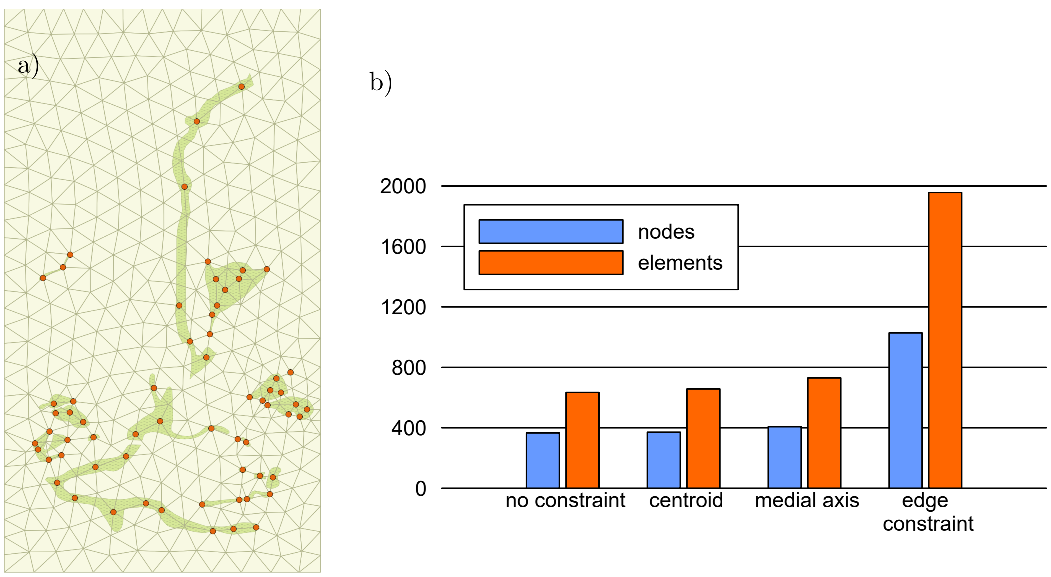

Figure D.3: a) Mesh design after the medial axis procedure (compare with Figure D.1); and b) cost statistics compared with alternative methods in terms of the number nodes and elements required for the given proceedure.

Appendix E

Finite element mesh: quality assessment

The final mesh used for this study contained 164,781 finite elements consisting of 82,668 nodes (see Figure 3.2). The longest elemental edge length was 946.0 m and the smallest element area was 19.2 m^2. Mesh quality was determined by four factors:

1. The Delaunay criterion requires that an element's circumcenter lies within itself. Failure to do so can lead to large interpolation errors; however with a constrained mesh, Delaunay criterion failures are commonly unavoidable. A total of 1,498 elements (0.9%) failed the Delaunay criterion.

2. Elements with obtuse interior angles cause similar issues as a Delaunay criterion failure. Elements with obtuse interior angles tend also to fail the Delaunay criterion. In total 10,611 elements (6.4%) were found to exhibit obtuse interior angles.

3. Elements with interior right angles can cause severe numerical instability. No right-angled elements occurred in the mesh.

4. Elemental aspect ratio is the ratio of an element's longest edge to its shortest edge, and is related to numerical accuracy. Ideally, an elements aspect ratio should be close to unity. Within the generated mesh, 1,213 (0.7%) elements with aspect ratios > 2.0.

Mesh quality can also be observed by creating a histogram of interior element angles (Figure E.1). The interior angle histogram relates to the four above criterion, but a further check of mesh quality can be observed by (i) the bell-shaped resemblance of the histogram, and (ii) the tendency for the histogram mode to approach 60°; recall that an equilateral triangle has all of its interior angles at 60°, aspect ratio of 1.0, and its circumcenter coincident with its centroid.

Figure E.1 also includes the cumulative distribution function of element area. This shows that close to 85% of elements in the model have areas less than a hectare, and the median area is roughly 0.36 ha or 3600 m^2, equivalent to a grid cell having 60 m sides. Recall that if a grid-based model were to be selected, and 60 m grid cells were to be used, 264,000 model cells would be required, a greater than 3-fold increase in computational requirements.

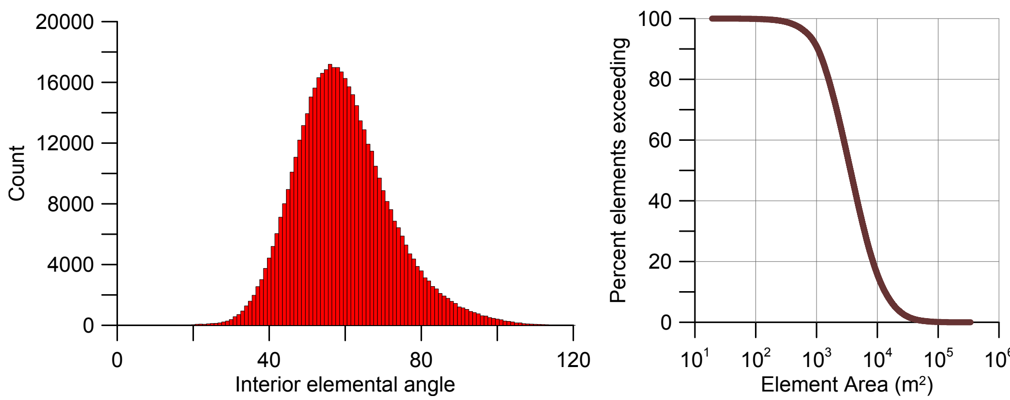

Figure E.1: Final mesh statistics: left) elemental interior angles, and right) cumulative distribution of elemental area.

Appendix F

Determination of late-summer antecedent moisture conditions

F.1 Model A

The late-summer antecedent state was defined first by separating the baseflow from all 13 Water Survey of Canada (WSC) stream gauges shown in Figure 3.4. To determine an average summer low-flow for the CRW streams, baseflow was separated using 13 automatic baseflow separation routines of:

1. The Wallingford (UKIH) method (Institute of Hydrology, 1980)

2–4. Three modified/extended Wallingford methods: sweeping minima, sweeping maxima, sweeping mean (Piggott et. al., 2005)

5. The Clarifica method (Clarifica, 2002)

6–8. The USGS Hydrograph Separation (HYSEP) method, three methods: fixed interval, sliding interval, local minimum (Sloto and Crouse, 1996)

9. The PART method (Rutledge, 1998)

10. The Lyne and Hollick digital filter (Nathan and McMahon, 1990)

11. The Chapman digital filter (Nathan and McMahon, 1991)

12. The Chapman and Maxwell digital filter (Chapman and Maxwell, 1996)

13. The Eckhardt digital filter (Eckhardt, 2005)

All of the above automatic baseflow separation routines lack any real physical basis; they are simply modelled after signal processing algorithms. For this reason, the best approach is to accept many baseflow separation routines as equally valid, and take the median of the reported baseflows as representative of reality (Figure F.2).

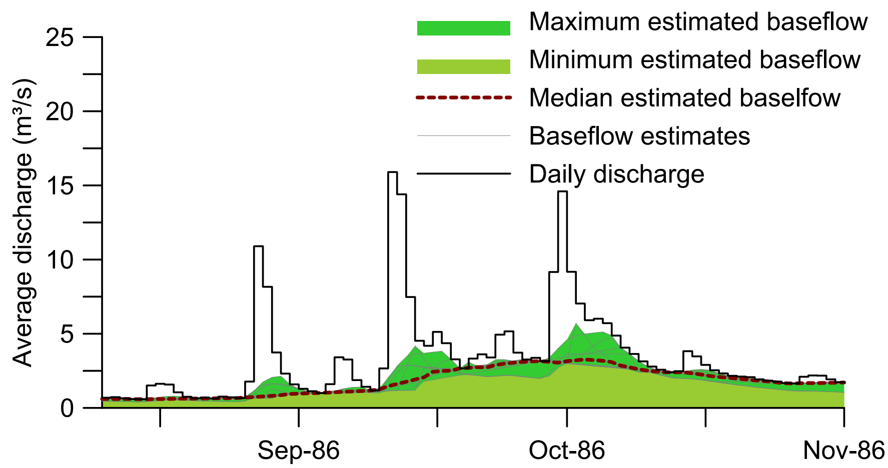

Figure F.1: Sample of baseflow separation from the methods listed above applied to 02HB008: Credit River West Branch at Norval.

The July–August–September median baseflow was then extracted from each gauge with the exception of 02HB030—Cooksville Creek near Cooksville and 02HB031—Credit River Erin Branch at Hillsburgh. On inspection, these stations appeared to have spurious results and were subsequently removed as outliers. Weighted by their catchment areas, the remaining 11 gauges averaged a median July–August–September baseflow discharge equivalent to 134 mm/year (Table F.1), with a 21% coefficient of variation.[1]

F.2 Model B

The preparation Model B's initial condition was based on the output of the Model A. The first step was to replicate the steady state model results from Model A. By applying Model A's final steady-state heads as the constant head boundary at the base of Model B, Model B will continue to be influenced by the lower layers without explicitly modelling them.

A preparatory run using Model B was accomplished to create an initial state prior to parameter estimation and scenario analysis. This preparatory run is commonly referred to as a "speed-up" run used to improve subsequent model runtimes. Recall that Model A had 134 mm/year constant rainfall applied. For the speed-up on Model B, zero precipitation and a potential evapotranspiration rate of 4 mm/day was applied to acquire a level of dryness used to represent the state of the CRW having no precipitation prior to the onset of an extreme rainfall event. The speed-up model was run for a period of 48 hours.

From Figure F.2, the median baseflow from eight gauges with long-term data (>10-years) is

[1]Coefficient of variation = sample standard deviation divided by its mean.

Table F.1: July–August–September median baseflow extracted from 13 WSC stream flow gauges within the CRW.

Gauge	Median summer baseflow (m^3/s)	Drainage area (km^2)	Equivalent baseflow (mm/year)	Period of record (years)
02HB001: Credit River Near Cataract	0.751	199.4	119	99.7
02HB002: Credit River At Erindale	2.460	769.6	101	48.0
02HB008: Credit River West Branch At Norval	0.406	136.5	94	54.2
02HB013: Credit River Near Orangeville	0.311	76.0	129	47.2
02HB018: Credit River At Boston Mills	2.231	389.8	181	32.3
02HB019: Credit River Alton Branch Above Alton	0.345	63.9	170	8.1
02HB020: Credit River Erin Branch Above Erin	0.256	58.3	139	31.8
02HB024: Black Creek Below Acton	0.097	28.2	108	27.3
02HB025: Credit River At Norval	2.835	666.9	134	26.2
02HB026: Credit River At Mississauga Golf Course	3.500	869.9	127	0.4
02HB029: Credit River At Streetsville	3.750	729.1	162	7.8
02HB030: Cooksville Creek Near Cooksville†	0.059	100.0	19	7.3
02HB031: Credit River Erin Branch At Hillsburgh†	0.134	120.8	35	8.8

† outliers not used for analysis.

compared to the speed-up Model B results. Overall there's a slight overestimation (≈20%) of the baseflow discharge, which would only imply that the initial state set from this method is slightly more moist than anticipated. Recall that the coefficient of variation of the estimated baseflow from Table F.1 was 21%; therefore the bias found here was taken to be within acceptable limits.

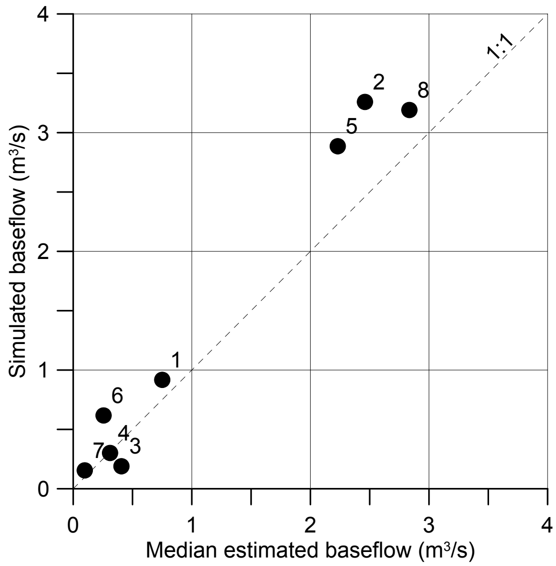

Figure F.2: Comparison of baseflow from the transient speed-up model compared to the median July–August–September baseflow reported at the following gauges (refer to Table F.1): 1) 02HB001; 2) 02HB002; 3) 02HB008; 4) 02HB013; 5) 02HB018; 6) 02HB020; 7) 02HB024; and, 8) 02HB025.

Overall, the determination of late-summer antecedent moisture conditions described here performed quite well, matching baseflow conditions observed within the CRW at eight locations simultaneously under a single model run. It is important to re-iterate that these results were accomplished using a distributed and integrated model simulation, demonstrating the advantage of incorporating the groundwater system when attempting to establish an antecedent state.

The established antecedent state resulting from this speed-up model run resulted in a number of wetlands remaining inundated, reducing their retention capacity, on the basis of their position on the landscape and local hydrostratigraphy. Without following such a procedure, the modeller would have had to define these water levels (i.e., retention capacity) manually prior to running scenario simulations, effectively biasing the model results. Model B results shown here confirm that the procedure established a typical late-summer moisture state, and was set to test wetland flood mitigation capacity.

Appendix G

Precipitation field temporal dissaggregation

The "very-high resolution urban-scale weather forecasting system" dataset prepared for the 2015 Pan- and Parapan-American Games in Toronto by Environment Canada was used to establish a dynamic precipitation event input for the model. The dataset came in a 1025×1025 250 m resolution, 15 minute snapshots of active weather distributions recorded in the southern Ontario region. The very-high resolution urban-scale weather forecasting system is a composite real-time dataset based on a double-moment microphysics planetary boundary-layer scheme. Simulations were obtained with the Global Environmental Multiscale model (GEM; Zadra et. al., 2008) with a specific limited-area configuration as described by Leroyer et. al., (2014), which incorporated:

- High-resolution vertical discretization of the surface boundary-layer where condensation processes were computed following an advanced double-moment microphysics scheme of Milbrandt and Yau (2005);
- Large-scale climate downscaling derived from the operational Regional Deterministic weather Prediction System (RDPS; Fillion et. al., 2010);
- Surface processes were modelled in built-up areas using the Town Energy Balance model (TEB; Masson, 2000), and for natural cover, the Interactions between the Surface, Biosphere and Atmosphere land surface model (ISBA; Belair et. al., 2003a; 2003b);
- Initial conditions for soil moisture and soil temperature was obtained from the 2.5 km Canadian Land Data Assimilation System (CaLDAS), the same used for the pan-Canadian modeling system (Milbrandt et. al., 2016); and,
- Surface temperatures for the Great Lakes were prescribed using 2 km hourly output from a coupled ocean-atmosphere forecasting system (Dupont et. al., 2012).

G.1 Rainfall intensity field

G.1.1 Surface cropping and translation

The dataset was first cropped from the 1025×1025 (250 m cells) to a 220×229 extent strategically chosen to capture the storm front and reduce the model input file size. The cropped surface, measuring 55×57 km, was the minimum extent that covered the entirety of the CRW. The cropped region was then translated 32 km due west to ensure that the storm front climax occurred directly over the study area. It is important to note that neither the orientation, direction, velocity, nor scale was modified, only the exact location of where the August 2$^{\text{nd}}$ storm occurred and the intensities it delivered. It was then assumed that the storm orientation, direction, velocity, and scale was representative of a typical late-summer southern Ontario convective storm event.

G.1.2 Temporal disaggregation

The dataset was provided in 15 minute increments, which provided instantaneous snap-shots of storm distribution. According to these snap-shots, the storm front, measuring roughly 2 km in width, travelled approximately 16 km per 15 minute increment (≈64 km/hr). Naturally, as the storm progressed in real time, the front would have swept across vast swaths of the CRW not captured by the 15 minute interval dataset. For example, Figure G.1 illustrates a series of 15 minute snapshots of the August 2$^{\text{nd}}$ storm progression obtained from Environment Canada. The storm front shown as the red-violet north-south oriented feature reflects the area of greatest rainfall intensity and it is apparent that much of the upper CRW is prevented from receiving these large intensities at the provided temporal resolution.

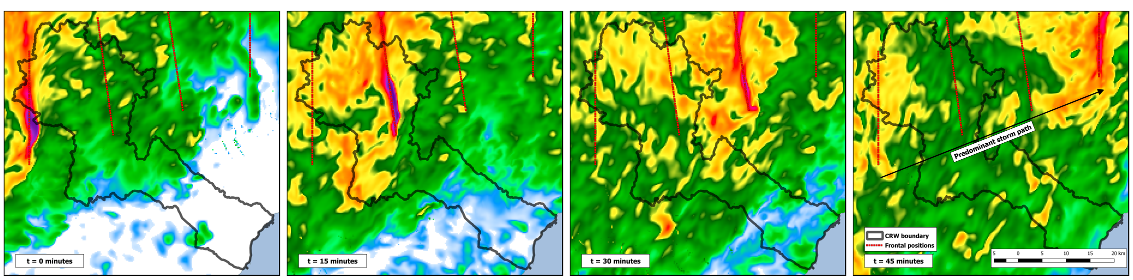

Figure G.1: A time series of the very-high resolution urban-scale weather forecasting system showing the August 2, 2015 storm in 15-minute intervals as provided by Environment Canada. Notice that if the dataset were used as is, much of the CRW (outlined in grey) would be devoid of high-intensity rainfall.

In tracing the storm front at these four (known) time steps, it was determined that the storm progressed at a velocity of 61.2 km/hr due east by 24.8 km/hr due north. Knowing the velocity of the predominant storm path ($\mathbf{v}_s$), a temporal disaggregation scheme was devised to interpolate sub-fields at 30 second intervals. Temporal disaggregation was accomplished by (forward-) translating storm distribution from a given time step and (backward-) translating from the subsequent time step using the calculated storm velocity. The forward- and backward-translations were then averaged, weighted by their interpolated time relative to the prior and subsequent known storm fields, following the equation:

$$\hat{P}_{t_i} = w\hat{\phi}^{-}(t_i) + (1-w)\hat{\phi}^{+}(t_i), \tag{G.1}$$

where $\hat{P}_{t_i}$ is the interpolated field at time step t_i. For every pixel x:

$$\begin{aligned}
\phi_x^{-}(t_i) &= P_{x-\lfloor \mathbf{v}_T\cdot(t_i-t_0)\rfloor,t_0} && \text{is the forecast projection,}\\
\phi_x^{+}(t_i) &= P_{x+\lfloor \mathbf{v}_T\cdot(t_1-t_i)\rfloor,t_1} && \text{is the hindcast projection,}\\
w &= \frac{t_i-t_0}{t_1-t_0} && \text{is a weighting coefficient,}
\end{aligned}$$

P_{x,t_0} is the known pixel value prior to time t_i and P_{x,t_1} is the known pixel value to follow t_i (i.e., $t_0 < t_i < t_1$), $\mathbf{v}_T = \frac{\mathbf{v}_s}{\mathbf{s}}$ is the training vector, and $\mathbf{s} = (l,h)$ is the dimension of the grid cells. The notation $\lfloor\cdot\rfloor$ is the floor function, the highest integer value less than value contained. On visual inspection, this approach was apparently quite effective.

Figure G.2 illustrates a sample series of disaggregated 30-second interval storm fields derived from the first two frames shown in Figure G.1. Only the first and last frames shown in Figure G.2 were provided, the remaining 29 sub-frames were interpolated using equation G.1.

G.1.3 Temporal (re-)aggregation and normalization

The next step was to accumulate the interpolated 30-second storm front fields into 15-minute rainfall accumulations. As shown in Figure G.3 the mapping of rainfall accumulation varies significantly from the mapping of instantaneous rainfall intensity (Figure G.1), filling in areas missed by the original dataset. Although the model can run at 30-second increments, it was decided that the model was to be structured to import climate data at 15-minute increments, to save on runtimes and memory requirements.

The 15-minute accumulation maps were then normalized such that they could be readily scaled to the necessary hypothetical intensities. The values were normalized to the median rainfall amount measured among all of the 15-minute accumulation maps derived from the steps described above (15 maps in total—storm duration was less than 4 hours). By this method, the median-normalized accumulation fields would represent an equal likelihood that a randomly placed rain gauge would measure either above or below the set intensity. Consequently, certain portions of the watershed will receive more than the set amount of rainfall used to scale the event.

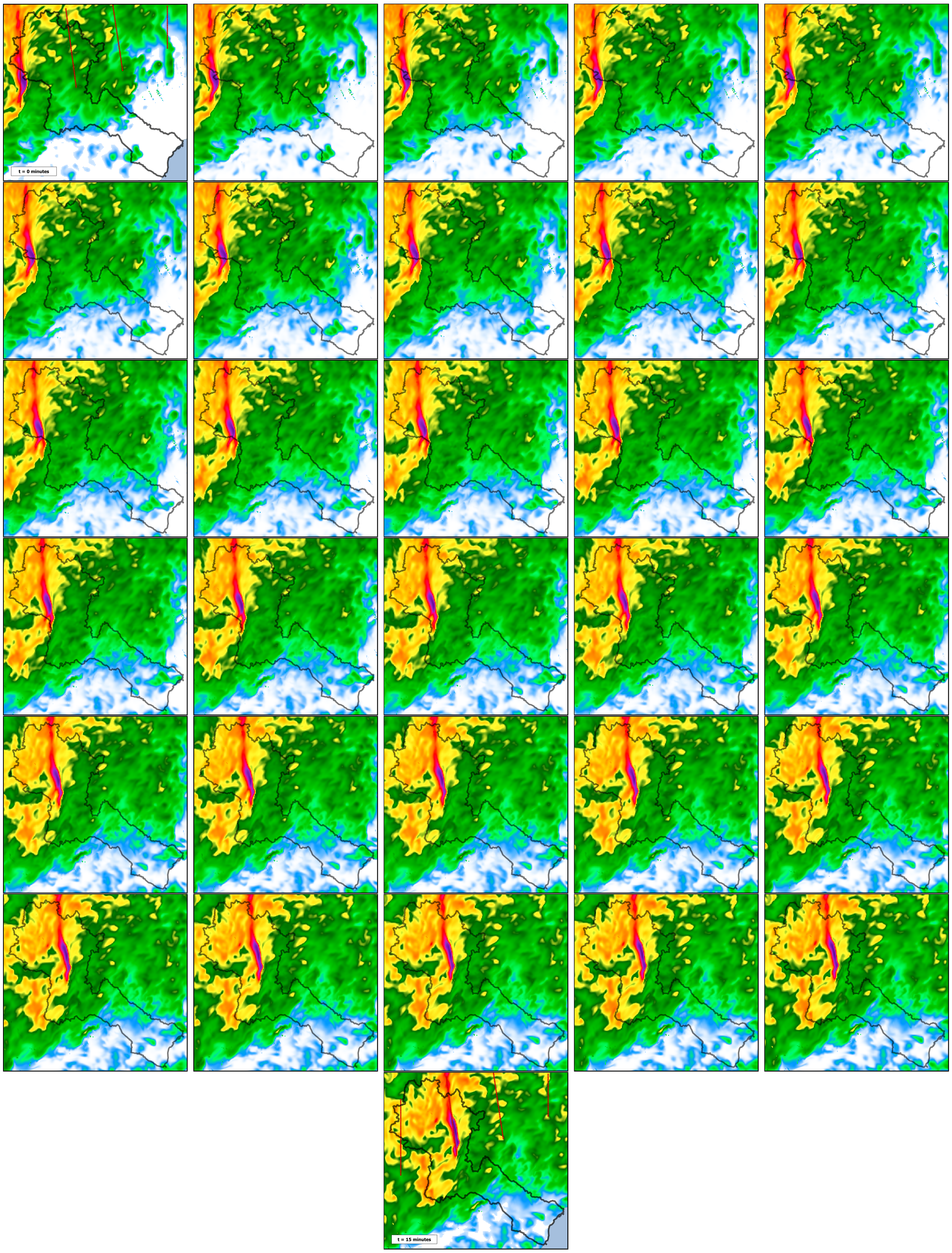

Figure G.2: A time series of the very-high resolution urban-scale weather forecasting system showing the August 2, 2015 storm in 30-second intervals interpolated using the described temporal disaggregation routine.

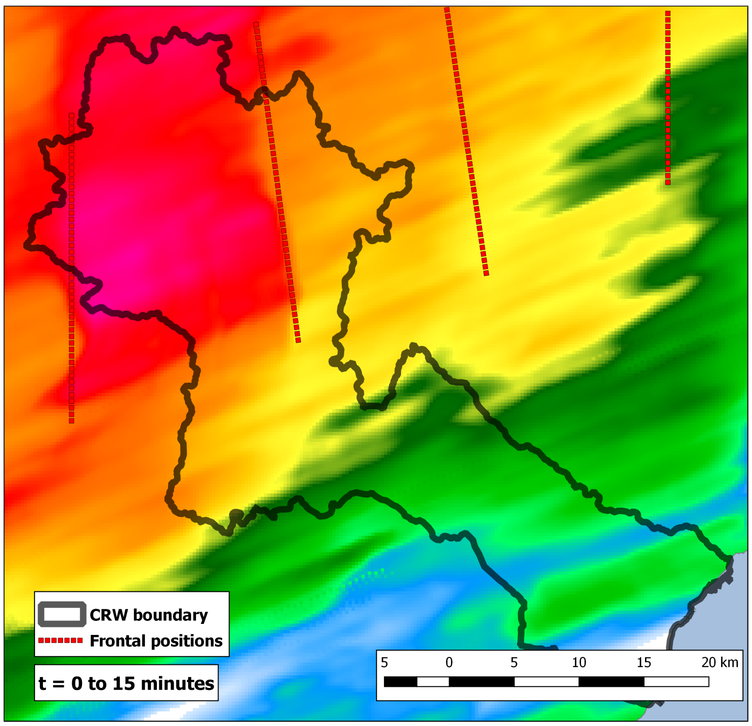

Figure G.3: 15-minute rainfall accumulation derived from the set of 30-second intensity fields shown in Figure G.2.

G.2 Storm event scaling

The modelling procedure of this study demanded the simulation of a set of 7 storms increasing in intensity over the Credit River watershed. The 2-, 5-, 10-, 25-, 50-, and 100-year return period, 15-minute duration events were retrieved from two Environment Canada engineering climate Intensity-Duration-Frequency (IDF) curves proximal to the study area, and include: Blue Springs Creek (6140818) and Orangeville MOE (6155790) (see Figure 2.13). Measured intensity-duration statistics are presented in Tables G.1 and G.2. The seventh intensity applied was the Ontario record highest 15-minute observed accumulation of 66.3 mm (Table 3.2).

These select 15-minute duration event intensities were applied as a scaling factor that when multiplied with the normalized intensity field resulted in a rainfall distribution representative of the given return period storm event.

Table G.1: Estimated return period rainfall amounts (mm) for Blue Springs Creek (6140818); Latitude: 43 38'N, Longitude: 80 7'W, Elevation: 373 masl.

Duration	2-yr	5-yr	10-yr	25-yr	50-yr	100-yr	number of years reporting
5 min	9.1	12.4	14.6	17.3	19.4	21.4	11
10 min	12.9	16.8	19.3	22.6	25.0	27.3	11
15 min	15.2	20.3	23.6	27.9	31.1	34.2	11
30 min	19.8	28.7	34.6	42.1	47.6	53.1	11
60 min	24.3	37.1	45.6	56.3	64.2	72.1	11
2 hour	30.7	44.6	53.8	65.5	74.1	82.7	11
6 hour	42.6	55.0	63.2	73.5	81.2	88.8	11
12 hour	48.9	62.4	71.3	82.7	91.0	99.4	11
24 hour	55.5	67.9	76.0	86.4	94.0	101.6	11

G.2.1 Confirmation of event creation

A hyetograph taken from a random location within the CRW illustrates the isolated (i.e., frontal) nature of the August 2nd storm (Figure G.4). As shown, the duration of the main pulse of the frontal storm lasts less than 5 minutes, and the event rainfall intensity is quite heterogeneous judging by its multi-modal distribution.

The scaled rainfall fields can also be extrapolated to their 5-, 10-, 15- 30- and 60-minute and 2-, 6-, 12- and 24-hour total accumulation to recreate IDF curves for the 2-, 5-, 20-, 25-, 50- and 100-year return period. Figures G.5 and G.6 show these results superimposed on top of the official short-duration IDF curves published for Blue Springs Creek and Orangeville MOE stations, respectively, and confirm that this procedure more than adequately recreated local event statistics.

Table G.2: Estimated return period rainfall amounts (mm) for Orangeville MOE (6155790); Latitude: 43 55'N, Longitude: 80 5'W, Elevation: 411 masl.

Duration	2-yr	5-yr	10-yr	25-yr	50-yr	100-yr	number of years reporting
5 min	7.4	9.9	11.5	13.6	15.2	16.7	10
10 min	10.8	15.7	19.1	23.2	26.3	29.4	10
15 min	12.5	19.1	23.5	29.1	33.3	37.4	10
30 min	15.9	24.1	29.5	36.4	41.5	46.5	10
60 min	18.4	26.5	31.8	38.6	43.6	48.6	10
2 hour	21.9	29.9	35.1	41.8	46.7	51.6	10
6 hour	30.9	38.4	43.3	49.6	54.2	58.9	10
12 hour	—	—	—	—	—	—	9
24 hour	39.7	50.9	58.2	67.6	74.5	81.4	10

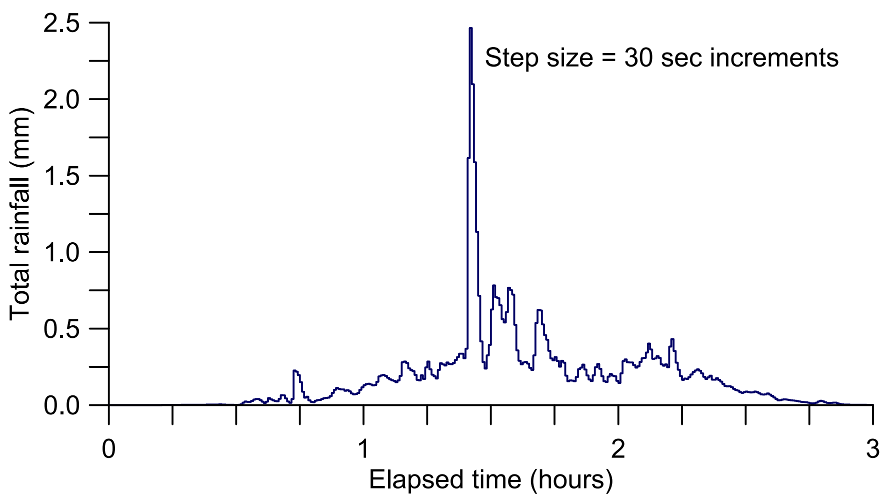

Figure G.4: Hyetograph of the August 2, 2015 storm, scaled to a 2-year return period intensity experienced at an arbitrary location within the CRW.

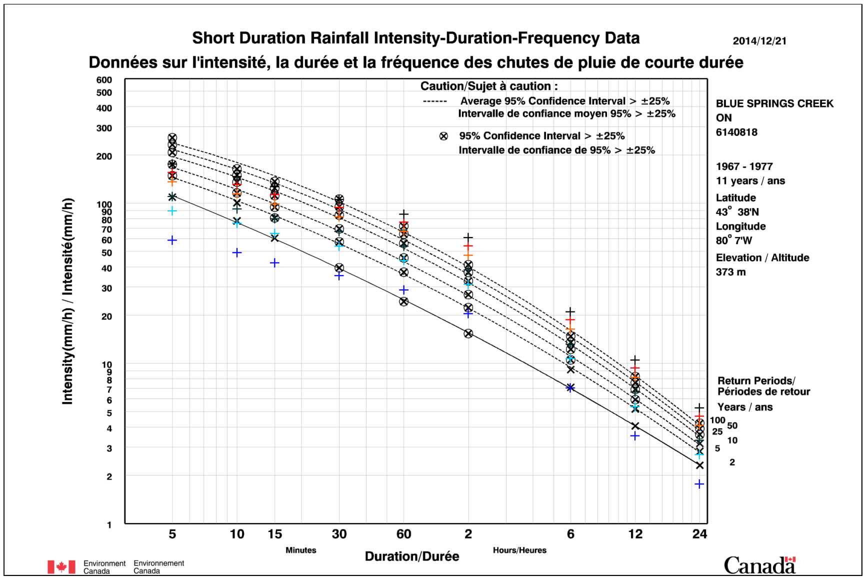

Figure G.5: Comparison of Blue Springs Creek (6140818) IDF curves to the August 2 storm field scaled to the 2-, 5-, 20-, 25-, 50- and 100-year return period events. (Coloured crosses are derived results.)

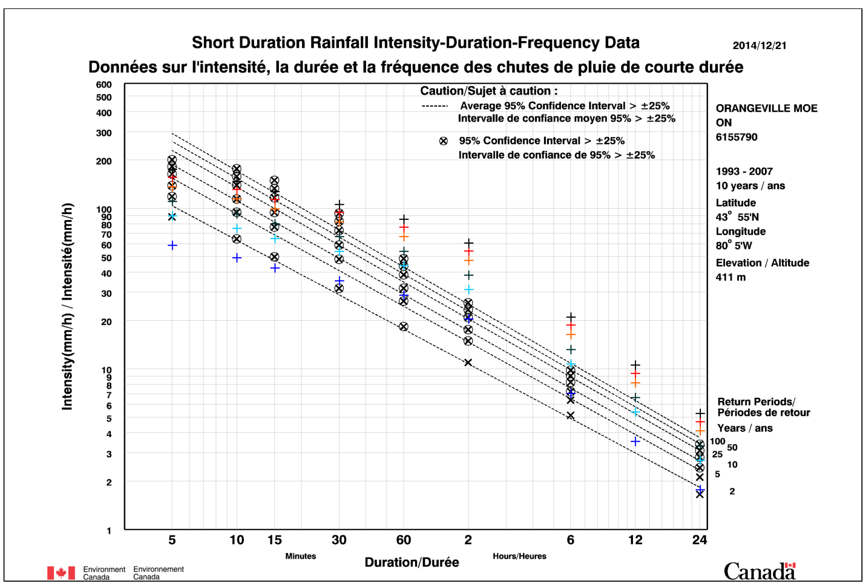

Figure G.6: Comparison of Orangeville MOE (6155790) IDF curves to the August 2 storm field scaled to the 2-, 5-, 20-, 25-, 50- and 100-year return period events. (Coloured crosses are derived results.)

Appendix H

Multi-model ensemble: Monte Carlo sampling plan

The multi-model ensemble approach began by building a Monte Carlo sampling plan (Lemieux, 2009), from which a pseudo-random selection of parameter values are combined for input into the model. The sampling plan used here is the Latin Hypercube sampling plan (Lemieux, 2009) used to permute a number of free parameters. The Latin Hypercube sampling plan provides parameter sampling from an independent and identically distributed (*i.i.d.*) set of uniform numbers between 0 and 1—formally expressed as $\mathrm{U}[0,1]$. The collection of uniform unit distributions must then be translated into a sampling range. Two transformations were applied: uniform $\mathrm{U}[a,b]$ and generalized trapezoid $\mathrm{Trap}[a,b,m,n]$ (van Dorp and Kotz, 2003; van Dorp et. al., 2007), where a and b are the lower and upper limits of a feasible range, respectively, and m and n are trapezoid shape parameters (Figure H.1).

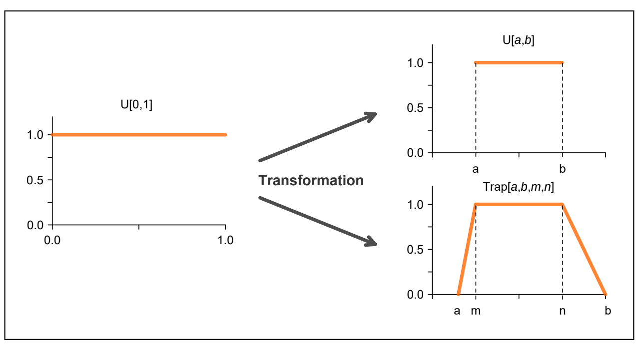

Figure H.1: A uniform sampling transformation.

The efficiency of a multi-model approach can be dependent on the number of parameters being sampled and the aim is to reduce the number of parameters as much as possible. Recent advances in high-dimensional dependence modelling have seen increased application of copulae to combine a number of parameters into a single "super-parameter," if there can be some assumed interdependence (Kurowicka and Cooke, 2006). A copula not only allows for the reduction of a number of dependent parameters to one sampling parameter, but the modeller can also assign the degree to which a pair of dependent parameters are correlated.

The copula used exclusively in this study, is known as Frank's Archimedean copula, with correlation of 0.8 and parameter θ set to 10.0 (Figure H.2). The Frank's copula is a symmetric copula of the Archimedean family commonly used for dependence sampling (Kurowicka and Cooke, 2006). The advantage of copula sampling is that while every parameter individually preserves their *i.i.d.*, the samples pairings are simply re-ordered to achieve a degree of correlation.

The correlation parameter ranges from -1 to 1 (i.e., from complete negative to positive correlation), where 0 would provide no correlation whatsoever. The parameter θ bounds the Frank's copula (C_F) by upper C_U and lower C_L copula bounds also known as the Fréchet copulae, where $C_L \leq C_F \leq C_U$ (see Kurowicka and Cooke, 2006).

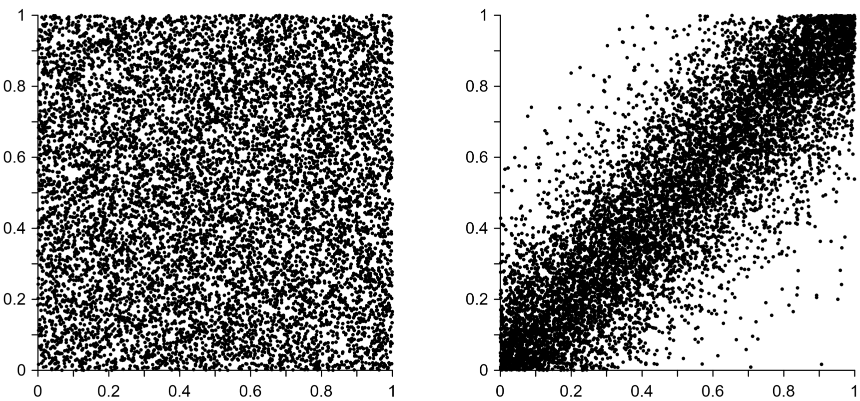

Figure H.2: left) uncorrelated bivariate sample; right) dependent bivariate sample built from a Frank's Archimedean copula, with correlation of 0.8 and θ =10.0.

A total of four model parameters (saturated hydraulic conductivity and porosity of the shallow soil zone, surface roughness, and ground vegetation height) were varied for the multi-model analysis, as shown in Table H.1. Two of the four parameters (hydraulic conductivity and porosity) affected all five surficial geology types (§3.2.3), while the third and fourth parameters affect three and two overland flow types (§2.2), respectively (see column 2 of Table H.1). In total, this came to 17 parameters being adjusted, 4 of which were reduced to 2 by use of copulae.

Only the saturated hydraulic conductivity was transformed to the trapezoidal distribution and was distributed over the logarithmic scale. Figure H.3 provides an illustrative example of the saturated hydraulic conductivity sampling strategy. The strategy was inspired from fuzzy-logic, which allows for the direct translation of the Chapman and Putnam (1984) permeability attribute to the multi-modelling strategy.

The remaining parameters not listed in Table H.1 were kept constant. See Aquanty (2016) for more information on model parameters.

Table H.1: List of parameter ranges sampled during the multi-model analysis.

Parameter	Surficial Geology/ Land use	Units	a	m	n	b
Saturated hydraulic conductivity[a]	Low	m/s	10^{-11}	10^{-9}	10^{-7}	10^{-6}
	Low-medium		10^{-9}	10^{-7}	10^{-6}	10^{-5}
	High		10^{-5}	10^{-4}	10^{-3}	10^{-2}
	Variable Materials		10^{-9}	10^{-7}	10^{-5}	10^{-3}
	Wetland Sediments		10^{-8}	10^{-7}	10^{-5}	10^{-4}
	Alluvium		10^{-8}	10^{-7}	10^{-5}	10^{-4}
Porosity	Low	–	0.35	–	–	0.55
	Low-medium		0.30	–	–	0.45
	High		0.25	–	–	0.35
	Variable Materials		0.35	–	–	0.45
	Wetland Sediments		0.35	–	–	0.60
	Alluvium		0.30	–	–	0.45
Manning's roughness coefficient	Short vegetation[b]	$\frac{s}{m^{1/3}}$	0.05	–	–	0.50
	Tall vegetation[b]		0.05	–	–	0.50
	Agriculture		0.01	–	–	0.50
Height of ground vegetation	Short vegetation[c]	m	0.05	–	–	1.0
	Tall vegetation[c]		0.05	–	–	1.0

[a] Sampling over the logarithmic (base-10) scale
[b] Manning's roughness coefficient co-sampled using a copula
[c] Height of ground vegetation co-sampled using a copula

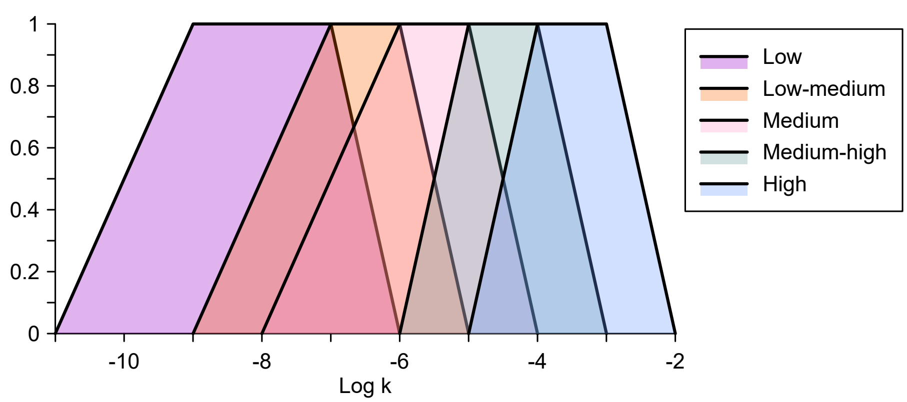

Figure H.3: Illustrative example of trapezoidal k-distributions.